# The role of vitamin D and β-defensin 103 on skin:

# from defence to pigmentation regulation

**Arrate Sevilla Mambrilla**

**2020**

**Supervisors: Santos Alonso and Isabel Smith**

This thesis is the result of the project carried out from 2015 to 2020 at the Department of Genetics, Physical Anthropology and Animal Physiology, at University of the Basque Country (UPV/EHU). This work was supported by a predoctoral fellowship from the Basque Government to Arrate Sevilla (PRE_2014_1_419), an EMBO Short-Term Fellowship (7014), a MINECO proyect grant (CGL2014-58526-P), by FEDER (Fondo Europeo de Desarrollo Regional), and by projects from the Basque Goverment (IT1138-16 and SAIOTEK2012: S-PE12UN051).

# Index

# Resumen

La pigmentación de la piel es uno de los rasgos fenotípicos humanos más diverso e interesante, porque constituye un buen ejemplo de la habilidad de los humanos para adaptarnos a diferentes ambientes. La distribución geográfica del color de la piel está altamente correlacionada con los niveles de radiación Ultravioleta (UV), mostrando un gradiente latitudinal desde pigmentación más oscura cerca del ecuador a pigmentación más clara cerca de los polos. Las hipótesis más aceptadas explican la pigmentación como un resultado de distintos intereses evolutivos. En regiones de alta radiación UV, una pigmentación más oscura sería ventajosa porque brinda protección contra los efectos nocivos de la UVR, como el daño al ADN, las quemaduras solares y la foto-degradación de folato. Por otro lado, en regiones de baja radiación UV, una piel más clara facilitaría la penetración de la luz UV en la piel promoviendo así la síntesis de vitamina D.

Sin embargo, se han propuesto otras hipótesis alternativas que también pueden haber tenido influencia en la evolución de la pigmentación de la piel, como por ejemplo, la necesitad de la conservación metabólica, conservación hídrica, selección sexual o camuflaje. Entre ellas, una hipótesis interesante propone que la pigmentación de la piel evolucionó para ofrecer protección contra los microorganismos patógenos, siendo los melanocitos parte del sistema de defensa.

En este sentido, la piel juega un importan papel como primera línea de defensa, actuando como barrera física y proporcionando actividad inmunológica a través de las células inmunes residentes, con las que también interactúan los melanocitos y los queratinocitos. Curiosamente, se ha observado que la síntesis de melanina aumenta tras algunas infecciones microbianas y, de manera similar, el péptido antimicrobiano β-defensina 103 se ha relacionado con la pigmentación en perros. Así, se descubrió que una deleción de 3 pb en el segundo exón del ortólogo canino de la β-defensina 103 que provoca la deleción de una glicina, era causante del color de pelo negro en los perros.

Estos resultados sugieren que la pigmentación podría estar asociada a la respuesta inmune innata.

Por su parte, la vitamina D tiene actividad inmunomoduladora y antiinflamatoria y se usa en el tratamiento de algunas enfermedades de la piel, como la psoriasis y el vitíligo. Asimismo, está involucrada en la protección contra el daño inducido por la radiación UV mediante la regulación de la respuesta al daño del ADN y las respuestas antioxidantes. Además, se ha visto que la vitamina D puede modular la expresión de algunos péptidos antimicrobianos, incluidas las catelicidinas y las β-defensinas.

Por lo tanto, el objetivo principal de este trabajo es explorar la posible relación entre la pigmentación de la piel humana y el sistema inmunitario de la piel. Para eso, analizamos el efecto de la β-defensina 103 (codificada por el gen *DEFB103*) y la vitamina D activa en la pigmentación de la piel.

En el capítulo 1, analizamos la diversidad de secuencia y variación en el número de copias (CNV) de *DEFB103*. Primero, recolectamos muestras de individuos del País Vasco y obtuvimos una distribución del color de la piel, medida por espectrometría de reflectancia en la superficie interna de la parte superior del brazo. Seleccionamos individuos de los extremos de la distribución (los individuos más pigmentados y los menos pigmentados) y analizamos la variabilidad de secuencia de *DEFB103* mediante clonación y resecuenciación de los exones y parte de la secuencia intrónica adyacente. También analizamos otros 30 individuos de Asia, África, Australia y Europa.

Observamos diversidad de secuencia detectando 30 variantes, aunque la mayoría de ellas eran raras, presentándose solo en una o unas pocas muestras. En total, 15 de las variantes no estaban previamente descritas en dbSNP (versión 154). Sin embargo, no detectamos ninguna variante similar a la observada en perros.

El gen *DEFB103* se encuentra dentro de una región variante en el número de copias (CNV, por sus siglas en inglés) cuyo rango oscila entre 1 y 12 copias por genoma diploide, siendo así otra fuente de variabilidad. Por lo tanto, también exploramos si el número de copias (NC) estaba relacionado con la pigmentación. Para eso, determinamos el NC de *DEFB103* en individuos de los extremos de la distribución de reflectancia de la piel (a partir de una muestra en el País Vasco; N = 122) y comparamos la frecuencia de NC entre los grupos, sin hallar diferencias significativas entre los grupos más y menos pigmentados. Además, para analizar si la radiación UV estaba relacionada con el número de copias, determinamos el NC en muestras de diferentes regiones de España (obtenidas del Banco Nacional de ADN). Obtuvimos datos para el promedio anual de incidencia de radiación UV-B (J / $m^2$) proporcionados por AEMET (Agencia Española de Meteorología) y comparamos la distribución del número de copias de *DEFB103* entre los grupos seleccionados en función de los valores de irradiación UV-B superficial.

La comparación se hizo entre individuos de provincias que se encuentran dentro del percentil inferior 15 frente a los pertenecientes a provincias por encima del percentil 85 de irradiación UV-B. En este caso, observamos diferencias estadísticamente significativas en la distribución del número de copias (prueba U de Mann-Whitney: $p = 0.022$), así como cuando se agruparon siguiendo el criterio de <4, 4 y > 4 copias (Prueba $X^2$, $p = 0.0078$). Estos datos indican una mayor frecuencia de valores bajos en el grupo del percentil 15 (individuos de provincias con menor irradiación superficial UV-B anual). Nuestros datos sugieren una posible asociación entre el número de copias de *DEFB103* y la irradiación UV-B superficial en España.

En el capítulo 2 exploramos el efecto de la radiación UV en la expresión de *DEFB103* en queratinocitos provenientes de individuos de pigmentación clara y oscura. Al mismo tiempo, también incubamos los queratinocitos con otros estimulantes relacionados con la inmunidad para comparar las respuestas. Así, los cultivos fueron irradiados con luz

UV-B, o se incubaron con *Staphylococcus aureus* inactivado mediante calor (HKSA, por sus siglas en inglés) y vitamina D activa ($1,25(OH)_2D_3$). El nivel de expresión de *DEFB103* se midió mediante PCR digital (dPCR) tras diferentes tiempos de incubación (12h, 24h y 48h).

Todas las líneas celulares analizadas mostraron un bajo nivel de expresión basal de *DEFB103* y había una gran variabilidad en la respuesta a los estimulantes. La respuesta parecía ser una característica particular de cada línea celular, en lugar de cada grupo (ligeramente pigmentadas o muy pigmentadas). Algunas líneas celulares no respondieron y otras líneas celulares respondieron en diferentes momentos.

Entre las células que respondieron a los estímulos, se dio un mayor aumento en la expresión de *DEFB103* con HKSA en comparación con irradiación UV. La respuesta máxima a HKSA fue 2-3 veces mayor que la respuesta máxima a UV. Tras la irradiación UV, 4 líneas celulares aumentaron la expresión (3 líneas celulares claras y una línea oscura), pero en momentos diferentes. Es de destacar que todas las líneas celulares claras respondieron a la irradiación UV-B, lo que podría sugerir que el fenotipo pigmentario podría ser relevante para la expresión de *DEFB103* en respuesta a UV. Respecto a la vitamina D, solo dos de las líneas celulares mostraron un aumento en la expresión en comparación con sus controles. Estos resultados sugieren que la radiación UV podría modular la expresión de *DEFB103*, al menos ligeramente, particularmente en queratinocitos de donantes de pigmentación clara.

Por otro lado, también tuvimos en cuenta otros factores genéticos que podrían influir en la expresión de *DEFB103*. Analizamos el número de copias y genotipamos un SNP ubicado en la región reguladora de *DEFB103* (rs2737902), el cual ha sido asociado a un mayor nivel de expresión. Sin embargo, ninguna de las líneas celulares poseía el SNP y no observamos ninguna correlación con el número de copias.

En el capítulo 3 analizamos la respuesta al péptido β-defensina 103 (HBD3) en melanocitos provenientes de individuos de pigmentación clara y oscura, mediante microarrays de expresión, tras diferentes tiempos de incubación. Queríamos determinar si HBD3 afecta a la melanogénesis en los melanocitos y qué vías de pigmentación se activan en humanos como consecuencia de la unión de HBD3 a MC1R. Los melanocitos se incubaron con péptido de tipo salvaje (WT-HBD3) o con un péptido que porta la mutación encontrada en perros (MUT-HBD3).

Basándonos en el análisis de componentes principales (PCA), planteamos la hipótesis de que el Componente Principal 1 (PC1) podría explicar un proceso de despigmentación de las líneas celulares a lo largo del tiempo en cultivo, ya que los controles a las 0h y a las 24h están en los extremos opuestos del PC1. Nuestra hipótesis es que los melanocitos en cultivo, sin ningún estimulante, tienden a perder la expresión de genes pigmentarios con el tiempo. Tras elaborar una lista de genes de melanocitos relacionados con la pigmentación, comprobamos mediante el test hipergeométrico si la lista de genes estaba sobrerrepresentada entre los genes diferencialmente expresados. La comparación del grupo formado por controles a las 0h y 12h versus el grupo formado por controles a las 24h mostró una regulación positiva (aumento) de los genes relacionados con la pigmentación a las 0h y 12h en melanocitos de pigmentación clara y oscura, confirmando así nuestra hipótesis.

Para analizar el efecto del péptido β-defensina 103 (HBD3), comparamos los perfiles transcriptómicos de las células incubadas con HBD3 y los controles correspondientes (no tratados), a las 12h y 24h. Observamos que a las 24h tras incubación con HBD3, se daba un aumento en la expresión de genes melanogénicos en comparación con los respectivos controles tanto en melanocitos claros como en oscuros. Los genes de pigmentación estaban sobrerrepresentados en cultivos tratados con HBD3. La regulación positiva fue más significativa en los melanocitos de pigmentación clara, lo que indica que la diferencia en la intensidad de la respuesta de los melanocitos a HBD3

podría estar relacionada con el fenotipo pigmentario. Además, la respuesta fue más significativa con HBD3 de tipo salvaje en comparación con HBD3 mutado.

Por lo tanto, si el efecto de HDB3 es a través de MC1R, la mutación observada en perros no parece aumentar la afinidad por el receptor en humanos, como ocurre en los cánidos. De hecho, esta mutación no se ha descrito en humanos y tampoco la encontramos en los individuos resecuenciados en el Capítulo 1.

También queríamos investigar cuál de las principales vías melanogénicas está sobrerrepresentada después de la incubación de HBD3. Sin embargo, observamos que genes de diferentes vías melanogénicas estaban sobreexpresados. Además de *MC1R*, los genes de las vías de señalización KIT y Wnt también se sobreexpresaron, especialmente en los melanocitos de pigmentación clara.

Por otro lado, genes relacionados con la reparación del ADN y la respuesta al estrés oxidativo también estaban sobrerrepresentados tras la incubación con HBD3 en melanocitos oscuros y claros, así como con HBD3 mutado en melanocitos claros. Curiosamente, muchos de estos genes se sabe que pueden ser regulados por la hormona estimulante de melanocitos alfa (α-MSH). Esta observación sugiere que HBD3 podría modular el daño del ADN y las respuestas de estrés oxidativo a través de MC1R, de manera similar a α-MSH.

Por lo tanto, aunque la ruta melanogénica específica no se puede dilucidar a partir de nuestros resultados, parece claro que HBD3 estimula la melanogénesis en los melanocitos humanos. Además, nuestros resultados sugieren que HBD3 podría modular otras respuestas de defensa asociadas con la señalización de MC1R, como la reparación del ADN y la respuesta al estrés oxidativo.

En el capítulo 4 exploramos el efecto de la vitamina D en los melanocitos de individuos de pigmentación clara y oscura. Nuestro objetivo principal era evaluar si la vitamina D

podía modular la pigmentación, especialmente en los melanocitos de pigmentación clara.

Como la mayoría de los efectos de la vitamina D están mediados por el receptor de vitamina D (VDR), evaluamos la implicación de VDR por Western Blot e inmunocitoquímica, confirmando que la incubación de melanocitos con vitamina D activa ($1,25(OH)_2D_3$) aumentaba los niveles proteicos de VDR. También analizamos la expresión de los genes melanogénicos *MITF* y *DCT* por PCR digital (dPCR) y observamos un aumento significativo en los niveles de ARN mensajero (ARNm) a las 12h y 24h tras incubación con $1,25(OH)_2D_3$.

Con el fin de analizar el efecto de la vitamina D activa en el transcriptoma de los melanocitos humanos, realizamos un análisis de secuenciación de ARN (RNA-Seq). Para ello, incubamos los melanocitos con $1,25(OH)_2D_3$ o el vehículo (control) y a las 18h se compararon los genes diferencialmente expresados entre las células tratadas y los controles.

Considerando juntas todas las muestras, observamos una sobreexpresión significativa (FDR <0.05) de *VDR*, confirmando la respuesta a la vitamina D. La regulación positiva de VDR también fue significativa cuando se consideraron solo los melanocitos oscuros, pero rondaba la significación para los melanocitos claros (FDR = 0.088).

Con respecto a los genes melanogénicos, observamos una sobreexpresión significativa de *MITF* en melanocitos claros, pero no en melanocitos oscuros. Otros genes relacionados con la pigmentación también aumentaron significativamente en melanocitos claros, incluidos *PRKACB, EDNRB, OSTM1* y *RAB27A*. Además, aunque los genes mencionados son los únicos significativos con FDR <0.05, en general, hubo una tendencia a una mayor expresión de genes relacionados con la pigmentación, incluidos *KIT, TYRP1* o *SLC24A5*.

También observamos en los melanocitos claros la modulación de otros genes asociados con funciones relacionadas con la pigmentación o que han sido asociados a pigmentación en ratones, como *MREG*. Estos resultados sugieren que la vitamina D tiene un efecto estimulante sobre la pigmentación en melanocitos de pigmentación clara.

Por otro lado, entre los genes diferencialmente expresados, hay varios genes que han sido relacionados con el melanoma, aunque son más abundantes en los melanocitos claros. En general, encontramos que los genes supresores de tumores como *PTEN* se sobreexpresan tras tratamiento con vitamina D, mientras que entre los genes subexpresados, hay varios relacionados con el riesgo o la progresión del melanoma o que se sobreexpresan. Estos resultados sugieren una respuesta transcripcional relacionada con la protección contra neoplasias malignas, específicamente en melanocitos de pigmentación clara.

Finalmente, con el objetivo de analizar si la selección natural ha afectado al *VD*R, resecuenciamos varias regiones del *VDR*, incluyendo todos los exones, en individuos españoles con diferentes niveles de pigmentación de la piel (reflectancia de la piel). Con fines comparativos, también obtuvimos datos del proyecto 1000 genomas (1000G) de individuos africanos y europeos.

Algunas de las regiones analizadas mostraron valores D positivos de Tajima en nuestras muestras de individuos españoles y en individuos europeos de 1000G. Los individuos ligeramente pigmentados mostraban más regiones con valores altos de la D de Tajima, en comparación con los más pigmentados. Curiosamente, en la población africana (Yoruba) de 1000G, no hubo valores positivos significativos. Estos resultados sugieren que la selección balanceadora ha afectado a *VDR* en los europeos. Debido a las muchas funciones asociadas con la vitamina D (y a su receptor), diferentes haplotipos podrían mantenerse, porque pueden suponer una ventaja relacionada con distintas funciones mediadas por VDR o pueden ser beneficiosos en diferentes etapas de la vida. Otra posibilidad relacionada con la pigmentación es que diferentes haplotipos se mantengan

debido a diferentes presiones que dependen de la irradiación solar: la necesidad de protegerse contra la irradiación solar en verano y menos pigmentado en invierno para permitir la síntesis suficiente de vitamina D.

En resumen, con este trabajo demostramos que la pigmentación de la piel puede ser modulada por moléculas que están implicadas en el sistema inmune. En particular, la β-defensina humana 103 (*DEFB103*) y la vitamina D activa, las cuales tienen la capacidad de influir en la expresión de genes melanogénicos. Además, el efecto de ambos factores parece estar relacionado con los niveles de pigmentación. El efecto de la vitamina D en los melanocitos es diferente con respecto al fenotipo pigmentario y su efecto en la pigmentación parece ser solo en melanocitos ligeramente pigmentados.

# Abstract

Skin pigmentation is one of the most diverse and interesting human phenotypic traits, because it constitutes a good example of the ability of humans to adapt to different environments. Geographical distribution of skin colour is highly correlated to the levels of Ultraviolet Radiation (UVR), showing a latitudinal gradient from dark pigmentation near the equator to light pigmentation near the poles. The most accepted hypotheses explain pigmentation as the result of different evolutionary interests. In regions of high UVR, a darker skin would be advantageous because it provides protection against the noxious effects of UVR, such as DNA damage, sunburn and folate photodegradation. On the other hand, lighter skin would be favoured in regions of low UVR, to facilitate the penetration of UV light into the skin in order to promote the synthesis of vitamin D.

However, other alternative hypotheses have also been proposed, which could also have influenced the evolution of skin pigmentation, such as the need for metabolic conservation, water conservation, sexual selection or camouflage. Among them, one interesting hypothesis is that skin pigmentation evolved to offer protection against pathogenic microorganisms and melanocytes would be part of the defence system.

In this regard, skin plays an important role as a first line of defence, acting as physical barrier and providing immunological activity through resident immune cells, with which melanocytes and keratinocytes also interact. Interestingly, melanin synthesis has been observed to increase after some microbial infections and, in a similar vein, the antimicrobial peptide β-defensin 103 has been related to pigmentation in dogs. Thus, a 3bp deletion in the second exon of the canine orthologue of β-defensin 103, which leads to a deletion of a glycine, was reported to cause black coat colour in dogs. These results suggest that pigmentation could be associated to the innate immune response.

Vitamin D is known to have immunomodulatory and anti-inflammatory activity and it is used in the treatment of some skin diseases, such as psoriasis and vitiligo. Furthermore, it is involved in the protection against UV-induced damage, through the regulation of DNA damage response and antioxidant responses. Besides, it has been reported that

vitamin D is able to modulate the expression of some antimicrobial peptides, including cathelicidins and β-defensins.

Therefore, the main objective of this work is to explore the possible relation between human skin pigmentation and the skin immune system. For that, we analyse the effect of β-defensin 103 (encoded by *DEFB103*) and active vitamin D on skin pigmentation.

In chapter 1, we analysed the sequence and copy number variation (CNV) diversity of *DEFB103*. First, we collected samples from Spanish individuals from the Basque Country and obtained a skin colour distribution, measured by reflectance spectrometry on the inner surface of the upper arm. We selected individuals from the extremes of the distribution (the most pigmented and the least pigmented individuals) and analysed the sequence variability of *DEFB103* by cloning and resequencing the exons and part of the adjacent intron sequence. We also analysed other 30 individuals from Asia, Africa, Australia and Europe.

We observed sequence diversity, detecting 30 variants, although the majority of the variants were rare, appearing only in one or a few samples. In total, 15 of the variants were not described in dbSNP (version 154). However, we did not detect any variant similar to that observed in dogs.

*DEFB103* is located within a Copy Number Variant (CNV) that can vary between 1 and 12 copies per diploid genome. We investigated if copy number (CN) was related with pigmentation. For that, we determined the copy number of *DEFB103* in individuals from the extremes of the skin reflectance distribution (from a sampling in the Basque Country; N=122) and compared the CN frequency among the groups, but we did not find significant differences between the most and least pigmented groups. Then, we wanted to study if UVR was related to CN, and we determined the CN in samples from different regions of Spain (obtained from the Spanish National DNA Bank). We obtained data for the daily annual average of incident UV-B radiation ($J/m^2$) provided by AEMET (Spanish

Agency of Meteorology) and compared the copy number distribution of *DEFB103* between selected groups based on the UV-B surface irradiation values. Comparison was made between individuals from provinces that lie in the lower 15th percentile versus those of provinces above the 85th percentile of UV-B surface irradiation. In this case, we observed statistical significant differences in the copy number distribution (Mann-Whitney U-test: $p = 0.022$), and when copy numbers were grouped in bins of <4 copies, 4 copies and > 4 copies (Chi-Square Test, $p= 0.0078$), indicating higher frequency of low copy numbers in the group of lower 15th percentile (individuals from provinces with the lower annual UV-B surface irradiation). Our data suggest a possible association between *DEFB103* copy number and surface UV-B irradiation in Spain.

In chapter 2 we explored the effect of UV on *DEFB103* expression in keratinocytes from lightly and darkly pigmented individuals. In parallel, we also incubated the keratinocytes with other immunity related stimulants in order to compare the responses. Thus, cultures were irradiated with UV-B, or incubated with Heat Killed *Staphylococcus aureus* (HKSA) and active vitamin D ($1,25(OH)_2D_3$). Expression level of *DEFB103* was measured by Digital PCR (dPCR) at different incubation times (12h, 24h, 48h).

All cell lines analysed showed a low basal expression level of *DEFB103* and there was a high variability in the response to the stimulants. The response was more particular of each cell line rather than of each group (darkly or lightly pigmented), some cell lines did not respond, and other cells lines responded at different times.

The increase in the expression of the responsive cell lines was higher with HKSA than with UV irradiation. The maximum response to HKSA was 2-3 times higher than the maximum response to UV. After UV exposure, four cell lines increased the expression (3 light cell lines and one dark cell line), but at a different times. Of note is that all the light cell lines responded to UV-B, which could suggest that the pigmentary phenotype could be relevant for the expression of *DEFB103* in response to UV. Regarding vitamin D, only two of the cell lines showed an increase in the expression in comparison with

their controls. These results suggest that UV radiation could modulate the expression of *DEFB103*, although to a limited amount, particularly in lightly pigmented keratinocytes.

We also took into account other genetic factors that could influence the expression of *DEFB103*. We analysed the copy number and genotyped a SNP located in the regulatory region of *DEFB103* (rs2737902) that has been reported to increase its expression level. However, none of the cell lines had the SNP and we did not observe any correlation with the copy number.

In chapter 3 we analysed the response of melanocytes from lightly and darkly pigmented individuals to β-defensin 103 peptide (HBD3) by means of expression microarrays at different incubation times. We wanted to determine if HBD3 affects melanogenesis in melanocytes and which pigmentation pathways are activated in humans as a consequence of HBD3 binding to MC1R. Melanocytes were incubated with either wild-type peptide (WT-HBD3) or with a peptide carrying the mutation found in dogs (MUT-HBD3).

Based on Principal Component Analysis, we hypothesized that Principal Component 1 (PC1) could explain a process of depigmentation of the cell lines along time in culture, as controls at 0h and at 24h are in opposite ends of the PC1. We hypothesised that melanocytes in culture, without any stimulant, tend to lose expression of pigmentary genes with time. We elaborated a list of pigmentation-related genes of melanocytes and tested, by means of Hypergeometric test, if the pigmentation-related gene list was overrepresented among differently expressed genes. The comparison of the group formed by controls at 0h and 12h versus the group formed by controls at 24h, showed an upregulation of the pigmentation-related genes in both light and dark melanocytes at 0h and 12h, which was in accordance with our hypothesis.

Then, to test the effect of the β-defensin 103 peptide, we compared HBD3-treated cells with the corresponding untreated controls at 12h and 24h and observed that at 24h after

incubation with HBD3, there was an increase in the expression of melanogenic genes in light and dark melanocytes in comparison with the respective controls. Pigmentation genes were overrepresented in cultures treated with HBD3. The upregulation was more significant in light melanocytes in general, indicating that the difference in the intensity of the response of melanocytes to HBD3 could be related to the pigmentary phenotype. Besides, the response was more significant with wild-type HBD3 in comparison with mutated HBD3.

Thus, if the effect of HDB3 is through MC1R, the mutation observed in dogs does not seem to increment the affinity for the receptor in humans, as it occurs in dogs. Indeed, this mutation has not been described in humans and we did not find it in the individuals resequenced in Chapter 1.

We also wanted to investigate which of the main melanogenic pathways is overrepresented after HBD3 incubation. However, we observed that genes from different melanogenic pathways were upregulated. Apart from *MC1R*, genes from KIT and Wnt signalling pathways were also overexpressed, especially in light melanocytes.

On the other hand, genes related with DNA repair and response to oxidative stress were also overrepresented after incubation with HBD3 in dark and light melanocytes and with mutated HBD3 in light melanocytes. Interestingly, many of these genes had been previously reported to be upregulated by the alpha-melanocyte-stimulating hormone (α-MSH). This observation suggests that HBD3 could modulate DNA damage and oxidative stress responses through MC1R, in a similar way than α-MSH.

Therefore, although the specific melanogenic pathway cannot be elucidated from our results, it seems clear that HBD3 stimulates melanogenesis in human melanocytes. Besides, our results suggest that HBD3 could be able to modulate other defence responses associated with MC1R signalling, such as DNA repair and oxidative stress response.

In chapter 4 we explored the effect of vitamin D on melanocytes from darkly and lightly pigmented individuals. Our principal aim was to evaluate if vitamin D was able to modulate pigmentation, especially in light melanocytes.

As most of the effects of vitamin D are mediated by vitamin D receptor (VDR), we evaluated the implication of VDR by western blot and immunocytochemistry, confirming that incubation of melanocytes with active vitamin D ($1,25(OH)_2D_3$) increased VDR protein levels. Then, we analysed the expression of the melanogenic genes *MITF* and *DCT* by Digital PCR (dPCR) and observed a significant increase in mRNA levels at 12h and 24h after incubation with $1,25(OH)_2D_3$.

In order to analyse the effect of active vitamin D on the transcriptome of human melanocytes we performed RNA Sequencing (RNA-Seq) analysis For that, we incubate melanocytes from darkly and lightly pigmented individuals with $10^{-7}$M $1,25(OH)_2D_3$ or vehicle (control), and 18h after incubation, compared the differentially expressed genes between treated cells and controls.

When all samples are considered together we observed a significant overexpression (FDR<0.05) of *VDR*, confirming the response to vitamin D. *VDR* upregulation was also significant when dark melanocytes alone were considered, but bordered genomic significance for light melanocytes alone (FDR = 0.088).

Regarding melanogenic genes, we observed a significant overexpression of *MITF* in light melanocytes, but not in dark melanocytes. Other pigmentation-related genes were also significantly upregulated in light melanocytes, including *PRKACB, EDNRB, OSTM1* and *RAB27A*. Besides, although the mentioned genes are the only ones significant at FDR<0.05, in general, there was a tendency of increased expression of pigmentation-related genes, including *KIT, TYRP1* or *SLC24A5*.

In addition, in light melanocytes, vitamin D also modulates the expression of other genes associated with pigmentation-related functions or reported to influence pigmentation in

mice, such as *MREG*. These results suggest that vitamin D has a stimulatory effect on pigmentation in lightly-pigmented melanocytes.

On the other hand, among differentially expressed genes, there are several genes that have been related with melanoma, both in dark and light melanocytes, although there are more abundant in light samples. In general, we found that tumour suppressor genes such as *PTEN* are overexpressed after vitamin D treatment, while among underexpressed genes, there are several related with melanoma risk or progression or that have been reported to be overexpressed in melanoma. These results suggest a transcriptional response related with protection against malignancy, specifically in lightly-pigmented melanocytes.

Finally, with the aim of analysing if natural selection has affected *VDR*, we resequenced several regions of *VDR*, covering all the exons in Spanish individuals with different level of skin pigmentation (skin reflectance). For comparative purposes, we also obtained data from 1000 genomes project (1000G) from African and European individuals.

Some of the regions analysed showed positive Tajima's D values in our samples of Spanish individuals and in European individuals from 1000G. There were more regions with positive values for Tajima's D in lightly pigmented Spanish individuals in comparison with most darkly pigmented individuals. Interestingly, in the African population (Yoruba) from 1000G, there were no significant positive values. These results suggest that balanced selection has affected *VDR* in Europeans. Due to the many functions associated to vitamin D (and VDR) different haplotypes could be maintained because they may suppose an advantage related with the different roles mediated by VDR or they may be beneficial in different stages of life. Another possibility related with pigmentation, is that different haplotypes are maintained due to different pressures depending on the solar irradiation: the need to be protected against solar irradiation in summer and more despigmented in winter to allow enough vitamin D synthesis.

In summary, with this work we demonstrate that skin pigmentation can be modulated by molecules that are implicated in the immune system. In particular, human β-defensin 103 (*DEFB103*) and active vitamin D, both have the ability of influence the expression of melanogenic genes. Besides, the effect of both factors seems to be related with pigmentation levels. The effect of vitamin D on melanocytes is different regarding pigmentary phenotype and seems to affect only pigmentation in lightly pigmented melanocytes.

# Introduction

## 1. Human pigmentation

Skin pigmentation is one of the most diverse and interesting human phenotypic traits, which constitudes a good example of the ability of humans to adapt to different environments.

The influence of UV radiation on skin pigmentation is undeniable. Geographical distribution of skin colour (reflectance values) is highly correlated to UVR (Chaplin, 2004). Chaplin (2004) created a map of skin colour reflectance of indigenous populations that shows a latitudinal gradient from dark pigmentation near the equator to light pigmentation near the poles, correlating with levels of UV radiation.

Highly melanised dark skin is thought to have evolved in hominins after the loss of fur that characterizes our lineage. Our naked skin possible arised as a mechanism for enhanced thermoregulation during high physical activity under the high environmental heat of the open savannahs in Africa. Presumably at the same time, the density of eccrine sweat glands increased in order to augment heat dissipation by evaporation from the surface of the skin (Jablonski and Chaplin, 2017).

There are different evolutionary hypotheses that aim at explaining the adaptive value of dark skin. Protection against skin cancer has been put forward as the adaptive driver for the development of black skin, based on the ability of melanin to protect skin cells from UV damage (Greaves, 2014). Other hypothesis highlights the protection against photodegradation of folate by UV radiation as the main selective force, due to the relevance of folate in fertility (Branda and Eaton, 1978; Jablonski and Chaplin, 2000). Another hypothesis proposes that skin pigmentation increased as a response to arid conditions. A thicker and acidified *stratum corneum* developed by greatest melanin content would enhance the skin permeability barrier function for water conservation (Elias et *al.*, 2009, 2010).

The hypothesis of protection of folate photolysis argues on its favour that folate has a direct effect on reproductive success, as folate deficiency is associated to abnormalities in the development of the embryonic neural tube and also with both male and female infertility (Jablonski and Chaplin, 2010). Thus, folate protection is argued to have an important selective value. Defendants of the "folate protection hypothesis" also argue against the "skin cancer protection hypothesis" that it is not clear whether mortality caused by skin cancer before reproductive age is high enough to affect fitness. Nevertheless, both hypothesis are related to the photoprotective effect of melanin and can be complementary. However, as humans migrated out of Africa to higher latitudes with low solar radiation, skin became less pigmented. Regarding skin depigmentation, there are also some different hypothesis. It has been proposed that dilution of epidermal pigmentation evolved as a consequence of the need for metabolic conservation (Elias et *al*., 2009, 2010; Elias and Williams, 2016). However, the most widely accepted hypothesis postulates that skin lightening was the consequence of an adaptive process to facilitate the synthesis of vitamin D (Loomis, 1967; Jablonski and Chaplin, 2000, 2010, 2017; Chaplin and Jablonski, 2009; Grant, 2016).

Since it was proposed, many lines of evidence have provided support for the vitamin D hypothesis. As stated before, skin pigmentation is strongly correlated with UVR (Chaplin, 2004), and interestingly, both are inversely correlated with the map of the potential for previtamin D3 in lightly pigmented human skin (Jablonski and Chaplin, 2000). In this sense, it has been reported that serum vitamin D levels (25OHD3) of individuals of African descent decrease with distance from the equator (Durazo-Arvizu et *al*., 2014). People with dark skin living in areas of high latitudes tend to have lower vitamin D serum concentration, because the UVB radiation is insufficient for optimal level of vitamin D production in a highly pigmented skin (Jablonski and Chaplin, 2017).

Furthermore, there is evidence that positive selection has acted favouring vitamin D synthesis under low UVB radiation (Norton et *al*., 2007; Wilde et *al*., 2014). Interestingly,

depigmentation seems to have evolved independently in Europeans and East Asians (Norton et *al*., 2007).

Finally, the relevance of vitamin D for overall health has been extensively demonstrated, supporting the idea that vitamin D deficiency has been a strong enough pressure to shape evolution (Yuen and Jablonski, 2010; Holick, 2017). Thus, vitamin D deficiency is important since early live, not only for being the most common cause of rickets, but also because it has been associated with problems during pregnancy and delivery, such as low birth weight, pre-eclampsia and neonatal mortality (Grant, 2016; Holick, 2017; Pilz et *al*., 2018), reproduction and fertility of both men and women (Lerchbaum and Obermayer-Pietsch, 2012; De Angelis et *al*., 2017; Voulgaris et *al*., 2017; Pilz et *al*., 2018; Arab et *al*., 2019), or more generally, with overall mortality rates (Grant, 2016; Heath et *al*., 2019).

## 2. Melanogenesis

Melanin is a pigmentary biopolymer synthetized in melanocytes, within specialized organelles called melanosomes. These melanin-packed melanosomes are transferred to keratinocytes, where they are laid out in an umbrella-shape around the nucleus in order to protect them from ultraviolet (UV) radiation. There are two main types of melanin: eumelanin, brown-black melanin, which is an insoluble polymer; and pheomelanin, yellow-reddish soluble polymer. The differences in skin pigmentation among humans are related with melanin-type, among other things, such as the number and size of the melanosomes and its distribution. The density of melanocytes in the skin varies according to the region of the skin under consideration, but per region, it is relatively constant among individuals of different pigmentary phenotype. However, it is the number and size of the melanosomes, its distribution and the type and amount of melanin

synthetized is variable; and together with the efficiency of melanocytes to transfer the melanosomes to the keratinocytes, which determines the basal pigmentation level in the skin. The melanosomes of dark-skinned individuals are larger, individualized, more numerous and contain a higher amount of eumelanin. On the contrary, light-skinned individuals have less melanosomes, which form aggregates and contain a higher amount of pheomelanin. These differences in melanosomes are present already at birth.

Interestingly, pigmentation levels can also be modulated by external stimuli, being the UV irradiation the most important one. Thus, pigmentation level is regulated by inducing/blocking melanin synthesis or switching between eumlenin/pheomelanin syntheses.

Among all of the cellular processes involved in pigmentation, we will focus now on melanogenesis. Melanogenesis is the process by which melanin is synthetized in melanosomes. The key enzyme in melanogenesis is tyrosinase (encoded by *TYR* gene), which catalyses the first steps in the synthesis of melanin, and which involves the hydroxylation of the amino acid tyrosine to L-3,4-dihydroxyphenilalanine (DOPA) and subsequent oxidation to DOPAquinone. The type of melanin produced will now depend on the function of the rest of melanogenic enzymes and the availability of substrates. In the presence of cysteine, DOPAquinone is reduced to cysteinylDOPA and then is oxidized to cysteinylDOPAquinona, to give benzothiazine intermediates, which gradually polymerize to form pheomelanin pigment. In the absence of cysteine, DOPAquinone is oxidated and converted to DOPAchrome. Then, DOPAchrome produces 5,6-dihydroxyindole (DHI) and 5,6-dihydroxyindole-2-carboxylic acid (DHICA). Finally, DHI and DHICA are oxidized and polymerizated to produce the eumelanin polymer (Ito, 2003; Slominski et *al*., 2004).

In the process of eumelanin synthesis the most important melanogenic enzymes involved are tyrosinase (TYR), tyrosinase-related protein 1 (TYRP1) and tyrosinase-related protein 2 (TYRP2), also known dopachrome tautomerase (DCT). TYRP2/DCT

catalizes the tautomerization of DOPAchrome to produce DHICA (Palumbo et *al*., 1991). TYRP1 is involved in the oxidation of DHICA and TYR, apart from mediating the first step, hydroxilation of tyrosine also oxidizes DHI (Ito, 2003). Premelanosome protein (PMEL/SILV) is also important, as it is involved in the polymerization of DHICA to form eumelanin (Figure 1).

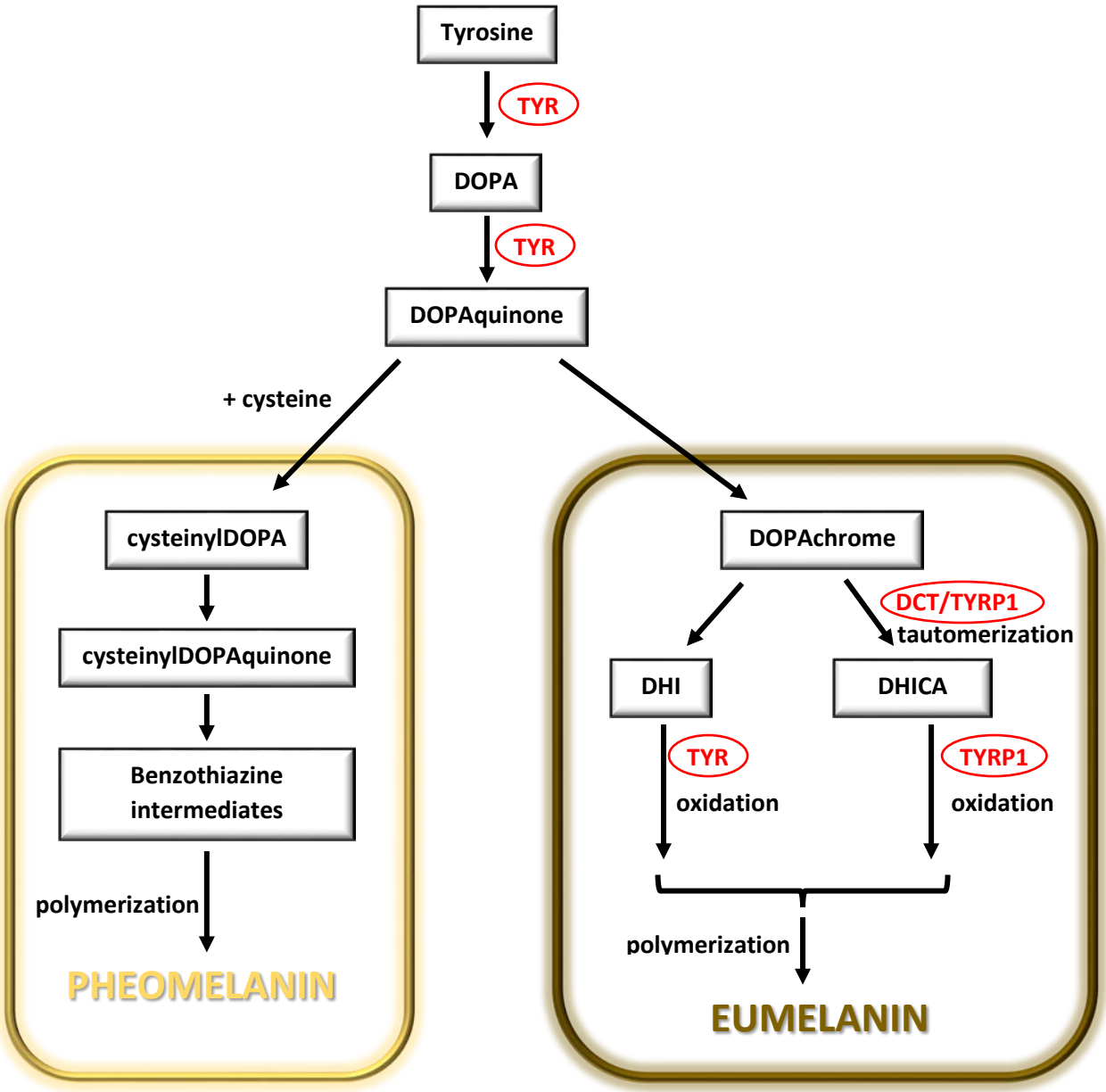


**Figure 1. Schematic overview of eumelanin and pheomelanin synthesis and the involvement of melanogenic enzymes.**

Apart from tyrosinase and tyrosinase-related proteins, there are other proteins in the melanosome that are important for the regulation of melanin synthesis and for maintaining melanosome homeostasis. Most of these proteins are located in the melanosomal membrane. For instance, the activation of tyrosinase requires the active uptake of tyrosine, which is mediated by OCA2. Melanosomal pH is also important in the regulation of skin pigmentation. In fact, tyrosinase activity is modulated by pH: melanosomes with a neutral pH have a higher tyrosinase activity (Fuller, Spaulding and Smith, 2001). Thus, it has been shown that melanosomes derived from dark-pigmented melanocytes have a more neutral pH, while melanosomes derived from light-pigmented melanocytes are more acidic. Several channels, pumps and transporters are implicated in the regulation of pH, coupling the transport of $H^+$, $Na^+$, $K^+$ and $Ca^{2+}$. Among them, the most relevant are SLC45A2/MATP, SLC24A5, ATP7A, V-ATPase and TPCN2. Solute carrier family 24 member 5 (SLC24A5) and solute carrier family 45 member 2 (SLC45A2/MATP) are sodium/calcium exchanger pumps that are located in the membrane of melanosomes (Bin et *al*., 2015). ATP7A is a copper transporting ATPase, which translocates copper from the cytosol to the melanosomes (Setty et *al*., 2008). Copper is necessary for the activity of tyrosinase (Petris, Strausak and Mercer, 2000). The vacuolar ATPase (V-ATPase) is an $H^+$ pump that has been reported to be upreglated by the alpha-melanocyte-stimulating hormone (α-MSH) (Cheli et *al*., 2009). The two pore segment channel 2 (TPCN2) is a sodium selective cannel and has been reported to control melanosome's membrane voltaje, which could modulate V-ATPase activity and thus melanosomal pH (Bellono, Escobar and Oancea, 2016).

## 2.1. Melanogenic pathways:

Melanogenesis is a complex process in which several proteins and efectors are directly or indirectly involved. α-MSH/MC1R pathway is the canonical and most studied melanogenic pathway. However, pathways known by being implicated in other cellular processes, such as as Wnt/β-catenin pathway, have also been reported to take part in melanogenesis. Below are explained the most important pathways related with melanin synthesis and a simplified squeme of all these pathways is shown in figure 4.

### 2.1.1. α-MSH/MC1R pathway

The canonical melanogenic pathway is initiated by the binding of the melanocortins, especially the alpha-melanocyte-stimulating hormone (α-MSH) to the melanocortin 1 receptor (MC1R). Melanocortins are peptide hormones derived from proopiomelanocortin (POMC), and include the adrenocorticotropic hormone (ACTH) and α-MSH (Figure 2). They are mainly expressed in the pituitary. However, different skin cells, including keratinocytes and melanocytes are also able to express and secrete melanocortins. Thus, α-MSH acts as a paracrine (also autocrine) factor secreted by keratinocytes, which is able to initiate melanogenesis in melanocytes.

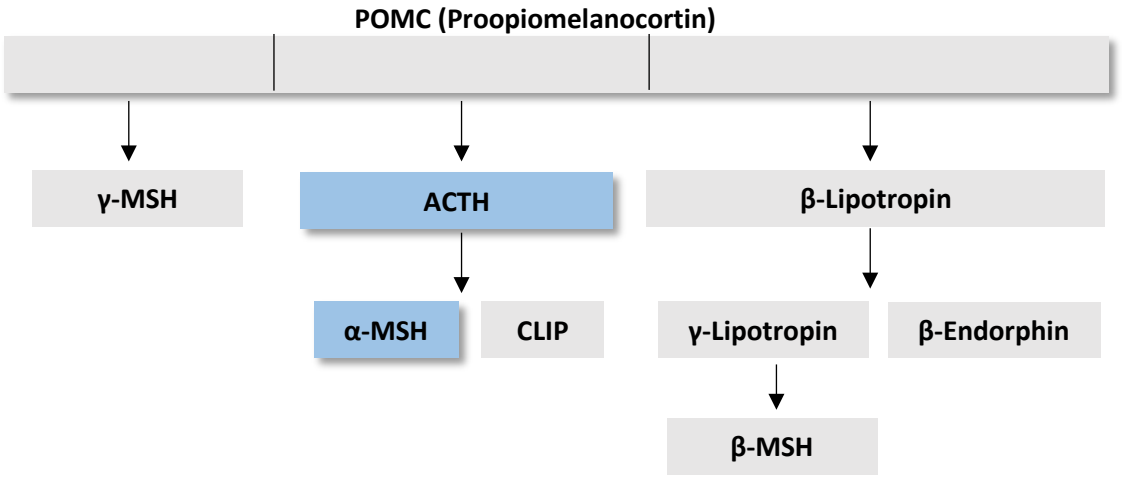


**Figure 2. Scheme of the formation of ACTH and α-MSH from POMC.**

The binding of α-MSH to MC1R, which is a membrane G-protein-coupled receptor, promotes the activation of adenyl cyclase (AC), which leads to a subsequent increase in cyclic adenosine monophosphate (cAMP) levels. The increase in cAMP levels leads to protein kinase A (PKA) activation, which translocates to the nucleous and phosphorylates and activates the cAMP responsive element binding proteins (CREB) and CREB binding protein (CBP) (Hagiwara et *al*., 1993). CREB upregulates the expression of microphthalmia transcription factor (*MITF*), a master regulator of melanogenesis, which after binding to response elements upregulates the expression of *TYR*, *TYRP1* and *TYRP2/DCT* (Abdel-Malek et *al*., 1995; Busca and Balloti, 2000) (Figure 3).

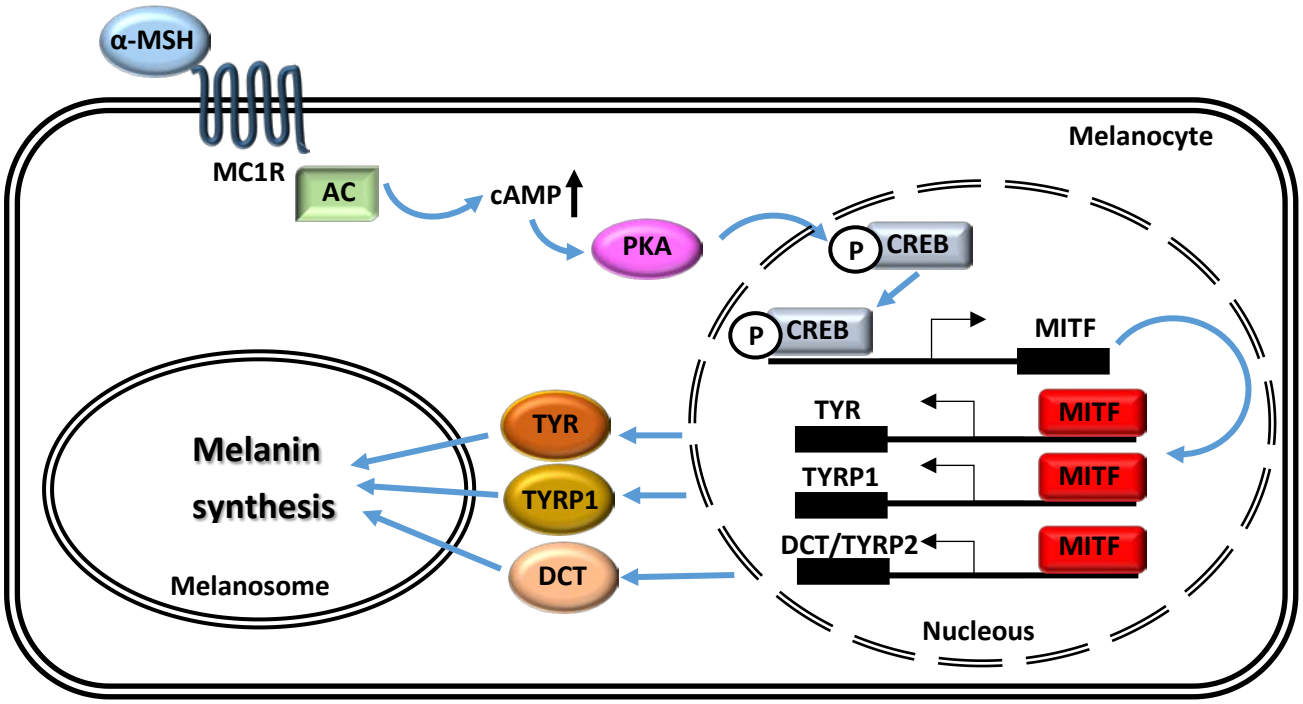


**Figure 3**. **Squeme of the canonic α-MSH/MC1R melanogenic pathway**. MC1R: the melanocortin 1 receptor, AC: adenyl cyclase, cAMP: cyclic adenosine monophosphate, PKA: protein kinase A, CREB: cAMP responsive element binding protein, MITF: microphthalmia transcription factor, TYR: tyrosinase, TYRP1: tyrosinase-related protein 1, DCT/TYRP2: dopachrome tautomerase/tyrosinase-related protein 2.

Activation of MC1R can also result in the activation of mitogen-activated protein kinase (MAPK) pathway. In humans, α-MSH binding to MC1R can lead to the transactivation of the stem cell factor receptor (KIT), a tyrosine kinase receptor (Herraiz et *al*., 2011). Transactivation of KIT results in the activation of MAPK pathway, leading to the activation of the Ser/Thr kinases ERK1 and ERK2 (Busca and Balloti, 2000), which in turn, phosphorylate MITF, activating it (Levy, Khaled and Fisher, 2006).

Prolonged exposure to agonists leads to desensitization of MC1R, i.e. the loss of responsiveness of MC1R to its ligand α-MSH (Sánchez-Más et *al*., 2005). In general, the desensitization of G-protein coupled receptors (GPCRs) is mediated by G-protein coupled receptor kinases (GRKs). GRKs specifically recognise and phosphorylate agonist-occupied GPCRs, which produces the inhibition or downstream signalling. Phosphorylation of GPCRs induces the recruitment of the cytosolic proteins β-arrestins, which uncouple the receptor from G proteins and bring it to clathrin-coated pits to initiate endocytosis (Luttrell and Lefkowitz, 2002; Wolfe and Trejo, 2007). In the case of MC1R, internalization is mediated principally by β-arrestin 2 (ARRB2) (Abrisqueta et *al*., 2013). Once internalized, the receptor can be degraded or recycled and brought to the membrane again. By the recycling mechanism, the cell can increase the number of receptors available in the membrane.

On the other hand, the agouti-signaling protein (ASIP) is an antagonist of MC1R. ASIP is a small protein that competes with α-MSH for MC1R binding. When ASIP binds to MC1R, it decreases constitutive signaling to the cAMP pathway, inhibiting the production of eumelanin, and pheomelanin is synthetized instead (Suzuki et *al*., 1997). Apart from competing with α-MSH for MC1R, ASIP is thought to promote pheomelanogenesis by a cAMP-independent pathway, for which other proteins such as mahogunin and attractin are also required (Hida et *al*., 2009).

### 2.1.2. SCF/KIT Pathway

The SCF/KIT Pathway is involved in the homeostasis, development and survival of melanocytes (Grichnik et *al*., 1998; Yoshida et *al*., 2001), and as such, it has also been shown to be an important pathway in melanogenesis, particularly in UV-B induced pigmentation (Hachiya et *al*., 2001) and pathological hyperpigmentation (Hattori et *al*., 2004). It has been demonstrated that keratinocytes and fibroblasts secrete stem cell factor (SCF) (Yamaguchi and Hearing, 2009; Wang et *al*., 2017a). Then, SCF (also known as KITLG or c-KIT ligand) binds KIT, a receptor tyrosine kinase (Zsebo et *al*., 1990), in melanocytes, promoting melanogenesis in a paracrine way. The secretion of SCF increases after UV irradiation (Baba, Uchiwa and Watanabe, 2005).

The binding of KITLG to KIT triggers the dimerization of the receptor KIT and the activation of its catalytic tyrosine kinase function (Lev, Yarden and Givol, 1992). The activated KIT phosphorylates and associates with SHC proteins (Src homology domain), GRB2 (growth factor receptor-bound protein 2) and the guanine nucleotide exchange factor SOS, leading to the phosphorylation of RAS. Then, RAS activates RAF1, which in its turncactivates the mitogen-activated protein kinase (MAPK) signalling pathway. Extracellular signal-regulated kinases (ERKs) 1 and 2 are then activated, which regulate the activities of several transcription factors, including MITF. MITF activation leads, as mentioned above, to the transcription of melanogenic enzymes TYR, TYRP1 and TYRP2/DCT.

SCF/KIT pathway induces a short-lived MITF activation, as MAPK signalling leads to two simultaneous phosphorylations, one that activates MITF and another one that targets MITF for its degradation by ubiquitin conjugating enzyme (Wu et *al*., 2000; Busca and Ballotti, 2000).

### 2.1.3. Endothelin pathway

Endothelin 1 (EDN1), a 21 amino acid peptide, was first identified in vascular endothelial cells, and was described as an endothelium-derived peptide with a potent vasoconstrictor activity (Yanagisawa et *al*., 1988). Later on, it was demonstrated that EDN1 is also expressed in the skin, being produced and secreted by keratinocytes (Imokawa, Yada and Miyagishi, 1992; Yohn et *al*., 1993). Subsequently, endothelins were reported to participate in the induction of proliferation of melanoblasts during melanocyte development and to be also stimulators of proliferation and dendrogenesis of adult melanocytes (Yada, Higuchi and Imokawa, 1991; Imokawa, Yada and Miyagishi, 1992; Hara, Yaar and Gilchrest, 1995). Endothelins, especially EDN1 seem also to be involved in human melanogenesis. For instance, the production of EDN1 by keratinocytes is increased after irradiation with ultraviolet B (Imokawa, Yada and Miyagishi, 1992). Similarly, Imokawa, Miyagishi and Yada (1995) reported that EDN1 is an important mediator for UVB-induced pigmentation in the epidermis *in vivo*, because they observed that the addition of EDN1 to cultured human melanocytes increased the expression levels of *TYR* and *TYRP1*.

Endothelins elicit their biologic effects by binding to G-protein coupled endothelin-B receptor (EDNRB) (Tada et *al*., 1998). The binding of EDN1 to EDNRB activates phospholipase Cγ (PLCγ) which increases the hydrolysis of the membrane phospholipid phosphatidylinositol 4,5-bisphosphate (PIP2), generating inositol-triphosphate (IP3) and diacylglycerol (DAG). IP3 increases the intracellular concentration of $Ca^{2+}$, and DAG induces the activation of protein kinase C (PKC) (Yada, Higuchi and Imokawa, 1991; Imokawa, Yada and Kimura, 1996; Swope and Abdel-Malek, 2016). Then, activated PKC phosphorylates RAF1, activating it. Activated RAF1 induces the MAPK phosphoylation cascade, which in its turn activates ERK1/2, leading to the phosporilation of the transcription factor CREB and inducing thereby the transcription of *MITF* (Imokawa, Kobayasi and Miyagishu, 2000; Imokawa and Ishida, 2014). Simultaneously, the

activation of PKC also promotes an increase in cAMP levels, leading to PKA activation, which in turn, induces the phosphorylation of CREB (Imokawa, Yada and Kimura, 1996), with the consequent induction of *MITF* expression.

EDN1 has also been shown to increase the expression of *MC1R* and the binding activity for α-MSH (Funasaka et *al*., 1998; Tada et *al*., 1998). This upregulation of *MC1R* expression by EDN1 takes place regardless of the melanin content of the cultured human melanocytes (Scott, Suzuki and Abdel-Malek, 2002).

Although the EDN1 is the most studied endothelin in relation to melanogenesis, the pigmentary effects of endothelins may not be restricted to EDN1. Some studies suggest that EDN3 has also the ability to induce melanin synthesis at least in a murine model (García et *al*., 2007; Li et *al*., 2017).

EDN1 has also be shown to be involved the maintenance of melanocyte homeostasis (Hyter et *al*., 2013; Swope and Abdel-Malek, 2016), which is the maintenance of a steady state in physical and chemical conditions. Kadekaro et *al*. (2005) observed that the activation of ENDBR by EDN1 reduced the generation of reactive oxygen species and enhanced the repair of cyclobutane pyrimidine dimers. Besides, Hyter et *al*. (2013) demonstrated that EDN1 is a target for p53 and that EDN1 controls melanocyte proliferation, migration, DNA damage protection, and apoptosis after UVB irradiation.

### 2.1.4. Wnt/β-catenin pathway

The Wnt/β-catenin pathway is involved in melanocyte development, as it is implicated in neural crest formation, and migration, proliferation, and differentiation of melanocytes (Wu, Saint-Jeannet and Klein, 2003). In this sense, Wnt/β-catenin signalling has been reported to also participate in melanogenesis.

WNTs are a family of cysteine-rich lipoglycoproteins that bind to Class Frizzled receptors (FZD) (Schulte, 2010). In the absence of WNT ligands, β-catenin is phosphorylated and marked for its degradation in proteasomes: Glycogen synthase kinase 3 β (GSK3β), in a complex with other proteins phosphorylates β-catenin leading to its ubiquitination (Liu et *al*., 2002) and thus maintaining the β-catenin levels low. But the binding of WNTs to FZD receptors causes β-catenin to be stabilized: Dishevelled protein (DVL) phosphorylates GSK3β, blocking its activity and avoiding the phosphorylation of β-catenin, and consequently, β-catenin accumulation occurs (Miller et *al*., 1999; Seidensticker et *al*., 2000). Then, β-catenin associates with lymphoid enhancer-binding factor 1 (LEF1) and together regulate the expression of target genes (Behrens et *al*., 1996; Huber et *al*., 1996).

The possible implication of Wnt/β-catenin pathway on melanogenesis was suggested several years ago. Takeda et *al*. (2000) first demonstrated that Wnt-3a upregulated the expression of *MITF* in mice. Later on, Guo et *al*. (2012) also reported an upregulation of *MITF* expression by Wnt-3a, together with its downstream target genes *TYR* and *TYRP1*. Also, GSK3β inhibition was proven to stimulate melanogenesis in murine melanoma cells and human melanocytes (Bellei et *al*., 2008). The mechanism consists on the formation of a complex between β-catenin and LEF1, which activates *MITF* expression (Takeda et *al*., 2000). Interestingly, MITF also associates with LEF1 to activate its own promoter (Saito et *al*., 2002) and to upregulate other MITF target genes, such as *DCT* (Yasumoto et *al*., 2002). Besides, Schepsky et *al*. (2006) demonstrated that β-catenin can also interact directly with MITF and that MITF/ β-catenin complex is able to upregulate *TYR* and *TYRP1* expression.

On the other hand, Dickkopf 1 (DKK1), an inhibitor of the Wnt/β-catenin pathway, supresses β-catenin accumulation and consequently *MITF* expression (Yamaguchi et *al*., 2004, Yamaguchi et *al*., 2008). DKK1 not only inhibits melanogenesis, but also

decreases the uptake of melanosomes by keratinocytes by the suppression of proteinase-activated receptor-2 (PAR-2) (Yamaguchi et *al*., 2008).

Finally, a crosstalk between the α-MSH/MC1R pathway and the Wnt/β-catenin pathway has also been suggested. PKA seems to phosphorylate both β-catenin at Ser675, preventing thus its ubiquitination (Hino et *al*., 2005) and GSK3β at Ser9, which leads to its inactivation (Suzuki et *al*. 2008). α-MSH induced stabilization of β-catenin protein was confirmed to be mediated by PKA phosphorylations in murine melanoma cells and human melanocytes (Bellei et *al*., 2011).

### 2.1.5. UV/PKCβ pathway

Several authors have reported that the PKCβ pathway is also involved in melanogenesis (Gordon and Gilchrest, 1989; Park et *al*., 1999). PKCs are serine/threonine protein kinases that are classified into three clases according to the needs for its activation: classical PKCs (cPKCs), which are activated by calcium and diacylglycerol and include PKCα, PKCβ, PKCγ; novel PKCs (nPKCs), which are activated by diacylglycerol but not calcium, and include PKCδ, PKCθ, PKCε, PKCη; and atypical PKCs (aPKCs), which are not activated by either calcium or diacylglycerol, and include PKCι and PKCζ

In this context, PKCβ isoform is normally inactive in the cytoplasm, until it is activated by DAG and/or calcium (Nishizuka, 1986; Gordon and Gilchrest, 1989; Denning, 2012). Then, the receptor for activated C-kinase 1 (RACK1), which is specific for activated PKCβ, binds to PKCβ and the PKCβ/RACK1 complex is translocated to the melanosome membrane (Mochly-Rosen, 1995; Park et *al*., 2004), where PKCβ activates tyrosinase by phosphorylations on serine residues at amino acid positions 505 and 509, on the cytoplasmic domain of tyrosinase (Park et *al*., 1999).

DAG is normally formed by the hydrolysis of phosphatidylinositol 4,5-bisphosphate (PIP2) by phospholipase C (PLC), a reaction in which inositol trisphosphate (PI3) is also generated (Nishizuka, 1986). It is normally cell membrane lipids which are cleaved into DAG and PI3, when some ligands bind their specific cell surface receptors, such as the above mentioned binding of EDN1 to endothelin B receptor (Park et *al*., 2009).

Interestingly, UV irradiation can also release DAG from cell membrane lipids (Friedmann, Wren and Matthews, 1990; Punnonen and Yuspa, 1992; Carsberg, Ohanian and Friedmann, 1995). As mentioned above DAG can activate PKCβ, and in this sense, several studies have confirmed the involvement of DAG and PKCβ in melanin synthesis. Gordon and Gilchrest (1989) demonstarted that the adittion of DAG increased the melanin content in cultured human melanocytes and that PKC was required. Friedmann Friedmann, Wren and Matthews (1990) showed that UV irradiation was implicated in the increase of melanogenesis by DAG. Furthermore, the ability of PKCβ to activate tyrosinase has been broadly demonstrated (Park et *al*., 1993; Park et *al*., 1999; Wu and Park, 2003; Park et *al*., 2004):, whereas incubation with PKCβ inhibitors, showed a decrease in melanin content and tyrosinase activity (Gordon and Gilchrest, 1989; Liu et *al*., 2015), and, on the contrary, incubation with PKCβ activators showed an increase in melanogenesis (Liu et *al*., 2015).

Finally, a crosstalk with the α-MSH pathway has also been proposed. Park et *al*. (1996) observed that incubation of melanocytes with α-MSH produced an increase in PKCβ levels in mouse melanoma cells, and that the inhibition of PKCβ blocked α-MSH induced melanogenesis. Interestingly, Park et *al*. (2006) then observed that the increase in the expression of PKCβ after α-MSH treatment is mediated by MITF. However, Herraiz et *al*. (2011) did not find evidence of PKC activation after incubation with the synthetic α-MSH analog NDP-MSH.

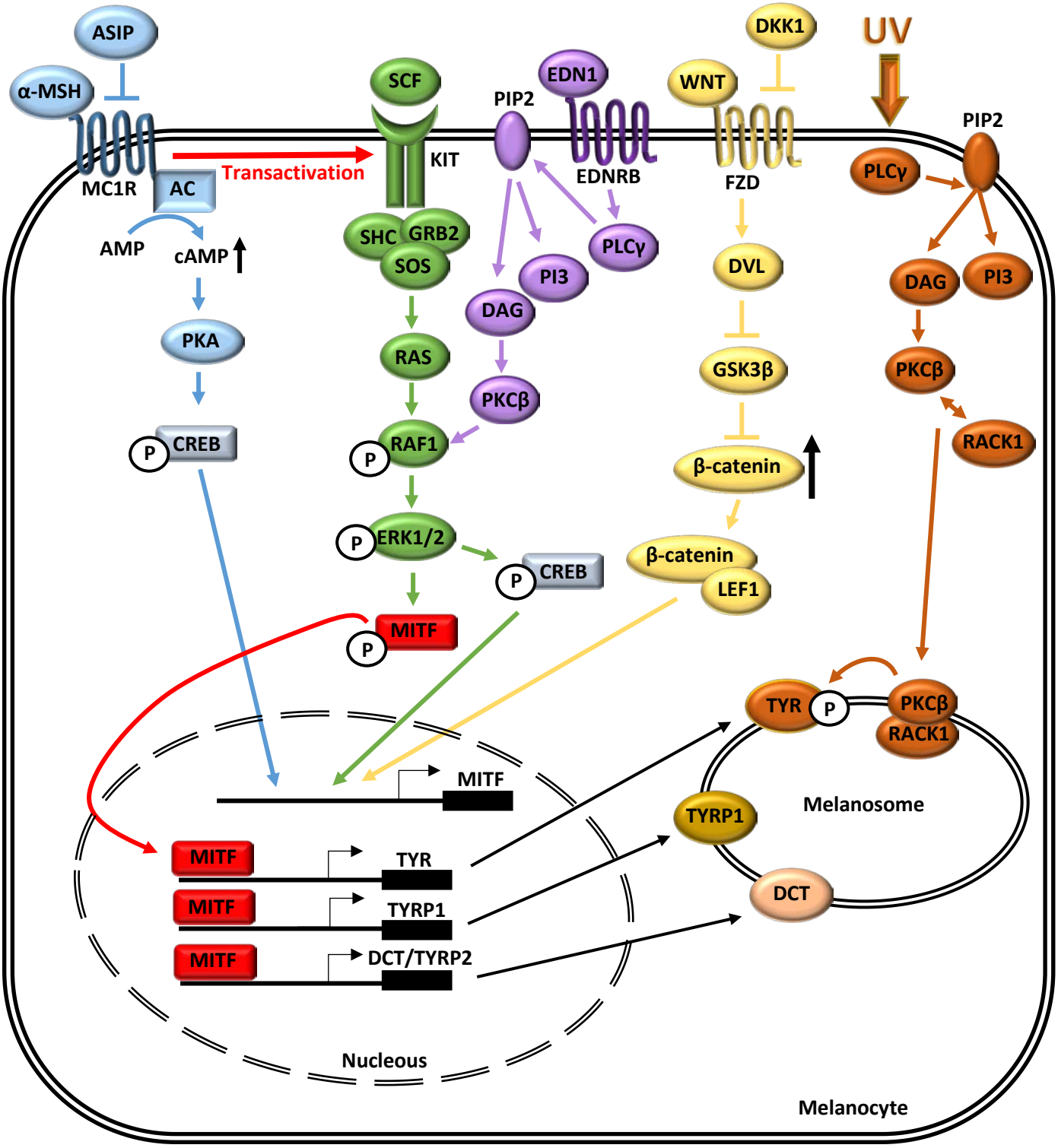


**Figure 4. Schematic overview of the melanogenic pathways.**

## 2.2. Skin immunity and pigmentation

The skin is a physical barrier between external and internal environments, which offers protection from external insults such as toxins, stress caused by injury, microbial pathogens and the harmful effects of UV irradiation. Therefore, skin acts a first line of defence.

Apart from the barrier function, skin has also immunological activity that is vital for maintaining skin homeostasis and overall protection. Skin contains different types of immune cells, distributed along the epidermis, the outermost layer of the skin, the deeper layer immediately below the epidermis (the dermis), and the subcutaneous fatty region underlying the dermis. Main resident immune cells of the epidermis are Langerhans dendritic cells, and T cells, especially CD8+ lymphocytes. On the dermis, there are several types of immune cells, including dermal dendritic cells, CD4+ lymphocytes, macrophages, mast cells, eosinophils and natural killer cells T cells (Nguyen and Soulika, 2019).

Furthermore, skin cells such as keratinocytes, melanocytes and fibroblasts interact with immune cells. These cells express pattern recognition receptors (PRRs), which recognize highly conserved pathogen-associated molecular patterns (PAMPs) (Nguyen and Soulika, 2019). These receptors have been reported to also recognize endogenous molecules derived from damaged cells, named damage‐associated molecular patterns (DAMPs) (Bianchi, 2007). The activation of PRRs leads to the production of cytokines and chemokines that can act on immune cells (Nguyen and Soulika, 2019). Besides, keratinocytes are also able to secrete antimicrobial peptides (AMPs) to protect against microbial infections, such as cathelicidins or defensins (see below) (Braff et *al*., 2005).

There is evidence that suggests a relation between human pigmentation and skin immune system. In fact, melanin also forms part of the skin barrier and protects from the noxious effects of UV radiation. There are reports that suggest that individuals with light skin are more prone to some skin infections than darkly pigmented individuals (Mackintosh, 2001), suggesting a protective function for pigmentation. Gunathilake et *al*. (2009) observed that individuals with darker skin showed enhanced epidermal function and possessed more acidic melanocytes. They proposed that in darkly pigmented skin, melanosome transfer to keratinocytes might acidify the *stratum corneum*, the outermost layer of the epidermis, resulting in enhanced skin barrier function. An acidic *stratum corneum* could also enhance antimicrobial function (Fluhr and Elias, 2002; Ali and Yosipovitch, 2013; Proksch, 2018).

Besides, pigmentation is disrupted in skin autoimmune diseases, such as vitiligo and psoriasis (Wang et *al*., 2013a; Picardo et *al*., 2015), and inflammation conditions often cause pigmentary alterations, such as post-inflammatory hyperpigmentation (Ortonne and Bissett, 2008). Immune cells are known to secrete cytokines, which can modulate melanogenesis in melanocytes (Yuan and Jin, 2018). Thus, there is a complex interaction between immune cells and the epidermal melanin unit.

Furthermore, melanin synthesis has been observed to increase after some microbial infections, including bacteria (Ahn, Jin and Kang, 2008) and yeast (Tapia et *al*., 2014). The mechanism of infection-induced melanogenesis has been reported to be mediated by the activation of Toll-like receptors (TLRs), a type of PRRs, which are important in pathogen recognition (Akira, Uematsu and Takeuchi, 2006). In fact, melanocytes express different types of TLRs and it has been demonstrated that the activation of some of them promote melanogenesis and melanosome transport (Koike et *al*., 2018). The observed interplay between TLRs and melanogenesis suggest a link between immune system and pigmentation. In this regard, Tam, Dzierżęga-Lęcznar and Stępień (2019)

observed the induction of melanogenesis by LPS-activated Toll-like receptor 4 (TLR4) and also reported differences in the expression of inflammatory cytokines and chemokines between melanocytes from lightly and darkly pigmented skin, suggesting that the pigmentary phenotype could influence the immune activity of melanocytes. Besides, Song et *al*. (2018) also observed that repeated UV irradiation induces the expression of *TLR4* and suggested that melanocytes could take part in the modulation of the immune system induced by UV radiation.

## 3. β-defensins and pigmentation

A likely relationship between β-defensins and pigmentation was first proposed by Candille et al. (2007), when they observed that a mutation in dog's K locus, which encodes a β-defensin, caused black coat colour in domestic dogs.

Defensins are small cationic antimicrobial peptides (AMPs) that play essential roles in the innate and adtive immune system (Fruitwala, El-Naccache and Chang, 2019). They are present in most multicellular organism and conserve a higly conserve structure consisting on a motive of six cysteine residues, stabilized by disulphure bonds. Based on the order of disulfide bonds, there are three classes of defensins in primates: α, β and θ (Yang et *al*., 2002). In humans, the genes that encode for θ-defensins are only present as pseudogenes, due to an early STOP-codon (Pazgier et *al*., 2006). The disulphide linkages of cysteine residues in α-defensins are between the first and the sixth cysteine residues Cys1-Cys6, Cys2-Cys4, and Cys3- Cys5, whereas in β-defensins, the linkage are Cys1-Cys5, Cys2-Cys4, Cys3-Cys6 (Pazgier et *al*., 2006).

β-defensins are of special relevance in skin defence. They have a broad spectrum of antimicrobial activity, acting against both Gram positive and negative bacteria, fungi and viruses (Pazgier et *al*., 2006; Chessa et *al*., 2020). β-defensins also contribute to skin's first line defence taking part in functions that improve skin physiological barrier and

enhance wound healing (Sørensen et *al*., 2003; . Niyonsaba et *al*., 2007; Hirsch et *al*., 2009; Kiatsurayanon et *al*., 2014).

Apart from their activity in innate immune system, β-defensins can act as chemiotactic agents, modulating the immune system, acting as a link between innate and adaptive immune systems (Froy, 2005; Pazgier et *al*., 2006; Fruitwala, El-Naccache and Chang, 2019). In this sense, it has been observed that they can contribute to the regulation of adaptive immune system, by means of signalling to cytokines' receptors of dendritic cells and T cells (Yang et *al.*, 1999; Yang et *al.*, 2002 Wu et *al*., 2003; Niyonsaba, Ogawa and Nagaoka, 2004). In fact, β-defensins have been reported to induce the expression of pro-inflammatory cytokines and chemokines in keratinocytes (Niyonsaba et al., 2007; van Kilsdonk et *al*., 2017). However, β-defensins have also been reported to attenuate pro-inflammatory response (Semple et *al*. 2010; Semple and Dorin, 2012).

The discovery of Candille et *al*. (2007) expanded β-defensins functions, linking immune system with pigmentation. They observed that a mutation in the dog's K locus, which encodes a β-defensin, caused black coat colour in domestic dogs; they also confirmed the influence of the mutation in transgenic mice. Later, the same mutation was found to cause melanism in in wolves and coyotes (Anderson et *al*., 2009).

The K locus, which is highly expressed in canine skin, encodes the canine β-defensin 103 (CBD103) peptide, the orthologue of human β-defensin 103 (*DEFB103*) peptide (HBD3). The K locus has three alleles, with a simple dominance order: black ($K^B$) > brindle ($k^{br}$) > yellow ($k^y$) (Kerns et *al*., 2007). The $K^B$ allele or *Dominant black* is defined by a 3 base pair deletion in the second exon that predicts an in-frame glycine deletion (ΔG23) and is the cause of the black coat colour in several dog breeds (Candille et *al*., 2007). Dogs with the wild-type alleles of Mc1r, Agouti and K locus have yellow coat, as a consequence of the repression of Mc1r activity by the binding of Agouti protein.

However, in dogs carrying the $K^B$ allele, CDB103 binds Mc1r with high affinity, displacing Agouti and leading to the development of black coat.

Interestingly, human β-defensin 103 (HBD3) has been also reported to bind MC1R (Candille et *al*., 2007; Beaumont et *al*., 2012; Swope et *al*., 2012; Nix et *al*., 2013, 2015), although with discordant results regarding the influence on MC1R signalling. Some authors reported that HBD3 is not able to increase cAMP levels in mouse and human melanocytes (Candille et *al*., 2007; Swope et *al*., 2012; Nix et *al*., 2013). However, Beaumont et *al*. (2012) observed a weak induction of cAMP signalling in human embryonic kidney cells (HEK293), transfected with MC1R. In addition, Ericson et *al*. (2018) reported the ability of HBD3 to increase cAMP at micromolar concentrations. However, HBD3 downregulates cAMP accumulation induced by α-MSH or NDP-MSH (a synthetic analogue of α-MSH) (Beaumont et *al*., 2012; Swope et *al*., 2012).

Based on its influence on MC1R-cAMP signalling, HBD3 has been considered as a MC1R antagonist (Swope et *al*., 2012) or a partial agonist (Beaumont et *al*., 2012). However, others have proposed that its role depends on the presence of other MC1R ligands, as it is able to block the action of α-MSH and ASIP, and therefore, it would be better considered as a neutral ligand (Nix et *al*., 2013).

Nevertheless, HBD3 signaling through MC1R could differ from other melanocortin ligands and it may lead to cAMP-independent signalling pathways. In fact, Beaumont et *al*. (2012) in their HEK293 model also observed the induction of MAPK signalling. Incubation with HBD3 increased ERK phosphorylation similar to NDP-MSH, but levels were maintained longer in time. They also observed an increase on p38 phosphorylation, suggesting that ERK phosphorylation was mediated by p38. Interestingly, ERK activation was similar in cells transfected with wild-type MC1R and with MC1R carrying some variants associated with RHC phenotype (red hair, fair skin and increased skin cancer risk), including V92M, R142H, R160W and D294H, but not R151C and D84E.

Although HBD3 is now considered as a third MC1R ligand, the way of binding differs from α-MSH and ASIP. It seem that HBD3 binding to MC1R does not need specific amino acid contact, instead, the interaction is based on electrostatic complementarity between the positively charged residues of HBD3 and the negatively charged regions on the surface of MC1R. This binding mode based on electrostatics confers higher affinity to HBD3 (Nix et *al*., 2013, 2015).

On the other hand, it has been proposed that UV radiation is able to upregulate *DEFB103* expression in human keratinocytes (Kim, Hong and Seo, 2003; Gläser et *al*., 2009) suggesting a role of *DEFB103* in UV response. Although Wolf Horrell and D'Orazio (2014) concluded that UV does not increase *DEFB103* expression in *ex vivo* neonatal skin explants. Further research would help understanding the influence of UV in *DEFB103* expression.

## 3.1. Keratinocytes as the source of HBD3

Keratinocytes are able to secrete antimicrobial peptides (AMPs) to protect against microbial infections, including cathelicidins and defensins (Braff et *al*., 2005). β-defensins are expressed and secreted by keratinocytes (Ali et *al*., 2001; Harder et *al*., 2001; Supp, Karpinski and Boyce, 2004), but also by several cell types residing in the skin, such as fibroblasts, sebocytes and different immune cells (Niyonsaba et *al*., 2017).

The expression of β-defensins can be constitutive or inducible in response to pro-inflammatory stimuli. Human β-defensin 1 (HBD1) is mainly constitutively expressed in the skin (Ganz, 2003), while it has been reported that in monocytes and lymphocytes, HBD1 can be also induced by microbe-derived molecules, such as lipopolysaccharides (LPS) and peptidoglycans (PGN) (Sørensen et *al*., 2005), which are components of bacteria cell wall. Human β-defensins 2-4 (HBD2-4) are inducible in response to different

stimuli such as pathogens (including bacteria, yeast and viruses) and inflammation (Ali et *al*., 2001; Ganz, 2003; Dhople, Krukemeyer and Ramamoorthy, 2006).

Expression of β-defensins is also dysregulated in some skin diseases. HBD2 and HBD3 are upregulated in psoriasis (Niyonsaba et al., 2017). In fact, both peptides were first isolated from human lesional psoriatic scales (Harder et al., 1997; Harder et al., 2001). In atopic dermatitis, HBD2 and HBD3 are downregulated when comparing with psoriatic skin (Nomura et al., 2003; Niyonsaba et al., 2017). However, an enhanced expression of these β-defensins has also been reported in the lesional skin of untreated atopic dermatitis patients in comparison with non-lesional skin and controls (Harder et al., 2010).

In healthy skin, keratinocytes show low basal expression of most of the inducible β-defensins, especially HBD3 (Kim et al., 2002; Harder et al., 2010; Wittersheim et al., 2013). However, upon a stimulant factor or situation, the expression can be rapidly increased. Apart from pathogenic microorganisms, HBD3 expression have been reported to be induced by tumor necrosis factor-α (TGF-α) and interferon-γ (IFN-γ) (Harder et al., 2001; Kim, Hong and Seo, 2003; Pernet et al., 2003). HBD3 is also highly expressed at wound sites and it is induced by insulin-like growth factor I (IGF-I) and TGF-α, which are important in wound healing (Sørensen et al., 2003). It has also been reported to be upregulated by histamine (Ishikawa et al., 2009) and prostaglandin D2 (Kanda, Ishikawa and Watanabe, 2010).

The differentiation state of keratinocytes also influences the expression of β-defensins. In keratinocytic cultures incubated with calcium, which induces keratinocyte differentiation, there is an increase in the expression of different β-defensins, including HBD3, after 4-6 days (Abiko et al., 2003; Pernet et al., 2003; Harder et al., 2004).

Interestingly, it has been proposed that UV radiation is also able to upregulate *DEFB103* expression in human keratinocytes (Kim, Hong and Seo, 2003; Gläser et al., 2009)

suggesting a role of HBD3 in UV response. Although Wolf Horrell and D'Orazio (2014) concluded that UV does not increase *DEFB103* expression in ex vivo neonatal skin explants. Further research would help understanding the influence of UV in *DEFB103* expression.

## 3.2. Genomic localization and Copy Number Variation

In humans, the genes encoding α and β-defensins form a multifunctional family, and most of them are located in clusters on chromosome 8. The α-defensin *DEFA1A3* and six β-defensins (*DEFB4, DEFB103, DEFB104, DEFB105, DEFB106* and *DEFB107*) are situated on chromosome 8p23.1 and vary in copy number independently: α-defensins vary as a 19-kb tandemly repeated unit and β-defensins are grouped in a repetitive unit, which is highly polymorphic in copy number (Hollox, Armour and Barber, 2003; Groth et *al*., 2008; Abu Bakar, Hollox and Armour, 2009). This cluster is called β-defensin CNV, and is at least 250Kb in size, but the exact size and breakpoints of the copy number variable region are not known (Hollox et *al*., 2008a). The copy numbers of the β-defensins within the CNV vary coordinately (Hollox, Armour and Barber, 2003; Linzmeier and Ganz 2005; Groth et *al*., 2008).

The diploid copy number of the β-defensins vary between 1 and 12 copies, but the most common is 2-7 copies per diploid genome, being very rare to have one or zero copies (Abu Bakar, Hollox and Armour, 2009; Sugawara et *al*., 2003). The *SPAG11* gene, formed by the fusion of two defensins is also located in this cluster. In this region, but outside the other three β-defensins are located (*DEFB1*, *DEFB108* and *DEFB109*), which only one copy per haploid genome (Hollox et *al*., 2008a).

The β-defensin CNV is located on a large genomic repeat unit within more complex CNVs involving retroviral elements and olfactory repeat (OR) regions, collectively known as “REPD” (for repeat distal) (Giglio et *al*. 2001). Another smaller OR region called

"REPP" (repeat proximal) is 5 Mb proximal on 8p23.1 and shares a high level of identity with REPD (Sugawara et *al*. 2003). In fact, the cluster of β-defensins is located at 2 distinct genomic *loci*, separated by ≈5 Mb of single-copy sequence and mapping to locations consistent with REPP and REPD repeat regions (Abu Bakar, Hollox and Armour, 2009) (Figure 5). The total copy number of these β-defensin genes is the sum of the genes of the two genomic locations.

Apart from the CNVs in this region, human 8p23 region harbors the largest polymorphic inversion known in the human genome, a 4Mb long paracentric inversion (Antonacci et *al*., 2009). The inverson breakpoints map to REPP and REPD regions (Giglio et *al*., 2001; Hollox et *al*., 2008a) (Figure 5).

Another three clusters of β-defensins are located in different chromosomes, one in chromosome 6p12.3 *(DEFB11O, DEFB112-114* and *DEFB134)* and two in chromosome 20, 20q1.21 *(DEFB115, DEFB116*, *DEFB118-124*) and 20p13 *(DEFB125-129, DEFB132*), but they do not seem to be variable in copy number (Schutte et *al*., 2002; Rodriguez-Jimenez et *al.*, 2003; Hollox and Armour, 2008).

The genetic structure of most β-defensins is composed by two exons, separated by an intron of variable length. The first exon codes for the peptide-signal, while the second exon codes for the mature peptide (White, Wimley and Selsted, 1995; Pazgier et *al*., 2006). *DEFB1* is an exception, in which the first exon codes for both the peptide-signal and the mature peptide (Liu et *al*., 1997; Pazgier et *al*., 2006).

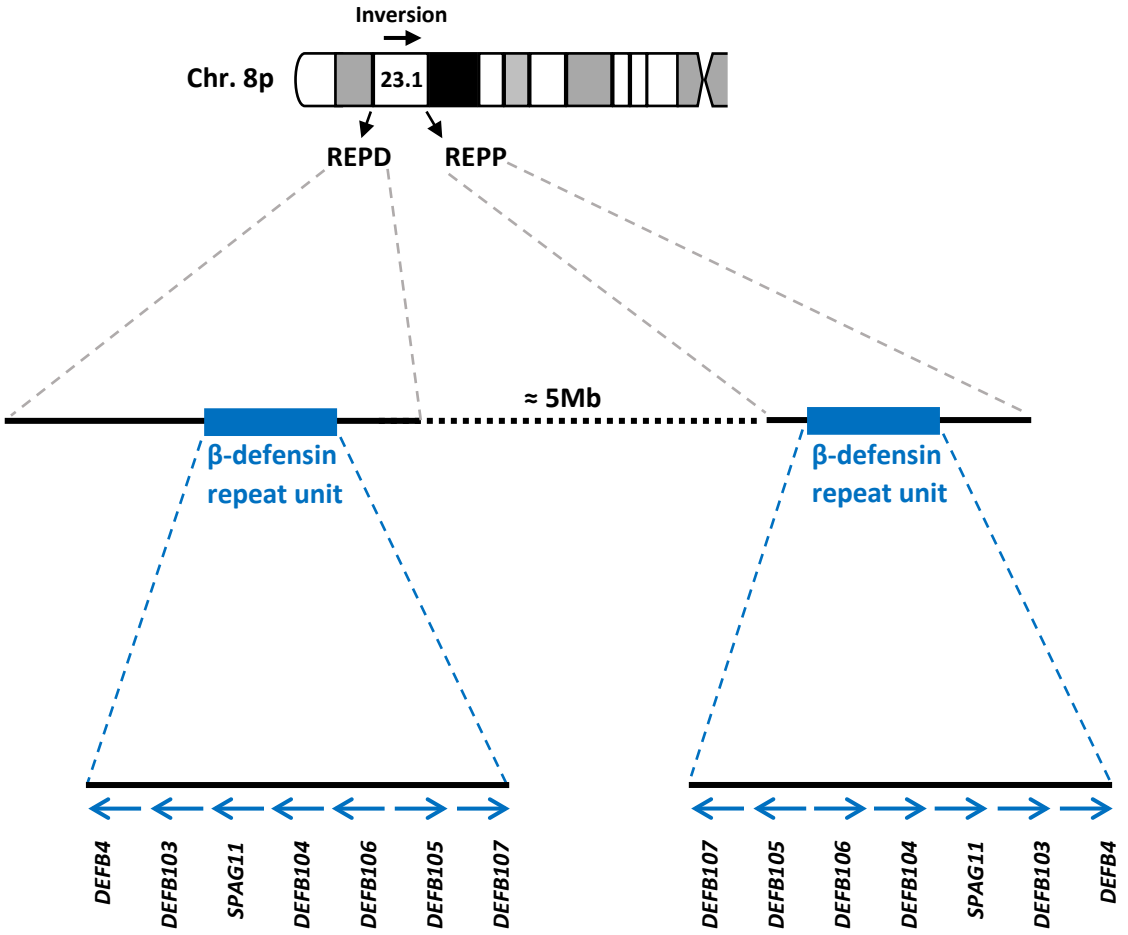


**Figure 5. A scheme of the location of the β-defensin repeat units on the 8p23.1 genomic region.** REPD and REPP are located on the extremes of the inversion in the 8p23.1 band. Genes within the β-defensin repeat units are highlighted and the arrows show their orientation.

### 3.2.1. β-defensin CNV and disease

Some β-defensin genes have been associated to the susceptibility to different diseases, especially in relation to their variation in copy number. Thus, for instance, it has been proposed that copy number is directly correlated to expression (Stranger et *al*., 2007; Groth et *al*., 2010), and then for instance, a high copy number of *DEFB4* has been associated to higher risk of developing psoriasis, an skin inflammatory disease (Hollox et *al*., 2008b; Stuart et *al*., 2012). Hollox et *al*. (2008b) observed that the increase in risk of psoriasis increased linearly with an increase in copy number dosage, supporting the idea that the risk factor is gene dosage itself and not some unknown sequence variant within the β-defensin region. High copy numbers of β-defensin cluster has also been associated with systemic lupus erythematosus (Zhou et *al*., 2012) or hidradenitis suppurativa/acne inversa (Giamarellos-Bourboulis et *al*., 2016). The CNV has also been associated with susceptibility to HIV infection, although the relation is not clear (Milanese et *al*., 2009; Hardwick et *al*., 2012; Mehlotra et *al*., 2012). On the other hand, high copy number has also been considered protective for some diseases, including celiac disease (Fernandez-Jiménez et *al*., 2010) and pancreatic ductal adenocarcinoma (Taudien et *al*., 2012).

In fact, results are not always conclusive and can even be conflicting. Fellermann et *al*. (2006) correlated low *DEFB4* copy numbers with Crohn's disease susceptibility, whereas Bentley et *al*. (2010) reported opposite results, associating the disease with high copy numbers; and Aldhous et *al*. (2010) failed to replicate any of the results. Thus, the relation of copy number variation with some diseases remains unclear.

### 3.2.2. Techniques for the analysis of copy number variation

*Real-time quantitative PCR (RT-qPCR)*

Real-time quantitative PCR (RT-qPCR) is the simplest PCR-based technique for the analysis of copy number polymorphisms. This method is based on the real-time measurement of amplicon accumulation. It uses fluorescent reporter molecules, such as SYBR™ Green, a DNA intercalating dye, which binds to double-stranded DNA, or Taqman® assays, which contain a primer set and a hydrolysis probe, which has a fluorophore covalently attached to the 5' end and a quencher attached at the 3' end. By using fluorescent techniques, it is possible to quantify the amount of PCR product generated in each cycle. At the exponential phase of the amplification reaction, fluorescence doubles every cycle and it is possible to relate the amount of the starting template to the number of cycles necessary to reach a defined threshold of fluorescence. For the determination of the copy number of a test *locus*, a reference *locus* with two fixed copies per diploid genome is simultaneously analysed.

However, it has been reported that the resolution of RT-qPCR could not be enough to accurately distinguish between copy numbers that differ only in one copy (Hollox et *al*., 2008a), especially with copy numbers higher than 3 (Weaver et *al*., 2010).

*Multiplex amplifiable probe hybridization (MAPH)*

Multiplex amplifiable probe hybridization (MAPH) is a simple method based on PCR to quantify DNA copy number (Armour et *al*., 2000; Hollox, Akrami and Armour, 2002). The technique relies on probes of 100-600pb that can be designed to bind to any target DNA sequence. Probes have an internal fragment that is complementary to the target sequence, flanked by additional known sequences, which are the same for all the probes. These flanking sequences allow the simultaneous amplification of all the fragments by a single set of primers. Analysis of the amplified fragments can be done by polyacrylamide

gel or by capillary electrophoresis (Hollox, Akrami and Armour, 2002) and copy number can be identified by comparing chromatograms to a refence sample.

*Multiplex ligation-dependent probe amplification (MLPA)*

Multiplex ligation-dependent probe amplification (MLPA) is very similar to MAPH, with small variations. In this technique, two probes are used for each target sequence: probes hybridize in adjacent sites the target sequence and then, a ligation step is needed to ligate the two probes by a thermostable ligase and form a unique probe. As in MAPH, probes contain sequences specific for the amplification with a single pair of primers. After the ligation, there is no need to wash unbounded probes, as only ligated probes serve as a template for PCR. Then, PCR is performed and the analysis is made by capillary electrophoresis (Schouten et *al*., 2002). One of the strength of MLPA in comparison to MAPH, is that less AND amount is needed, it can be performed with 20ng of DNA.

In both MAPH and MLPA techniques the hybridization is proportional to the amount of target DNA sequence. Using a single pair of primers for the amplification of all the target *loci* avoids the problem generated by differences in amplification efficiencies.

*Paralog ratio test (PRT)*

Paralog ratio test (PRT) is a comparative PCR method based on the amplification of dispersed repeat sequences with a single pair of primers (Armour et *al*., 2007). As test and reference *loci* belong to the same family of dispersed elements, they can simultaneously be amplified with the same primer pair (but amplicons of different size are formed). Precisely because of that, PRT is an accurate technique, comparable with MAPH and MLPA (Armour et *al*., 2007), because amplifying test and reference *locus* with the same primers avoids the possible bias that is usually present in multiplex RT-qPCR experiments, due to different amplification properties of the test and reference *loci*

(Armour et *al*., 2007). However, due to the requirements of primer design it is not always performable for all the test *loci*.

*Array-CGH*

Comparative genomic hybridization (CGH) was initially developed to discover and gauge genome-wide copy number variation. Array-CGH is based on the hybridization of DNA to immobilized oligonucleotides on a slide or platform. Test and reference DNA are hybridized in the same platform and the signal ratio between test and reference DNA is used to determine the copy number of the test sample. Initially, bacterial artificial chromosomes (BACs) were used and it was possible to measure the copy number of a large segment of DNA (100 kb) (Carter, 2007). Nowadays, the platforms can use short and long oligonucleotides.

*Digital PCR (dPCR)*

Digital PCR (dPCR) is an end-point PCR method that allows the absolute quantification of the nucleic acid molecules present in the sample. In dPCR, the sample is partitioned into many aliquots (or partitions), in which individual PCRs are carried out in parallel. The partition is assumed to follow a Poisson distribution, and in each alliquote 0, 1, or 2 copies are usually distributed. Thus, some of the alliquotes contain the target molecule, and amplification is performed (positive reactions) and some other partitions do not contain target molecules, so no amplification will occur (negative reactions). For the detection of target molecules, TaqMan chemistry with dye-labeled probes is usually used. Following PCR, the fluorescent signal is measured and used to assign each reaction as positive or negative. Then, the calculation of the ratio between positive and negative reactions is used to estimate the total number of target molecules in the sample. As it is not guaranteed that each positive reaction receives only a single molecule, Poisson modelling is implemented for the correction of the count of total number of target molecules (Majumdar, Wessel and Marks, 2015).

To the date, two platforms are available to perform dPCR: droplet digital PCR (ddPCR), from Bio-rad, is based on water-oil emulsion droplets.Here, the sample is distributed into 20,000 micelles (Mazaika and Homsy, 2014). The alternative to ddPCR is the approach developed by ThermoFisher Scientific, named QuantStudio™ 3D Digital PCR System, in which the sample is partitioned into 20,000 wells on a nanofluidic chip (Laig, Fekete and Majumdar, 2020). Both are based on the same principle: the sample is divided into many individual reactions, the fluorescent signal is then read to determine positive and negative reactions and the absolute count of the molecules is calculated based on a Poisson distribution.

dPCR has many applications, including Copy Number analysis. For that, two different Taqman assays (containing primers and dye-labeled probes) are used simultaneously: one for the detection of the target *locus*, and another one for the detection of a reference *locus*, which is known to have two copies in the diploid genome. After determining the target and reference concentrations in the sample, the genomic copy number of the target is then estimated as follows: 2 * (concentration of the target/concentration of the reference).

dPCR is an accurate and precise technique, as it does not need standards or endogenous controls. Besides, as it is and end-point technique, the efficiency of the reaction has not influence in the results, and it is more resistant to inhibitors. This avoids the problems shown by RT-qPCR regarding different amplification efficiencies for each *loci*. Furthermore, an advantage of dPCR is that it has a wider dynamic range than RT-qPCR. As it is based on linear detection, it allows the detection of small fold changes (Laig, Fekete and Majumdar, 2020).

*Next-Generation Sequencing (NGS)*

Next-generation sequencing (NGS) has also recently been used for the detection of copy number variants. The most widely used approach is based on sequence read depth (SRD). The principle of this methodology is that the number of reads that map to a specific region is proportional to the number of copies in the genome (Medvedev, Stanciu and Brudno, 2009). Thus, if an individual has a higher/lower copy number for a particular region, the number of reads aligned to that region would be higher/lower than those expected for a normal diploid region.

Copy number analysis can be performed from whole genome sequencing (WGS) data, but also from whole exome sequencing (WES) data (Kadalayil et *al*., 2015). One of the advantages of using NGS data is that at the same time, it is possible to analyse sequence variation and CN. There are different programs available for the analysis of CNVs from exome data (Krumm et *al*., 2012; Kadalayil et *al*., 2015; Yao et *al*., 2017). However, results obtained by different methods may differ if coverage is not high (Yao et *al*., 2017).

However, in some cases, assessing the exact copy number, especially for higher copy numbers is complicated, and different techniques could give different results.

## 4. Vitamin D and melanogenesis

The principal role of vitamin D is related to the maintenance of calcium and phosphate homeostasis and bone metabolism. Vitamin D regulates calcium levels through different processes including intestinal calcium absorption, storage and retention (DeLuca, 2004) and its deficiency is related with impairment of bone mineralization, and several diseases such as rickets and osteomalacia (Whyte and Thakker, 2005).

Apart from its relevance in calcium metabolism, vitamin D is essential for other important physiological processes and vitamin D deficiency has been associated to many illnesses (Holick and Chen, 2008; Daraghmeh et *al*., 2016). Further, vitamin D is involved in the regulation of signalling pathways related to cell proliferation and differentiation, apoptosis, angiogenesis and immune responses. Besides, it has also been demonstrated to have antioxidant properties and to be relevant in the defence against DNA damage (Samuel and String, 2008; Bikle, 2010). Thus, it has also been related with cancer, where a protective role for vitamin D has been suggested (Feldman et *al*., 2014; Mostafa and Hegazy, 2015; Slominski et *al*., 2017; Khammissa et *al*., 2020).

Regarding the skin, vitamin D has been proven to be important for defence against the negative effects of Ultraviolet Radiation (UVR), through the regulation of DNA damage response and antioxidant responses (Mostafa and Hegazy, 2015; Pawlowska Wysokinski, and Blasiak, 2016; Jagoda and Dixon, 2020).

It has been reported that 1α,25-dihydroxyvitamin D3 (1α,25(OH)2D3), the active form of vitamin D (also known as calcitriol) is also able to modulate melanogenesis, although results are conflicting, and the exact effect of vitamin D on pigmentation is actually not clear.

Effect of vitamin D compounds on tyrosinase activity was long ago reported in B16 mouse melanoma cell line. Oikawa and Nakayasu (1974) observed and increase in tyrosinase activity in cultured B16 cells after treatment with cholecalciferol. 1α,25(OH)2D3 was also reported to have the same effect on tyrosinase activity in the same cell line (Hosoi et *al*., 1985).

Regarding melanocytes, reports offer contrasting results. Thus, while some authors reported an increase in tyrosinase activity, others show the opposite effect or find not differences. Thus, Ranson, Posen and Mason (1988) observed an increase on tyrosinase activity after 48h of treatment with $10^{-9}$M of 1α,25(OH)2D3 in cultured human

melanocytes. In the same vein, Tomita, Torinuki and Tagami (1988), despite not finding any effect by 1α,25(OH)2D3, nevertheless reported an increase in immunoactive tyrosinase with 1.3 μM of cholecalciferol after 6 days. And Watabe et *al*. (2002) observed an increase on tyrosine activity together with an induction of differentiation and inhibition of proliferation in immature mouse melanocytes incubated with 1α,25(OH)2D3. However, Abdel-Malek et *al*. (1988) observed instead a suppression of the tyrosinase activity with $10^{-7}$-$10^{-9}$M. And, similarly, Mansur et *al*. (1988) incubated melanocytes with different vitamin D derivatives, including 1α,25(OH)2D3 and found no effect after 10 days, although this observation may be possibly due to the high variability observed between cell cultures. Recently, Kawakami et *al*. (2014) reported a dose-dependent upregulation of tyrosine activity in human melanocytes and melanoblasts after treatment with 1α,25(OH)2D3 for 72h. Furthermore, in melanoblasts they observed melanosomes at more advanced stages.

Further evidence suggesting the implication of vitamin D on melanogenesis comes from research in two skin autoimmune diseases: psoriasis and vitiligo. Psoriasis is a chronic inflammatory disease, characterized by the abnormal proliferation of keratinocytes and disordered maturation of the epidermis. The influence of vitamin D on melanogenesis was suggested by the observation that psoriasis patients treated with calcipotriol (synthetic 1α,25(OH)2D3), developed hyperpigmentation in the treated skin area as a secondary effect (Gläser, Röwert and Mrowietz, 1998; Rutter and Schwarz, 2000). However, the patients were also simultaneously treated with other therapies, such as UV irradiation.

Vitiligo is an autoimmune disease characterized by the destruction of functional melanocytes from the epidermis through a combination of multiple processes influencing melanocyte function and survival. The most frequent treatments involve the use of calcipotriol or tacalcitol (analogues of calcitriol) together with different therapies that involve corticotherapy, or irradiation, such as psoralen photochemotherapy (PUVA) or

narrow-band UVB therapy (NB-UVB). This makes difficult to elucidate the mechanism of action of vitamin D. Thus, for instance, Katayama et *al*. (2003) reported an upregulation of c-kit by tacalcitol in vitiligo melanocytes. However, melanocytes were also irradiated, so the effect could be due to irradiation.

In general, patients treated with vitamin D show improvement as a result of melanocyte proliferation or increase in repigmentation. However, there are contradictory reports. Some authors reported that the addition of calcipotriol to the NB-UVB therapy increased its outcome (Kullavanijaya and Lim, 2004; Goktas et *al*., 2006; Leone et *al*., 2006), while others did not found significant differences (Ada et *al*., 2005; Hartmann et *al*., 2005; Arca et *al*., 2006). Nevertheless, in general, the use of calcipotriol as a monoterapy has also been reported to be effective (Ameen et *al*., 2001; Gargoom et *al*., 2004).

Genomic analyses of *VDR* also suggest a relation of vitamin D pathway with pigmentation. In a ChIP-seq (chromatin immunoprecipitation sequencing) experiment with VDR in lymphoblastoid cell lines (LCLs) treated with 1α,25(OH)2D3, Ramagopalan et *al*. (2010) showed enrichment of VDR binding to genomic regions related to traits such as tanning, skin sensitivity to sun or hair pigmentation (among others). Meyer et *al*. (2014) also performed ChIP-seq for VDR in osteoblasts and among the enriched peaks, there were *TYRP1* and *DCT*, two pigmentation-related genes.

## 4.1. Synthesis of vitamin D

The main part of body's requirements for vitamin D is endogenously generated. This process starts in the skin by the effect of UV radiation, although a small proportion (10%) can be obtained from the diet.

The synthesis starts with the photochemical transformation of 7-dehydrocholesterol (7-DHC) to pre-vitamin D3 by the effect of UVB radiation (λ=280-320 nm) (Holick, Smith

and Pincus, 1987). Previtamin D3 is a thermodynamically unstable sterol that subsequently is isomerized to vitamin D3 (cholecalciferol). Both are non-enzymatic steps. Then, vitamin D3 is released from keratinocyte membranes to the extracellular space and it enters the circulating system bound to vitamin D3-binding protein (DBP). Vitamin D3 is then metabolized in the liver by the 25-hydroxylases (CYP2R1 and CYP27A1) to form 25-hydroxyvitamin D3 (25OHD3) (calcidiol), which is the major circulating metabolite of vitamin D in serum. 25OHD3 3 is further hydroxylated in the kidney by 1α-hydroxylase (CYP27B1) to produce 1α,25-diydroxyvitamin D3 (1α,25(OH)2D3) (calcitriol), the most biologically active form of vitamin D. Finally, 1α,25(OH)2D3 binds DBP and it is delivered through the circulating system to target tissues (olick, Smith and Pincus, 1987; Slominski et *al*., 2004).

The levels of 25OHD3 and 1α,25(OH)2D3 are regulated by CYP24A1, a 24-hydroxylase, which is key to the catabolism of both 25OHD3 and 1α,25(OH)2D3. CYP24A1, initially hydroxylates 1α,25(OH)2D3 at C24 and then further oxidizes the side chain to produce calcitroic acid, a biliar catabolite. CYP24A1 can also inactivate 1α,25(OH)2D3 through a lactone pathway. 1α,25(OH)2D3 indirectly regulates its own levels via a negative feedback mechanism by the induction of the production of CYP24A1 (Jones, Prosser and Kaufmann, 2012).

Interestingly, the synthesis of vitamin D can be entirely completed in the skin. Keratinocytes are the only human cells that possess all the enzymes needed for the complete synthesis of vitamin D from 7-dehydrocholesterol to 1α,25(OH)2D3 (Bikle, 2011) (Figure 7). The ability of the skin to synthetize 1α,25(OH)2D3 has been demonstrated in human keratinocytes (Bikle et *al*., 1986a, b; Lehmann, Knuschke and Meurer, 2000), human skin equivalent models (Lehmann et *al*., 2000, 2001) and also *in vivo* in human skin by microdialysis (Lehmann et *al*., 2003).

7-DHC is also the last substrate for cholesterol synthesis in the Kandutsch-Russell pathway (Prabhu et *al*., 2016a). Thus, both pathways depend on the availability of 7-DHC, and there can be a competition for it. Shin et *al*. (2019) observed that in cultured human keratinocytes UV irradiation reduced the expression of dehydrocholesterol reductase 7 (DHCR7), the enzyme that converts 7-DHC into cholesterol, and at the same time increased the expression of *CYP27B1*, which remember hydroxilates 25OHD3 into 1,25(OH)2D3, suggesting a UV-mediated shift from cholesterol synthesis to vitamin D synthesis.

It has also been reported that other cells in the skin also possess some of the enzymes implicated in the vitamin D synthesis. For instance, fibroblast express CYP27A1, but not CYP27B1 (Vantieghem et *al*., 2006); thus, they can be donors of intermediate metabolites, such as 25OHD3, for vitamin D synthesis. Interestingly, CYP27B1 is expressed in nevi and melanoma (Brożyna et *al*., 2013), Thus, it is possible that melanocytes are able to mediate the final step in 1α,25(OH)2D3 synthesis.

It has been also demonstrated that many skin cells have functional VDR, the receptor of vitamin D. Keratinocytes, melanocytes and fibroblasts all express VDR (Abdel-Malek et *al*., 1988; Pillai, Bikle and Elias, 1988; Reichrath et *al*., 1996; Carlson et *al*., 2007). Thus, skin is the source and also target of vitamin D action.

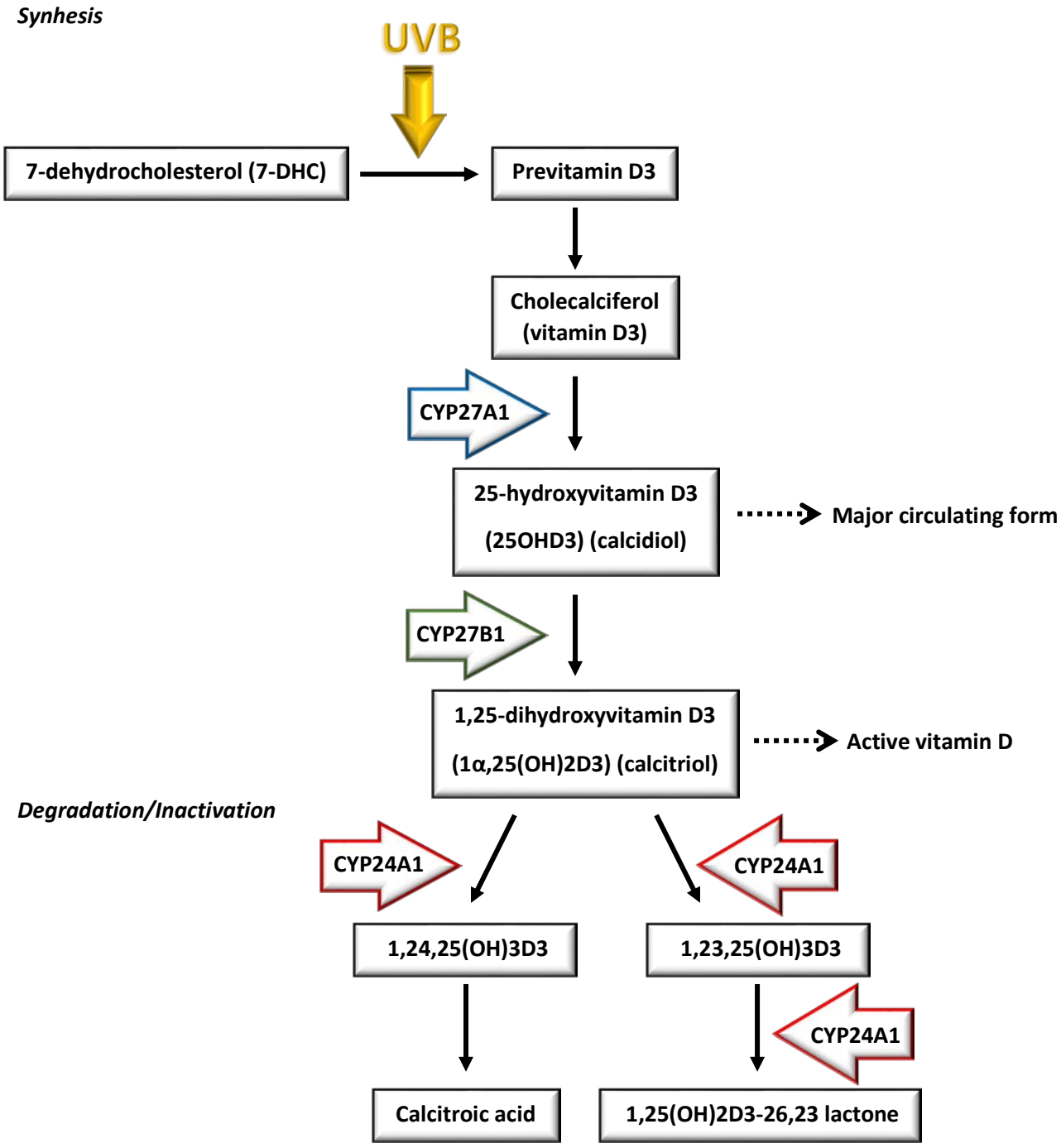


**Figure 7. Metabolism of vitamin D.**

## 4.2. 25OHD3 (calcidiol) serum level and pigmentation

Serum levels of calcidiol (25OHD3), the main circulating form of vitamin D, have been investigated and associated with several diseases, including those typical of the skin, such as psoriasis, vitiligo and melanoma. Although 25OHD3 serum levels are widely measured and vitamin D status is considered very important for health in general, there are still discrepancies about what are considered normal, insufficient and deficient levels. In general, the minimum desirable serum level is considered to be between 20 and 30 ng/ml (50-75 nmol/L), whereas the normal range would be 30-80 ng/mL. It has been stated that levels higher than 20 ng/ml are needed for good bone and general health for almost all individuals (Ross et *al*., 2011). Besides, levels between 30 and 40 ng/ml have been suggested to be necessary to reduce mortality (Zittermann et *al*., 2012). Although the boundaries among the categories are not well defined and widely accepted, in general levels below 30-20 ng/ml would be considered as vitamin D insufficiency and levels below 20-10 ng/ml deficiency (Holick and Chen, 2008; De Smedt et *al*., 2017; Spath et *al*., 2017; Bikle, 2020).

In general, it is assumed that higher skin pigmentation is associated with lower vitamin D production (Holick 2003, 2007). This assumption is based on the fact that melanin has the ability to absorb and filter out UVB radiation. In fact, the main function of this pigment is to protect the cells from the noxious effects of UV. Thus, higher melanin content would imply that lower UVB photons are available to reach basal and suprabasal layers of epidermis to convert 7-dehydrocholesterol (7-DHC) into previtamin D3. Some authors have showed evidence for this hypothesis. Armas et *al*. (2007) irradiated the skin of individuals of different skin tone three times a week for four weeks and measured serum 25OHD3 weekly. They observed that the response was dependent on skin pigmentation. Chen et *al*. (2007) also irradiated the skin of volunteers of different skin types for 12 weeks, and found that lightly pigmented individuals produced more 25OHD3. Nevertheless, other authors found no correlation between melanin content and 25OHD3

levels (Bogh et *al*., 2010). Disparities among studies could be the result of the different radiation spectra used. Thus, while Bogh et *al*. (2010) used short-wavelength radiation, which does not penetrate far into the epidermis, but can convert the 7-DHC in the superficial layers, above the melanin (Björn et *al*., 2010), and Chen et al (2007) used tanning beds mimicking sunlight.

There are also observational studies that provide evidence of the differences among skin types. In general, individuals with skin types V-VI (dark) tend to have lower vitamin D levels and need longer sun exposure (or more UV radiation) to make the same amount of vitamin D than light-skinned individuals (Farra et *al*., 2011; Webb et *al*., 2018). Similarly, mean vitamin D levels are lower in individuals with darker skin, such as South Asian, African and African Americans, than in white Caucasian, and vitamin D deficiency or insufficiency are more common among them (Ford et *al*., 2006; Harris, 2006; Aloia, 2008; Egan et *al*., 2008; Powe et *al*., 2013; Schleicher et *al*., 2016; Cashman et *al*., 2016).

Recently, an association between 25OHD3 serum level and polymorphisms in genes involved in skin pigmentation has been proposed. Saternus et *al*. (2015) genotyped SNPs within 29 melanogenic genes in 2970 Caucasian individuals and measured the concentration of 25OHD3 in serum. 46 SNPs in 16 of the genes were associated with lower or higher 25OHD3 levels. After correction for multiple tests, 12 SNPs remained significant in the genes *EXOC2*, *TYR*, *PRKACG*, *EDN1*, *TYRP1* and *MITF*. They proposed that up to 5.6% of the variation in 25OHD3 concentration can be explained by these 12 SNPs. However, this could be limited to the population studied. An important detail of this work is that the mean 25OHD3 serum level was 17.30 ng/mL (median, 15.5 ng/mL), a value considered as insufficient. The reason could be that the participants are from a hospital-based cohort study for coronary artery disease, and their sun exposure may be limited. This study suggests that there is a genetic relation between the melanin

synthesis pathway and vitamin D serum levels, at least in the population analysed. It would be interesting to analyse if it was also related with skin pigmentation levels.

More recently, another group studied the relation of solar exposition, skin pigmentation and 25OHD3 levels in an Australian population with predominantly European ancestry (Mitchell et *al*., 2019). They found an inverse relationship between skin pigmentation (skin reflectance values at 650nm) and 25OHD3 concentration. Individuals with darker skin had significantly lower 25OHD3 levels than individuals with lighter skin. They also found association between self-reported sun exposure and 25OHD3 concentration in serum.

These studies suggest a relation between melanin content and vitamin D pathway and support the general assumption of the relation between higher pigmentation level and lower 25OHD3 serum levels.

On the other hand, the endogenous synthesis of active vitamin D (1α,25(OH)2D3) in the skin itself is another form of vitamin D production that has not been analysed in the context of pigmentation differences. 1α,25(OH)2D3 acts locally in the skin and it is important for protection against UV. The cutaneous synthesis of 1α,25(OH)2D3 could also vary between individuals with different skin type.

## 4.3. Vitamin D receptor and mechanism of action

The numerous actions of vitamin D are mediated through the interaction of the active form of vitamin D (1α,25(OH)2D3) and vitamin D receptor (VDR), which is a transcription factor. VDR binds 1α,25(OH)2D3 with high affinity and specificity. Two mechanism are known for vitamin D and VDR action: genomic and non-genomic responses (Figure 6). The non-genomic rapid responses are generated within 1-45 minutes, whereas the

genomic responses can take several hours or days (Haussler et *al*., 2011; Hii and Ferrante, 2016).

In the genomic response, the most studied, 1α,25(OH)2D3 enters the cytoplasm and binds to VDR in the binding site called “genomic pocket”. The binding of vitamin D triggers VDR to interact and form a heterodimer with the retinoid X receptor (RXR). The VDR-RXR heterodimer translocates to the nucleus and binds DNA at vitamin D responsive elements (VDREs). Then, by recruiting complexes of either coactivators or corepressors, VDR-RXR regulate the transcription of several genes. The most common VDRE possess a direct repeat of two hexanucleotide half elements with a spacer of three nucleotides and it is known as DR3 motif. Other VDREs are also present in the genome, such as ER6 motif, which consists on an everted repeat of two half-elements with a spacer of six nucleotides (Haussler et *al*., 2011; Carlberg and Campbell, 2012).

In the non-genomic response, also known as the rapid response pathway, 1α,25(OH)2D3 binds to an alternative pocket of VDR. In this case, VDR is located in the plasma membrane, associated with *caveolae* (Huhtakangas et *al*., 2004). The binding of vitamin D to membrane-associated VDR leads to the activation of kinases, phosphatases and ion channels. This process can include the activation of G protein-coupled receptors, phosphatidylinositol-3-kinase (PI3K), phospholipase C (PLC) or protein kinase C (PKC). Besides, the activation of second messengers can also lead to the regulation of the transcription of other genes. Apart from caveolae-associated VDR, 1,25D3-membrane-associated rapid response steroid-binding protein (1,25D3-MARRS) has also been proposed to mediate non-genomic rapid responses of vitamin D (Nemere et *al*., 2004). It has been reported that 1,25D3-MARRS, also known as protein disulfide isomerase family A, member 3 (PDIA3) or endoplasmic reticulum stress protein 57 (ERP57), co-localizes and interacts with VDR, at least in osteoblasts and fibroblasts (Sequeira et *al*. 2012; Chen et *al*., 2013), and that it may contribute to the vitamin D-induced DNA damage response (Sequeira et *al*. 2012).

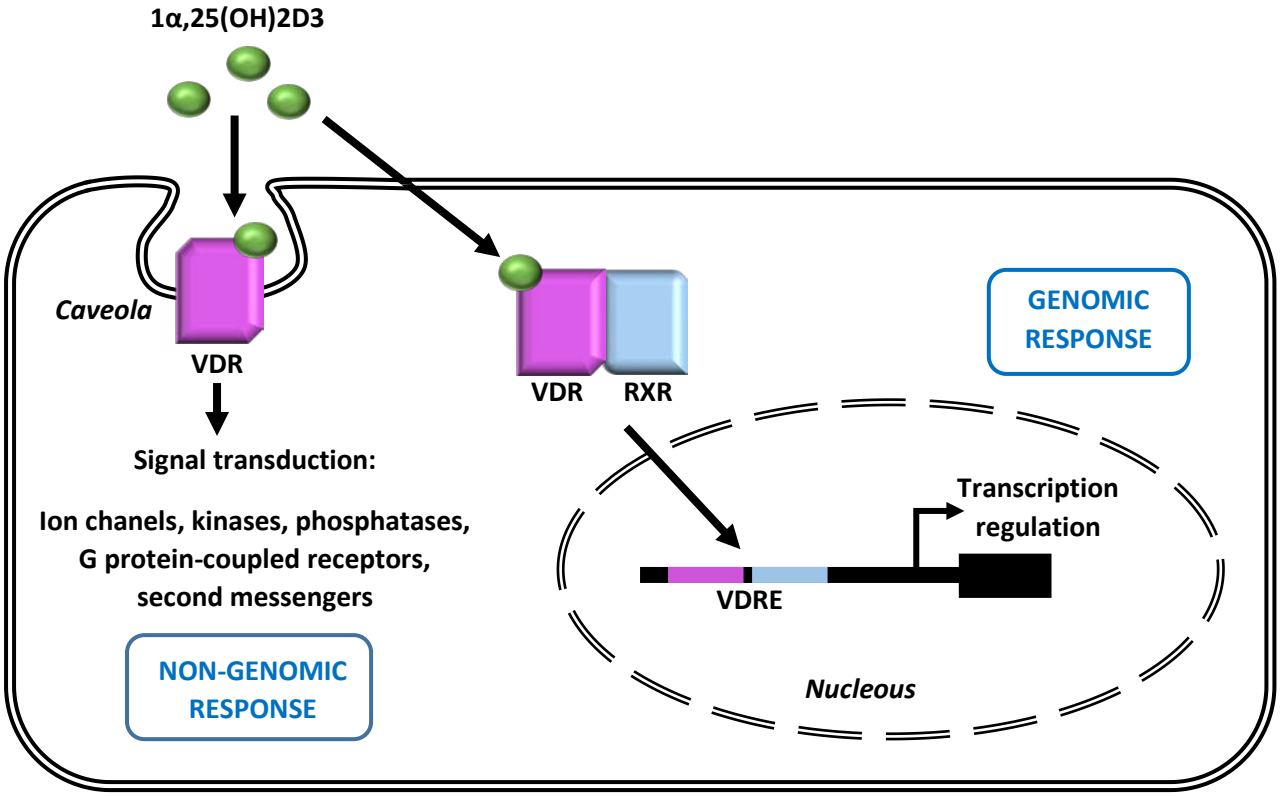


**Figure 6. Mechanisms of action of active vitamin D (1α,25(OH)2D3): genomic and non-genomic responses.**

## 4.4. Vitamin D mediated protection against UV induced damage

1α,25(OH)2D3 synthetized by keratinocytes is able to exert its actions in the skin, in a autocrine and paracrine way to melanocytes and other cells in the skin. Probably one of the most important actions of vitamin D in the skin is the protection against negative effects of UV radiation. In fact, vitamin D reduces UV-induced damage, including inflammation, sunburn, DNA-damage accumulation, immunosuppression and photocarcinogenesis.

UV radiation can damage DNA in different ways. UVB radiation (280–320 nm), when absorbed by DNA, induces the formation of cyclobutane pyrimidine dimers (CPDs) and

pyrimidine (6-4) pyrimidone photoproducts (6-4PP). The most common CPDs are thymine dimers. If they are not repaired properly, they result in mutations that can cause cancer. Besides, UVA radiation (320–400 nm) causes mainly oxidative processes that can also damage DNA. UVA radiation can be also absorbed by DNA, although it is mostly absorbed by other chromophores, (such as pterins, porphyrins, heme and bilirubin, melanin and melanin precursors, flavins and NADPH oxidase), leading to the production and accumulation of reactive oxygen species (ROS), reactive nitrogen species (RNS) and other toxic photoproducts, which all can damage DNA in different ways (Schuch et *al*., 2017; Cadet and Douki, 2018). ROS oxidate nucleotide bases leading to base pair mismatch and mutagenesis, if they are not repaired. A common base pair mismatch is caused by the oxidation of guanine, which produces primarily 8-oxo-7,8-dihydroguanine (8-oxodG), which tends to pair with adenine, instead of cytosine. ROS can also damage other molecules such as proteins and lipids. Oxidation of proteins involved in DNA repair impairs their function, contributing to the mutagenic effect of UV (Schuch et *al*., 2017). Nucleotide excision repair (NER) and Base Excision Repair (BER) are the systems responsible for the reparation of DNA damages. NER repairs nucleotide dimmers and BER eliminates the oxidized bases.

Although the exact process by which vitamin D helps in the protection against UV-induced DNA damage is not clear, several evidences suggest that it could be due to the interaction with NER (Pawlowska Wysokinski, and Blasiak, 2016). Many authors have reported the increase in DNA repair in keratinocytes treated with vitamin D, before or after UV irradiation.

It has been demonstrated that vitamin D and other analogues reduce the amount of CPDs in UV irradiated keratinocytes (De Haes et *al*., 2005, Gupta et *al*., 2007; Song et *al*., 2013; Rybchyn et *al*., 2018; Chaiprasongsuk et *al*., 2019; Wong et *al*., 2004; Sequeria et *al*., 2012). Furthermore, Moll et *al*. (2007) observed that after treatment with vitamin D, keratinocytes upregulated the expression of *XPC* (xeroderma pigmentosum,

complementation group C) and *DDB2* (damage specific DNA binding protein 2), two genes implicated in NER. There is also evidence from experiments made with mice. Dixon et al. (2005) induced tumours by UV irradiation in hairless mice and then observed that after topic application of vitamin D, the amount of CPD decreased. Chaiprasongsuk et *al*. (2019) also observed that in human keratinocytes, vitamin D and other derivatives, induced DNA reparation, by enhancing the repair of 6-4PP and attenuating CPD levels.

The effects of vitamin D on the protection from oxidative processes have been also demonstrated (Jagoda and Dixon, 2020). Song et *al*. (2013) observed that in human skin explants 1α,25(OH)2D3 not only reduces thymine dimmers formed by UV, but also other lesions related with ROS, such as 8-oxodG. In human keratinocytes, 1α,25(OH)2D3 and other vitamin D derivatives also reduced the amount of oxidant compounds created by the effect of UV (Chaiprasongsuk et *al*., 2019). Furthermore, it has been suggested that vitamin D regulates pathways involved in redox balance. Some authors have found an association between vitamin D and *NRF2* (nuclear factor, erythroid 2 like 2). *NRF2* is a transcription factor implicated in the antioxidant response and has been reported to act against UV-induced oxidative damage in human skin cells (Jeayeng et *al*., 2017). Chaiprasongsuk et *al*. (2019) observed the upregulation of the expression of several genes that are target of the transcription factor *NRF2* and which are involved in antioxidant response, what was further demonstrated with the upregulation of the antioxidant enzymes heme oxygenase-1; (HO-1), catalase (CAT) and superoxide dismutase/Mn (MnSOD). The translocation of NRF2 to the nucleus was also increased. Further, they also observed an increase in the phosphorylation of p53 at Ser-15 and an increase in its nuclear concentration. Besides, Tang et *al*. (2018b) observed that Vitamin D protects against oxidative damage by activation of Wnt/β-catenin signalling in normal and vitiligo melanocytes. On the other hand, Rybchyn et *al*. (2018) observed, along with an increase in the repair of CPDs, a decrease in the oxidative damage in vitamin D-treated primary keratinocytes. Interestingly, they reported an increase in the glycolysis

and other processes related to energy conservation, such as autophagy and mitophagy and suggested that energy availability is an important contributor to DNA repair in skin after UV exposure.

Another protective role of vitamin D against UV effects is the reduction of nitric oxide (NO). UV induces the overproduction of NO, by upregulation of NO synthases. NO may cause the nitrosylation of the enzymes responsible for DNA repair (Bau, Gurr and Jan, 2001; Tang, Wei and Liu, 2012). An excess of NO can also form RNS, which can also damage DNA and proteins. Besides, NO can combine with ROS to form more genotoxic NO derivatives such as peroxynitrite (OONO−), which can cause modifications in DNA by oxidation or nitration. In this sense, it has been demonstrated that in irradiated keratinocytes 1α,25(OH)2D3 reduced the accumulation of NO derivatives, such as nitrite, the product of peroxynitrite degradation (Gupta et *al*., 2007) and nitrotyrosine, the product of nitration of tyrosine from proteins (Dixon et *al*., 2011). Song et *al*. 2013 also observed the reduction of 8-nitroguanosine (8-NG), the product of nitration in guanine in DNA in human skin explants. In addition, Gordon-Thomson et *al*. (2012) apart from a reduction in thymine dimers also observed a decrease in accumulation of RNS in keratinocytes, and Wong et *al*. (2004) observed a decrease in NO amount in melanocytes, keratinocytes and fibroblasts that had been pre-treated with 1α,25(OH)2D3 before UV irradiation.

Besides, vitamin D has also been reported to inhibit apoptosis after UV irradiation in keratinocytes (Lee and Youn, 1998; Manggau et *al*., 2001; De Haes et *al*., 2003; Wong et *al*., 2004), melanocytes (Wong et *al*., 2004; Mason et *al*., 2010) and fibroblasts (Wong et *al*., 2004). However, the opposite effect has been reported instead in malignant cells. Thus, vitamin D has been reported to show pro-apoptotic activity in several tumours, including melanoma (Brożyna, Hoffman and Slominski, 2020). One possible explanation for the different effects on apoptosis could be the vitamin D role in DNA damage and oxidative response in normal skin cells. Thus, UV-triggered apoptosis is the result of

induced DNA damage, and as it is prevented by vitamin D, because it decreases DNA damage at least to levels that do not need programmed cell death.

Although the exact mechanisms of vitamin D protective actions against UV irradiation are not fully understood, some evidence suggests that at least some of the effects are carried out by the non-genomic rapid response. 1α,25(OH)2D3 analogues that only participate in the rapid response or have little effect on the genomic response, have been reported to exert some of the responses to UV, such as reducing CPDs and apoptosis (Wong et *al*., 2004; Dixon et *al*., 2007; Mason et *al*., 2010). Besides, an antagonist of the non-genomic pathway reversed the protective effects (Wong et *al*., 2004), while antagonist of the genomic pathway did not (Dixon et *al*., 2007). Furthermore, Sequeira et *al*. (2012) showed that VDR is implicated in the reduction of thymine dimers, and that even defective VDR with no ability to mediate genomic responses were also effective in removal of thymine dimers in human fibroblasts.

In addition, there is ample evidence that indicates that the vitamin D pathway may play a role in melanoma, including observational analysis of low 25OHD3 serum levels, *VDR* polymorphisms, altered *VDR* expression in melanoma cell lines and tumours, and experiments that demonstrate the anti-tumorigenic properties of 1α,25(OH)2D3 in melanoma.

Lower 25OHD3 serum levels are associated with melanoma susceptivility (Spath et *al*., 2017, Cattaruzza et *al*., 2019) and poor clinical outcome (Newton-Bishop et *al*., 2009; Nurnberg et *al*., 2009; Gambichler et *al*., 2013; Bade et *al*., 2014; Wyatt et *al*., 2015; Fang et *al*., 2016; Timerman et *al*., 2017).

Vitamin D receptor has been suggested to act as a tumour suppressor, based on the evidences that mice lacking *VDR* were more prone to develop UV-induced tumours (Ellison et *al*., 2008; Bikle, Oda and Teichert, 2011) and on the anti-tumorigenic activities mediated by VDR (Bikle et *al*., 2015). In this sense, in melanoma, *VDR* expression is

decreased in comparison with normal skin (Brożyna et *al*., 2011; Del Puerto et *al*., 2017) and it is inversely correlated with metastatic potential (Brożyna, Jóźwicki and Slominski, 2014).

VDR variants have also been associated with susceptibility of developing melanoma (Li et *al*., 2007; Denzer, Vogt and Reichrath, 2011; Mandelcorn-Monson et *al*., 2011; Orlow et *al*., 2012; Zeljic et *al*., 2014), and also with progression and prognosis (Hutchinson et *al*., 2000; Birke et *al*. (2020).

Apart from vitamin D's role in the protection against UV-induced damage, which prevents the malignant transformation of skin cells, and thus the formation of tumours, some other activities of 1α,25(OH)2D3 provide anti-cancer effects. These activities include the regulation of important processes such as cell-cycle arrest, the induction of apoptosis, the inhibition of angiogenesis or the repression of oncogenic genes (Holick et *al*., 2007; Picotto et al., 2012; Bolerazska et al., 2017; Slominski et al., 2017; Brożyna, Hoffman and Slominski, 2020).

## 4.5. Vitamin D and β-defensins

It is interesting that a link between vitamin D and β-defensins has been proposed. It has been reported that vitamin D is able to modulate the expression of some antimicrobial peptides, including cathelicidins and β-defensins. In fact, human β-defensin 2 (HBD2) encoded by *DEFB4* and cathelicidin (*CAMP*), also known as *LL37*, contain VDREs in their promoter regions (Wang et *al*., 2004, 2005). Besides, although *DEFB103* does not contain the consensus VDREs (DR3 or ER6), upstream the gene there is a DR3 element with a single nucleotide substitution, which could be also functional (Wang et *al*., 2005).

In fact, it has been demonstrated that vitamin D upregulates the expression of cathelicidin, HBD2 and HBD3 (Wang et *al*., 2004; Gonzalez-Curiel et *al*., 2014; Dai et

*al*., 2010; De Filippis et *al*., 2017). And, more interestingly, Hong et *al*. (2008) reported that in hairless mice, UV stimulated the expression of mouse defensins 2 and 3, and the inhibition of vitamin D system blocked their expression.

However, vitamin D induced downregulation of β-defensins has also been reported (Kim et *al*., 2009; Peric et *al*., 2009). The discrepancies could be the result of different conditions and the experimental design. For instance, Dai et *al*. (2010) observed an increase in *DEFB103* expression after treating normal human keratinocytes with calcitriol, whereas the downregulation of HBD2 and HBD3 by calcipotriol observed by Peric et *al*. (2009) was in lesional psoriatic plaques, where β-defensin expression is known to be increased comparing with normal skin. On the other hand, in the experiments by Kim et *al*. (2009), keratinocytes were first treated with other stimulants before the additional treatment with calcipotriol. It has also been suggested that the induction of HBD2 expression by vitamin D may require additional signalling pathways (Liu et *al*., 2009; Wang et *al*., 2010).

# Objectives

The main objective of this work is to investigate the relation between human skin pigmentation and skin immunity. In particular, we focus on the study of the effect of the antimicrobial peptide beta-defensin 103 (*DEFB103*), and vitamin D on skin pigmentation.

The specific objectives of this work are:

1. To analyse the sequence and copy number variations in *DEFB103* and identify if there is any variation associated to pigmentation in humans (Chapter 1).
2. To analyse the effect of UV radiation on the expression of *DEFB103* in human keratinocytes; and if there are differences in the response of keratinocytes from dark and light pigmented individuals (Chapter 2).
3. To analyse the response to wild-type and mutated HBD3 (the peptide encoded by *DEFB103*) of melanocytes from darkly and lightly pigmented individuals using gene expression microarrays (Chapter 3).
4. To analyse the response to active vitamin D of melanocytes from darkly and lightly pigmented individuals (Chapter 4).

# Chapter 1.

## Sequence and copy number variability of DEFB103 gene and its possible relation with skin pigmentation

## 1.1. Introduction

β-defensins are principally known for their role as antimicrobial peptides in the innate immune system (Ganz, 2003). They have also been proposed as a link between the innate and the adaptative immune systems, as they are able to act as chemotactic agents (Yang et *al*., 1999; Niyonsaba, Ogawa and Nagaoka, 2004), that is, β-defensins are able to attract cells from the adaptive immune system to infection and inflammation sites (Yang et *al*., 1999; Wu et al., 2003; Niyonsaba, Ogawa and Nagaoka, 2004).

Interestingly, β-defensins have also been related with pigmentation. In a study made with domestic dogs, Candille et *al*. (2007) showed that a *locus* named K had an important role in the determination of coat colour. This K locus turned out to be the canine orthologue of human β-defensin 103 (*DEFB103*).

The K locus is expressed at high levels in canine skin and presents three alleles, one of them, the $K_B$ allele (or *Dominant black*) seems to be the cause of black coat colour in several dog breeds. The $K_B$ allele contains a 3bp deletion in the second exon, which leads to a deletion of a glycine in the peptide (ΔG23). Thus, Candille et *al*. (2007) demonstrated that in the presence of the wild-type alleles of *Mc1r* and *Agouti* (the main genes implicated in coat melanin synthesis) and of CDB103 (the peptide encoded by the *K* locus), Agouti protein binds Mc1r, resulting in a yellow coat colour. However, in dogs carrying the $K_B$ allele, CDB103 peptide binds with higher affinity to Mc1r, competing with Agouti, and promoting melanogenesis. The deletion has also been found to produce a black colour in wolves (Anderson et *al*., 2009).

The discovery of Candille et *al*. (2007) associates a new function to β-defensin 103 in mammals. Consequently, this finding opened the possibility that *DEFB103* could also be implicated in human skin pigmentation, and that this, perhaps, could also be related to the innate immune system.

On the other hand, an important characteristic of *DEFB103* to bear in mind is that in humans the gene is located in an extended region variable in copy number, which includes other β-defensins (Hollox *et al.*, 2003). The copy number of β-defensins is highly polymorphic, and all of the genes within the region vary concordantly in copy number (Groth *et al*., 2008). The common copy numbers range between 2 and 7 copies per diploid genome (Abu Bakar *et al.*, 2009).

In this context, we aimed at analysing the genetic diversity of *DEFB103* in order to search for sequence or copy number variants, implicated in human skin pigmentation.

## 1.2. Material and Methods

### 1.2.1. DNA Samples

DNA samples used in this study were obtained from different sources. Thus, we collected samples from donors living in the Basque Country; we also used samples obtained from the Spanish National DNA Bank from different regions of Spain; and finally we purchased, from Coriell Cell Repository and from European Collection of Authenticated Cell Cultures (Public Health England), DNA samples of African, Asian and European descent.

### 1.2.2. Sample Collection from donors

After approval of the Ethics Committee of The University of the Basque Country, and informed consent of the donors, we collected 1267 samples from unrelated Spanish individuals living in the Basque Country. We took approximately 5 ml of saliva from each donor. We also recorded information about sex, age, sun exposure behaviour, presence/abundance of facial nevi, eye and hair colour and skin phototype according to the Fitzpatrick scale (Fitzpatrick, 1988). To obtain a more accurate measure of the pigmentary phenotype, we also measured the constitutive pigmentation, the pigmentation that is not influenced by environmental factors such as solar radiation. The measurement was made by reflectance spectrometry at 685 nm using MiniScan EZ

4500L spectrophotometer (HunterLab). In order to avoid the effects of solar radiation in the skin, samples were collected during the winter season. Reflectance measures (five per individual) were taken on the inner surface of the upper arm. Samples were collected in two different periods obtaining 650 valid samples in the first sampling and 617 samples in the second sampling.

### 1.2.3. DNA extraction of collected samples from donors

DNA was isolated from saliva collected from donors and DNA extraction was performed following a standard phenol-chloroform protocol: Briefly, 700µl of saliva were transferred into a 1.5ml Eppendorf tube to which we added 800µl of 1x SSC (saline sodium citrate buffer. Tubes were centrifuged for 1 minute at 13,000 rpm and the supernatant was discarded. This step was repeated twice. Then, 375µl of sodium acetate (0.2M, pH 7.0), 10µl proteinase K (10mg/ml in Tris 10mM, pH 8.0) and 25µl of sodium lauryl sulphate 10x (SDS) were added to the pellet. The tube was gently vortexed and incubated for at least 1 hour at 56ºC with agitation. Once the pellet was completely dissolved, 120µl phenol-chloroform-isoamyl alcohol in a proportion of 20:19:1 was added and the tube was vigorously vortexed until obtaining a white emulsion. Then, the sample was centrifuged for 3 minutes at 13,000 rpm, to separate the sample in different layers. The aqueous layer (upper layer), which contains nucleic acids, was carefully transferred to a clean 1.5ml Eppendorf tube. DNA precipitation was performed by adding one volume of 100% ethanol and freezing at -20ºC for at least 1 hour. Then, the sample was centrifuged for 30 minutes at 13,000 rpm and the supernatant was discarded. The pellet was rinsed with 70% ethanol and the tube was centrifuged again for 10 minutes at 13,000 rpm. The supernatant was discarded and the pellet was dried at room temperature. DNA was resuspended in 50µl TE (Tris-EDTA) buffer and stored at -20ºC.

DNA quantitation was performed by spectrophotometry, measured at 260nm. To assess DNA purity the ratio of absorptions at 260nm vs 280nm (A260/280) was used.

***Analysis of sequence variability: resequencing of DEFB103***

For the analysis of sequence variability in *DEFB103*, we initially resequenced the exons of *DEFB103* in 13 of the samples described above. We selected samples from the extremes of the distribution of pigmentation levels, measured by reflectance spectrometry, in order to select individuals with lowest and highest levels of constitutive pigmentation: seven of the most pigmented and the six of the least pigmented of the series. In addition, we also used an additional set of 30 samples from different world-wide population groups: 5 North-Saharan Africans (NSA), 5 Sub-Saharan Africans (SSA), 3 Japanese (JPT), 2 Chinese (CHN), 5 Australian aborigines, 5 Europeans, all of them purchased from Coriell Cell Repositories, except the European samples, which were from HRC-panel 1 (European Collection of Authenticated Cell Cultures, Public Health England), and 5 Bantus (a gift from D. Comas, UPF).

### 1.2.4. Polymerase Chain Reaction (PCR)

The entire sequence of *DEFB103* was amplified using custom designed primers: 5´-TTCCTCCCTTACCTCACTACC-3´ (forward) and 5´-GGCTCCCTTATAGATTTCTCCA-3´ (reverse), which encompass a total length of 1.8kb (Figure 1.1). PCR reactions were carried out using a high fidelity enzyme, in order to minimize the misincorporation of nucleotide by the polymerase that could be erroneously interpreted as variants present within the different copies of *DEFB103* in a given individual. The PCR mixture included 50ng of genomic DNA as template, 0.25µl (2 units) of Q5 High-Fidelity DNA polymerase (New England BioLabs), 5µl 5X Q5 reaction buffer containing 2mM $Mg^{2+}$ at final reaction concentration, 5µl Q5 High GC enhancer, 10 mM dNTPS (dGTP, dATP, dCTP, and dTTP) and 1.25µl of each primer (10µM). Thermocycling conditions included a denaturation step at 98 ºC for 2 min, followed by 30 cycles of 98 ºC for 10 s, 61 ºC for 30s, and 72 ºC for 1 min, plus a final extension cycle of 72 ºC for 2 min.

PCR products were analysed by gel electrophoresis in a 1% agarose gel and the products with correct size were purified using illustra™ MicroSpin™ S-400 HR purification columns (GE Healthcare, Life Sciences, UK).

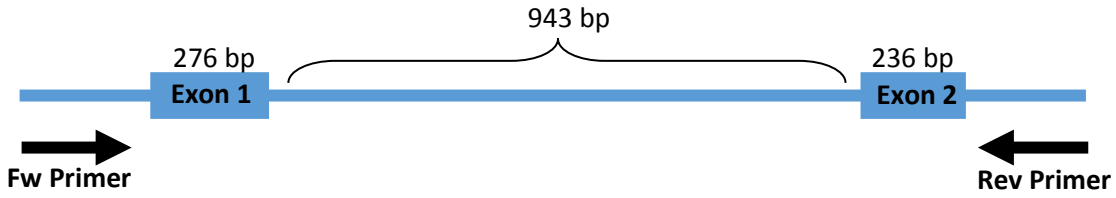


**Figure 1.1**. **Schematic drawing of the *DEFB103* gene and the position of the primers**. *DEFB103* contains two exons of 276bp (exon 1) and 236bp (exon 2), separated by one intron of 943bp. Primers are located flanking the gene.

### 1.2.5. Cloning

As *DEFB103* falls within a structural variation region, we decided to clone the PCR products with the aim of detecting the sequences of all the possible copies of *DEFB103* present in each sample. Had we sequenced PCR products directly, the sequence obtained would be the consensus sequence of all the copies of *DEFB103*. That strategy would have not allowed us detect variations that only appear on one copy out of the several possible, as if the sample has several additional copies that do not contain the variation this would have passed unnoticed. Only if the variation is present in ~50% of the copies per sample it could have been feasible to identify it with confidence. For that reason, we decided to clone the PCR products, and sequence 10-20 colonies per sample, in order to get the sequence individual copies of *DEFB103* (per sample). In this way, each colony would have a unique sequence of the gene, and it would be possible to sequence most of the copies individually.

Q5 High-Fidelity DNA polymerase generates PCR products with blunt ends, so before cloning, we added to the PCR products 3´ A-overhangs, which are needed for cloning in pCR™ 2.1-TOPO® vector. Thus, 4µl of purified PCR products were incubated with 1µl Taq polimerase (Bioline), 2µl dATP (1mM), 1µl of 10X Reaction Buffer (containing 160 mM $(NH_4)_2SO_4$ and 670 mM Tris-HCl (pH 8.8)) and 0.6µl $MgCl_2$ (25mM) for 20 minutes at 72ºC.

PCR products with 3´ A-overhangs were cloned into pCR™ 2.1-TOPO® vector using TOPO TA Cloning® Kit (Invitrogen, Life Technologies) following the manufacturer's protocol. After ligation of the insert and the vector, E.coli One Shot Top10, chemically competent cells were transformed with the vector. Then, transformed cells were seeded in tempered petri dishes with solid medium (LB broth with agar and ampicillin) for 24-48h. Before the seeding, IPTG (Isopropyl β-D-1-thiogalactopyranoside) and X-Gal (5-bromo-4-chloro-3-indolyl-β-D-galactopyranoside) (40mg/ml) were added to the petri dishes for blue/white screening of the colonies. White colonies, those containing the insert, were further grown in liquid LB medium with ampicillin for 24h. Plasmidic DNA was then isolated using the QIAprep Spin Miniprep kit (QIAGen, Hilden, Germany). Then, purified plasmid DNA was linearized by digestion with the restriction enzyme Hind-III (New England Biolabs). For digestion, 10µl of plasmid DNA were incubated with 20 units of Hind III and 2µl of 10X CutSmart Buffer, for 15 minutes at 37ºC, followed by 20 minutes at 80ºC. The digested products were again visualized by electrophoresis on a 1% agarose gel.

### 1.2.6. Resequencing

From every clone, 10-20 colonies were sequenced. Sequencing reactions were performed immediately after digestion using 10ng of PCR purified product, BigDye 3.1 Terminator Cycle Sequencing kit (Life Technologies) and primers flanking, but not including, the exons. We performed forward and reverse reactions for each exon, with the following primers: 5'-GCATACTTGCTCATGCCAGC-3'and 5'-TGGTCTTGAACTCCTGAC-3' for the first exon and 5'-CCACAAGCCTTGTACGTG-3' and 5'-GAATATCTGAGGAAGAGCCAG-3´ for the second exon). Thermocycling conditions included a denaturation step at 96ºC for 1 minute, followed by 35 cycles of 96ºC for 20 seconds, 58ºC for 20 seconds and 60ºC for 4 minutes, plus a final extension cycle of 60ºC for 10 minutes. Sequencing reaction products were then purified with Illustra™ Microspin G-50 Columns (GE Healthcare, Life Sciences, UK), and after adding 25µl of formamide they were run on an ABI 310 Genetic Analyzer (Applied Biosystems, Foster City, USA). Sequences were manually edited with Genalys v.2.8 (Takahashi et *al*., 2002).

***CNV analysis of DEFB103***

For Copy Number Variant (CNV) analysis, we used those samples from unrelated individuals living in the Basque Country collected by us. We analysed by RT-qPCR and digital PCR selected samples from the extremes of the distribution of pigmentation levels, measured by reflectance spectrometry: 29 of the most pigmented (<69.23) and 29 of the least pigmented (>74) individuals. We also analysed by digital PCR 356 samples from different regions of Spain from the Spanish National DNA Bank.

### 1.2.7. Copy number (CN) determination by real-time quantitative PCR (RT-qPCR)

Gene copy number analyses by RT-qPCR were initially performed on StepOne Real-Time PCR System (Applied Biosystems, Foster City, USA). We used target gene-specific primers and an oligonucleotide probe labelled with FAM dye designed by us. As a

reference gene, we used *DEFB1*, a beta-defensin gene that is also located in chromosome 8, but outside the block of beta-defensins, and has not been described to vary in copy number. Custom-designed primers and a VIC-labelled probe were used for *DEFB1* (Table 1.1).

**Table 1.1. Primer and probe sets used for β-defensin gene copy number analyses by RT-qPCR.**

| Gene | Oligonucleotide | Sequence (5´→ 3´) |
|---|---|---|
| ***DEFB103*** | Forward primer | TATGACAAGAATTGCAGCTGTGG |
| | Reverse primer | CCACGCTGAGACTGGATGAA |
| | Probe * | [6FAM]TTATAAAG[+T]GACC[+A]AGCACACCT[BHQ1] |
| ***DEFB1*** | Forward primer | GTCAGCTCAGCCTCCAAAGG |
| | Reverse primer | GCAGGCAACACCCAGGAT |
| | Probe * | [HEX]CCAGCGT[+C]TC[+C]CCAGTTCCTG[BHQ1] |

* [+N] indicates LNAs (Locked Nucleic Acids)

Data were analysed by the comparative Ct method. All comparisons between groups were performed using Fisher exact test.

### 1.2.8. Copy Number determination by Digital PCR (dPCR)

Digital PCR (dPCR) was also used to calculate de copy number of beta-defensin 103 (*DEFB103*). dPCR was performed by means of a QuantStudio™ 3D Digital PCR System (Thermo Fisher Scientific), using Digital PCR 20K Chips. These chips are high-density nanofluidic chips which contain 20,000 reaction wells to partition a sample into thousands of independent PCR reactions. When performing a PCR, some of these wells will contain a target molecule and will be amplified (positives) and some wells will not contain any molecule and there will not be amplification (negatives).

We used a FAM™ dye–labeled Custom Taqman Copy Number Assay for *DEFB103* (Cat. No. 4400291) and VIC™ dye–labeled TaqMan™ Copy Number Reference Assay for RNase P (Cat. No. 4403326), as a reference of 2 copies per diploid genome.

Reaction mixes were set up containing the QuantStudio™ 3D Digital PCR Master Mix v1, TaqMan Copy Number Assay for *DEFB103*, RNase P Reference Assay, and genomic DNA (gDNA) sample. A total volume of 15µL PCR reaction mix was prepared for each sample, and 14.5µL was loaded onto the chip.

For optimal dPCR results, each reaction well in the chip should receive, on average, 0.6–1.6 copies of the target sequence. To fit to these values, the recommended final DNA concentration on the chips is 2.29-6.1 ng/µl. However, an initial optimization of the optimal DNA concentration should be done. The concentration of the gDNA used was of 30ng/µl (5ng/µl in the chip). Amplification was done using the ProFlex™ flat PCR System and chips were read on the QuantStudio® 3D Digital PCR System. PCR conditions were set as recommended from ThermoFisher: a denaturation step at 96ºC for 10 minutes, followed by 39 cycles of 60ºC for 2 minutes and 98ºC for 30 seconds, plus a final extension cycle of 60ºC for 2 minutes and a final holding step at 10ºC.

Data analysis was performed with the AnalysisSuite Cloud Software v3.1.4 (Applied Biosystems), applying a Poisson model as quantification algorithm to estimate the number of copies per microliter of the target molecules. The genomic copy number of *DEFB103* was determined as:

$$\frac{DEFB103\ copies/ul}{RNaseP\ copies/ul}\ x\ 2$$

Differences in the distribution of copy numbers between groups was analysed by Mann-Whitney's U-test and by Fisher's exact test or Chi-Square test.

## 1.3. Results and Discussion

### 1.3.1. Skin color (Reflectance) distribution in the sample set collected from donors living in the Basque Country

Skin pigmentation was measured in 650 individuals (415 females and 235 males) living in the Basque Country by means of reflectance spectrophotometry in the first sampling. Skin reflectance values ranged from 54.5 to 80 and followed a near normal distribution, although Kolmogorov-Smirnov test indicated that the distribution is not normal ($p = 0.001$) (Figure 1.2). Mean reflectance values were 69.48 and 69.28 for females and males respectively and there were not differences between sexes (Mann-Whitney U-test: $p = 0.775$) (Figure 1.3).

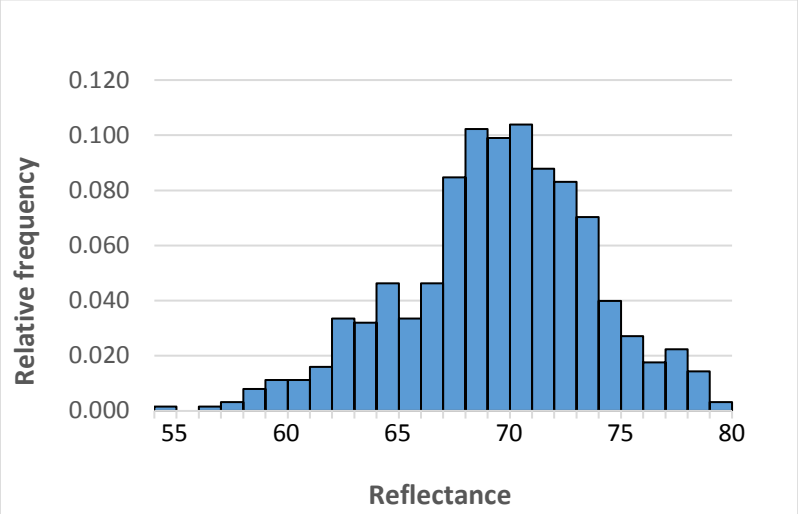


**Figure 1.2 Distribution of skin reflectance values for Spanish individuals, males and females together, living in the Basque Country.**

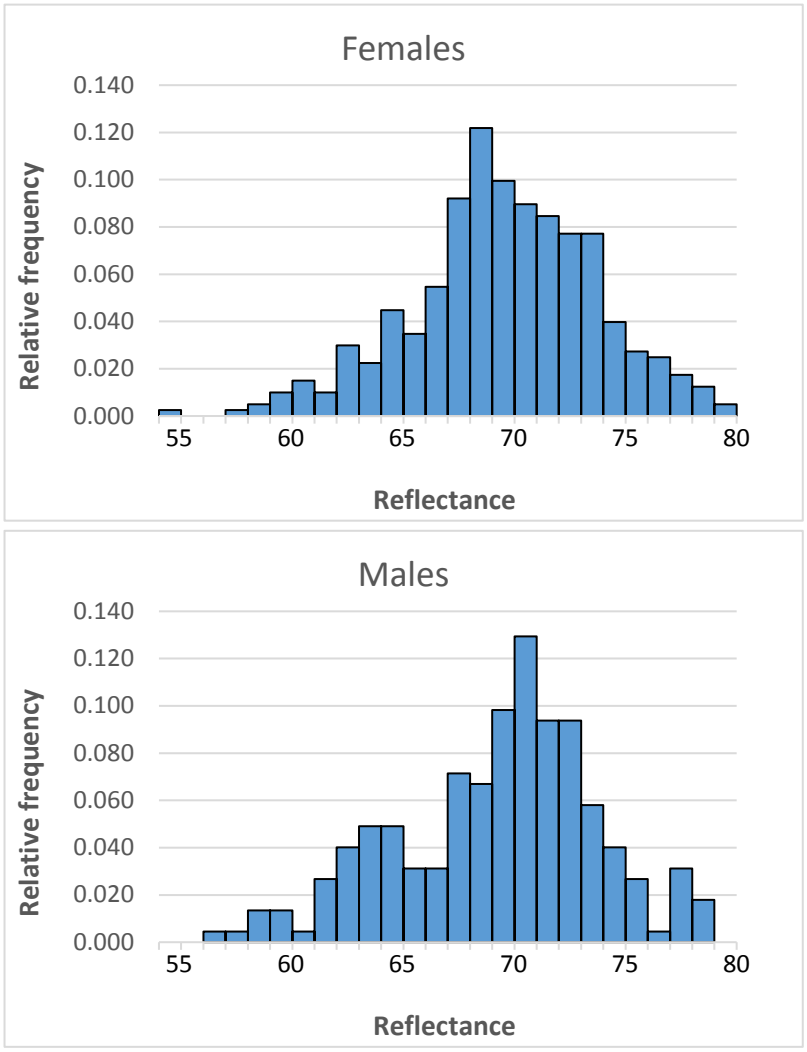


**Figure 1.3. Distributions of skin reflectance values for Spanish individuals living in the Basque Country, separated by sex**. Distributions show no statistical differences (Mann-Whitney U-test: p = 0.775).

Population stratification analysis had been previously performed by López et *al*. (2014). Briefly, the 34 most and the 34 least pigmented individuals were genotyped using the Genome-wide Human SNP Array 6.0 (Affymetrix, Santa Clara, CA). A total of 106,521 SNPs were used for population stratification analysis by means of EIGENSOFT 4.2 package (http://genetics.med.harvard.edu/reich/Reich_Lab/Software.html), which computes the Tracy-Widom statistics to evaluate the statistical significance of each principal component identified. To further assess a possible substructure, 15 STRs were

also typed and results were analyzed with the software STRUCTURE v.2.3.3, which uses a Bayesian model-based clustering algorithm to infer the number of genetically distinct groups represented in a sample.

In a second sampling period, 617 samples from the same population were collected. The procedure for data and sample collection was the same. In this second sample set, mean reflectance value was 68.89 and the reflectance distribution was also not normal (Kolmogorov-Smirnov test: p = 0.002) (Figure 1.4). Mean reflectance values for females (N = 454) and males (N = 163) were 68.92 and 68.81 respectively and there were not differences between sexes (Mann-Whitney U-test: p = 0.643) (Figure 1.5).

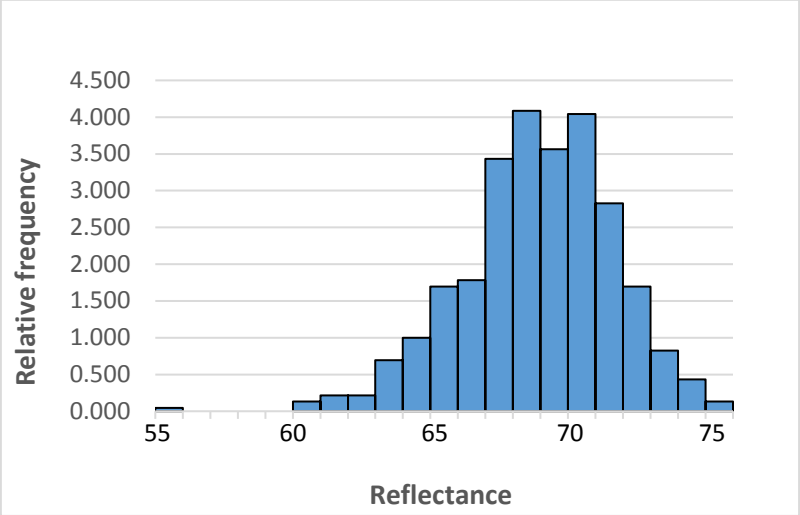


**Figure 1.4. Distribution of skin reflectance values for Spanish individuals living in the Basque Country from the second sample collection.**

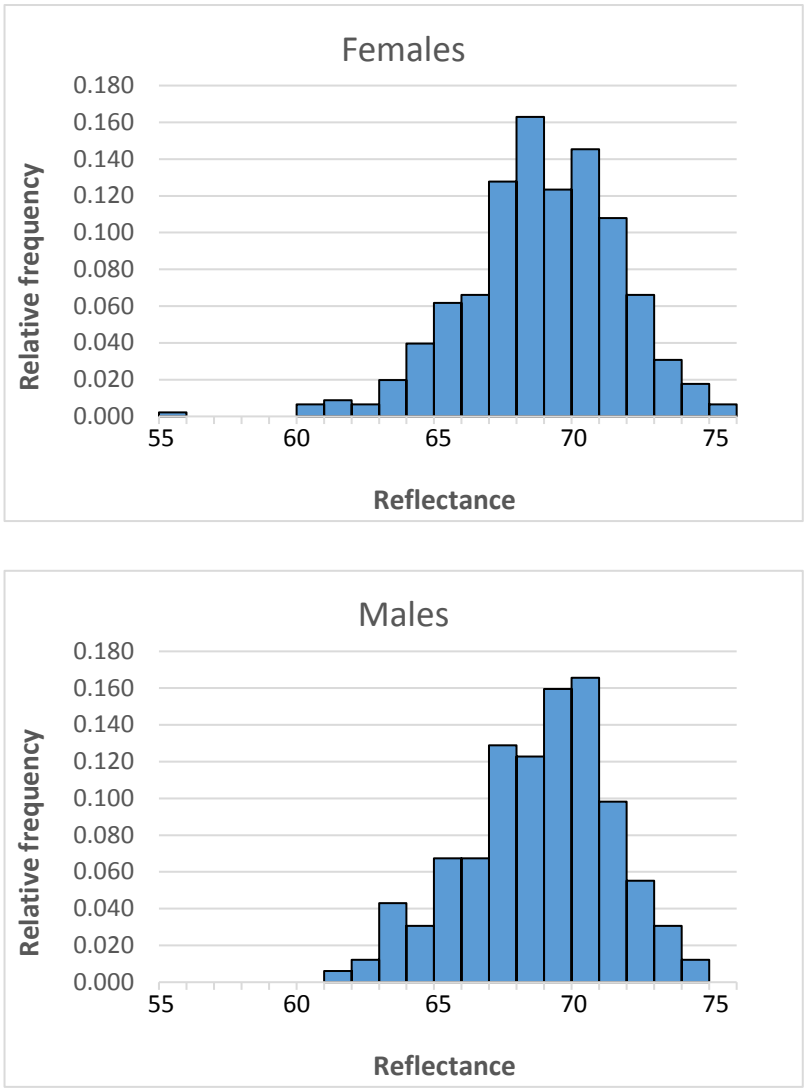


**Figure 1.5. Distributions of skin reflectance values for Spanish individuals living in the Basque Country from the second sample collection, separated by sex**. Distributions show no statistical differences (Mann-Whitney U-test: p = 0.643).

As expected, there were not statistical differences between the two sample sets regarding skin reflectance values (Mann-Whitney U-test: p = 0.473). Thus, for some of the subsequent analyses, in order to increase the sample size, we dedided to join all samples and analyse them as one population. Also, as there were either not statistical differences between sexes we decided to analyse females and males together. For subsequent analyses individuals from the extremes of the reflectance distribution were selected, i.e. the least pigmented (right tail) and the most pigmented (left tail) individuals.

### 1.3.2. Analysis of sequence variability: resequencing of *DEFB103*

For the analysis of *DEFB103* sequence variability we selected seven of the more pigmented and six of the less pigmented individuals from the Spanish population. We also resequenced 30 individuals from other populations: 15 Africans, 5 Asians, 5 Australians and 5 Europeans (as described in Material and Methods). In total, we sequenced about 750 bp in 43 individuals.

Among the 43 samples resequenced we detected 30 variants within the exons and part of the adjacent intron sequence. These variants comprised 26 SNPs, 3 insertions and 1 deletion (Table 1.2). The majority of the variants were rare, appearing only in one or a few samples.

Within the exons' sequence, we found eight variants, six in untranslated regions and two in the coding regions: one non-synonymous substitution in the first exon and a deletion of 1 bp in the second exon, which causes a change in the reading frame, producing a shorter protein. Among the eight variants, two were not present in dbSNP (154) (April 21, 2020). In total, 15 of the variants have not been described in dbSNP. All the variations found in 5'UTR and coding region were only observed in samples from Africa. The two variants found in the 3'UTR region were also present in samples from other continents.

**Table 1.2**. **Sequence variations found in *DEFB103* gene. Position of the variants is based on one of the chromosomic positions of *DEFB103* (chr8:7881204-7882664). Coordinates corresponding to the GRCh38/hg38 ssembly.**

| Position (GRCh38/hg38) | Function | Class (Alleles) | Reference number |
|---|---|---|---|
| chr8:7881358 | 5´UTR variant | SNP (C/A) | Not in dbSNP |
| chr8:7881383 | 5´UTR variant | SNP (T/G) | rs868060132 |
| chr8:7881404 | 5´UTR variant | SNP (G/A) | rs202127294 |
| chr8:7881405 | 5´UTR variant | SNP (G/A) | rs867429834 |
| chr8:7881435 | Missense variant | SNP (A/G) | rs866766054 |
| chr8:7881575 | Intron variant | SNP (A/G) | Not in dbSNP |
| chr8:7881576 | Intron variant | SNP (G/T) | Not in dbSNP |
| chr8:7881595 | Intron variant | SNP (A/T) | Not in dbSNP |
| chr8:7881611 | Intron variant | SNP (T/C) | Not in dbSNP |
| chr8:7881690 | Intron variant | SNP (C/T) | Not in dbSNP |
| chr8:7881691 | Intron variant | SNP (G/A) | rs865925547 |
| chr8:7881693 | Intron variant | SNP (A/T) | Not in dbSNP |
| chr8:7881697 | Intron variant | SNP (C/G) | rs3789862 |
| chr8:7881708 | Intron variant | SNP (G/A) | rs868833983 |
| chr8:7881734 | Intron variant | SNP (T/C) | Not in dbSNP |
| chr8:7881739 | Intron variant | Insertion (-/C) | Not in dbSNP |
| chr8:7881767 | Intron variant | SNP (A/G) | Not in dbSNP |
| chr8:7881836 | Intron variant | SNP (C/T) | Not in dbSNP |
| chr8:7881844 | Intron variant | SNP (C/T) | Not in dbSNP |
| chr8:7881900 | Intron variant | SNP (G/T) | Not in dbSNP |
| chr8:7881908 | Intron variant | SNP (A/G) | rs1301545701 |
| chr8:7881916 | Intron variant | SNP (A/T) | Not in dbSNP |
| chr8:7882333 | Intron variant | SNP (G/A) | rs768045203 |
| chr8:7882544 | Nonsense variant | Deletion (A/-) | Not in dbSNP |
| chr8:7882647 | 3´UTR variant | Insertion (-/T) | rs1171126592 |
| chr8:7882661 | 3´UTR variant | SNP (A/C) | rs201695119 |

The non-synonymous substitution observed in the first exon, rs866766054, was only present in one individual from North Sahara. The variation implies an amino acidic change from tyrosine to cysteine on the fifth amino acid. The amino acid is located in the signal sequence of the peptide (amino acids 1-22). The functional consequences of this change are not known. However, the change is predicted to be benign according to the databases PolyPhen-2 (http://genetics.bwh.harvard.edu/pph2/index.shtml) and SIFT (https://sift.bii.a-star.edu.sg/www/SIFT_seq_submit2.html).

The deletion found in the second exon causes changes in the reading frame from the 61 amino acid onwards, resulting in a longer protein of 71 amino acids. In particular, the deletion implies the change of the cysteines in the positions 62 and 63 to two alanines. These cysteines take part in the disulphide bridges, which are fundamental for the structure of the β-defensin. Thus, the resulting protein is likely non-functional.

### 1.3.3. CNV analysis of DEFB103

In humans, *DEFB103* is within a copy number region that can vary between 1 and 12 copies per diploid genome. We aimed at investigating if copy number variation of this cluster could be related to pigmentation diversity in humans.

Thus, we analysed the variability in copy number of *DEFB103* by means of Taqman assays in samples with known pigmentation level, measured by reflectance spectrometry. In a first analysis, forty individuals were included in the study, 20 of the higher and 20 of the lower pigmentation level groups.

First, we determined the copy number by RT-qPCR in a Step-ONE machine (Life Technologies). The copy numbers observed (CN) ranged from 2 to 7 (median, 2), with numbers higher than 4 uncommon (Table 1.3). We compared the CN distribution between groups of different pigmentation level, and did not find statistical differences (Fisher exact test: $p = 0.4192$).

**Table 1.3**. **Comparison of the Copy Number determination by RT-qPCR and dPCR on samples with different pigmentation level.**

| Sample ID | Phenotype | Reflectance (*L) | *DEFB103* Copy Number | |
|---|---|---|---|---|
| | | | RT-qPCR | dPCR |
| 1 | most pigmented | 61.97 | 2 | 4 |
| 2 | most pigmented | 62.47 | 4 | 3 |
| 3 | most pigmented | 64.73 | 2 | 4 |
| 4 | most pigmented | 64.77 | 1 | 2 |
| 5 | most pigmented | 64.97 | 3 | 3 |
| 6 | most pigmented | 65.03 | 2 | 3 |
| 7 | most pigmented | 66.13 | 3 | 5 |
| 8 | most pigmented | 66.20 | 2 | 4 |
| 9 | most pigmented | 66.39 | 2 | 4 |
| 10 | most pigmented | 66.53 | 3 | 5 |
| 11 | most pigmented | 66.63 | 7 | 6 |
| 12 | most pigmented | 66.70 | 3 | 7 |
| 13 | most pigmented | 66.80 | 5 | 4 |
| 14 | most pigmented | 67.13 | 2 | 5 |
| 15 | most pigmented | 67.20 | 4 | 4 |
| 16 | most pigmented | 67.27 | 2 | 4 |
| 17 | most pigmented | 67.33 | 1 | 4 |
| 18 | most pigmented | 67.33 | 1 | 4 |
| 19 | most pigmented | 67.37 | 1 | 3 |
| 20 | most pigmented | 67.50 | 2 | 4 |
| 21 | least pigmented | 74.97 | 2 | 4 |
| 22 | least pigmented | 75.00 | 2 | 5 |
| 23 | least pigmented | 75.03 | 2 | 4 |
| 24 | least pigmented | 75.17 | 2 | 4 |
| 25 | least pigmented | 75.20 | 3 | 5 |
| 26 | least pigmented | 75.27 | 1 | 2 |
| 27 | least pigmented | 75.40 | 2 | 5 |
| 28 | least pigmented | 75.50 | 2 | 4 |
| 29 | least pigmented | 75.80 | 2 | 4 |
| 30 | least pigmented | 75.90 | 1 | 3 |
| 31 | least pigmented | 76.10 | 1 | 3 |
| 32 | least pigmented | 76.17 | 2 | 4 |
| 33 | least pigmented | 76.50 | 2 | 5 |
| 34 | least pigmented | 77.10 | 2 | 6 |
| 35 | least pigmented | 77.63 | 2 | 4 |
| 36 | least pigmented | 77.97 | 1 | 4 |
| 37 | least pigmented | 78.03 | 2 | 5 |
| 38 | least pigmented | 78.13 | 2 | 4 |
| 39 | least pigmented | 78.23 | 2 | 5 |
| 40 | least pigmented | 79.67 | 2 | 4 |

The copy number distribution of our sample set, was unusual comparing with data reported by other authors for a European population, in which median copy number is used to be around 4 (Hollox, 2008; Wain et *al*., 2014). Besides, in 13 samples, we estimated the minimum copy number, based on the number of different sequences found by clone resequencing, assuming that the samples have at least the number of different sequences found. When comparing both results, we observed that in three cases, the minimum number of copies was higher than the total copy number estimated by qPCR (Table 1.4), suggesting that the CN calls from qPCR were underestimated in general.

**Table 1.4**. **Copy number determination by RT-qPCR and the minimum copy number estimated from clone resequencing on 13 samples with different pigmentation level.**

| Sample | Copy Number (RT-qPCR) | Minimum CN (Resequencing) |
|---|---|---|
| 1 | 2 | 2 |
| 2 | 2 | 4 |
| 3 | 5 | 2 |
| 4 | 1 | 4 |
| 5 | 3 | 2 |
| 6 | 1 | 4 |
| 7 | 2 | 1 |
| 8 | 3 | 4 |
| 9 | 4 | 3 |
| 10 | 1 | 3 |
| 11 | 3 | 1 |
| 12 | 2 | 2 |
| 13 | 1 | 1 |

Real-time quantitative PCR (RT-qPCR) has been broadly used to analyse copy number variation (Fellermann et *al*., 2006; Fernández-Jiménez et *al*., 2010; Abe et *al*., 2013; Willie et *al*., 2017). However, given the results obtained, we decided to use digital PCR to get a more accurate calling of copy numbers.

With dPCR, we are able to overcome some of the problems of RT-qPCR. Firstly, dPCR does not need standard curves, as it does absolute quantification, based in end-point

PCR. Secondly, as it performs a linear detection of small-fold changes, there is no need to worry about PCR efficiency. Thirdly, it has higher tolerance for inhibitors. Lastly, dPCR has higher accuracy and sensitivity.

Thus, we determined CN of the same sample sets by dPCR (Table 1.3) and added more samples from the extremes of the pigmentation level distribution. In total, we determined the CN in 122 samples: 58 of the most pigmented and 64 of the least pigmented individuals. The copy numbers now ranged from 2 to 7 (median, 4) and there weren't differences regarding sex. Copy number distribution was not normal (Kolmogorov-Smirnov test: p = 0.000), and we did not observe differences in the CN distribution between groups with different pigmentation levels (Mann-Whitney U-test: p = 0.333) (Figure 1.6, Table 1.5).

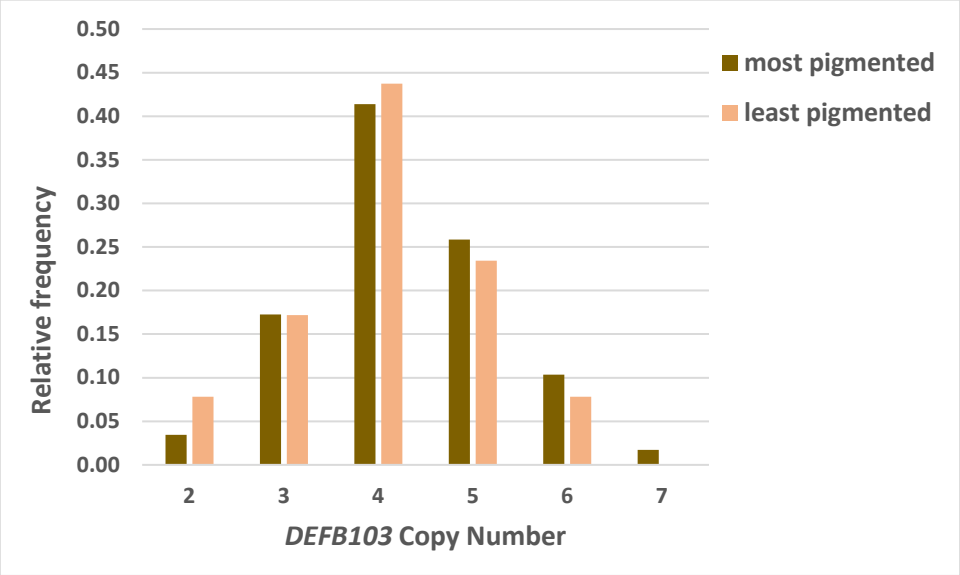


**Figure 1.6**. **Copy number distribution of the samples from the extremes of the reflectance distribution (the most and least pigmented individuals) from dPCR results.** Mann-Whitney U-test: p = 0.592.

**Table 1.5. Copy number determination by dPCR in the 58 of the most pigmented and 64 of the least pigmented individuals.**

| Copy Number | Most pigmented | Least pigmented |
|---|---|---|
| **2** | 2 | 5 |
| **3** | 10 | 11 |
| **4** | 24 | 28 |
| **5** | 15 | 15 |
| **6** | 6 | 5 |
| **7** | 1 | 0 |

Then, we determined CN of *DEFB103* by dPCR in 568 samples from different regions of Spain (with all grandparents from the same region), from the Spanish National DNA Bank: 284 males and 284 females. Copy numbers ranged from 1 to 8 and the median was 4 and there were not statistically significant differences regarding sex (Mann-Whitney U-test: p = 0.330). We also grouped the samples in bins of <4 copies, 4 copies and > 4 copies and observed no significant differences in the frequencies (Chi-Square Test, p= 0.4426) (Figure 1.7, Table 1.6).

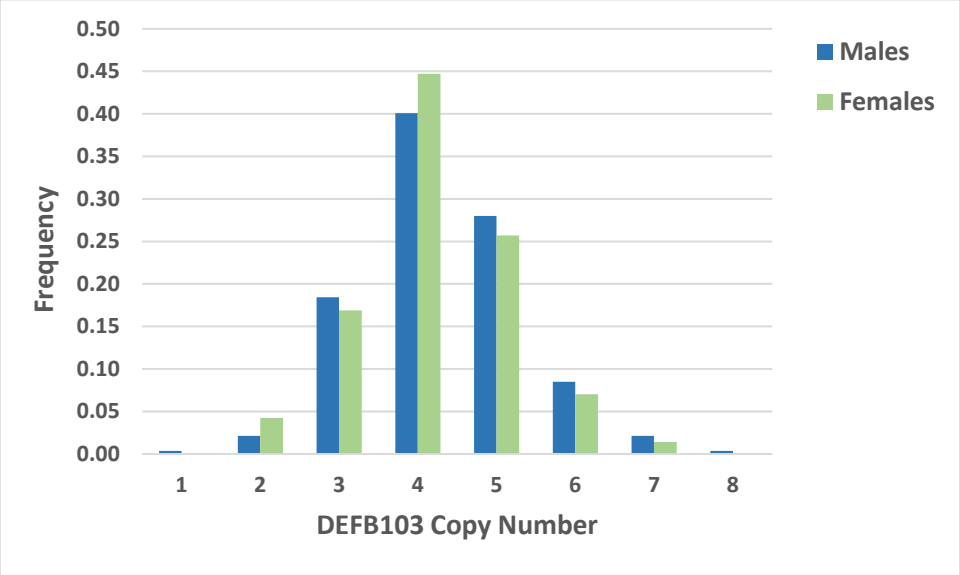


**Figure 1.7. Copy number distribution of the samples from the Spanish National DNA Bank.**

**Table 1.6**. **Copy number determination by dPCR in the 568 samples from the Spanish National DNA Bank.**

| Copy Number | Females | Males |
|---|---|---|
| **1** | 0 | 1 |
| **2** | 12 | 6 |
| **3** | 48 | 52 |
| **4** | 127 | 113 |
| **5** | 73 | 79 |
| **6** | 20 | 24 |
| **7** | 4 | 6 |
| **8** | 0 | 1 |

Next, we wanted to analyse if there were differences related with solar irradiation. To try to correlate the daily annual average of incident UV-B radiation ($J/m^2$) with *DEFB103* copy number, we used a UV-radiation map of Spain, previously elaborated by our group from surface UV-B data (from 1995 to 2010, although not for all the provinces) supplied by AEMET (the Spanish National Meteorological Agency), who used sixteen meteorological stations spread over the Spanish territory.

A positive correlation was found between copy number and UV-B surface irradiation (Pearson's correlation coefficient = 0.135; bilateral p-value = 0.004), still significant excluding Canary Islands (Pearson's correlation coefficient = -0.118, bilateral p-value = 0.012). Next, we selected groups based on the UV-B surface irradiation values and compared the copy number distribution of *DEFB103* between them. The groups were made based on the percentiles of UV-B radiation values: We compared the copy number distribuction of individuals of provinces that lie in the lower $15^h$ percentile versus those of provinces above the $85^{th}$ percentile of UV-B surface irradiation. The election of the percentiles was made with the intention of achieving a good balance between maintaining the extremes of the distribution of UV-B surface irradiation and at the same time, maintaining a good sample size. The provinces included in the $15^{th}$ percentile were

Asturias, Bizkaia, Gipuzkoa, Araba, Cantabria, Lugo, Navarre and La Coruña, all of them from the North of Spain, while in the 85$^{th}$ percentile were included Canary Islands, Cadiz, Granada, Almería, Huelva, Cáceres, Seville and Jaen, all of them from the South of Spain (for the possible exception of the Canary Islands, see below). We observed significant differences in the copy number distribution (Mann-Whitney U-test: p = 0.022). We also grouped the samples in bins of <4 copies, 4 copies and > 4 copies and observed significant differences in the frequencies (Chi-Square Test, p= 0.0078) (Tables 1.7 a, b). The distribution of individuals from the 15$^{th}$ percentile is shifted toward lower copy numbers (Figure 1.8). When we separate the samples by the sex, this difference is only significant for males (Mann-Whitney U-test: p = 0.009; Fisher exact test: p = 0.0133), but not for females (Mann-Whitney U-test: p = 0.566; Fisher exact test: p = 0.1063).

We also tested if the differences were maintained after removing Canary Islanders from the sample, because the population from Canary Islands is distint from that of the Iberian Peninsula, due to their distinct geographical location, history and African ancestry. In this case (when excluding individuals from Canary Islands), the differences were also significant (Mann-Whitney U-test: p = 0.038; Chi-Square Test, p = 0.0160); and again, when analysing by sexes, it was only significant for males (Mann-Whitney U-test: p = 0.025; Chi-Square Test, p= 0.0385).

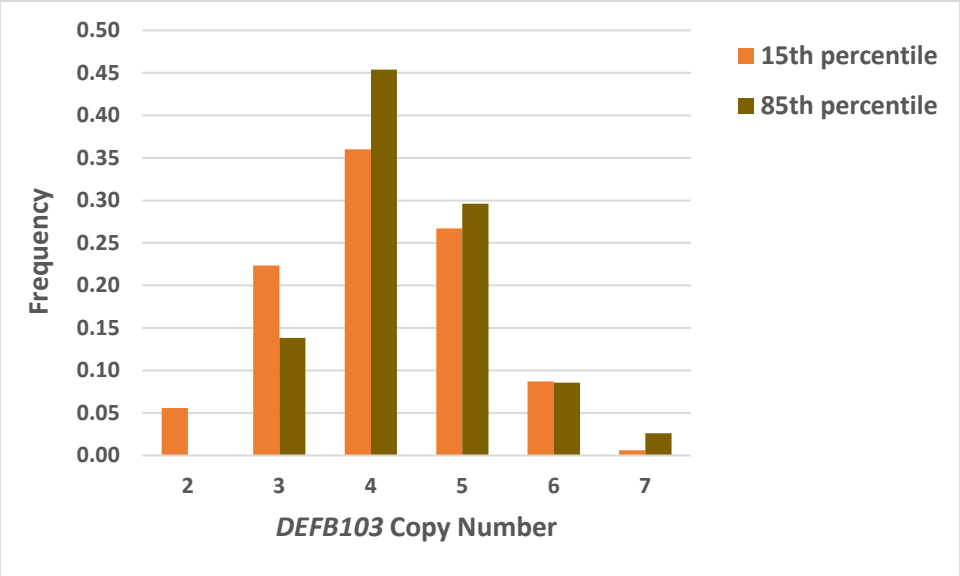


**Figure 1.8. Copy number distribution of the individuals from the 15th and 85th percentiles (regarding UV-B irradiation) from Spanish National DNA Bank.**

**Table 1.7a. Comparison of *DEFB103* copy number frequencies for the bins <4, 4 and >4 copies, between individuals from 15th and 85th percentiles (absolute frequency and relative frequency between brackets).** Chi-Square Test, p= 0.0078.

| CN set | N (Relative frequency) | |
|---|---|---|
| | 15th percentile | 85th percentile |
| **< 4 copies** | 45 (0.28) | 21 (0.14) |
| **4 copies** | 58 (0.36) | 69 (0.45) |
| **> 4 copies** | 58 (0.36) | 63 (0.41) |

**Table 1.7b. Comparison of *DEFB103* copy number frequencies for the bins <4, 4 and >4 copies, between individuals from 15th and 85th percentiles, separated by sex (absolute frequency and relative frequency between brackets).** Fisher exact test for females (p = 0.1063) and males (p = 0.0133).

| CN set | Females | | Males | |
|---|---|---|---|---|
| | N (relative frequency) | | N (Relative frequency) | |
| | 15th percentile | 85th percentile | 15th percentile | 85th percentile |
| **< 4 copies** | 21 (0.26) | 12 (0.16) | 24 (0.30) | 9 (0.12) |
| **4 copies** | 29 (0.36) | 39 (0.51) | 29 (0.36) | 30 (0.39) |
| **> 4 copies** | 31 (0.38) | 25 (0.33) | 27 (0.34) | 38 (0.49) |

Our results suggest that at least in Spanish population there could be an association between copy number of *DEFB103* and solar irradiation, given that previous work have indicted lack of general population structure (López et al, 2014) . Although the median copy number in all the groups analysed is 4, and the distributions are similar, there is a small tendency in the areas with less UV-B irradiation to have higher frequencies of lower copy numbers than in the areas with more UV-B irradiation.

***CN data from other sources***

In order to analyse the CN of β-defensins in other populations, we used copy number data reported by Forni et *al*. (2015). To our knowledge, this study uses the highest number of samples from the highest number of different populations. They used high-coverage phase 3 exome sequences of the 1000 Genomes project to infer diploid copy number of the β-defensin genomic region. They determined the copy number in 2455 samples from 26 populations. The range of common variation in all the continental populations goes from 2 copies to 8 copies per diploid genome and the modal copy number is 4 in all but one. In sub-Saharan Africans, the modal CN is 5. We compared copy number distributions among continental populations, and observed that there is a

statistically significant difference (Mann-Whitney U-test) between sub-Saharan Africans and the rest of populations (Table 1.8). We also observed significant differences when grouping the copy numbers in three bins (<4 copies, 4 copies and > 4 copies) (Table 1.8). The differences are still significant after Bonferroni correction for multiple testing, except for Shout European population. In this population, there is also a tendency towards higher copy numbers (>4). In fact, although the difference does not reach statistic significance (Chi-Square Test: p = 0.0547) in comparison with North European population, Shout Europeans have a higher relative frequency for > 4 copies.

**Table 1.8. Comparison of the copy number distribution between Africans and different populations from the 1000G project.**

| Population | Mann-Whitney U-test (corrected p-values) | Chi-Square Test (corrected p-value) |
|---|---|---|
| **North European** | 0.001 * | 0.0001 * |
| **South European** | 0.003 * | 0.0420 |
| **East Asian** | 0.000 * | 0.0005 * |
| **South Asian** | 0.010 * | 0.0070 * |

***** Significant after Bonferroni correction

## 1.4. Conclusions

One of our aim was to analyse sequence diversity of *DEFB103* in order to search for a variant that, similarly to the one observed in dogs, could be involved in human pigmentation. Although we detected some new variants, they were rare. The two variations observed in the coding region and the four variations observed in 5'UTR region were only present in African samples. Therefore, it seems that sequence variation do not regulate pigmentation in humans. However, our data suggest a possible association between *DEFB103* copy number and surface UV-B irradiation, at least in the Spanish sample analysed.

# Chapter 2.

## Comparative analysis of the influence of UV irradiation on *DEFB103* expression in keratinocytes

## 2.1. Introduction

Keratinocytes actively contribute to the the cutaneous defence. In this sense, they express and secrete antimicrobial peptides (AMPs), including β-defensins (Ali et *al*., 2001; Harder et *al*., 2001; Supp et *al*., 2004).

In normal conditions, the expression level of most of the β-defensins is low, especially that of human β-defensin 103 (*DEFB103*) (Kim et al., 2002; Harder et al., 2010; Wittersheim et al., 2013). However, they are upregulated in response to several pathogens or inflammation conditions (Ali et al., 2001; Ganz, 2003; Dhople et al., 2006). *DEFB103* is also highly expressed in some skin diseases, such as psoriasis (Niyonsaba et *al*., 2017) and at wound sites (Sørensen et *al*., 2003).

Interestingly, some authors have reported that Ultra Violet (UV) light is also able to increase the expression of *DEFB103* in HaCat cells (Kim et *al*., 2003), or in normal human keratinocytes and *ex vivo* explants of adult skin (Gläser et *al*., 2009). However, the influence of UV radiation is not clear. Wolf Horrell and D'Orazio (2014) reported that UV exposure of e*x vivo* neonatal skin explants did not induce *DEFB103* expression, as they observed an increase in *DEFB103* levels over time both in untreated controls and in irradiated explants, which led to suggest that the observed increase was independent of the UV irradiation.

Keratinocytes play an important role on the regulation of skin pigmentation in response of UV radiation, thought the secretion of melanogenic factors, such as α-MSH or endothelins. As UV irradiation is one of the most relevant external factors influencing skin pigmentation, determining its implication on *DEFB103* expression is important to understand if *DEFB103* is indeed an UV-inducible factor, which could modulate skin pigmentation. Thus, our aim was to further investigate the influence of UV-B irradiation on the expression of *DEFB103* in human keratinocytes. In this sense, in order to have an idea of the biological relevance of the response, we also wanted to compare the

strength of the response to UV with that to a pathogenic stimulus, as pathogens are the natural inducers of β-defensins.

Vitamin D has also been linked to the modulation of expression of some β-defensins. Dai et *al*. (2010) reported that in keratinocytes treated with $10^{-7}$M 1α,25-dihydroxyvitamin D3 (the active form of vitamin D), the expression of *DEFB103* was upregulated. De Filippis et *al*. (2017) also observed an increase in *DEFB103* expression in human gingival epithelium after treatment with vitamin D.

Genetic variation has also been reported to influence the expression of some β-defensins. On the one hand, Copy Number (CN) of β-defensins is though to be correlated with their expression level (Hollox et al., 2003; Groth et al., 2010). On the other hand, sequence variations have been reported to also affect the expression of different β-defensins. The single nucleotide polymorphism (SNP) rs2737902, upstream *DEFB103,* has been reported to influence the expression level of the peptide (Hardwick et al., 2011). Besides, as there are differences between dark and light skin in the response to UV (López et al., 2015a,b), the pigmentary phenotype could also influence the response to UV on the expression of *DEFB103.*

Therefore, we aimed at measuring the effect of UV-B in *DEFB103* expression in human normal keratinocytes in donors of different pigmentary phenotype, in order to further investigate if a) UV-B irradiation affects *DEFB103* expression, b) skin pigmentation level influences the expression of *DEFB103* c) the response to UV-B in comparison to against a bacterial stimulus or to active vitamin D. Besides, we also analysed the expression related SNP (rs2737902).

## 2.2. Material and Methods

### 2.2.1. Cell Cultures

Normal human epidermal keratinocytes (NHEKs) were purchased from Cell Applications Inc. (San Diego, CA, USA): three lines isolated from lightly pigmented neonatal foreskin (NHEK-LP) and three lines from darkly pigmented neonatal foreskin (NHEK-DP). Cells were cultured in EpiLife medium with 60 µM calcium (Cascade Biologics, Life technologies, Carlsbad, CA, USA) supplemented with human keratinocyte growth supplement (HKGS), consisting of 0.2 ng/ml human recombinant epidermal growth factor (EGF), 0.18 µg/ml hydrocortisone, 5 µg/ml insulin, 5 µg/ml transferrin and 0.2% bovine pituitary extract. All the cell lines were maintained in an incubator under an atmosphere of 5% $CO_2$ at 37°C. Media were refreshed every two days.

### 2.2.2. Cell culture conditions and stimulation

Cultured keratinocytes were exposed to different stimulants: Heat Killed *Staphylococcus aureus* (HKSA), purified Lipoteichoic Acid (LTA), vitamin D or Ultraviolet B light (UV-B) (for specific conditions see below). Cells were seeded in 6-well plates at a density of $2x10^4$ cells/well. When cultures reached a confluence of 70%, medium was removed, cultures were washed with PBS and medium was replaced by Epilife medium without supplements or conditioned medium.

*a) UV-B irradiation*

UV irradiation was performed in an ICH2 photoreactor (LuzChem, Canada), using UVB lamps (290–320 nm) at 37°C. Cultures were irradiated at 75 mJ/cm$^2$ UV-B, based on previous work of our lab (López et *al*., 2015a). The time of exposure for 75 mJ/cm$^2$ dose with our set of lamps was 3'12''. Irradiation of the cell cultures was done under normal incubation conditions. Immediately before irradiation, medium was replaced with Epilife

medium without supplements. Non-irradiated cultures used as controls were subjected to the same procedure but covered with aluminium foil.

*b) Stimulation with alternatives to Staphylococcus aureus*

Heat Killed *Staphylococcus aureus* (HKSA) and purified LipoTeichoic Acid (LTA) from *Staphylococcus aureus* were purchased from InvivoGen (San Diego, CA, USA). All experiments were approved by the Ethics Committee of The University of the Basque Country (M30_2018_177). HKSA stock solution ($10^{10}$ HKSA/ml) was prepared by rehydrating the lyophilized HKSA ($10^{10}$ cells) into 1ml of endotoxin-free water. LTA stock solution was prepared by resuspending 5 mg of LTA in 1 ml of sterile endotoxin-free water. Concentrations were selected based on the literature, thus final working solutions were HKSA ($10^{8}$ HKSA/ml) and LTA (100 ng/ml). Control cultures were incubated with Epilife medium alone.

c) *Incubation with biologically active vitamin D*

1α,25-Dihydroxyvitamin D3, the biologically active form of vitamin D3 ($1,25(OH)_2D_3$) was purchased from Sigma-Aldrich (St. Louis, MO, USA). A 10 µM stock solution was prepared in 95% ethanol. Working solution was $10^{-7}$M, diluted into Epilife medium. Control cultures were incubated with Epilife medium containing the same amount of ethanol used for vitamin D working solution.

### 2.2.3. *DEFB103* gene expression

Cells were harvested after the experiment by treatment with TrypLE Express (Life Technologies), centrifuged at 1500 rpm, for 5 minutes and resuspended in lysis buffer for subsequent mRNA extraction. RNA was extracted from the cell pellets by means of the RNAqueous kit (Ambion), following the manufacturers' protocol. Then RNA was DNAse-treated (DNA-free Kit, Ambion), and retrotranscribed using Maxima First Strand cDNA Synthesis (Thermo Fisher Scientific).

Quantification of the gene expression of *DEFB103* was done by means of Real Time Quantitative PCR (RT-qPCR). Initially, RT-qPCR was performed in a Step-One thermocycler (Life Technologies), and analyses were performed using SYBR Green reagents (Life technologies). Expression was normalized to the reference housekeeping gene *GAPDH*. The following primers were used: for *DEFB103*: 5´-TTCCAGGTCATGGAGGAATC-3´ and 5´-CTTCGGCAGCATTTTCGG-3´and for *GAPDH*: 5´-CGACCAAATCCGTTGACTCC-3´and 5´-CCTGTTCGACAGTCAGCCG-3´. Four replicates were performed for each sample. Given the low expression observed, expression was subseqeuntly measured with Taqman probes. A TaqMan® Gene Expression Assay was used for the quantification of *DEFB103* cDNA (Assay ID: Hs04194486_g1; FAM™ dye–labelled) (Thermo Fisher Scientific), and the expression of the housekeeping gene *GAPDH* was used again for normalization (Assay ID: Hs02758991_g1, VIC™ dye–labelled).

As this was not still fully satisfactory due to the low expression level of *DEFB103*, to further increase the sensitivity of the analysis, digital PCR (dPCR) was performed with the QuantStudio 3D Digital PCR System (Thermo Fisher Scientific) on the same set of samples. The analysis was performed with the same Taqman assays as with RT-qPCR. In the first experiments, we set up the PCR reaction as recommended by the manufacturers: the reaction contained 7.5µl of QuantStudio™ 3D Digital PCR Master Mix v.1, 0.725µl of each 20x TaqMan® Gene Expression Assays (Hs04194486_g1 and Hs02758991_g1) and 45-90ng of cDNA sample. A total volume of 15µL PCR reaction mix was prepared for each sample, and 14.5µL was loaded onto the chips. Thermocycling conditions were as follows: 96 ºC for 10 minutes, followed by 39 cycles of 55 ºC for 2 minutes and 98 ºC for 30 seconds, plus a final cycle of 60 ºC for 2 minutes.

As the expression of *DEFB103* was many times lower than that of *GAPDH*, the correct evaluation of *DEFB103* expression was challenging, even after attempting to optimize the reaction set-up. Consequently, we decided to perform the dPCR reactions for

*DEFB103* and *GAPDH* separately, in different dPCR chips. In this way, we added different amounts of cDNA for each gene, allowing thus a correct measurement of the expression of both genes.

The number of copies per microliter was estimated by means of the AnalysisSuite Cloud Software v.3.1.4 (Applied Biosystems). The expression level of *DEFB103* was reported as the ratio between *DEFB103* (copies/µl) and *GAPDH* (copies/µl).

### 2.2.4. Copy Number determination of the *DEFB103* locus in cell lines

As mentioned before, cells were seeded in 6-well plates at a density of $2x10^4$ cells/well. For every cell line, one of the wells was used for DNA extraction. Cells were harvested by treatment with TrypLE Express (Life Technologies) and centrifuged at 5000 rpm for 5 minutes. Then, DNA was isolated from cell pellets following a standard phenol-chloroform protocol. Isolated DNA quantitation was performed by spectrophotometry by measuring absorbance at 260nm, and DNA purity was assessed by the ratio of absorptions at 260nm vs 280nm (A260/280). Copy number determination of *DEFB103* was calculated by Digital PCR, as described before (see section 1.2.8 of Chapter 1).

### 2.2.5. HDB3 protein production: Enzyme-linked immunosorbent assay (ELISA)

Supernatants from two cell lines (1 NHEK-LP and 1 NHEK-DP) of the cultured keratinocytes described above were also analysed for the production of secreted HBD3. Thus, 100µL of supernatant of each cell culture was measured using ELISA (Phoenix Pharmaceuticals Inc. Cat. Nº: EK-072-38. The detection limit for ELISA was 0.063 ng/ml.

### 2.2.6. Genotyping

rs2737902, a SNP previously reported to be associated with expression of *DEFB103* (Hardwick et al., 2011), was genotyped by digital PCR. We used a Custom TaqMan SNP Genotyping Assay, containing primers for the amplification of *DEFB103* region where the SNP lies, and probes for the detection of both alleles: FAM™ dye–labeled probe for the

detection of the derived allele and VIC™ dye–labeled probe for the detection of ancestral allele.

Reaction mixes were set up containing the QuantStudio™ 3D Digital PCR Master Mix v.1, TaqMan Assay and gDNA sample. A total volume of 15µL PCR reaction mix was prepared for each sample, and 14.5µL was loaded onto the chip. PCR conditions were as follows: a denaturation step at 96ºC for 10 minutes, followed by 39 cycles of 56ºC for 2 minutes and 98ºC for 30 seconds, plus a final extension cycle of 60ºC for 2 minutes and a final holding step at 10ºC.

## 2.3. Results and Discussion

In order to analyse if keratinocytes increase the expression of *DEFB103* in response to UV irradiation, and to compare this response to that produced after contact with pathogens (given the immunological role of β-defensins), we measured *DEFB103* expression after irradiating the keratinocytes with UV-B and after exposing the keratinocytes to different candidate microbial, pathogenic stimulants.

For the selection of a good representative pathogen for *DEFB103* expression induction, we first considered lipopolysaccharides (LPS), as it has been reported that *DEFB103* expression increases in the presence of LPS in HaCaT cells (Kim et *al*., 2003). However, other authors only detected minor effects (Sorensen et *al*., 2005) or were not able to detect an increase in *DEFB103* mRNA levels (Chadebech et *al*. 2003; Kalus et *al*., 2009). For this reason, we then considered another pathogen candidates, such as *Staphylococcus aureus,* as HBD3 has been reported to be able to bind and kill *S. aureus* (Schibli et *al*., 2002; Kisich et *al*., 2007) and *DEFB103* expression has been reported to increase after contact with *S. aureus* (Zanger et *al*., 2010). However, due to the health risk involved in manipulating live *S. aureus*, we chose two alternatives to live *S. aureus*

as pathogenic stimulants: Heat Killed *Staphylococcus aureus* (HKSA) and purified lipoteichoic acid from *S. aureus* (LTA).

To get an overview of the cellular response to the pathogenic stimulants and in order to decide which of the bacterial derived stimulants would be better for comparison with UV-B response, we performed preliminary experiments with two cell lines (one Normal Human Epidermal Keratinocyte (NHEK) cell line, whose donor was Lightly Pigmented: NHEK-LP; and one Darkly Pigmented: NHEK-DP) and different incubation times to estimate the most effective time-points for subsequent experiments. Incubation times considered were 12h, 24h, 48h and 72h.

Expression of *DEFB103* was measured by RT-qPCR and SYBR Green or TaqMan Assays. The detection of *DEFB103* mRNA was very challenging due to the low expression of this gene. In fact, in controls, the expression was not detectable. With some treatments it was only possible to detect a very weak expression after 40 cycles, but we dismissed these results as unreliable. Thus, due to the very low expression level of *DEFB103*, we could not efficiently compare the effect of different treatments with this technique.

In order to try to circumvent this problem, we used the QuantStudio™ 3D Digital PCR System (dPCR), as it offers higher accuracy and sensitivity (Millier et *al*., 2017). Initial experiments were made with the same two cell lines as before. With dPCR we were able to detect *DEFB103* mRNA expression in all the conditions (including controls) and we were able to infer small fold changes. The results showed that LTA did not induced any response in the expression of *DEFB103* at the times analysed (12h, 24h, 48h and 72h), contrary to the work of Menzies and Kenoyer (2006), in which they showed and induction of HBD3 expression (although at a different time: after 5h of incubation). Besides, the expression of all the conditions at 72h was similar to that of the controls. Thus, LTA was

not further used with the rest of the cell lines and the subsequent analyses were made at 12h, 24h and 48h (Figure 2.1).

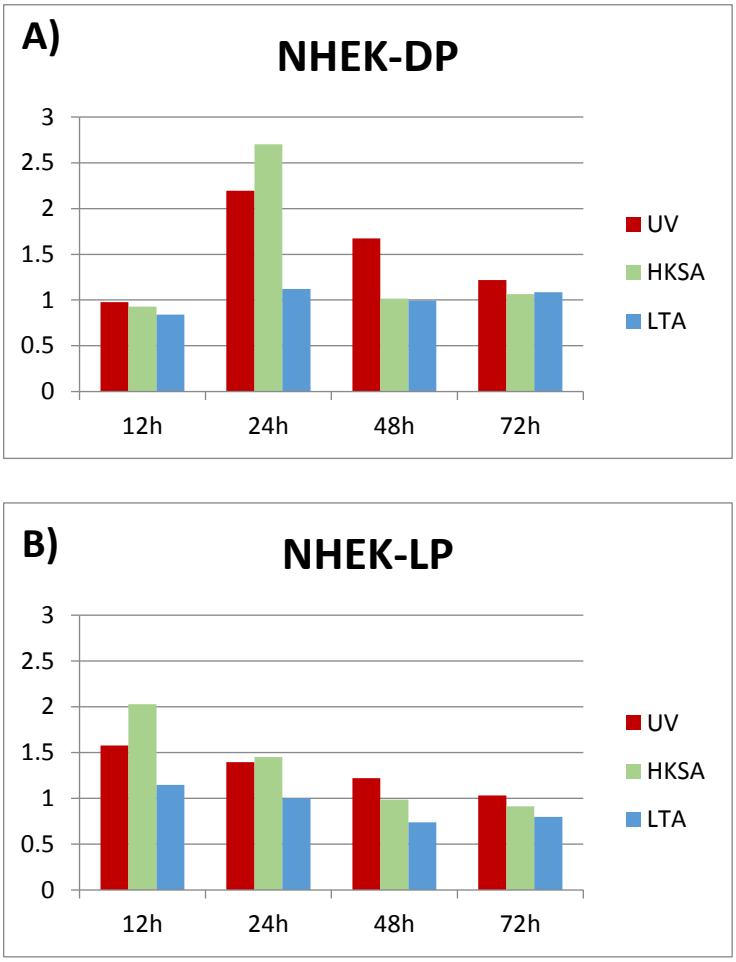


**Figure 2.1**. **Preliminary analysis of *DEFB103* expression in one darkly pigmented NHEK (NHEK-DP) (A) and one lightly pigmented NHEK (NHEK-LP) (B) cell lines, after UV irradiation or treatment with lipoteichoic acid (LTA) and Heat Killed *Staphylococcus aureus* (HKSA).** *DEFB103* mRNA is normalized by *GAPDH* mRNA and expressed as the ratio between the treatment and the control at each time-point.

Although with dPCR we were able to detect *DEFB103* mRNA, in comparison with the expression of *GAPDH*, the amount of *DEFB103* mRNA was actually very low, and thus, finding the right concentration of cDNA to be able to detect enough *DEFB103* mRNA and

not saturate the chip with *GAPDH* mRNA at the same time was challenging. For that reason, in subsequent experiments we decided to analyse separatedly the expression of *DEFB103* and *GAPDH* by using two chips per sample: one for *DEFB103* and one for *GAPDH*.

For subsequent experiments, six keratinocytic cell lines were used: three NHEK-LP and three NHEK-DP. Keratinocyte cell lines were seeded in 6-well plates again at a density of $2x10^4$ cells/well. As before, when cultures reached a confluence of 70%, medium was changed for conditioned medium containing HKSA ($10^8$ HKSA/ml), $1,25(OH)_2D_3$ ($10^{-7}$M) or irradiated with UV-B, and cells were incubated for 12h, 24h or 48h.

Using dPCR, keratinocytes showed, in general, a weak response to UV-B irradiation and to HKSA treatment. However, this response was more particular of each cell line rather than of each group (dark or light) (Figures 2.2 and 2.3). In addition, the response varied in intensity and time of maximum response (Figures 2.2 and 2.3). Thus, the variability observed in our results seems to confirm the results reported by Wolf-Horrell and D'Orazio (2014).

As regards HKSA, this variability included some cell lines that did not respond. But those who respond (LP7, DP2 and DP8), showed an increase in expression correlated with time, with a maximum at 48h (both light and dark) (Figure 2.2). Some of the cell lines did not respond either to UV irradiation. In contrast to HKSA, under UV treatment, responsive cells have the maximum at different time points: two light NHEKs (LP6 and LP7) showed a maximum response at 12h after treatment, LP8 showed a maximum at 48h, whereas the only dark responsive line (DP2) showed the maximum response at 24h (Figure 2.3). An interesting observation is that all the light cell lines responded to UV-B, which could suggest that the pigmentary phenotype could be relevant in the response to UV in the expression of *DEFB103*. Regarding response intensity, of those cells who respond well to HKSA, the maximum response to HKSA (at 48h: LP7 and DP2), was 2-3 times higher than their maximum response to UV (at 12h: LP6).

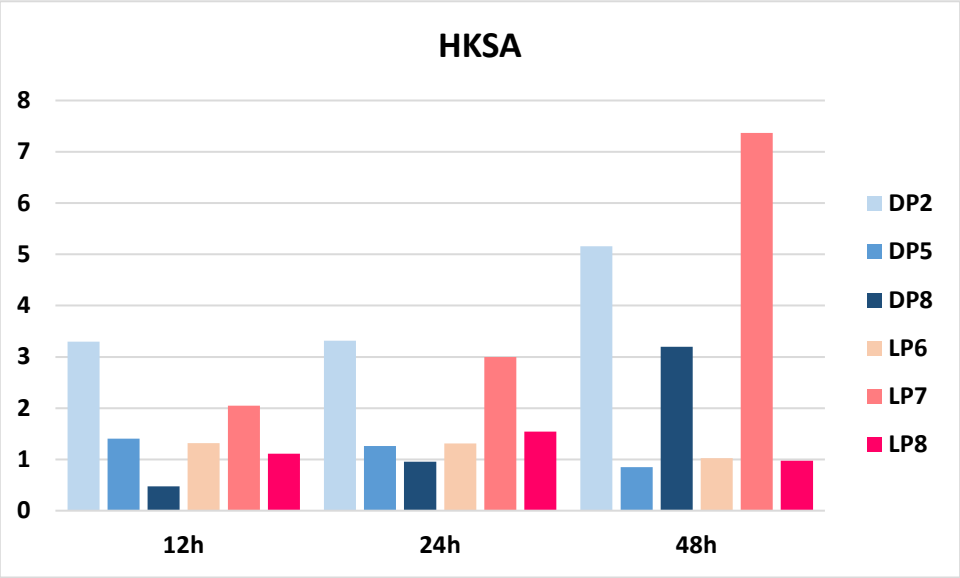


**Figure 2.2. *DEFB103* expression after treatment with Heat Killed *Staphylococcus aureus* (HKSA) in six NHEK cell lines**. *DEFB103* mRNA is normalized by *GAPDH* mRNA and expressed as the ratio between the treatment and the control at each time-point. Expression levels correspond to three NHEK-LP cell lines (LP6, LP7 and LP8) and three NHEK-DP cell lines (DP2, DP5 and DP8).

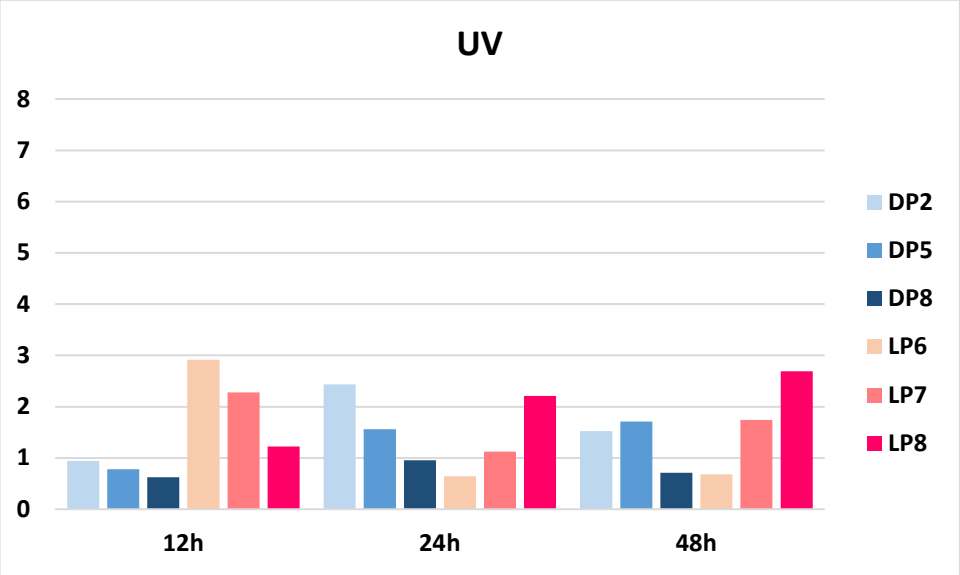


**Figure 2.3**. ***DEFB103* expression after irradiation with UV-B (75 mJ/cm$^2$) in six NHEK cell lines.** *DEFB103* mRNA is normalized by *GAPDH* mRNA and expressed as the ratio between the treatment and the control at each time-point. Expression levels correspond to three NHEK-LP cell lines (LP6, LP7 and LP8) and three NHEK-DP cell lines (DP2, DP5 and DP8).

Besides, we also wanted to test if vitamin D has any influence on the expression of *DEFB103* as it has been previously reported (Dai et al., 2010; De Filippis et *al*., 2017). The same six keratinocytic cell lines were treated with $10^{-7}$M 1α,25-dihydroxyvitamin D3 (active vitamin D). In this case, the variability in the response was even higher than with other stimulants. Only two of the cell lines showed an increase in the expression in comparison with their controls, at 12h (LP7) or 24h (DP2) (Figure 2.4). In this case, the response does not seem to be related with the pigmentary phenotype.

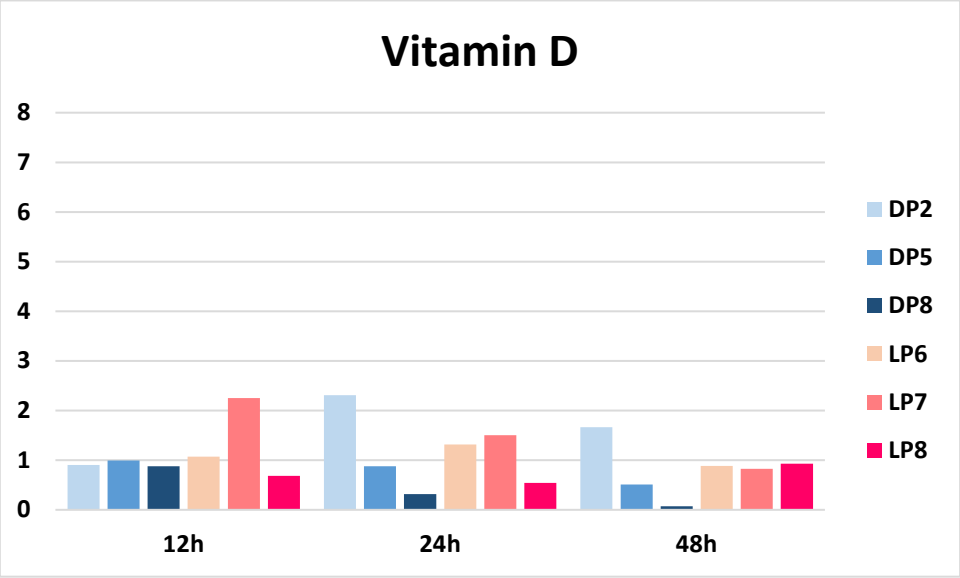


**Figure 2.4**. ***DEFB103*** **expression after treatment with $10^{-7}$M active vitamin D ($1,25(OH)_2D_3$) in six NHEK cell lines.** *DEFB103* mRNA is normalized by *GAPDH* mRNA and expressed as the ratio between the treatment and the control at each time-point. Expression levels correspond to three NHEK-LP cell lines (LP6, LP7 and LP8) and three NHEK-DP cell lines (DP2, DP5 and DP8).

We have additionally observed that, when comparing the basal levels of *DEFB103* mRNA, there are differences between dark and light keratinocytes. In two light cell lines, the expression levels in controls were smaller than in the dark lines. This could be related to the later response to UV-B observed in dark lines, compared with light lines (two NHEK-LP respond at 12h and one NHEK-DP responds at 24h). Interestingly, the light

cell line that showed a later response to UV and no response to HKSA (LP8), has basal mRNA levels similar to the dark lines. It could be possible that the response to the stimuli depends on the initial mRNA levels of *DEFB103*. Thus, in the lines with a high basal level of expression, the HBD3 quantity could be enough and there would not need to increase the expression in response to a stimulus.

However, it could as well be that *DEFB103* copy number could be influencing this response. Thus, we determined the copy number in each cell line (Table 2.1). However, we did not observe any trend regarding copy number and basal or induced expression of *DEFB103* in the cell lines analysed. A correlation between *DEFB4* copy number and expression level had been reported by other authors in lymphoblastoid cell lines (Hollox et *al*., 2003; Groth et *al*., 2010). However, Groth et *al*. (2010) also observed that several lymphoblastoid cell lines with different copy numbers exhibited similar expression levels. Interestingly, they also observed a weak correlation (r = 0.4) in normal human epidermal keratinocytes (NHEK) (n = 4). James et *al*. (2018) also reported a positive association between *DEFB4* copy number and cervicovaginal HBD2 (the peptide encoded by *DEFB4*) concentration (Spearman r = 0.21, p = 0.0032). However, they did not observe a correlation for HBD3 concentration (encoded by *DEFB103*) (p-value not shown). β-defensin genes lying in the copy number repeat of chromosome 8 are considered to vary together in copy number (Linzmeier and Ganz 2005; Groth et *al*., 2008). Thus, a similar expression level of all the genes within the repeat could be expected. The results of James et *al*. (2018), however, suggest that other factors, that could include sequence variants, influence the expression of β-defensins, leading to different expression levels among different defensin genes.

**Table 2.1**. ***DEFB103*** **copy number (CN) of NHEK cell lines.**

| Cell line | DP2 | DP5 | DP8 | LP6 | LP7 | LP8 |
|---|---|---|---|---|---|---|
| ***DEFB103*** **CN** | 5 | 6 | 5 | 3 | 6 | 4 |

Although skin is among the tissues in which *DEFB103* is apparently more expressed (Harder et *al*., 2001), many authors have reported that, in general, the basal expression of *DEFB103* is low. If fact, ee also performed an ELISA analysis to try to quantify the protein level of HBD3, to analyse if the secretion of the peptide is enhanced after the treatments. However, the values were below the detection limit of the kit (0.063 ng/ml) in all the conditions,

Thus, a number of studies have failed to detect HBD3 in basal conditions or healthy skin, at both mRNA level or protein level (Kim et *al*., 2003; Harder et *al*., 2010; Wittersheim et *al*., 2013). The reason of the low expression could be related with the inducible nature of some β-defensins (HBD2 and HBD3). Thus, only when a low basal expression level already pre-exists, , only different stimuli will be able to modify the expression level of these genes.. In this regard, Fan et *al*. (2015) analysed the RNA-Seq data of 76 cell lines and tissues and confirmed the low expression across all the samples analysed. They suggested that the reason for the low expression of β-defensins could be in the in the structure of the chromatin in that region, which exerts a repressive effect on the gene expression. They observed that the intensity for DNase I hypersensitive sites (DHSs), transcription factors (TFs) and histone modifications were weaker in the β-defensin region than those in the adjacent regions.

***Genotyping of the expression-level associated SNP rs2737902***

We also thought it interesting to explore if expression levels of *DEFB103* would have any impact on pigmentation. In this sense, Hardwick et *al*. (2011) found that a SNP in the promotor of *DEFB103* (rs2737902) increases its expression. Thus, we genotyped rs2737902 in the cell lines and in some of our samples by means of digital PCR. We

decided to use dPCR because if the SNP also shows copy number variation we would also be able to detect it with precision. Thus, we analysed the SNP in darkly an lightly pigmented cell lines and also in the most and least pigmented Spanish samples (the same from Chapter 1) and also in samples from Asia, because the SNP has been reported to be more frequent in Asia (Hardwick et *al*., 2011). However, we did not detect the derived allele in any of the samples.

## 2.4. Conclusions

Although the changes in *DEFB103* expression are low, our results suggest that UV radiation could nevertheless modulate the expression of *DEFB103,* although to a limited amount, particularly in lightly-pigmented NHEKs. Our results suggest that when comparing the same cell lines, the response to UV is lower than the response to HKSA. Notwithstanding, small increases in HBD3 levels could be biologically relevant, and thus, although the principal function of β-defensins might still be immunological, HBD3 could also have a photo-protective role. This observation suggests a new role for HBD3 and it would be interesting to study if HBD3 takes part in the response to UV radiation.

# Chapter 3.

# Response of melanocytes from lightly and darkly pigmented individuals to wild-type and mutant human β-defensin 103: transcriptional profile analysis

## 3.1. Introduction

As mentioned above, β-defensin 103 has been related to pigmentation in dogs. Candille et *al*. (2007) demonstrated that the canine peptide carrying a 3bp deletion (the $K_B$ allele) has the ability to bind the mc1r receptor and trigger melanogenesis. Furthermore, several studies have demonstrated that human β-defensin 3 peptide (HBD3) is also able to bind the melanocortin 1 receptor (*MC1R*) (Beaumont et *al*., 2012; Swope et *al*., 2012; Nix et *al*., 2013, 2015) and that the binding is based on electrostatic complementarity between the differently charged surfaces of the ligand and the receptor (Nix et *al*., 2013, 2015).

Nevertheless, the pathway downstream the binding of HBD3 to MC1R is not clear. Some authors reported that cAMP levels are not altered by the interaction of β-defensin 3 and MC1R in mouse melanocytes (Candille et *al*., 2007) and in human melanocytes (Swope et *al*., 2012), suggesting that other signalling pathways could mediate the response to HBD3. However, Beaumont et *al*. (2012) observed a small increase in cAMP levels in human embryonic kidney cells incubated with HBD3. Besides, they also observed an effect of HBD3 on the MAPK signalling pathway. Thus, incubation with HBD3 produced and increase in ERK phosphorylation, which was mostly independent of protein kinase A (PKA). On the other hand, Ericson et *al*. (2018) also reported that HBD3 is a MC1R agonist and it is able to induce cAMP at micromolar concentrations.

Thus, our aim was to analyse the effect of HBD3 on human melanocytes expression, in order to confirm if HBD3 is able to trigger melanogenesis in human skin and to understand which are the pathways involved. Furthermore, we also wanted to investigate if the response to HBD3 varies between melanocytes from donors with different pigmentary phenotype. And, finally, we also tested if there are differences in the response to wild-type HBD3 and to mutated HBD3 (a peptide carrying the deletion observed in dogs, ΔG23), to test if the mutation is also important in humans as it is in dogs. For that purpose, we analysed the transcriptional profiles of melanocytes from lightly and darkly pigmented individuals treated with wild-type and mutated HBD3.

## 3.2. Material and Methods

### 3.2.1. Cell cultures

Human epidermal melanocytes (HEMs) were purchased from Cascade Biologics: four lines isolated from lightly pigmented neonatal foreskin, termed “light melanocytes” (HEM-LP), and three lines from darkly pigmented neonatal foreskin, termed “dark melanocytes” (HEM-DP). Cells were cultured in Medium 254 (Gibco™, ThermoFisher) supplemented with human melanocyte growth supplement (HMGS), consisting of 0.2% (v/v) bovine pituitary extract (BPE), 0.5% (v/v) fetal bovine serum, 1 µg/ml recombinant human insulin-like growth factor-I , 5 µg/ml bovine transferrin, 3 ng/ml basic fibroblast growth factor, 0.18 µg/ml hydrocortisone, 3 µg/ml heparin and 10 ng/ml phorbol 12-myristate 13-acetate (PMA). The cell lines were maintained in an incubator under an atmosphere of 5% $CO_2$ at 37°C. Media were refreshed every two days.

### 3.2.2. Incubation with HBD3

The peptide of wild type beta-defensin 3 (HBD3) (WT-HBD3) was purchased from Aapptec (Louisville, Kentucky) and the mutated HBD3 (MUT-HBD3) was purchased from Almac Sciences (Edinburgh). Sequences of the peptides are shown in table 3.1. The mutated HBD3 peptide includes the mutation found to cause black coat colour in dogs: a 3–base pair deletion in the second exon of CBD103, the orthologue of human *DEFB103*, which predicts an in-frame glycine deletion (ΔG23).

**Table 3.1. Sequences of beta-defensin 103 (HBD3) peptides used in this work**.

| Peptide name | Sequences of mature peptides |
|---|---|
| **WT-HBD3** | **G**IINTLQKYYCRVRGGRCAVLSCLPKEEQIGKCSTRGRKCCRRKK |
| **MUT-HBD3** | IINTLQKYYCRVRGGRCAVLSCLPKEEQIGKCSTRGRKCCRRKK |

The four HEM-LP cell lines and the four HEM-DP cell lines were seeded in 6-well plates at a density of $2.5x10^5$ cells/well. When cultures reached a confluence of 70%, medium was removed and changed by a conditioned medium, consisting of 100nM of either WT-HBD3 or MUT-HBD3 (see Table 3.1) in Medium 254. In the case of controls, normal medium 254 was refreshed. Cells were incubated for 12h and 24h. 0h controls (without HBD3) were also used.

To facilitate the reading of this chapter, I define next the abbreviations for the cell lines, times and conditions used:

D: dark pigmented melanocytes

L: light pigmented melanocytes

HBD3: Human beta-defensin 103 peptide (encoded by *DEFB103*)

W: melanocytes treated with wild-type HBD3

M: melanocytes treated with mutated HBD3

C: untreated melanocytes (controls)

0h: melanocytes at 0h

12h: melanocytes at 12h

24h: melanocytes at 24h

1, 2..n: cell line number

Thus, for instance, D1_12h_C indicates dark melanocytes, cell line #1, at 12h without any treatment (12h control); D2_12h_W indicates dark melanocytes, cell line #2, treated with wild-type HBD3 at 12h; and similarly for the rest of combinations.

### 3.2.3. Microarrays

Four Dark (HEM-DP) and four light (HEM-LP) melanocyte cell lines were incubated with wild-type or mutated HBD3 and were harvested at 12h and 24h. Controls were also harvested at 0h, 12h and 24h. RNA of HEM-DP and HEM–LP cells at 0h and HEM-DP and HEM-LP at 12h and 24h treated and untreated was extracted using the RNAqueous kit (Ambion). RNA samples were quantified using an UV/VIS NanoDrop 8000 (Thermo Fisher) and RNA integrity was analyzed using an Agilent 2100 Bioanalyzer, with RNA 6000 Nano Chips.

After quality control, samples were analysed using SurePrint G3 Human Gene Expression 8x60K v2 Microarrays (Agilent). Microarray preparation was performed by the Advanced Research Facilities (SGIker) of the University of the Basque Country (UPV/EHU), following the protocol "One-Color Microarray-Based Gene Expression Analysis. Low Input Quick Amp Labeling, v.6.5". This protocol is as follows: firstly, Spike-Ins are added, consisting on a mix of 10 polyadenilated transcripts, synthesized *in vitro*, with are derived from the Adenovirus gene E1A and hybridize with probes for positive internal controls. Spike-Ins will be used for the evaluation of the processing of the microarrays. Secondly, the total RNA (and Spike-Ins) is retrotranscribed with the AffinityScript Reverse Transcriptase enzyme (AffinityScript RT), using Oligo dT primers coupled to the T7 promotor. The RNA quantity used for the labeling reaction was 25ng. Thirdly, the double-strand cDNA is transcribed *in vitro* by T7 RNA polymerase, in presence of Cyanine 3-CTP (Cy3-CTP), in order to generate labeled cRNA. Then, labeled samples are purified with the RNeasy Mini kit (Qiagen) and quantified by means of an UV/VIS NanoDrop ND-1000 apparatus. As a quality control, the samples had to pass the following requirements: Yield > 0.825 µg per reaction and specific activity of Cyanine-3 > 6 pmol/µg. After labeling, hybridization is performed using SureHyb hybridization chambers (Agilent Technologies). For the hybridization step, 600ng of labeled cRNA are used. Hybridization is performed in a 40L hybridization oven (Agilent

Technologies) with the following conditions: 65ºC for 17h at 10rpm. Then, washing is performed following the Agilent protocol with ozone-barrier slide covers to avoid ozone-induced dye degradation. Finally, scanning was performed in G2565CA DNA microarray scanner (Agilent Technologies) using Scan Control software v 8.5.1 and default settings for the profile AgilentG3_GX_1Color.

### 3.2.4. Microarray data preprocessing

Image processing of the microarrays was performed using the Agilent Feature Extraction software, v. 10.7.3.1. This software extracts the information of the fluorescence raw signal (mean signal) for the fluorochrome (Cy3: green channel) both for the spot that contains the control and non-control probes and for the background (obtained from negative controls), and processes the signals to generate Raw Data Files and a Quality Control Report. Positive controls are probes that hybridize with Spike-Ins and negative controls are probes that contain sequences for which no hybridization is expected, thus, are indicators of unspecific unions.

Quality Control Report:

To check the quality of the microarray, nine parameters are taken into account. In the preparation of the microarray, spike-Ins are included in order to evaluate the quality of the microarray. The most important evaluated parameters are: the coefficient of variation of the processed signal from non-control probes and spike-ins (%CV), the percentage of outlier probes in the replicated probes population, the intensity of the signals of the negative controls, and the limit of detection and linearity of the spike-ins signal.

Raw data preprocessing:

The raw data files were processed with GeneSpring GX software v. 11.5.1 (Agilent). All raw data are processed together and a unique file is obtained, which contains the data for every biological probe (without positive and negative controls) and for all the samples.

Feature extraction flags were transformed as follows: if a feature was not positive and significant, *not uniform*, or was a population outlier: *compromised*. If a feature was saturated or its signal not clearly above background: *not detected.* We filtered the probes according to the following criterion: We made seven groups (0h, 12h_C, 12h_W, 12h_M, 24h_C, 24h_W and 24h_M) and consider the probe if it was detected in at least 50% of the samples in at least one group.

Then, a variance-stabilizing transformation of the data was performed. Many standard statistical techniques are effective on data that are normally distributed with constant variance, independent of the mean of the data. However, gene-expression microarray data come from non-Gaussian distributions, in which the mean-variance relation is not linear. There are several methods to transform the data to have a Gaussian distribution, but most of them, rely on log transformations, and can increase the variance of observations near background (Motakis et *al*., 2006). We used DDHF (Data-Driven Haar-Fisz) transformation for variance stabilization, with the R package DDHF for microarrays (DDHFm) (Motakis et *al*., 2006). This method does not require specifying a parametric model for the underlying microarray data and produces transformed intensities that are approximately normally distributed. Transformed data were then further normalized following the quantile method, using the R package DNAMR (Cabrera, 2011).

### 3.2.5. Principal Component Analysis (PCA)

After removing those samples that did not pass the quality control, an unsupervised analysis was performed with transformed data by means of Principal Component Analysis (PCA). The analysis was performed in R with the *prcomp* function from the *stats* package (R Core Team, 2018) and plotted using the *ggplot2* package (Wickham, 2016).

### 3.2.6. Comparison of expression profiles

Statistical analysis for the comparison of expression profiles was performed with SAM (Significance Analysis of Microarrays) software. We compared expression profiles of the

treated samples (WT-HBD3 or MUT-HBD3) and the controls. Two-class paired comparisons were made in all but some comparisons: in three groups, three samples did not pass the quality control; thus, to allow comparisons with these groups, we performed two-class unpaired test. In each test, 100 permutations were set. The significance of the tests was given by the q-value, which is the lowest False Discovery Rate (FDR) at which that gene is called significant. For subsequent analysis, we chose the genes for which $q<0.05$.

### 3.2.7. Enrichment analysis

We performed an analysis with a custom-made category of "Pigmentation". For that, we created a list of genes related with human melanogenic genes related to melanocytes. First, we considered genes known to be implicated in melanogenesis based on the databases Gene Ontology (GO) and The Kyoto Encyclopedia of Genes and Genomes (KEGG) and literature. Then, we curated that list based on the following criteria: We included the genes implicated in different pathways of melanogenesis, which usually change in expression level during melanogenesis (excluding the genes that code for proteins that in these proceses are regulated by phosphorylation, but which do not change in transcription levels, apparently). Besides, we only chose genes that are known to be expressed in melanocytes. For that, we excluded some ligands of the melanogenic receptors, because they are expressed and secreted by other cell-types, such as keratinocytes and fibroblasts. Selected genes include: genes implicated in the different pathways of melanogenesis (α-MSH/MC1R pathway, SCF/KIT pathway, endothelin pathway, WNT pathway and PKC pathway) and genes related with melanosome biogenesis and transport (Table 3.2). The significance analysis was performed using the Hypergeometric test.

We also tested the enrichment of pigmentation-related genes in HBD3 treated melanocytes by performing Hypergeometric test on additional custom gene lists elaborated from different sources. One list was elaborated by searching the terms

"melanin", "melanosome" and "pigmentation" in the AmiGO 2 database (http://amigo.geneontology.org/amigo). We obtained a set of 194 genes, and 175 genes remained after the removal of those that were not included in the microarray (Table S3.1). We also made use of the gene list proposed by Baxter et *al*. (2018), which was curated based on the information from four public databases: Online Mendelian Inheritance in Man (OMIM), Mouse Genome Informatics (MGI), Zebrafish Information Network (ZFIN) and the Gene Ontology Consortium (GO). The list contains genes directly or indirectly related with integument pigmentation in human, mouse and zebrafish, encompassing 650 genes. We used the complete Baxter's list (558 genes after removing those that were not present in the array) (Table S3.2) and also a smaller list containing only the *loci* validated to be associated with skin pigmentation in humans (including 120 genes after the removal of those not present in the array) (Table S3.3).

Pathway enrichment analysis was also performed using Web-based Gene Set Analysis Toolkit (WebGestalt) (http://www.webgestalt.org/). As a reference list, we used all the genes included in the microarray. We used the pathways from The Kyoto Encyclopedia of Genes and Genomes (KEGG), Wikipathway and Panther.

**Table 3.2**. **List of genes included in the "Pigmentation" category.**

| Gene symbol | Description | Subcategory |
|---|---|---|
| ***POMC*** | Proopiomelanocortin | α-MSH/MC1R pathway |
| ***MC1R*** | Melanocortin 1 receptor | α-MSH/MC1R pathway |
| ***PRKACA*** | Protein kinase cAMP-activated catalytic subunit alpha | α-MSH/MC1R pathway |
| ***PRKACB*** | Protein kinase cAMP-activated catalytic subunit beta | α-MSH/MC1R pathway |
| ***MITF*** | Microphthalmia-associated transcription factor | Regulator of melanogenic enzymes |
| ***TYR*** | Tyrosinase | Mmelanogenic enzyme |
| ***TYRP1*** | Tyrosinase-related protein 1 | Melanogenic enzyme |
| ***DCT /TYRP2*** | Dopachrome tautomerase | Melanogenic enzyme |
| ***KIT*** | KIT proto-oncogene, receptor tyrosine kinase | SCF/KIT pathway |

| | | |
|---|---|---|
| ***HRAS*** | Harvey rat sarcoma viral oncogene homolog | SCF/KIT pathway |
| ***RAF1*** | v-raf-1 murine leukemia viral oncogene homolog 1 | SCF/KIT pathway |
| ***DVL1*** | Dishevelled segment polarity protein 1 | WNT pathway |
| ***DVL2*** | Dishevelled segment polarity protein 2 | WNT pathway |
| ***DVL3*** | Dishevelled segment polarity protein 3 | WNT pathway |
| ***CTNNB1*** | Catenin beta 1 | WNT pathway |
| ***LEF1*** | Lymphoid enhancer-binding factor 1 | WNT pathway |
| ***EDN3*** | Endothelin 3 | Endothelin pathway |
| ***EDNRB*** | Endothelin receptor type B | Endothelin pathway |
| ***PLCB1*** | Phospholipase C, beta 1 | PKC pathway |
| ***PLCB2*** | Phospholipase C, beta 2 | PKC pathway |
| ***PLCB3*** | Phospholipase C, beta 3 | PKC pathway |
| ***PRKCA*** | Protein kinase C, alpha | PKC pathway |
| ***PRKCB*** | Protein kinase C, beta | PKC pathway |
| ***PAX3*** | Paired box 3 | MITF transcription factor |
| ***SOX10*** | SRY(sex determining region Y)-box transcription factor 10 | MITF transcription factor |
| ***ZEB2*** | Zinc finger E-box binding homeobox 2 | MITF transcription factor |
| ***PMEL*** | Premelanosome protein | Melanosome biogenesis |
| ***SLC24A5*** | Solute carrier family 24, member 5 | Melanosome biogenesis |
| ***SLC45A2*** | Solute carrier family 45, member 2 | Melanosome biogenesis |
| ***OCA2*** | OCA2 melanosomal transmembrane protein | Melanosome biogenesis |
| ***ATP7A*** | ATPase copper transporting, alpha | Melanosome component |
| ***GPR143 / OA1*** | G protein-coupled receptor 143 | Melanosome biogenesis |
| ***MLANA*** | Melan-A | Melanosome biogenesis |
| ***OSTM1*** | Osteopetrosis associated transmembrane protein 1 | Melanosome biogenesis |
| ***LYST*** | Lysosomal trafficking regulator | Melanosome biogenesis |
| ***RAB7A*** | RAB7B, member RAS oncogene family | Melanosome transport |
| ***RAB27A*** | RAB27A, member RAS oncogene family | Melanosome transport |
| ***MYO5A*** | Myosin VA | Melanosome component |
| ***IRF4*** | Interferon regulatory factor 4 | Cooperates with MITF to activate TYR |

## 3.3. Results and Discussion

### 3.3.1. Quality control (QC)

QC Metrics performed with GeneSpring revealed three arrays that did not satisfy the quality parameters: D2_0h, L4_0h and L4_24h_M. In the visualization of the profiles of all the samples by means of Box-Plot, D2_0h, L4_0h and L4_24h_M showed dispersion levels and variability higher than those for the rest of the samples in the same conditions (Figure S3.1). Therefore, we removed those three samples (D2_0h, L4_0h and L4_24h_M) from the subsequent analyses.

### 3.3.2. Principal Components Analysis (PCA) and enrichment analysis

After removing the arrays that did not meet the initial quality filter, we performed, as a preliminary exploratory tool, an unsupervised classification of the 53 remaining microarrays by means of Principal Component Analysis (PCA).

In the PCA plot of the first two principal components, we can distinguish five different clusters (Figure 3.2):

cluster #1: dark melanocytes treated with WT-HBD3 at 24h (D_24h_W)

cluster #2: all samples at 0h (untreated controls) and 12h (treated and untreated), and light melanocytes treated with WT-HBD3 at 24h (L_24h_W)

cluster #3: dark melanocytes treated with MUT-HBD3 at 24h (D_24h_M)

cluster #4 contains controls at 24h (both light and dark)

cluster #5 contains light melanocytes treated with MUT-HBD3 at 24h (L_24h_M).

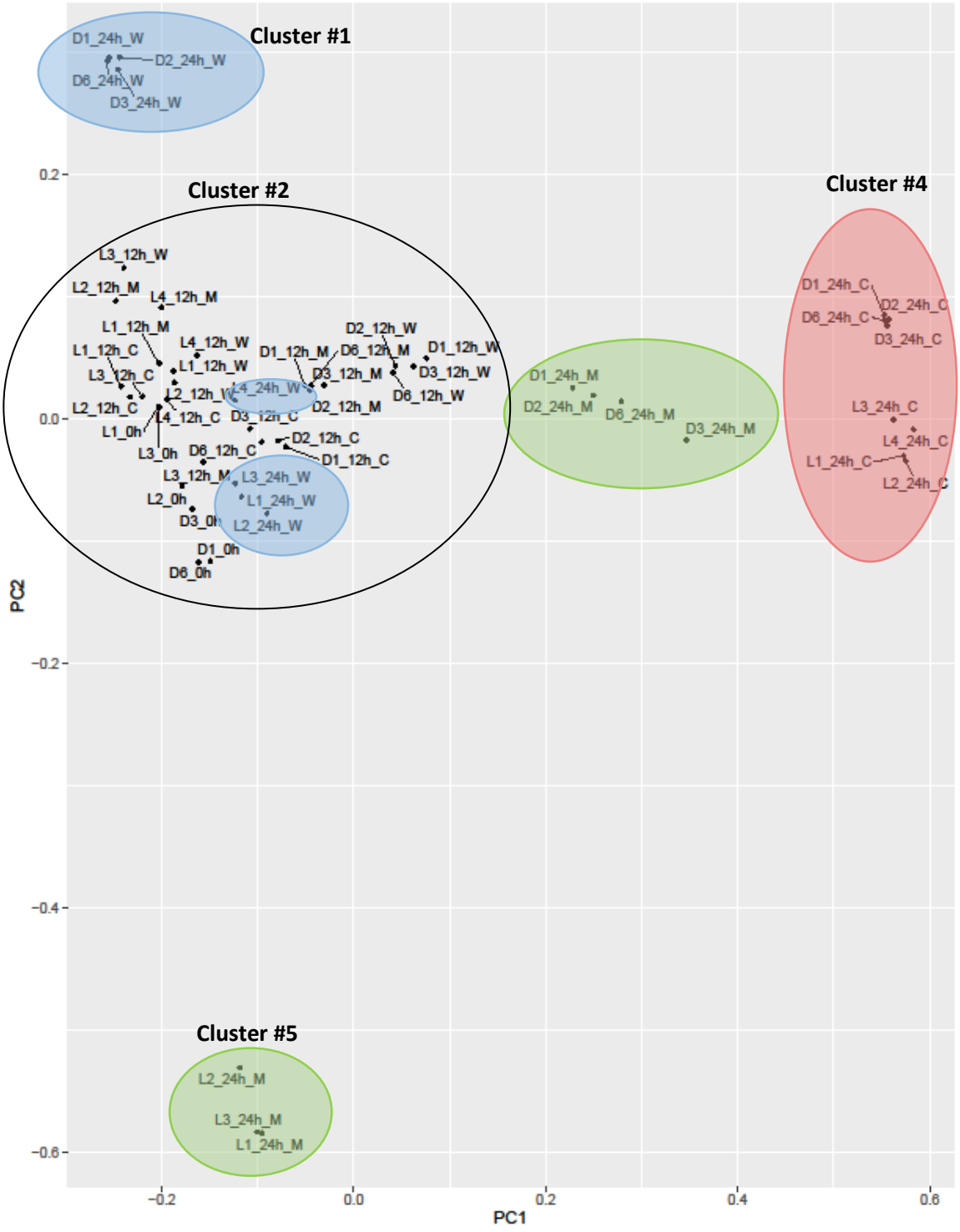


**Figure 3.2. Principal Component Analysis showing the first (36% of variance) and second (16% of variance) components.** Samples at 24h are highlighted: controls in red, melanocytes treated with wild-type HBD3 in blue and treated with mutated HBD3 in green. “D” is for dark melanocytes and “L” for light melanocytes. “W” is for wild-type HBD3 and “M” for mutated HBD3. Five clusters are also indicated.

We can observe (Figure 3.2) that the first principal component (PC1), which explains 36% of the variance, separates mainly the control groups at 24h of both pigmentary phenotypes (D+L_24h_C) (cluster #4) vs. the corresponding 0h groups, control groups at 12h and treated groups (both with WT or MUT HDB3) at 12h and 24h (clusters #1, 2, 3 and 5). However, the group of dark melanocytes treated with mutated HBD3 at 24h (D_24h_M) (cluster #3), lies in an intermediate position, closer to the cluster D+L_24h_C (cluster #4).

To interpret the distribution in PC1, we performed an enrichment test with the custom-made category of “Pigmentation” described above and which contains genes listed in Table 3.2. Then, we analysed if the overexpressed or underexpresed genes in each comparison were over- or under-represented in the category of “Pigmentation”. The significance analysis was performed using the Hypergeometric test.

We compared the group formed by controls at 0h and 12h with the group formed by controls at 24h, and observed an upregulation of the “Pigmentation” category in both light and dark melanocytes at 0h and at 12h. These results indicate that PC1 could explain a process of depigmentation of the cell lines along time in culture, as we can see the D+L_0h on one end of PC1 and the D+L_24_C at the other. We hypothesised that melanocytes in culture, without any stimulant, tend to lose expression of pigmentary genes with time.

In this scenario, we may hypothesize that adding HBD3 to the cultures could prevent depigmentation, promoting the maintenance of the initial level of melanogenesis based on the location of samples at 24h in PC1: in figure 3.2, the group formed by controls at 24h locate at one end of PC1 and the group formed by treated melanocytes at 24h locate at the opposite end of PC1, with the rest of the samples. Dark melanocytes treated with mutated HBD3 (D_24h_M) are an exception, as they locate between controls at 24h and

the rest of the samples. The explanation to this can be that mutated HBD3 has a lower effect in dark melanocytes than wild-type HBD3.

To further investigate this hypothesis we performed an enrichment test with the custom-made category of “Pigmentation” comparing melanocytes treated with HBD3 (WT and MUT) and the respective controls at 24h. We performed comparisons with all cell lines together (dark and light pigmented cell lines) and also dark cell lines and light cell lines separatedly, to analyse if the pigmentary phenotype influences the response to HBD3. We observed an upregulation of the “Pigmentation” category in both light and dark melanocytes, treated with either WT or MUT-HBD3, compared to their respective untreated controls at 24h. Results are shown in table 3.3. The upregulation was more significant in light melanocytes in general and more significant with WT-HBD3 (Hypergeometric test: p= 1E-06). Thus, there is a difference in the intensity of the response of melanocytes to HBD3 that could be related to the pigmentary phenotype. One possible explanation is that in dark melanocytes the basal pigmentation level is higher than in light melanocytes, and the binding of HBD3 to MC1R could induce a smaller response. This could explain the location of D_24h_M samples between controls at 24h and the rest of the samples in PC1.

Looking at the genes overexpressed, we see that the most relevant genes in melanogenesis such as *MITF*, *TYR* and *TYRP1,* are overexpressed, with both treatments, and *DCT* in all but in dark melanocytes with MUT-HBD3 (Table 3.3).

Thus, we wanted to investigate which of the main melanogenesis pathways is overrepresented. It has been demonstrated that HBD3 is able to bind MC1R (Candille et *al*., 2007; Nix et *al*., 2013). But a crosstalk between different pigmentation pathways could occur after the binding of HBD3 to MC1R. In fact, it has been reported that HBD3 does not seem to induce an increase of cAMP levels (Candille et *al*., 2007; Swope et *al*., 2012; Nix et *al*., 2013). In this sense, we observed that genes from different

melanogenesis pathways are upregulated. Apart from *MC1R*, genes from KIT and Wnt signaling pathways are also overexpressed, especially in light melanocytes (Table 3.3).

We also performed a pathway enrichment analysis, using Web-based Gene Set Analysis Toolkit (WebGestalt), based on pathways from The Kyoto Encyclopedia of Genes and Genomes (KEGG). We compared overrepresented genes in wild type and mutated HBD3 in relation with the controls at 24h. We did not find any relevant pathway in any of the comparisons. The pathways obtained were too general and we were not able to find any pattern.

We tried to discern which of the pathways implicated in melanogenesis could be activated by HBD3. We wanted to define categories of the genes implicated in each melanogenic pathway, in order to evaluate if the pathway is upregulated. However, the amount of genes in each category was too small to do any statistical calculation. The reason is tha most of the effectors implicated in the different pathways do not need to be transcriptionally modulated. Some proteins are present in the cell and they are activated or inactivated during the melanogenic process. For instance, some of the pathways do not lead to an increase in *TYR* expression, but they increase the activity of the tyrosinase present in the cell.

**Table 3.3. Genes from the "Pigmentation" category overexpressed (+) in each condition, at 24h in comparison with the corresponding control at 24h.**

| Gene symbol | Conditions vs respective Control at 24h | | | |
|---|---|---|---|---|
| | D_24h_W [1] | D_24h_M [2] | L_24h_W [3] | L_24h_M [4] |
| ***POMC*** | | | | |
| ***MC1R*** | + | | + | + |
| ***PRKACA*** | | | + | |
| ***PRKACB*** | + | + | + | |
| ***MITF*** | + | + | + | + |
| ***TYR*** | + | + | + | + |
| ***TYRP1*** | + | + | + | + |
| ***DCT*** | + | | + | + |
| ***KIT*** | + | | + | + |
| ***HRAS*** | | | + | |
| ***RAF1*** | | | + | |
| ***DVL1*** | + | | + | + |
| ***DVL2*** | | | + | |
| ***DVL3*** | | | + | + |
| ***CTNNB1*** | + | | + | + |
| ***LEF1*** | | | + | + |
| ***EDN3*** | | | | |
| ***EDNRB*** | | | + | |
| ***PLCB1*** | | | | + |
| ***PLCB2*** | | | + | |
| ***PLCB3*** | + | | | |
| ***PRKCA*** | | | | |
| ***PRKCB*** | | | + | |
| ***PAX3*** | | | + | + |
| ***SOX10*** | | | + | + |
| ***ZEB2*** | | | + | |
| ***PMEL*** | + | + | + | + |
| ***SLC24A5*** | + | | + | + |
| ***SLC45A2*** | | | + | + |
| ***OCA2*** | + | | + | + |
| ***ATP7A*** | + | | + | |
| ***GPR143 /OA1*** | + | | + | + |
| ***MLANA*** | + | + | + | + |
| ***OSTM1*** | + | | + | + |
| ***LYST*** | | | + | + |
| ***RAB7A*** | + | | + | + |
| ***RAB27A*** | | | + | + |
| ***MYO5A*** | + | | + | + |
| ***IRF4*** | | | + | + |
| **Number of genes (n)** | n = 19 | n = 6 | n = 34 | n = 24 |
| **Hypergeometric test (p)** | p= 0.0134 | p= 0.0419 | p= $1x10^{-06}$ | p=$1x10^{-05}$ |

[1] D_24h_W: dark melanocytes treated with wild-type HBD3; [2] D_24h_M: dark melanocytes treated with mutated HBD3, [3] L_24h_W: light melanocytes treated with wild-type HBD3; [4] L_24h_M: light melanocytes treated with mutated HBD3.

Therefore, we only can speculate. Several authors have demonstrated that HBD3 is able to bind MC1R. However, according to most authors, it does not seem to produce an increase of cAMP in melanocytes (Candille et *al*., 2007; Swope et *al*., 2012; Nix et *al*., 2013), although Beaumont et *al*. (2012) reported a small increment in cAMP levels produced by HBD3 in human embryonic kidney (HEK293) cells. Thus, HBD3 may activate other cAMP-independent pathways downstream MC1R. In our results, we observe an upregulation of the receptor tyrosine kinase KIT in dark and light melanocytes incubated with wild-type HBD3. Although KIT is normally activated by SCF (Stem Cell Factor, KITLG), Herraiz et *al*. (2011) reported that α-MSH binding to MC1R could lead to the transactivation of KIT. When activated, KIT activates a RAS GTPase, which in turn activates members of RAF family of protein kinases, leading to the phosphorylation of ERK1 and ERK2 kinases and finally activation of MITF (Wu et *al*., 2000). In this sense, Beamount et *al*. (2012) demonstrated that incubation of HEK293 cells with HBD3 induces ERK phosphorylation. Therefore, KIT is a candidate for HBD3-induced melanogenesis. However, in light melanocytes we also observe an upregulation of the endothelin B receptor (*EDNRB*) and genes related with WNT pathway.

As regards the melanogenic activity of WT-HBD3 vs MUT-HDB3, in our data at 24h, which is the time period showing the biggest differentiation, we observe that WT-HBD3 has a greater effect on the expression of melanogenic genes than MUT-HBD3, both in dark and light melanocytes, but especially so in light melanocytes. As table 3.3 shows, hypergeometric tests are more significant with WT-HBD3. Thus, if the effect of HDB3 is through MC1R, the ΔG23 mutation does not seem to increment in humans the affinity for the receptor, as it occurs in dogs (Candille et *al*., 2007). Indeed, this mutation has not been described in humans. We neither found it in the individuals resequenced for *DEF1B03* (Chaper 1).

On the other hand, although cluster #1 (D_24h_W), cluster #2 (L+D 0h, L+D 12h treated and untreated, and L_24h_W), and cluster #5 (L_24h_M) locate on the same end on

PC1, they are however separated along the second principal component (PC2). Along this axis, which explains 16% of total variance, cluster #1 occupies the positive coordinates, cluster #5 the negative coordinates and cluster #2 the intermediate coordinates around 0 (Figure 3.2). As we assume that pigmentation is explained by PC1, it has no sense to test if the PC2 explains pigmentation. Anyway, we tested it. As the group L_24h_M is the most differentiated one from the rest, we compared this group with the rest, we analysed if the genes in the custom-made "Pigmentation" category were upregulated by means of the hypergeometric test and it was not significant. In order to elucidate the possible reason of this differentiation, we performed an enrichment analysis, comparing the expression profile of L_24h_M against the rest. We did not observe any clear tendency in the pathways upregulated/downregulated, with any of the database used (KEGG, Wikipathway and Panther).

In order to confirm the overrepresentation of pigmentation-related genes in HBD3 treated melanocytes at 24h, we elaborated a gene list based on AmiGO 2 database, by searching the terms "melanin", "melanosome" and "pigmentation" (Table S3.1). The comparisons were all significative (Table 3.4). Furthermore, with the aim of providing more robust results, we also used gene lists curated by Baxter et *al*. (2018): one including genes related to integument pigmnetation on human, mice and zebrafish (Table S3.2) and other containing only genes validated in humans (Table S3.3). Genes involved in pigmentation were overrepresented in light melanocytes treated with wild-type or mutated HBD3 and in dark melanocytes treated with wild-type HBD3, in comparison with their respective untreated controls when the complete gene list was used. However, when only the human-validated genes were used the comparisons were only significative for light melanocytes (Table 3.4). The reason could be that the human-validated gene list is more restrictive, leaving out important genes such as *DCT*.

**Table 3.4. Hypergeometric test p-values for the over-representation of pigmentation-related genes in HBD3-treated melanocytes in comparison with non-treated controls, using different gene lists: based on AmiGO database term search or modified from Baxter et *al*. (2018).** D_24h_W: dark melanocytes treated with wild-type HBD3; D_24h_M: dark melanocytes treated with mutated HBD3, L_24h_W: light melanocytes treated with wild-type HBD3; L_24h_M: light melanocytes treated with mutated HBD3.

| | AmiGO | Baxter et *al*. 2018 | |
|---|---|---|---|
| | | ALL | Human-validated |
| **D_24h_W** | $1x10^{-11}$ | 0.0002 | 0.0914 |
| **D_24h_M** | 0.0424 | 0.0998 | 0.8155 |
| **L_24h_W** | $1x10^{-16}$ | 9x10-11 | 0.0021 |
| **L_24h_M** | $3x10^{-12}$ | 0.0002 | 0.0429 |

We also observed changes in the expression of genes related with oxidative stress response and DNA repair. Many genes associated with both functions were upregulated in light melanocytes treated with wild-type and mutated HBD3 and in dark melanocytes treated with wild-type HBD3. Although these categories were not significant in enrichment analyses based on the KEGG, Wikipathway and Panther information, we observed several genes with important functions. Among them, many codify antioxidant enzymes, such as catalase (CAT), superoxide dismutase (SOD1), heme oxygenase 1 (HMOX1), glutamate cysteine ligase (encoded by GCLM and GCLC) and glutathione-S-transferase Pi (GSTP1). Interestingly, genes previously reported to be upregulated by α-MSH (Kokot et *al*., 2009; Song et *al*., 2009; Kadekaro et *al*., 2010, 2012; Abdel-Malek et *al*., 2014) were also upregulated by HBD3. In particular, nearly all of the genes overexpressed after α-MSH treatment included in the categories “Oxidative Stress” and “DNA Repair” in the experiments made by Kadekaro et *al*. (2010), were upregulated by

HBD3 in our experiments. This observation suggests that HBD3 could modulate DNA damage and oxidative stress responses through MC1R, in a similar way than α-MSH.

Finally, in the third principal component (PC3) we observe that most dark cell lines lie at values above 0, whereas most of the light cell lines lie at values below 0, regardless of their condition (treated and untreated) (Figure 3.3). It is possible that this component could explain intrinsic differences between light and dark lines.


**Figure 3.3**. **Principal Component Analysis showing the second (16%) and the third (13%) components.** Samples from L4 cell line (light melanocytes, replicate 4) are highlighted.

## 3.4. Conclusions

In summary, although the specific melanogenic pathway cannot be elucidated from our results, it seems clear that HBD3 stimulates melanogenesis in human melanocytes. It is possible that a crosstalk between SCF/KIT or WNT pathways occurs in the presence of HBD3. Although HBD3 has been described either as an antagonist of MC1R (Swope et *al*., 2012) or as a partial agonist (Beaumont et *al*., 2012), however, the most accepted idea is that HBD3 acts as a neutral antagonist (Nix et *al*., 2013) and that the response depends on the presence of other MC1R ligands such as α-MSH and ASIP. Based on our results we speculated that melanocytes in culture (without complements) would loss pigmentation activity due to the absence of stimulatory factors. Therefore, the observed increase in the expression of melanogenesis related genes induced by HBD3 at 24h could be different if other factors are present. Anyway, we propose that in the absence of other MC1R ligands, HBD3 promotes melanogenesis.

On the other hand, our results suggest that HBD3 could be able to modulate other defence responses associated with MC1R signalling, such as DNA repair and oxidative stress response.

## 3.5. Supplementary Material

**Table S3.1. Gene list elaborated from AmiGO 2 database by searching the terms "melanin", "melanosome" and "pigmentation".** Out of 194 genes, 19 (*) were not present in the microarray and were removed from our final list.

| Gene symbol | Description |
|---|---|
| * *ADAMTS20* | ADAM metallopeptidase with thrombospondin type 1 motif 20 |
| ***ADAMTS9*** | ADAM metallopeptidase with thrombospondin type 1 motif 9 |
| ***AHCY*** | Adenosylhomocysteinase |
| ***ANKRD27*** | Ankyrin repeat domain 27 |
| ***ANXA11*** | Annexin A11 |
| ***ANXA2*** | Annexin A2 |
| * *ANXA2P2* | Annexin A2 pseudogene 2 |
| ***ANXA6*** | Annexin A6 |
| ***AP1G1*** | Adaptor related protein complex 1 subunit gamma 1 |
| ***AP1M1*** | Adaptor related protein complex 1 subunit mu 1 |
| ***AP3B1*** | Adaptor related protein complex 3 subunit beta 1 |
| ***AP3D1*** | Adaptor related protein complex 3 subunit delta 1 |
| ***APPL1*** | Adaptor protein, phosphotyrosine interacting with PH domain and leucine zipper 1 |
| ***ARCN1*** | Archain 1 |
| ***ARL6*** | ADP ribosylation factor like GTPase 6 |
| * *ASIP* | Agouti signaling protein |
| ***ATP1A1*** | ATPase Na+/K+ transporting subunit alpha 1 |
| ***ATP1B3*** | ATPase Na+/K+ transporting subunit beta 3 |
| ***ATP6AP2*** | ATPase H+ transporting accessory protein 2 |
| ***ATP6V0A1*** | ATPase H+ transporting V0 subunit a1 |
| ***ATP6V1B2*** | ATPase H+ transporting V1 subunit B2 |
| ***ATP6V1G2*** | ATPase H+ transporting V1 subunit G2 |
| ***ATP7A*** | ATPase copper transporting alpha |
| ***ATRN*** | Attractin |
| ***BAX*** | BCL2 associated X, apoptosis regulator |
| ***BBS2*** | Bardet-Biedl syndrome 2 |
| ***BBS4*** | Bardet-Biedl syndrome 4 |
| ***BBS5*** | Bardet-Biedl syndrome 5 |
| ***BBS7*** | Bardet-Biedl syndrome 7 |
| ***BCL2*** | BCL2 apoptosis regulator |
| ***BCL2L11*** | BCL2 like 11 |
| ***BLOC1S1*** | Biogenesis of lysosomal organelles complex 1 subunit 1 |
| ***BLOC1S2*** | Biogenesis of lysosomal organelles complex 1 subunit 2 |
| ***BLOC1S3*** | Biogenesis of lysosomal organelles complex 1 subunit 3 |
| ***BLOC1S4*** | Biogenesis of lysosomal organelles complex 1 subunit 4 |

| | |
|---|---|
| ***BLOC1S5*** | Biogenesis of lysosomal organelles complex 1 subunit 5 |
| ***BLOC1S6*** | Biogenesis of lysosomal organelles complex 1 subunit 6 |
| ***BSG*** | Basigin (Ok blood group) |
| ***CALU*** | Calumenin |
| ***CANX*** | Calnexin |
| ***CAPG*** | Capping actin protein, gelsolin like |
| ***CCT4*** | Chaperonin containing TCP1 subunit 4 |
| ***CD63*** | CD63 molecule |
| ***CDH3*** | Cadherin 3 |
| ***CITED1*** | Cbp/p300 interacting transactivator with Glu/Asp rich carboxy-terminal domain 1 |
| ***CLTC*** | Clathrin heavy chain |
| ***CNP*** | 2',3'-cyclic nucleotide 3' phosphodiesterase |
| ***CTNS*** | Cystinosin, lysosomal cystine transporter |
| ***CTSB*** | Cathepsin B |
| ***CTSD*** | Cathepsin D |
| ***DCT*** | Dopachrome tautomerase |
| ***DCTN2*** | Dynactin subunit 2 |
| ***DDT*** | D-dopachrome tautomerase |
| ***DNAJC5*** | DnaJ heat shock protein family (Hsp40) member C5 |
| * *DRD2* | Dopamine receptor D2 |
| ***DTNBP1*** | Dystrobrevin binding protein 1 |
| ***EDA*** | Ectodysplasin A |
| * *EDAR* | Ectodysplasin A receptor |
| ***EDN3*** | Endothelin 3 |
| ***EDNRB*** | Endothelin receptor type B |
| * *EN1* | Engrailed homeobox 1 |
| ***ENPP1*** | Ectonucleotide pyrophosphatase/phosphodiesterase 1 |
| ***ERP29*** | Endoplasmic reticulum protein 29 |
| ***FASN*** | Fatty acid synthase |
| ***FIG4*** | FIG4 phosphoinositide 5-phosphatase |
| ***FLOT1*** | Flotillin 1 |
| ***GANAB*** | Glucosidase II alpha subunit |
| ***GCHFR*** | GTP cyclohydrolase I feedback regulator |
| ***GGH*** | Gamma-glutamyl hydrolase |
| ***GIPC1*** | GIPC PDZ domain containing family member 1 |
| ***GLI3*** | GLI family zinc finger 3 |
| ***GNA11*** | G protein subunit alpha 11 |
| ***GNA13*** | G protein subunit alpha 13 |
| ***GPNMB*** | Glycoprotein nmb |
| ***GPR143*** | G protein-coupled receptor 143 |
| ***HPS1*** | HPS1 biogenesis of lysosomal organelles complex 3 subunit 1 |
| ***HPS3*** | HPS3 biogenesis of lysosomal organelles complex 2 subunit 1 |
| ***HPS4*** | HPS4 biogenesis of lysosomal organelles complex 3 subunit 2 |
| ***HPS5*** | HPS5 biogenesis of lysosomal organelles complex 2 subunit 2 |

| | |
|---|---|
| ***HPS6*** | HPS6 biogenesis of lysosomal organelles complex 2 subunit 3 |
| ***HSP90AA1*** | Heat shock protein 90 alpha family class A member 1 |
| ***HSP90AB1*** | Heat shock protein 90 alpha family class B member 1 |
| ***HSP90B1*** | Heat shock protein 90 beta family member 1 |
| ***HSPA5*** | Heat shock protein family A (Hsp70) member 5 |
| ***HSPA8*** | Heat shock protein family A (Hsp70) member 8 |
| ***IHH*** | Indian hedgehog signaling molecule |
| ***ITGB1*** | Integrin subunit beta 1 |
| ***ITGB3*** | Integrin subunit beta 3 |
| ***KIF13A*** | Kinesin family member 13A |
| ***KIT*** | KIT proto-oncogene, receptor tyrosine kinase |
| ***KITLG*** | KIT ligand |
| * *KRT76* | Keratin 76 |
| ***LAMP1*** | Lysosomal associated membrane protein 1 |
| ***LEF1*** | Lymphoid enhancer-binding factor 1 |
| * *LRMDA* | Leucine rich melanocyte differentiation associated |
| ***LYST*** | Lysosomal trafficking regulator |
| ***MC1R*** | Melanocortin 1 receptor |
| * *MCHR1* | Melanin concentrating hormone receptor 1 |
| * *MCHR2* | Melanin concentrating hormone receptor 2 |
| ***MEF2C*** | Myocyte enhancer factor 2C |
| ***MFSD12*** | Major facilitator superfamily domain containing 12 |
| ***MITF*** | Microphthalmia-associated transcription factor |
| ***MKKS*** | McKusick-Kaufman syndrome |
| ***MLANA*** | Melan-A |
| ***MLPH*** | Melanophilin |
| ***MMP14*** | Matrix metallopeptidase 14 |
| ***MREG*** | Melanoregulin |
| ***MYH11*** | Myosin heavy chain 11 |
| ***MYO5A*** | Myosin VA (heavy chain 12, myoxin) |
| * *MYO7A* | Myosin VIIA |
| ***MYSM1*** | Myb like, SWIRM and MPN domains 1 |
| ***NAP1L1*** | Nucleosome assembly protein 1 like 1 |
| ***NCSTN*** | Nicastrin |
| ***NF1*** | Neurofibromin 1 |
| ***OCA2*** | OCA2 melanosomal transmembrane protein |
| * *OR51E2* | Olfactory receptor family 51 subfamily E member 2 |
| ***P4HB*** | Prolyl 4-hydroxylase subunit beta |
| ***PDCD6IP*** | Programmed cell death 6 interacting protein |
| ***PDIA3*** | Protein disulfide isomerase family A member 3 |
| ***PDIA4*** | Protein disulfide isomerase family A member 4 |
| ***PDIA6*** | Protein disulfide isomerase family A member 6 |
| * *PMCH* | Pro-melanin concentrating hormone |
| * *PMCHL1* | Pro-melanin concentrating hormone like 1 (pseudogene) |
| * *PMCHL2* | Pro-melanin concentrating hormone like 2 (pseudogene) |

| | |
|---|---|
| ***PMEL*** | Premelanosome protein |
| ***POMC*** | Proopiomelanocortin |
| ***PPIB*** | Peptidylprolyl isomerase B |
| ***PRDX1*** | Peroxiredoxin 1 |
| ***RAB11A*** | RAB11A, member RAS oncogene family |
| ***RAB11B*** | RAB11B, member RAS oncogene family |
| ***RAB17*** | RAB17, member RAS oncogene family |
| ***RAB1A*** | RAB1A, member RAS oncogene family |
| ***RAB27A*** | RAB27A, member RAS oncogene family |
| * *RAB27B* | RAB27B, member RAS oncogene family |
| * *RAB29* | RAB29, member RAS oncogene family |
| ***RAB2A*** | RAB2A, member RAS oncogene family |
| ***RAB32*** | RAB32, member RAS oncogene family |
| ***RAB35*** | RAB35, member RAS oncogene family |
| ***RAB38*** | RAB38, member RAS oncogene family |
| ***RAB5A*** | RAB5A, member RAS oncogene family |
| ***RAB5B*** | RAB5B, member RAS oncogene family |
| ***RAB5C*** | RAB5C, member RAS oncogene family |
| ***RAB7A*** | RAB7A, member RAS oncogene family |
| ***RAB9A*** | RAB9A, member RAS oncogene family |
| ***RAC1*** | Rac family small GTPase 1 |
| * *RACK1* | Receptor for activated C kinase 1 |
| ***RAN*** | RAN, member RAS oncogene family |
| ***RAPGEF2*** | Rap guanine nucleotide exchange factor 2 |
| ***RPN1*** | Ribophorin I |
| ***SDCBP*** | Syndecan binding protein |
| ***SEC22B*** | SEC22 homolog B, vesicle trafficking protein |
| ***SERPINF1*** | Serpin family F member 1 |
| ***SGSM2*** | Small G protein signaling modulator 2 |
| ***SHROOM2*** | Shroom family member 2 |
| * *SHROOM3* | Shroom family member 3 |
| ***SLC1A4*** | Solute carrier family 1 member 4 |
| ***SLC1A5*** | Solute carrier family 1 member 5 |
| ***SLC24A5*** | Solute carrier family 24 member 5 |
| ***SLC2A1*** | Solute carrier family 2 member 1 |
| ***SLC3A2*** | Solute carrier family 3 member 2 |
| ***SLC45A2*** | Solute carrier family 45 member 2 |
| ***SLC7A11*** | Solute carrier family 7 member 11 |
| ***SNAI2*** | Snail family transcriptional repressor 2 |
| ***SNAPIN*** | SNAP associated protein |
| ***SND1*** | Staphylococcal nuclease and tudor domain containing 1 |
| ***SOX10*** | SRY(sex determining region Y)-box transcription factor 10 |
| ***SPARC*** | Secreted protein acidic and cysteine rich |
| ***SPNS2*** | Sphingolipid transporter 2 |
| ***STOM*** | Stomatin |

| | |
|---|---|
| ***STX3*** | Syntaxin 3 |
| ***SYNGR1*** | Synaptogyrin 1 |
| ***SYPL1*** | Synaptophysin like 1 |
| ***SYTL1*** | Synaptotagmin like 1 |
| ***SYTL2*** | Synaptotagmin like 2 |
| ***SZT2*** | SZT2 subunit of KICSTOR complex |
| ***TFRC*** | Transferrin receptor |
| ***TH*** | Tyrosine hydroxylase |
| ***TMED10*** | Transmembrane p24 trafficking protein 10 |
| ***TMEM33*** | Transmembrane protein 33 |
| ***TPP1*** | Tripeptidyl peptidase 1 |
| ***TRAPPC6A*** | Trafficking protein particle complex 6A |
| ***TRPC1*** | Transient receptor potential cation channel subfamily C member 1 |
| ***TRPV2*** | Transient receptor potential cation channel subfamily V member 2 |
| ***TYR*** | Tyrosinase |
| ***TYRP1*** | Tyrosinase-related protein 1 |
| ***USP13*** | Ubiquitin specific peptidase 13 |
| ***VANGL1*** | VANGL planar cell polarity protein 1 |
| ***VPS33A*** | VPS33A core subunit of CORVET and HOPS complexes |
| ***VPS33B*** | VPS33B late endosome and lysosome associated |
| ***WNT5A*** | Wnt family member 5A |
| ***YWHAB*** | Tyrosine 3-monooxygenase/tryptophan 5-monooxygenase activation protein beta |
| ***YWHAE*** | Tyrosine 3-monooxygenase/tryptophan 5-monooxygenase activation protein epsilon |
| ***YWHAZ*** | Tyrosine 3-monooxygenase/tryptophan 5-monooxygenase activation protein zeta |
| ***ZEB2*** | Zinc finger E-box binding homeobox 2 |

* Not present in the microarray

**Table S3.2. Gene list elaborated from Baxter et *al*. (2018) including genes related with pigmentation in human, mice and zebrafish.** Out of 650 genes, 92 (*) were not present in the microarray and were removed from our final list (we also removed genes with not clear human orthologues).

| Gene Symbol | Description |
|---|---|
| ***ABCA12*** | ATP binding cassette subfamily A member 12 |
| ***ABCB6*** | ATP binding cassette subfamily B member 6 |
| ***ABHD11*** | Abhydrolase domain containing 11 |
| ***ACD*** | ACD shelterin complex subunit and telomerase recruitment factor |
| ***ACVR2A*** | Activin A receptor type 2A |
| ***ADAM10*** | ADAM metallopeptidase domain 10 |
| ***ADAM17*** | ADAM metallopeptidase domain 17 |
| * *ADAMTS20* | ADAM metallopeptidase with thrombospondin type 1 motif 20 |
| ***ADAMTS9*** | ADAM metallopeptidase with thrombospondin type 1 motif 9 |
| ***ADAR*** | Adenosine deaminase RNA specific |
| * *ADCY5* | Adenylate cyclase 5 |
| * *ADGRA2* | Adhesion G protein-coupled receptor A2 |
| ***ADRB2*** | Adrenoceptor beta 2 |
| ***AEBP2*** | AE binding protein 2 |
| ***AFG3L2*** | AFG3 like matrix AAA peptidase subunit 2 |
| ***AHCY*** | Adenosylhomocysteinase |
| ***ALCAM*** | Activated leukocyte cell adhesion molecule |
| ***ALDH2*** | Aldehyde dehydrogenase 2 family member |
| ***ALDOA*** | Aldolase, fructose-bisphosphate A |
| ***ALG13*** | ALG13 UDP-N-acetylglucosaminyltransferase subunit |
| * *ALX3* | ALX homeobox 3 |
| ***AMBRA1*** | Autophagy and beclin 1 regulator 1 |
| ***ANXA2*** | Annexin A2 |
| ***AP1S1*** | Adaptor related protein complex 3 subunit sigma 1 |
| ***AP3B1*** | Adaptor related protein complex 3 subunit beta 1 |
| ***AP3D1*** | Adaptor related protein complex 3 subunit delta 1 |
| ***AP3S2*** | Adaptor related protein complex 3 subunit sigma 2 |
| ***APC*** | APC regulator of WNT signaling pathway |
| ***ARCN1*** | Archain 1 |
| ***ARL6*** | ADP ribosylation factor like GTPase 6 |
| ***ARL6IP1*** | ADP ribosylation factor like GTPase 6 interacting protein 1 |
| * *ASIP* | Agouti signaling protein |
| ***ATE1*** | Arginyltransferase 1 |
| ***ATG7*** | Autophagy related 7 |
| ***ATM*** | ATM serine/threonine kinase |
| * *ATOH7* | Atonal bHLH transcription factor 7 |

| | |
|---|---|
| ***ATOX1*** | Antioxidant 1 copper chaperone |
| ***ATP1A1*** | ATPase Na+/K+ transporting subunit alpha 1 |
| ***ATP6AP1*** | ATPase H+ transporting accessory protein 1 |
| ***ATP6AP2*** | ATPase H+ transporting accessory protein 2 |
| ***ATP6V0B*** | ATPase H+ transporting V0 subunit B |
| ***ATP6V0C*** | ATPase H+ transporting V0 subunit C |
| ***ATP6V0D1*** | ATPase H+ transporting V0 subunit D1 |
| ***ATP6V1E1 / ATP6V1E2*** | ATPase H+ transporting V0 subunit E1 /E2 |
| ***ATP6V1F*** | ATPase H+ transporting V1 subunit F |
| ***ATP6V1H*** | ATPase H+ transporting V1 subunit H |
| ***ATP7A*** | ATPase copper transporting, alpha |
| ***ATP7B*** | ATPase copper transporting,beta |
| ***ATR*** | ATR serine/threonine kinase |
| ***ATRN*** | Attractin |
| ***BACE2*** | Beta-secretase 2 |
| * *BARX2* | BARX homeobox 2 |
| ***BBIP1*** | BBSome interacting protein 1 |
| ***BBS1*** | Bardet-Biedl syndrome 1 |
| ***BBS2*** | Bardet-Biedl syndrome 2 |
| ***BBS4*** | Bardet-Biedl syndrome 4 |
| ***BBS7*** | Bardet-Biedl syndrome 7 |
| ***BCL2*** | BCL2 apoptosis regulator |
| ***BCL2L11*** | BCL2 like 11 |
| ***BLM*** | BLM RecQ like helicase |
| ***BLOC1S3*** | Biogenesis of lysosomal organelles complex 1 subunit 3 |
| ***BLOC1S4*** | Biogenesis of lysosomal organelles complex 1 subunit 4 |
| ***BLOC1S5*** | Biogenesis of lysosomal organelles complex 1 subunit 5 |
| ***BLOC1S6*** | Biogenesis of lysosomal organelles complex 1 subunit 6 |
| * *BMP5* | Bone morphogenetic protein 5 |
| ***BMPR2*** | Bone morphogenetic protein receptor type 2 |
| ***BNC2*** | Basonuclin 2 |
| ***BRAF*** | B-Raf proto-oncogene, serine/threonine kinase |
| ***BRCA1*** | Basonuclin 2 |
| ***BRCA2*** | BRCA2 DNA repair associated |
| ***BRIP1*** | BRCA1 interacting protein C-terminal helicase 1 |
| ***BTD*** | Biotinase |
| ***C3ORF38*** | Chromosome 3 open reading frame 38 |
| ***C8ORF37*** | Chromosome 8 open reading frame 37 |
| ***CARS*** | Cysteinyl-tRNA synthetase |
| ***CAV1*** | Caveolin 1 |
| ***CBL*** | Cbl proto-oncogene |
| ***CBS*** | Cystathionine beta-synthase |

| | |
|---|---|
| ***CCDC28B*** | Coiled-coil domain containing 28B |
| ***CCT2*** | Chaperonin containing TCP1 subunit 2 |
| ***CDC25A / CDC25B*** | Cell division cycle 25A/B |
| ***CDC42*** | Cell division cycle 42 |
| ***CDC73*** | Cell division cycle 42 |
| ***CDH11*** | Cadherin 11 |
| ***CDH2*** | Cadherin 2 |
| ***CDH3*** | Cadherin 3 |
| ***CDK5*** | Cyclin dependent kinase 5 |
| ***CDK7*** | Cyclin dependent kinase 7 |
| ***CDKN2A*** | Cyclin dependent kinase inhibitor 2A |
| ***CDX1*** | Caudal type homeobox 1 |
| * *CEP131* | Centrosomal protein 131 |
| ***CEP290*** | Centrosomal protein 290 |
| * *CGA* | Glycoprotein hormones, alpha polypeptide |
| ***CHD7*** | Chromodomain helicase DNA binding protein 7 |
| ***CHEK1*** | Checkpoint kinase 1 |
| ***CIB2*** | Calcium and integrin binding family member 2 |
| ***CISD2*** | CDGSH iron sulfur domain 2 |
| ***CITED1*** | Cbp/p300 interacting transactivator with Glu/Asp rich carboxy-terminal domain 1 |
| ***CLCN7*** | Chloride voltage-gated channel 7 |
| * *COL17A1* | Collagen type XVII alpha 1 chain |
| ***COL6A2*** | Collagen type VI alpha 2 chain |
| * *COLEC11* | Collectin subfamily member 11 |
| * *COP1* | COP1 E3 ubiquitin ligase |
| ***COPA*** | COPI coat complex subunit alpha |
| ***COPB1*** | COPI coat complex subunit beta 1 |
| ***COPB2*** | COPI coat complex subunit beta 2 |
| * *CORIN* | Corin, serine peptidase |
| ***CORO1A*** | Coronin 1A |
| * *CPLX4* | Complexin 4 |
| ***CPSF1*** | Cleavage and polyadenylation specific factor 1 |
| * *CRB2* | Crumbs cell polarity complex component 2 |
| ***CREB3L2*** | cAMP responsive element binding protein 3 like 2 |
| * *CRH* | Corticotropin releasing hormone |
| * *CSF1R* | Colony stimulating factor 1 receptor |
| ***CSNK1A1*** | Casein kinase 1 alpha 1 |
| ***CTBP2*** | C-terminal binding protein 2 |
| ***CTC1*** | CST telomere replication complex component 1 |
| ***CTLA4*** | Cytotoxic T-lymphocyte associated protein 4 |
| ***CTNNB1*** | Catenin beta 1 |

| | |
|---|---|
| ***CTNS*** | Cystinosin, lysosomal cystine transporter |
| ***CTR9*** | CTR9 homolog, Paf1/RNA polymerase II complex component |
| ***CTSD*** | Cathepsin D |
| ***CXCL12*** | C-X-C motif chemokine ligand 12 |
| ***CYP11A1*** | Cytochrome P450 family 11 subfamily A member 1 |
| ***DCT*** | Dopachrome tautomerase |
| ***DCTN1*** | Dynactin subunit |
| ***DCTN2*** | Dynactin subunit 2 |
| ***DDB2*** | Damage specific DNA binding protein 2 |
| ***DDX3X*** | DEAD-box helicase 3 X-linked |
| ***DHRSX*** | dehydrogenase/reductase X-linked |
| ***DIO2*** | Iodothyronine deiodinase 2 |
| ***DISC1*** | DISC1 scaffold protein |
| ***DKC1*** | Dyskerin pseudouridine synthase 1 |
| ***DLAT*** | Dihydrolipoamide S-acetyltransferase |
| ***DMXL2*** | Dmx like 2 |
| ***DNM2*** | Dynamin 2 |
| ***DOCK7*** | Dedicator of cytokinesis 7 |
| * *DRD2* | Dopamine receptor D2 |
| * *DSG4* | Desmoglein 4 |
| ***DSTYK*** | Dual serine/threonine and tyrosine protein kinase |
| ***DTNBP1*** | Dystrobrevin binding protein 1 |
| ***DYNC1H1*** | Dynein cytoplasmic 1 heavy chain 1 |
| ***DZANK1*** | Double zinc ribbon and ankyrin repeat domains 1 |
| ***EBNA1BP2*** | EBNA1 binding protein 2 |
| ***ECE1*** | Endothelin converting enzyme 1 |
| ***ECE2*** | Endothelin converting enzyme 2 |
| ***EDA*** | Ectodysplasin A |
| * *EDAR* | Ectodysplasin A receptor |
| ***EDARADD*** | EDAR associated death domain |
| * *EDN1* | Endothelin 1 |
| ***EDN3*** | Endothelin 3 |
| ***EDNRB*** | Endothelin receptor type B |
| ***EED*** | Embryonic ectoderm development |
| ***EGFR*** | Epidermal growth factor receptor |
| ***EIF3B*** | Eukaryotic translation initiation factor 3 subunit B |
| ***EIF3C*** | Eukaryotic translation initiation factor 3 subunit C |
| ***EIF3E*** | Eukaryotic translation initiation factor 3 subunit E |
| ***EIF3G*** | Eukaryotic translation initiation factor 3 subunit G |
| ***EIF3H*** | Eukaryotic translation initiation factor 3 subunit H |
| ***EIF3I*** | Eukaryotic translation initiation factor 3 subunit I |
| * *EN1* | Engrailed homeobox 1 |

| | |
|---|---|
| ***ENPP1*** | Ectonucleotide pyrophosphatase/phosphodiesterase 1 |
| ***EPG5*** | Ectopic P-granules autophagy protein 5 homolog |
| ***ERBB3*** | Erb-b2 receptor tyrosine kinase 3 |
| ***ERCC2*** | ERCC excision repair 2, TFIIH core complex helicase subunit |
| ***ERCC3*** | ERCC excision repair 3, TFIIH core complex helicase subunit |
| ***ERCC4*** | ERCC excision repair 4, endonuclease catalytic subunit |
| ***ERCC5*** | ERCC excision repair 5, endonuclease |
| ***ERCC6*** | ERCC excision repair 6, chromatin remodeling factor |
| ***ESCO2*** | Establishment of sister chromatid cohesion N-acetyltransferase 2 |
| ***ETS1*** | ETS proto-oncogene 1, transcription factor |
| ***EXOC5*** | Exocyst complex component 5 |
| ***FAM57B / TLCD3B*** | TLC domain containing 3B |
| ***FANCA*** | FA complementation group A |
| ***FANCC*** | FA complementation group C |
| ***FANCD2*** | FA complementation group D2 |
| ***FANCE*** | FA complementation group E |
| ***FANCI*** | FA complementation group I |
| ***FBXO5*** | F-box protein 5 |
| ***FBXW4*** | F-box and WD repeat domain containing 4 |
| ***FGFR3*** | Fibroblast growth factor receptor 3 |
| ***FHL1*** | Four and a half LIM domains 1 |
| ***FIG4*** | FIG4 phosphoinositide 5-phosphatase |
| ***FLNA*** | Filamin A |
| ***FMR1*** | FMRP translational regulator 1 |
| ***FOXD3*** | Forkhead box D3 |
| ***FOXM1*** | Forkhead box M1 |
| ***FOXN1*** | Forkhead box N1 |
| * *FREM2* | FRAS1 related extracellular matrix 2 |
| ***FSCN1*** | Fascin actin-bundling protein 1 |
| ***FTO*** | FTO alpha-ketoglutarate dependent dioxygenase |
| ***FZD4*** | Frizzled class receptor 4 |
| ***GART*** | Phosphoribosylglycinamide formyltransferase, phosphoribosylglycinamide synthetase, phosphoribosylaminoimidazole |
| ***GAS7*** | Growth arrest specific 7 |
| * *GATA3* | GATA binding protein 3 |
| ***GBF1*** | Golgi brefeldin A resistant guanine nucleotide exchange factor 1 |
| * *GDF6* | Growth differentiation factor 6 |
| ***GDPD3*** | Glycerophosphodiester phosphodiesterase domain containing 3 |
| ***GFPT1*** | Glutamine--fructose-6-phosphate transaminase 1 |
| ***GGT1*** | Gamma-glutamyltransferase 1 |
| * *GJA4* | Gap junction protein alpha 4 |
| * *GJA5* | Gap junction protein alpha 5 |

| | |
|---|---|
| ***GLI3*** | GLI family zinc finger 3 |
| ***GMPPB*** | GDP-mannose pyrophosphorylase B |
| ***GMPS*** | Guanine monophosphate synthase |
| ***GNA11*** | G protein subunit alpha 11 |
| ***GNAI3*** | G protein subunit alpha i3 |
| ***GNAQ*** | G protein subunit alpha q |
| ***GNAS*** | GNAS complex locus |
| * *GNAT2* | G protein subunit alpha transducin 2 |
| ***GPATCH3*** | G-patch domain containing 3 |
| ***GPC3*** | Glypican 3 |
| ***GPER1*** | G protein-coupled estrogen receptor 1 |
| ***GPNMB*** | Glycoprotein nmb |
| ***GPR143*** | G protein-coupled receptor 143 |
| ***GPR161*** | G protein-coupled receptor 161 |
| ***GPR89A / GPR89B*** | G protein-coupled receptor 89A/B |
| * *GRK3* | G protein-coupled receptor kinase 3 |
| ***GRM1*** | Glutamate metabotropic receptor 1 |
| ***GTF2IRD1*** | GTF2I repeat domain containing 1 |
| ***GTPBP3*** | GTP binding protein 3, mitochondrial |
| ***H3F3A*** | H3.3 histone A |
| ***HDAC1*** | Histone deacetylase 1 |
| ***HDAC2*** | Histone deacetylase 2 |
| ***HELLS*** | Helicase, lymphoid specific |
| ***HES1*** | Hes family bHLH transcription factor 1 |
| ***HEXIM1*** | HEXIM P-TEFb complex subunit 1 |
| + *HGF* | Hepatocyte growth factor |
| ***HIPK2*** | Homeodomain interacting protein kinase 2 |
| ***HIRIP3*** | HIRA interacting protein 3 |
| * *HOXA13* | Homeobox A13 |
| ***HOXB7*** | Homeobox B7 |
| ***HPS1*** | HPS1 biogenesis of lysosomal organelles complex 3 subunit 1 |
| ***HPS3*** | HPS3 biogenesis of lysosomal organelles complex 2 subunit 1 |
| ***HPS4*** | HPS4 biogenesis of lysosomal organelles complex 3 subunit 2 |
| ***HPS5*** | HPS5 biogenesis of lysosomal organelles complex 2 subunit 2 |
| ***HPS6*** | HPS6 biogenesis of lysosomal organelles complex 2 subunit 3 |
| ***HRAS*** | Harvey rat sarcoma viral oncogene homolog |
| * *HSD3B1* | Hydroxy-delta-5-steroid dehydrogenase, 3 beta- and steroid delta-isomerase 1 |
| ***HSP90B1*** | Heat shock protein 90 beta family member 1 |
| ***HTRA1*** | HtrA serine peptidase 1 |
| ***HTT*** | Huntingtin |
| ***IDS*** | Iduronate 2-sulfatase |
| ***IDUA*** | Alpha-L-iduronidase |

| | |
|---|---|
| ***IER3IP1*** | Immediate early response 3 interacting protein 1 |
| ***IFT122*** | Intraflagellar transport 122 |
| ***IFT27*** | Intraflagellar transport 27 |
| ***IGFBP7*** | Insulin like growth factor binding protein 7 |
| ***IGSF11*** | Immunoglobulin superfamily member 11 |
| ***IKBKB*** | Inhibitor of nuclear factor kappa B kinase subunit beta |
| ***IKBKG*** | Inhibitor of nuclear factor kappa B kinase regulatory subunit gamma |
| * *IL17A* | Interleukin 17A |
| ***ILK*** | Integrin linked kinase |
| ***IMPDH1*** | Inosine monophosphate dehydrogenase 1 |
| ***INO80E*** | INO80 complex subunit E |
| ***INPP5B*** | Inositol polyphosphate-5-phosphatase B |
| ***INPP5E*** | Inositol polyphosphate-5-phosphatase E |
| ***IPPK*** | Inositol-pentakisphosphate 2-kinase |
| ***IRF4*** | Interferon regulatory factor 4 |
| ***IRX1*** | Iroquois homeobox 1 |
| * *IRX2* | Iroquois homeobox 2 |
| ***ITGA3*** | Integrin subunit alpha 3 |
| ***ITGB1*** | Integrin subunit beta 1 |
| ***JAM3*** | Junctional adhesion molecule 3 |
| ***KBTBD8*** | Kelch repeat and BTB domain containing 8 |
| ***KCNJ13*** | Potassium inwardly rectifying channel subfamily J member 13 |
| ***KCTD15*** | Potassium channel tetramerization domain containing 15 |
| ***KIF13A*** | Kinesin family member 13A |
| ***KIF3A*** | Kinesin family member 3A |
| ***KIF5A*** | Kinesin family member 5A |
| ***KIT*** | KIT proto-oncogene, receptor tyrosine kinase |
| ***KITLG*** | KIT ligand |
| ***KRAS*** | KRAS proto-oncogene, GTPase |
| * *KRT1* | Keratin 1 |
| * *KRT14* | Keratin 14 |
| * *KRT17* | Keratin 17 |
| * *KRT2* | Keratin 2 |
| ***KRT27*** | Keratin 27 |
| ***KRT4*** | Keratin 4 |
| * *KRT5* | Keratin 5 |
| * *KRT75* | Keratin 75 |
| * *KRT76* | Keratin 76 |
| ***KRT9*** | Keratin 9 |
| ***LARP7*** | La ribonucleoprotein 7, transcriptional regulator |
| ***LEF1*** | Lymphoid enhancer-binding factor 1 |
| ***LEO1*** | LEO1 homolog, Paf1/RNA polymerase II complex component |
| * *LEP* | Leptin |

| | |
|---|---|
| * *LHX2* | LIM homeobox 2 |
| * *LIPH* | Lipase H |
| ***LMLN*** | Leishmanolysin like peptidase |
| ***LMNA*** | Lamin A/C |
| * *LMX1A* | LIM homeobox transcription factor 1 alpha |
| ***LOX*** | Lysyl oxidase |
| * *LRMDA* | Leucine rich melanocyte differentiation associated |
| ***LRSAM1*** | Leucine rich repeat and sterile alpha motif containing 1 |
| ***LTK*** | Leukocyte receptor tyrosine kinase |
| * *LVRN* | Laeverin |
| ***LYST*** | Lysosomal trafficking regulator |
| ***MAFB*** | MAF bZIP transcription factor B |
| ***MAGOH*** | Mago homolog, exon junction complex subunit |
| ***MAP1LC3A*** | Microtubule associated protein 1 light chain 3 alpha |
| ***MAP2K1*** | Mitogen-activated protein kinase kinase 1 |
| ***MAP2K2*** | Mitogen-activated protein kinase kinase 2 |
| ***MAPK3*** | Mitogen-activated protein kinase kinase 3 |
| * *MASP1* | mannan binding lectin serine peptidase 1 |
| ***MATN1*** | Matrilin 1 |
| ***MBTPS1*** | Membrane bound transcription factor peptidase, site 1 |
| ***MC1R*** | Melanocortin 1 receptor |
| * *MC2R* | Melanocortin 2 receptor |
| ***MCM2*** | Minichromosome maintenance complex component 2 |
| ***MCM4*** | Minichromosome maintenance complex component 4 |
| ***MCOLN3*** | Mucolipin 3 |
| ***MCRS1*** | Microspherule protein 1 |
| ***MDM2*** | MDM2 proto-oncogene |
| ***MDM4*** | MDM4 regulator of p53 |
| ***MDN1*** | Midasin AAA ATPase 1 |
| ***MED12*** | Mediator complex subunit 12 |
| ***MED14*** | Mediator complex subunit 14 |
| ***MED23*** | Mediator complex subunit 23 |
| ***MEF2C*** | Myocyte enhancer factor 2C |
| ***MEMO1*** | Mediator of cell motility 1 |
| ***MEN1*** | Menin 1 |
| * *MEOX1* | Mesenchyme homeobox 1 |
| ***MEPCE*** | Methylphosphate capping enzyme |
| ***MESP1*** | Mesoderm posterior bHLH transcription factor 1 |
| ***MFSD12*** | Major facilitator superfamily domain containing 12 |
| ***MGRN1*** | Mahogunin ring finger 1 |
| ***MIB1*** | Mindbomb E3 ubiquitin protein ligase 1 |
| ***MIB2*** | Mindbomb E3 ubiquitin protein ligase 2 |
| ***MITF*** | Microphthalmia-associated transcription factor |

| | |
|---|---|
| ***MKKS*** | McKusick-Kaufman syndrome |
| ***MKLN1*** | Muskelin 1 |
| ***MLANA*** | Melan-A |
| ***MLH1*** | MutL homolog 1 |
| ***MLPH*** | Melanophilin |
| ***MMP17*** | Matrix metallopeptidase 17 |
| ***MPND*** | MPN domain containing |
| ***MPP5*** | Membrane palmitoylated protein 5 |
| ***MPV17*** | Mitochondrial inner membrane protein MPV17 |
| ***MPZL3*** | Myelin protein zero like 3 |
| *MRAP* * | Melanocortin 2 receptor accessory protein |
| ***MREG*** | Melanoregulin |
| ***MSH2*** | MutS homolog 2 |
| ***MSH6*** | MutS homolog 6 |
| * *MTREX* | Mtr4 exosome RNA helicase |
| ***MYC*** | MYC proto-oncogene, bHLH transcription factor |
| ***MYCBP2*** | MYC binding protein 2 |
| ***MYH9*** | Myosin heavy chain 9 |
| ***MYO10*** | Myosin X |
| ***MYO5A*** | Myosin VA (heavy chain 12, myoxin) |
| ***MYO6*** | Myosin VI |
| * *MYRIP* | Myosin VIIA and Rab interacting protein |
| ***MYSM1*** | Myb like, SWIRM and MPN domains 1 |
| ***NAA10*** | N-alpha-acetyltransferase 10, NatA catalytic subunit |
| ***NBN*** | Nibrin |
| ***NCSTN*** | Nicastrin |
| ***NF1*** | Neurofibromin 1 |
| ***NFIB*** | nuclear factor I B |
| ***NINL*** | Ninein like |
| ***NNT*** | Nicotinamide nucleotide transhydrogenase |
| ***NOC3L*** | NOC3 like DNA replication regulator |
| ***NOTCH1*** | Notch receptor 1 |
| ***NOTCH2*** | Notch receptor 2 |
| * *NOTO* | Notochord homeobox |
| ***NR0B1*** | Nclear receptor subfamily 0 group B member 1 |
| ***NR3C1*** | Nuclear receptor subfamily 3 group C member 1 |
| ***NR4A3*** | Nuclear receptor subfamily 4 group A member 3 |
| ***NRARP*** | NOTCH regulated ankyrin repeat protein |
| ***NRAS*** | NRAS proto-oncogene, GTPase |
| ***NSDHL*** | NAD(P) dependent steroid dehydrogenase-like |
| ***NSF*** | N-ethylmaleimide sensitive factor, vesicle fusing ATPase |
| ***NSMCE2*** | NSE2 (MMS21) homolog, SMC5-SMC6 complex SUMO ligase |
| ***NUP88*** | Nucleoporin 88 |

| | |
|---|---|
| ***OAT*** | Ornithine aminotransferase |
| ***OCA2*** | OCA2 melanosomal transmembrane protein |
| ***OCRL*** | OCRL inositol polyphosphate-5-phosphatase |
| ***OPHN1*** | Oligophrenin 1 |
| ***OPTN*** | Optineurin |
| ***OSTM1*** | Osteopetrosis associated transmembrane protein 1 |
| ***OTUD5*** | OTU deubiquitinase 5 |
| ***OVOL1*** | Ovo like transcriptional repressor 1p |
| ***PAFAH1B1*** | Platelet activating factor acetylhydrolase 1b regulatory subunit 1 |
| *PAH* * | Phenylalanine hydroxylase |
| ***PAICS*** | Phosphoribosylaminoimidazole carboxylase and phosphoribosylaminoimidazolesuccinocarboxamide synthase |
| ***PAK1*** | p21 (RAC1) activated kinase 1 |
| ***PALB2*** | Partner and localizer of BRCA2 |
| ***PAQR7*** | Progestin and adipoQ receptor family member 7 |
| ***PARD3*** | Par-3 family cell polarity regulator |
| ***PARN*** | Poly(A)-specific ribonuclease |
| ***PARP3*** | Poly(ADP-ribose) polymerase family member 3 |
| ***PAX3*** | Paired box 3 |
| ***PAX7*** | Paired box 7 |
| ***PCBD1*** | Pterin-4 alpha-carbinolamine dehydratase 1 |
| * *PCDH10* | Protocadherin 10 |
| ***PCNT*** | pericentrin |
| ***PDHB*** | Pyruvate dehydrogenase E1 subunit beta |
| ***PEPD*** | Peptidase D |
| ***PFAS*** | Phosphoribosylformylglycinamidine synthase |
| ***PICALM*** | Phosphatidylinositol binding clathrin assembly protein |
| ***PIGK*** | Phosphatidylinositol glycan anchor biosynthesis class K |
| ***PIKFYVE*** | Phosphoinositide kinase, FYVE-type zinc finger containing |
| ***PKN2*** | Protein kinase N2 |
| ***PKNOX1*** | PBX/knotted 1 homeobox 1 |
| ***PLK4*** | Polo like kinase 4 |
| ***PLXNB2*** | Plexin B2 |
| * *PMCH* | Pro-melanin concentrating hormone |
| ***PMEL*** | Premelanosome protein |
| ***PMS2*** | PMS1 homolog 2, mismatch repair system component |
| ***PNN*** | Pinin, desmosome associated protein |
| ***POC1B*** | POC1 centriolar protein B |
| ***POFUT1*** | Protein O-fucosyltransferase 1 |
| ***POGLUT1*** | Protein O-glucosyltransferase 1 |
| ***POGZ*** | Pogo transposable element derived with ZNF domain |
| ***POLA1*** | DNA polymerase alpha 1, catalytic subunit |
| ***POLG*** | DNA polymerase gamma |

| | |
|---|---|
| ***POLH*** | DNA polymerase eta |
| ***POLR1A*** | RNA polymerase I subunit A |
| ***POLR2G*** | RNA polymerase II subunit G |
| ***POMC*** | Proopiomelanocortin |
| ***PPARGC1A*** | PPARG coactivator 1 alpha |
| ***PPP4C*** | Protein phosphatase 4 catalytic subunit |
| ***PRDM1*** | PR/SET domain 1 |
| ***PRICKLE2*** | Prickle planar cell polarity protein 2 |
| ***PRKAR1A*** | Protein kinase cAMP-dependent type I regulatory subunit alpha |
| ***PRKDC*** | Protein kinase, DNA-activated, catalytic subunit |
| ***PRPS1*** | Phosphoribosyl pyrophosphate synthetase 1 |
| ***PSEN1*** | Presenilin 1 |
| ***PSEN2*** | Presenilin 2 |
| ***PSENEN*** | Presenilin enhancer, gamma-secretase subunit |
| ***PTCH1*** | Patched 1 |
| ***PTCH2*** | Patched 2 |
| ***PTEN*** | Phosphatase and tensin homolog |
| ***PTPN11*** | Protein tyrosine phosphatase non-receptor type 11 |
| ***PTPN21*** | Protein tyrosine phosphatase non-receptor type 21 |
| * *PTPN6* | Protein tyrosine phosphatase non-receptor type 6 |
| ***PTS*** | 6-pyruvoyltetrahydropterin synthase |
| ***PXDN*** | Peroxidasin |
| ***RAB11A*** | RAB11A, member RAS oncogene family |
| ***RAB11B*** | RAB11B, member RAS oncogene family |
| ***RAB17*** | RAB17, member RAS oncogene family |
| ***RAB1A*** | RAB1A, member RAS oncogene family |
| ***RAB27A*** | RAB27A, member RAS oncogene family |
| ***RAB32*** | RAB32, member RAS oncogene family |
| ***RAB36*** | RAB36, member RAS oncogene family |
| ***RAB38*** | RAB38, member RAS oncogene family |
| ***RAB3IP*** | RAB3A interacting protein |
| ***RAB7A*** | RAB7A, member RAS oncogene family |
| ***RAB8A*** | RAB8A, member RAS oncogene family |
| ***RAB9A*** | RAB9A, member RAS oncogene family |
| ***RABGGTA*** | Rab geranylgeranyltransferase subunit alpha |
| ***RAC1*** | Rac family small GTPase 1 |
| * *RACK1* | Receptor for activated C kinase 1 |
| ***RAD21*** | RAD21 cohesin complex component |
| ***RAD50*** | RAD50 double strand break repair protein |
| ***RADIL*** | Rap associating with DIL domain |
| ***RAF1*** | v-raf-1 murine leukemia viral oncogene homolog 1 |
| ***RAG1*** | Recombination activating 1 |
| ***RAPGEF2*** | Rap guanine nucleotide exchange factor 2 |

| | |
|---|---|
| ***RAPH1*** | Ras association (RalGDS/AF-6) and pleckstrin homology domains 1 |
| ***RAX*** | Retina and anterior neural fold homeobox |
| ***RB1*** | RB transcriptional corepressor 1 |
| ***RBPJ*** | Recombination signal binding protein for immunoglobulin kappa J region |
| ***RECQL4*** | RecQ like helicase 4 |
| ***REST*** | RE1 silencing transcription factor |
| ***RHBDF2*** | Rhomboid 5 homolog 2 |
| ***RIC8B*** | RIC8 guanine nucleotide exchange factor B |
| ***RILP*** | Rab interacting lysosomal protein |
| ***RIT1*** | Ras like without CAAX 1 |
| ***RNF2*** | Ring finger protein 2 |
| ***RNF41*** | Ring finger protein 41 |
| ***RPGR*** | Retinitis pigmentosa GTPase regulator |
| ***RPL24*** | Ribosomal protein L24 |
| ***RPL27A*** | Ribosomal protein L27A |
| ***RPL38*** | Ribosomal protein L38 |
| ***RPS14*** | Ribosomal protein S14 |
| ***RPS19*** | Ribosomal protein S19 |
| ***RPS20*** | Ribosomal protein S20 |
| ***RPS6*** | Ribosomal protein S6 |
| ***RPS7*** | Ribosomal protein S7 |
| ***RTF1*** | RTF1 homolog, Paf1/RNA polymerase II complex component |
| ***RUVBL2*** | RuvB like AAA ATPase 2 |
| ***RXRA*** | Retinoid X receptor alpha |
| ***SAMD9*** | Sterile alpha motif domain containing 9 |
| ***SASH1*** | SAM and SH3 domain containing 1 |
| ***SCARB2*** | Scavenger receptor class B member 2 |
| ***SCUBE2*** | Signal peptide, CUB domain and EGF like domain containing 2 |
| * *SDC2* | Syndecan 2 |
| ***SDC4*** | Syndecan 4 |
| ***SDF4*** | Stromal cell derived factor 4 |
| ***SEMA4C*** | Semaphorin 4C |
| ***SF3B1*** | Splicing factor 3b subunit 1 |
| ***SFPQ*** | Splicing factor proline and glutamine rich |
| * *SFRP4* | Secreted frizzled related protein 4 |
| ***SGPL1*** | Sphingosine-1-phosphate lyase 1 |
| ***SGSM2*** | Small G protein signaling modulator 2 |
| ***SH3BP4*** | SH3 domain binding protein 4 |
| ***SH3PXD2A*** | SH3 and PX domains 2A |
| ***SHH*** | Sonic hedgehog signaling molecule |
| ***SHOC2*** | SHOC2 leucine rich repeat scaffold protein |
| ***SHROOM2*** | Shroom family member 2 |

| | |
|---|---|
| ***SIK2*** | Salt inducible kinase 2 |
| * *SIX6* | SIX homeobox 6 |
| ***SLC12A2*** | Solute carrier family 12 member 2 |
| ***SLC16A2*** | Solute carrier family 16 member 2 |
| ***SLC17A5*** | Solute carrier family 17 member 5 |
| * *SLC17A6* | Solute carrier family 17 member 6 |
| ***SLC22A7*** | Solute carrier family 22 member 7 |
| ***SLC24A5*** | Solute carrier family 24, member 5 |
| ***SLC29A3*** | Solute carrier family 29, member 3 |
| ***SLC2A1*** | Solute carrier family 2, member 1 |
| ***SLC2A11*** | Solute carrier family 2, member 11 |
| ***SLC30A4*** | Solute carrier family 30, member 4 |
| ***SLC31A1*** | Solute carrier family 31, member 1 |
| ***SLC36A1*** | Solute carrier family 36, member 1 |
| *SLC40A1 | Solute carrier family 40, member 1 |
| ***SLC45A2*** | Solute carrier family 45, member 2 |
| ***SLC7A11*** | Solute carrier family 7, member 11 |
| ***SMARCA4*** | SWI/SNF related, matrix associated, actin dependent regulator of chromatin, subfamily a, member 4 |
| ***SMARCA5*** | SWI/SNF related, matrix associated, actin dependent regulator of chromatin, subfamily a, member 5 |
| ***SMARCAL1*** | SWI/SNF related, matrix associated, actin dependent regulator of chromatin, subfamily a like 1 |
| ***SMARCD1*** | SWI/SNF related, matrix associated, actin dependent regulator of chromatin, subfamily d, member 1 |
| ***SMCHD1*** | Structural maintenance of chromosomes flexible hinge domain containing 1 |
| ***SMO*** | Smoothened, frizzled class receptor |
| ***SNAI2*** | Snail family transcriptional repressor 2 |
| ***SNAP29*** | synaptosome associated protein 29 |
| ***SNRPC*** | Small nuclear ribonucleoprotein polypeptide C |
| ***SOX10*** | SRY(sex determining region Y)-box transcription factor 10 |
| * *SOX18* | SRY-box transcription factor 18 |
| * *SOX2* | SRY-box transcription factor 2 |
| ***SOX5*** | SRY-box transcription factor 5 |
| ***SOX9*** | SRY-box transcription factor 9 |
| ***SPAG9*** | Sperm associated antigen 9 |
| ***SPRED1*** | Sprouty related EVH1 domain containing 1 |
| ***SRC*** | SRC proto-oncogene, non-receptor tyrosine kinase |
| ***SRM*** | Spermidine synthase |
| ***ST3GAL5*** | ST3 beta-galactoside alpha-2,3-sialyltransferase 5 |
| * *STAR* | Steroidogenic acute regulatory protein |
| ***STIM1*** | Stromal interaction molecule 1 |
| ***STK11*** | Serine/threonine kinase 11 |
| ***STX12*** | Syntaxin 12 |

| | |
|---|---|
| ***STX17*** | Syntaxin 17 |
| ***STX3*** | Syntaxin 3 |
| ***STXBP1*** | Syntaxin binding protein 1 |
| ***SUFU*** | SUFU negative regulator of hedgehog signaling |
| ***SULF1*** | Sulfatase 1 |
| ***SUPT5H*** | SPT5 homolog, DSIF elongation factor subunit |
| ***SUPT6H*** | SPT6 homolog, histone chaperone and transcription elongation factor |
| ***SYTL2*** | Synaptotagmin like 2 |
| ***SZT2*** | SZT2 subunit of KICSTOR complex |
| ***TACO1*** | Translational activator of cytochrome c oxidase I |
| ***TAF4*** | TATA-box binding protein associated factor 4 |
| ***TBC1D10A*** | TBC1 domain family member 10A |
| ***TBC1D10B*** | TBC1 domain family member 10B |
| ***TBCD*** | Tubulin folding cofactor D |
| ***TBX10*** | T-box transcription factor 10 |
| * *TBX15* | T-box transcription factor 15 |
| ***TBX19*** | T-box transcription factor 19 |
| ***TENM3*** | Teneurin transmembrane protein 3 |
| ***TERF1*** | Telomeric repeat binding factor 1 |
| ***TERF2*** | Telomeric repeat binding factor 2 |
| ***TERF2IP*** | TERF2 interacting protein |
| ***TERT*** | Telomerase reverse transcriptase |
| ***TET2*** | Tet methylcytosine dioxygenase 2 |
| ***TET3*** | Tet methylcytosine dioxygenase 3 |
| ***TFAP2A*** | Transcription factor AP-2 alpha |
| ***TFAP2C*** | Transcription factor AP-2 gamma |
| ***TFAP2E*** | Transcription factor AP-2 epsilon |
| ***TFPI2*** | Tissue factor pathway inhibitor 2 |
| ***TGFBR2*** | Transforming growth factor beta receptor 2 |
| ***THRA*** | Thyroid hormone receptor alpha |
| ***TINF2*** | TERF1 interacting nuclear factor 2 |
| ***TJP1*** | Tight junction protein 1 |
| ***TMPRSS6*** | Transmembrane serine protease 6 |
| ***TP53*** | Tumor protein p53 |
| * *TP63* | Tumor protein p63 |
| ***TPCN2*** | Two pore segment channel 2 |
| ***TRAF6*** | TNF receptor associated factor 6 |
| ***TRAPPC6A*** | Trafficking protein particle complex 6A |
| ***TRIM32*** | Tripartite motif containing 32 |
| ***TRIM33*** | Tripartite motif containing 33 |
| ***TRPM1*** | Transient receptor potential cation channel subfamily M member 1 |
| ***TRPM7*** | Transient receptor potential cation channel subfamily M member 7 |
| ***TSC1*** | TSC complex subunit 1 |

| | |
|---|---|
| ***TSC2*** | TSC complex subunit 2 |
| * *TSHR* | Thyroid stimulating hormone receptor |
| ***TTC8*** | Tetratricopeptide repeat domain 8 |
| ***TYMS*** | Thymidylate synthetase |
| ***TYR*** | Tyrosinase |
| ***TYRP1*** | Tyrosinase-related protein 1 |
| ***UBXN4*** | UBX domain protein 4 |
| ***UCHL3*** | Ubiquitin C-terminal hydrolase L3 |
| ***UQCRFS1*** | Ubiquinol-cytochrome c reductase, Rieske iron-sulfur polypeptide 1 |
| ***USB1*** | U6 snRNA biogenesis phosphodiesterase 1 |
| ***USF2*** | Upstream transcription factor 2, c-fos interacting |
| ***USP10*** | Ubiquitin specific peptidase 10 |
| ***USP13*** | Ubiquitin specific peptidase 13 |
| ***USP20*** | Ubiquitin specific peptidase 20 |
| ***USP28*** | Ubiquitin specific peptidase 28 |
| ***USP3*** | Ubiquitin specific peptidase 3 |
| ***USP36*** | Ubiquitin specific peptidase 36 |
| ***USP43*** | Ubiquitin specific peptidase 43 |
| ***USP45*** | Ubiquitin specific peptidase 45 |
| ***USP48*** | Ubiquitin specific peptidase 48 |
| ***USP53*** | Ubiquitin specific peptidase 53 |
| ***USP7*** | Ubiquitin specific peptidase 7 |
| ***USP9X*** | Ubiquitin specific peptidase 9 X-linked |
| ***UVSSA*** | UV stimulated scaffold protein A |
| ***UXT*** | Ubiquitously expressed prefoldin like chaperone |
| ***VAC14*** | VAC14 component of PIKFYVE complex |
| ***VAMP7*** | Vesicle associated membrane protein 7 |
| ***VANGL1*** | VANGL planar cell polarity protein 1 |
| ***VDR*** | Vitamin D receptor |
| ***VPS11*** | VPS11 core subunit of CORVET and HOPS complexes |
| ***VPS18*** | VPS18 core subunit of CORVET and HOPS complexes |
| ***VPS33A*** | VPS33A core subunit of CORVET and HOPS complexes |
| ***VPS39*** | VPS39 subunit of HOPS complex |
| ***WDPCP*** | WD repeat containing planar cell polarity effector |
| ***WDR73*** | WD repeat domain 73 |
| * *WIF1* | WNT inhibitory factor 1 |
| ***WIPI1*** | WD repeat domain, phosphoinositide interacting 1 |
| * *WNT1* | Wnt family member 1 |
| * *WNT3A* | Wnt family member 3A |
| * *WNT7A* | Wnt family member 7A |
| ***WRAP53*** | WD repeat containing antisense to TP53 |
| ***WRN*** | WRN RecQ like helicase |
| ***XPA*** | XPA, DNA damage recognition and repair factor |

| | |
|---|---|
| ***XPC*** | XPC complex subunit, DNA damage recognition and repair factor |
| ***YWHAE*** | Tyrosine 3-monooxygenase/tryptophan 5-monooxygenase activation protein epsilon |
| ***YWHAZ*** | Tyrosine 3-monooxygenase/tryptophan 5-monooxygenase activation protein zeta |
| ***YY1*** | YY1 transcription factor |
| ***ZBTB17*** | Zinc finger and BTB domain containing 17 |
| ***ZDHHC21*** | Zinc finger DHHC-type palmitoyltransferase 21 |
| ***ZEB2*** | Zinc finger E-box binding homeobox 2 |
| * *ZIC2* | Zic family member 2 |
| ***ZMPSTE24*** | Zinc metallopeptidase STE24 |

* Not present in the microarray

**Table S3.3. Gene list elaborated from Baxter et *al*. (2018) including genes related with skin pigmentation validated in human.** Out of 128 genes, 8 (*) were not present in the microarray and were removed from our final list.

| Gene symbol | Description |
|---|---|
| ***ABCB6*** | ATP binding cassette subfamily B member 6 |
| ***ADAM10*** | ADAM metallopeptidase domain 10 |
| ***ADAR*** | Adenosine deaminase RNA specific |
| ***AP3B1*** | Adaptor related protein complex 3 subunit beta 1 |
| ***ATM*** | ATM serine/threonine kinase |
| ***ATP7A*** | ATPase copper transporting, alpha |
| ***BLM*** | BLM RecQ like helicase |
| ***BLOC1S3*** | Biogenesis of lysosomal organelles complex 1 subunit 3 |
| ***BLOC1S6*** | Biogenesis of lysosomal organelles complex 1 subunit 6 |
| ***BRAF*** | B-Raf proto-oncogene, serine/threonine kinase |
| ***BRCA2*** | BRCA2 DNA repair associated |
| ***BRIP1*** | BRCA1 interacting protein C-terminal helicase 1 |
| ***CBS*** | Cystathionine beta-synthase |
| ***CDH3*** | Cadherin 3 |
| ***CDKN2A*** | Cyclin dependent kinase inhibitor 2A |
| ***CTC1*** | CST telomere replication complex component 1 |
| ***CTNS*** | Cystinosin, lysosomal cystine transporter |
| ***CYP11A1*** | Cytochrome P450 family 11 subfamily A member 1 |
| ***DDB2*** | Damage specific DNA binding protein 2 |
| ***DDX3X*** | DEAD-box helicase 3 X-linked |
| ***DKC1*** | Dyskerin pseudouridine synthase 1 |
| ***DSTYK*** | Dual serine/threonine and tyrosine protein kinase |
| ***DTNBP1*** | Dystrobrevin binding protein 1 |
| ***EDN3*** | Endothelin 3 |
| ***EDNRB*** | Endothelin receptor type B |
| ***ENPP1*** | Ectonucleotide pyrophosphatase/phosphodiesterase 1 |
| ***EPG5*** | Ectopic P-granules autophagy protein 5 homolog |
| ***ERCC2*** | ERCC excision repair 2, TFIIH core complex helicase subunit |
| ***ERCC3*** | ERCC excision repair 3, TFIIH core complex helicase subunit |
| ***ERCC4*** | ERCC excision repair 4, endonuclease catalytic subunit |
| ***ERCC5*** | ERCC excision repair 5, endonuclease |
| ***ERCC6*** | ERCC excision repair 6, chromatin remodeling factor |
| ***ESCO2*** | Establishment of sister chromatid cohesion N-acetyltransferase 2 |
| ***FANCA*** | FA complementation group A |
| ***FANCC*** | FA complementation group C |
| ***FANCD2*** | FA complementation group D2 |

| | |
|---|---|
| ***FANCE*** | FA complementation group E |
| ***FANCI*** | FA complementation group I |
| ***FGFR3*** | Fibroblast growth factor receptor 3 |
| ***FLNA*** | Filamin A |
| ***FMR1*** | FMRP translational regulator 1 |
| ***GNAI3*** | G protein subunit alpha i3 |
| ***GNAS*** | GNAS complex locus |
| ***GPNMB*** | Glycoprotein nmb |
| ***GPR143*** | G protein-coupled receptor 143 |
| ***HPS1*** | HPS1 biogenesis of lysosomal organelles complex 3 subunit 1 |
| ***HPS3*** | HPS3 biogenesis of lysosomal organelles complex 2 subunit 1 |
| ***HPS4*** | HPS4 biogenesis of lysosomal organelles complex 3 subunit 2 |
| ***HPS5*** | HPS5 biogenesis of lysosomal organelles complex 2 subunit 2 |
| ***HPS6*** | HPS6 biogenesis of lysosomal organelles complex 2 subunit 3 |
| ***HRAS*** | Harvey rat sarcoma viral oncogene homolog |
| ***IDS*** | Iduronate 2-sulfatase |
| ***IDUA*** | Alpha-L-iduronidase |
| ***IKBKG*** | Inhibitor of nuclear factor kappa B kinase regulatory subunit gamma |
| ***IRF4*** | Interferon regulatory factor 4 |
| ***KIT*** | KIT proto-oncogene, receptor tyrosine kinase |
| ***KITLG*** | KIT ligand |
| ** KRT14* | keratin 14 |
| ** KRT5* | keratin 5 |
| ** LRMDA* | Leucine rich melanocyte differentiation associated |
| ***LYST*** | Lysosomal trafficking regulator |
| ***MC1R*** | Melanocortin 1 receptor |
| ** MC2R* | Melanocortin 2 receptor |
| ***MCM4*** | Minichromosome maintenance complex component 4 |
| ***MEN1*** | Menin 1 |
| ***MITF*** | Microphthalmia-associated transcription factor |
| ***MLH1*** | MutL homolog 1 |
| ***MLPH*** | Melanophilin |
| ** MRAP* | Melanocortin 2 receptor accessory protein |
| ***MSH2*** | MutS homolog 2 |
| ***MSH6*** | MutS homolog 6 |
| ***MYO5A*** | Myosin VA (heavy chain 12, myoxin) |
| ***NBN*** | Nibrin |
| ***NF1*** | Neurofibromin 1 |
| ***NNT*** | Nicotinamide nucleotide transhydrogenase |
| ***NR0B1*** | Nclear receptor subfamily 0 group B member 1 |
| ***NRAS*** | NRAS proto-oncogene, GTPase |

| | |
|---|---|
| ***OCA2*** | OCA2 melanosomal transmembrane protein |
| ** PAH* | Phenylalanine hydroxylase |
| ***PALB2*** | Partner and localizer of BRCA2 |
| ***PARN*** | Poly(A)-specific ribonuclease |
| ***PAX3*** | Paired box 3 |
| ***PCNT*** | pericentrin |
| ***PMS2*** | PMS1 homolog 2, mismatch repair system component |
| ***POFUT1*** | Protein O-fucosyltransferase 1 |
| ***POGLUT1*** | Protein O-glucosyltransferase 1 |
| ***POLA1*** | DNA polymerase alpha 1, catalytic subunit |
| ***POLH*** | DNA polymerase eta |
| ***POMC*** | Proopiomelanocortin |
| ***PRKAR1A*** | Protein kinase cAMP-dependent type I regulatory subunit alpha |
| ***PSENEN*** | Presenilin enhancer, gamma-secretase subunit |
| ***PTEN*** | Phosphatase and tensin homolog |
| ***PTPN11*** | Protein tyrosine phosphatase non-receptor type 11 |
| ***RAB27A*** | RAB27A, member RAS oncogene family |
| ***RAF1*** | v-raf-1 murine leukemia viral oncogene homolog 1 |
| ***RECQL4*** | RecQ like helicase 4 |
| ***RIT1*** | Ras like without CAAX 1 |
| ***SAMD9*** | Sterile alpha motif domain containing 9 |
| ***SASH1*** | SAM and SH3 domain containing 1 |
| ***SGPL1*** | Sphingosine-1-phosphate lyase 1 |
| ***SHOC2*** | SHOC2 leucine rich repeat scaffold protein |
| ***SLC17A5*** | Solute carrier family 17 member 5 |
| ***SLC24A5*** | Solute carrier family 24, member 5 |
| ***SLC29A3*** | Solute carrier family 29, member 3 |
| ***SLC45A2*** | Solute carrier family 45, member 2 |
| ***SMARCAL1*** | SWI/SNF related, matrix associated, actin dependent regulator of chromatin, subfamily a like 1 |
| ***SMO*** | Smoothened, frizzled class receptor |
| ***SNAI2*** | Snail family transcriptional repressor 2 |
| ***SOX10*** | SRY(sex determining region Y)-box transcription factor 10 |
| ***SPRED1*** | Sprouty related EVH1 domain containing 1 |
| ***ST3GAL5*** | ST3 beta-galactoside alpha-2,3-sialyltransferase 5 |
| ** STAR* | Steroidogenic acute regulatory protein |
| ***STK11*** | Serine/threonine kinase 11 |
| ***TERT*** | Telomerase reverse transcriptase |
| ***TINF2*** | TERF1 interacting nuclear factor 2 |
| ** TP63* | Tumor protein p63 |
| ***TPCN2*** | Two pore segment channel 2 |

| | |
|---|---|
| ***TSC1*** | TSC complex subunit 1 |
| ***TSC2*** | TSC complex subunit 2 |
| ***TYR*** | Tyrosinase |
| ***TYRP1*** | Tyrosinase-related protein 1 |
| ***USP9X*** | Ubiquitin specific peptidase 9 X-linked |
| ***UVSSA*** | UV stimulated scaffold protein A |
| ***WRAP53*** | WD repeat containing antisense to TP53 |
| ***WRN*** | WRN RecQ like helicase |
| ***XPA*** | XPA, DNA damage recognition and repair factor |
| ***XPC*** | XPC complex subunit, DNA damage recognition and repair factor |
| ***ZMPSTE24*** | Zinc metallopeptidase STE24 |

* Not present in the microarray

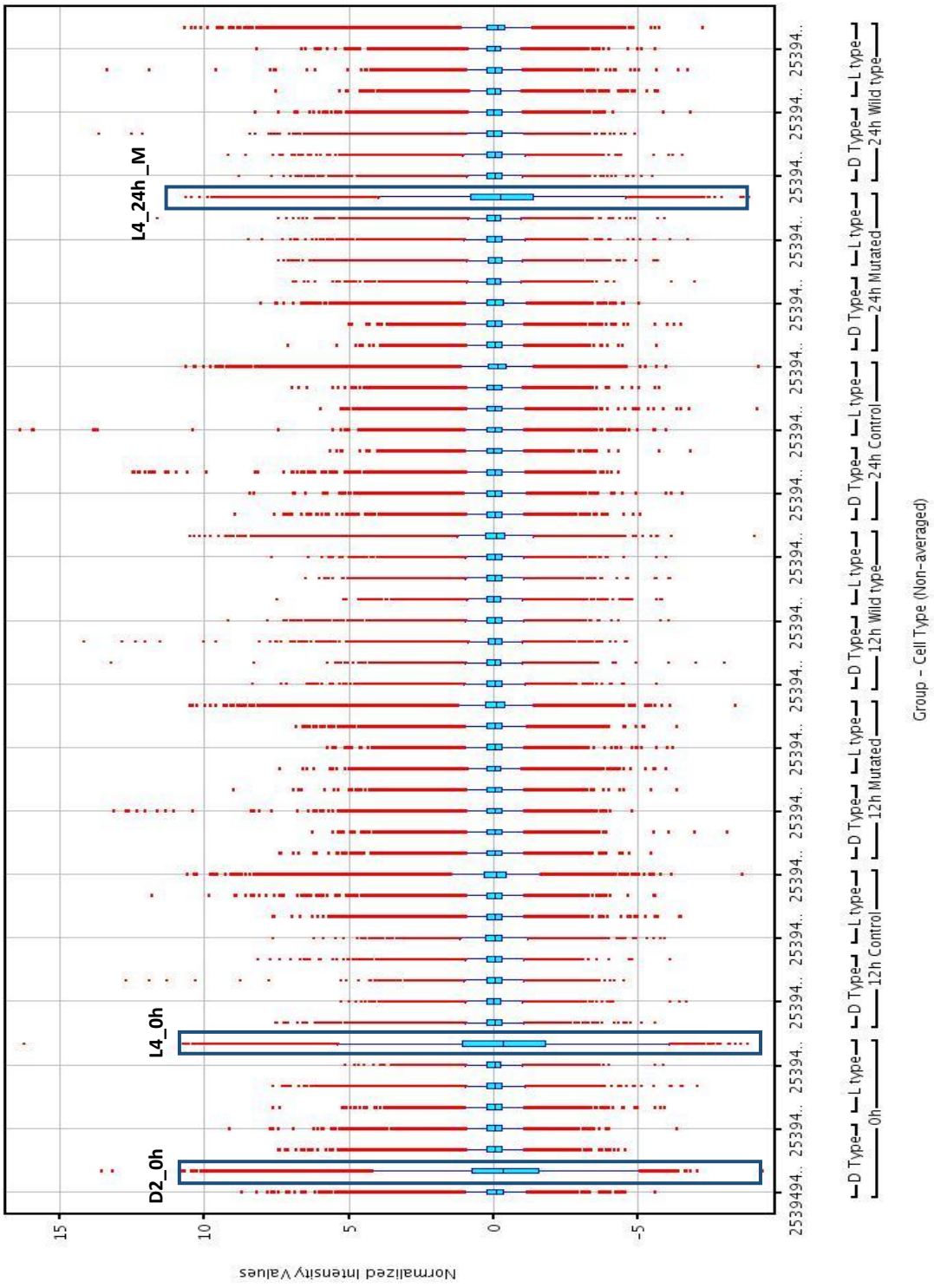


**Figure S3.1**. **Box-plots of the normalized intensity values of all the samples.**

# Chapter 4.

## Effect of active vitamin D on the transcriptome of human melanocytes

## 4.1. Introduction

It is thought that black skin in hominins was an adaptation to the noxious effects of ultra violet radiation (UVR) after the loss of fur that characterizes our lineage. Hairless skin and increased density of eccrine sweat glands possible evolved at roughly the same time as a mechanism for enhanced thermoregulation during high physical activity under high environmental heat (Jablonski and Chaplin, 2017).

Two main hypotheses have been put forward to explain the adaptive value of dark skin. One is protection against skin cancer (Greaves, 2014); the other one is protection against photodegradation of folate under high UVR conditions, primarily to prevent the reduction of fertility (due to loss of folate) (Jablonski and Chaplin, 2000). A third, less supported alternative includes increasing the skin's resistance to desiccation under arid conditions (Elias et *al*., 2009, 2010).

But, as regards light skin in particular, the most accepted evolutionary hypothesis explains this depigmentation process as a consequence of the out-of-Africa exodous and colonization of high latitude geographical areas by modern *Homo sapiens*. Thus, depigmentation arises as an adaptive process that facilitates vitamin D synthesis in regions of low solar radiation (Loomis, 1967; Jablonski and Chaplin, 2000, 2010, 2017; Chaplin and Jablonski, 2009; Grant, 2016).

There is evidence for a clear evolutionary interest in favouring light skin (Norton et *al*., 2007; Martínez-Cadenas et *al*., 2013; Basu Mallick et *al*., 2013; López et *al*., 2014), despite that some mutations that are associated to a light skin, and which seem to be the target of positive selection, are also simultaneously associated to an increased risk of melanoma (Martínez-Cadenas et *al*., 2013; López et *al*., 2014). It has thus been hypothesized that skin depigmentation would have evolved to prevent a number of reproductive or health issues leading to an early death, consequence of the scant UV light available for vitamin D synthesis in northern latitudes (Jablonski and Chaplin, 2010).

In fact, our own results show that in cultured primary melanocytes from donors of dark and light skin there is an increase in the expression of the receptor of vitamin D (*VDR*) 24h after irradiation with UV-light (López S, unpublished). Further, it has been reported that keratinocytes possess the enzymatic machinery needed to synthesize calcitriol (1α,25(OH)2D3, the active form of vitamin D), and it has been proven that the skin is not only source, but also target of calcitriol activities (Bikle, 2011). Interestingly, it has proposed that vitamin D is able to regulate melanogenesis (Kawakami et *al*., 2014). In this regard, it has been shown by means of Chromatin Immunoprecipitation Sequencing (ChIP-Seq) that limphoblastoid cell lines (LCLs) incubated with active vitamin D show a highly significant (adjusted p-value < 0.0001) enrichment of VDR binding to genomic regions related to traits such as tanning, skin sensitivity to sun or hair pigmentation (among other more expected targets such as multiple sclerosis, type I diabetes or systemic lupus erythematosus) (Ramagopalan et *al*., 2010). In another ChIP-Seq experiment in osteoblasts, the pigmentation-associated genes *DCT* and *TYRP1* also showed enrichment for VDR binding (Meyer et *al*., 2014). In this context, our aim with this work is to identify the effect of 1α,25(OH)2D3 on the expression of human melanocytes in order to see if there is a bidirectional influence between vitamin D and melanogenesis and which are the main genes involved.

## 4.2. Material and Methods

### 4.2.1. Cell cultures

Human epidermal melanocytes were purchased from Thermo Fisher Scientific: four lines isolated from lightly pigmented neonatal foreskin (HEMn-LP), and five lines from darkly pigmented neonatal foreskin (HEMn-DP). Melanocytes were cultivated in Medium 254 supplemented with human melanocyte growth supplement (HMGS). All the cell lines were maintained in an incubator under an atmosphere of 5% $CO_2$ at 37°C. Media were refreshed every two days and cells from the third to fifth passage were used.

### 4.2.2. Gene expression by Digital PCR (dPCR)

For the optimization of incubation parameters, six melanocytic cell lines were used (3 HEMn-LP and 3 HEMn-DP). Cells were seeded in 6-well plates at a density of $2x10^5$ cells/well. After 24h, medium was removed and changed by a conditioned medium: Medium 254 with $10^{-7}$ or $10^{-8}$ M of $1,25(OH)_2D_3$ (Sigma) or vehicle, in combination with two incubation times (12h and 24h).

Melanocytes (≈$2x10^6$) were harvested by treatment with TrypLE Express (Life Technologies) and RNA was extracted from the cell pellets by means of the RNAqueous kit (Ambion). RNA was DNAse-treated (DNA-free Kit, Ambion), and then RNA integrity was analysed through an Agilent 2100 Bioanalyzer, using Agilent RNA 6000 Nano Chips (Agilent Technologies, Santa Clara, CA, USA). Then, RNA was retrotranscribed using Maxima First Strand cDNA Synthesis (Thermo Fisher Scientific). Quantification of the gene expression of melanogenic loci *MITF* (microphthalmia-associated transcription factor), *DCT* (dopachrome tautomerase) and *TYRP1* (tyrosinase-related protein 1), and of the vitamin-D receptor gene (*VDR*), was done by means of Digital PCR (dPCR) in a QuantStudio 3D apparatus with Taqman probes (Thermo Fisher Scientific) (Assay IDs: Hs01117294_m1 (*MITF*), Hs01098278_m1 (*DCT*), Hs00167051_m1 (*TYRP1*) and Hs01045843_m1 (*VDR*)). The expression of glyceraldehyde-3-phosphate dehydrogenase (*GAPDH*) was used as a reference (Assay ID: Hs02758991_g1).

### 4.2.3. VDR and RXRα Immunocytochemistry

In order to determine the capability of $1,25(OH)_2D_3$ to induce the expression of *VDR* we performed an immunocytochemistry assay with melanocytes 12h after incubation with $1,25(OH)_2D_3$ or vehicle (control).

Melanocytes cultured on coverslips were washed with phosphate buffered saline (PBS) and fixed with 1% fresh paraformaldehyde (PFA) in phosphate buffer saline on ice for

15 minutes. The coverslips were washed with PBS. Next, the cells were permeabilized with 0.1% (v/v) Triton X-100 in PBS for 10 minutes at room temperature followed by incubation with the blocking solution containing 3% of bovine serum albumin (BSA) in PBS for 20 minutes at room temperature. Cells were incubated with primary anti-VDR mouse monoclonal antibody (sc-13133, from Santa Cruz Biotechnology) (5µg/ml) for 1h at RT and was followed by 2h incubation with a secondary antibody (anti-mouse Alexa Fluor 594; 1:250 from Invitrogen) at RT in a humidity chamber. Cells incubated with only the secondary antibody were used to evaluate the secondary antibody background. Finally, the coverslips were mounted on slides with medium containing DAPI (Thermo Fisher Scientific). For *RXRα* (Retinoid X Receptor alpha) expression, sc-774 rabbit polyclonal antibody (Santa Cruz Biotechnology) was used and anti-rabbit Alexa Fluor 488 (Invitrogen) as a secondary antibody. The immunofluorescence images were captured by a wide field fluorescence microscope (Zeiss AxioObserver Z1) with Zeiss Axiocam MRm R3 camera and Plan Apochromat 20X objective. Images were processed using FIJI/ImageJ and display settings were adjusted according to negative controls.

### 4.2.4. Western Blotting

The expression of VDR was also analysed through immunoblotting, 12h and 18h after incubation with 10-7M 1,25(OH)2D3. Melanocytes were harvested by trypsinization, washed with PBS and lysed in RIPA lysis buffer (80 mM Tris-HCl pH 8, 150 mM NaCl, 1% NP-40, 0.5% sodium deoxycholate, 0.1% SDS) containing Protease Inhibitor Cocktail (Sigma-Aldrich) for 15 minutes on ice. Lysates were then cleared by centrifugation at 10,000 g for 5 minutes and total protein concentration was determined using the Biuret protein assay. Total protein lysates (40 µg) were separated by 10% SDS-polyacrylamide gel and transferred onto nitrocellulose membrane. Non-specific binding sites were blocked by 1h incubation with blocking buffer (5% non-fat milk, 1% TBS (Tris-Buffered Saline), 0.1% Tween-20). Incubation with primary anti-VDR antibody (#12550 from Cell Signaling Technology) (dilution 1:1000) was performed overnight at

4°C. Membranes were washed three times with PBS with Tween-20 and then incubated for 2 h with horseradish peroxidase-linked secondary goat anti-rabbit IgG (#ab102279 from Abcam). Finally, the VDR protein was visualized by enhanced chemiluminescence using the SuperSignalH West Pico Chemiluminescent Substrate (Thermo Fisher Scientific) and the intensity of each band was measured using Fiji/ImageJ software. Western blotting of GAPDH as a control was performed using the same blot as that prepared for VDR after deprobing. A monoclonal anti-GAPDH antibody (diluted 1:2500; #ab9485 from Abcam) was used as primary antibody.

### 4.2.5. Melanin quantification

After incubation with 10-7M of 1,25(OH)2D3 for 18h, 24h and 36h, melanocytes were washed with PBS, harvested and centrifuged. Cell pellets were then lysed and melanin was solubilized with 1N NaOH containing 10% DMSO. The solution was incubated at 80°C for 1 hour and absorbance was measured at 405 nm. Melanin concentration was determined from a standard curve prepared with synthetic melanin (Sigma, USA). Melanin content was expressed as fold change with respect to controls.

### 4.2.6. RNA-sequencing (RNA-Seq)

For RNA-sequencing (RNA-Seq), four cell lines from *light* skin donors (HEMn-LP) and five cell lines from *dark* skin donors (HEMn-DP) were used. For every cell line, cells were seeded in two T75 culture flasks (at a density of $2x10^6$ cells/flask). After 24h, medium was changed to conditioned medium ($10^{-7}$ M of active vitamin D ($1,25(OH)_2D_3$) or vehicle alone (1µl of 95% ethanol diluted in 1ml of medium) and cells were incubated for 18h. Cells incubated with the vehicle alone served as the control. A total of 18 RNA samples were analysed, corresponding to melanocytic cell lines incubated with vitamin D and the corresponding controls. RNA was isolated and DNAse-treated by means of RNAqueous kit (Ambion) and DNA-free Kit (Ambion). About 2 µg of total RNA of good quality (average RIN 9.7; minimum RIN 8.2) were sent to Sistemas Genómicos S.L. (Valencia, Spain),

where libraries were generated with the Illumina TruSeq Stranded Total RNA kit. Samples were sequenced in a HiSeq 2500 (Illumina) at a minimum of 50 million reads at read length 100X2, to analyse gene expression differences between $1,25(OH)_2D_3$-treated and non-treated conditions.

The quality control of the raw data was performed using the FastQC tool (the Babraham Institute, https://www.bioinformatics.babraham.ac.uk/index.html). Insufficient quality reads (phred score < 10) were eliminated using the Picard Tools software (v1.129) (https://broadinstitute.github.io/picard/). Reads were mapped by means of HISAT2 v2.1.0 (Kim, Langmead and Salzberg, 2015) against GRCh38; read counting was done with featureCounts v1.6.2 (Liao, Smyth and Shi, 2014). Percentage of GC of mappable reads centered about 50-55%, indicating no bias. Ribosomal RNA genes were removed from the analysis. For the differential expression analysis between treated and untreated samples, DESeq2 (Love, Huber and Anders, 2014), and edgeR (Robinson, McCarthy and Smyth, 2010) were used, as implemented in RNA-Seq 2G (http://rnaseq2g.awsomics.org) (Zhang et *al*., 2017). Read counts were TMM normalized and paired analyses were performed according to the method. Genes with less than 100 counts across all cell lines were discarded. An FDR value <= 0.05 was considered as significant unless otherwise stated. Gene ontology and pathway analyses were done on WebGestalt (http://www.webgestalt.org/), version 2019 (Wang et *al*., 2017b). The GWAS associations for the genes were searched in the GWAS catalog, version: gwas_catalog_v1.0.2-associations_e95_r2019-03-22.

### 4.2.7. Genetic variant calling from RNA-Seq data and PCA

Using RNA-Seq data, we performed a variant calling analysis based on the Variant Analysis Pipeline (VAP) proposed by Adetunji et al. (2019). RNA-seq reads from treated and untreated (control) samples were analysed independetely (although we expect to find the same variants). Reads were mapped to the reference genome (GRCh38) by

means of HISAT2 v2.1.0 (Kim, Langmead and Salzberg, 2015) and STAR v2.7.1a (Dobin et *al*., 2013) independently. SNP calling and filtering was performed by GATK v4, with the following criteria: ReadRankPosSum (RRPS) < -8, Quality by depth (QD) < 5, Read depth (DP) < 10, Fisher's exact test p-value (FS) > 60, Mapping Quality (MQ) < 40, SnpCluster of 3 SNPs in 35bp, Mann-Whitney Rank-Sum (MQRankSum) < -12.5 and Alternative allele supporting read depth ALTreads < 5. After filtering, the variants were annotated using the SnpSift 4.3T (Cingolani et *al*., 2012). Only SNPs obtained from the reads of treated and untreated samples of each cell line and obtained with both mapping tools (HISAT2 and STAR) were considered.

### 4.2.8. Principal Component Analysis

We also obtained data from the 1000 genomes (1000G) project populations, for the same SNPs detected in our samples and performed a Principal Component Analysis (PCA) with all the samples.

### 4.2.9. Methylated DNA Immunoprecipitation Sequencing (MeDIP-Seq)

*DNA isolation, Methylated DNA Immunoprecipitation (MeDIP) and library preparation*

A total of 12 samples corresponding to three cell lines from *light* skin donors (HEMn-LP) and three cell lines from *dark* skin donors (HEMn-DP) were used for MeDIP-Seq analysis. Culture conditions were the same used for RNA-Seq.

After incubation with $10^{-7}$ M of $1,25(OH)_2D_3$ or vehicle for 18h, cells were harvested by treatment with TrypLE Express (Life Technologies) and cell pellets were resuspended in 1 ml of lysis buffer, consisting of 2% CTAB (cetyltrimethyl ammonium bromide), 100 mM Tris HCl pH 8.0, 1.4 M NaCl, 20 mM EDTA 5% PVP (Polyvinylpyrrolidone) and 5% β-mercaptoethanol. Resuspended cell pellets were incubated for at least 1h at 56ºC. Then, genomic DNA isolation was performed from the cell pellets by means of a standard

phenol-chloroform method combined with a CTAB-based lysis buffer to circumvent the problem caused by melanin attachment to DNA.

About 1-1.5µg of isolated DNA were sheared by sonication in a Bioruptor Pico sonication device (Diagenode): After the optimization of the sonication parameters, 25 cycles of 30''ON / 30'' OFF were applied to the samples, to generate fragments around 200 bp. DNA sharing performance was analysed by Agilent 2100 Bioanalyzer, with Agilent High Sensitivity DNA chips (Agilent Technologies). Methylated DNA Immunoprecipitation was performed with 1 µg of sheared DNA, using the MagMeDIP Kit (Diagenode) and IPure Kit v2 (Diagenode) was used for for DNA elution. Library preparation was performed with iDeal Library Preparation Kit (Diagenode), using 15 cycles for PCR amplification. Finally, the libraries of methylated DNA were analysed with Agilent 2100 Bioanalyzer, with Agilent High Sensitivity DNA chips (Agilent Technologies) and quantified with a Qubit Fluorometer.

Enriched DNA (0.5-1 µg) was sent to ITER S.A. (Instituto Tecnológico y de Energias Renovables) (Santa Cruz de Tenerife, Spain), where samples were sequenced in a HiSeq 4000 (Illumina) at an expected minimum of 100 million reads at read length 75X2 (paired-end).

*Bioinformatic Analysis*

Paired end reads were mapped to human genome (hg19) with BWA (Li and Durbin, 2010). MEDIPS R package (Lienhard et *al*., 2014) was used to perform quality control and identify differentially methylated regions (DMRs). We scanned the genome for differentially methylated regions using the default parameters except window size, which was set at of 1kb, and minimum reads per window, which was set at 50 (ws=1000 and minRowSum=50). edgeR was used to test differential methylation. Three light (HEMn-LP) and three dark (HEMn-DP) samples were studied together to increase sample size, therefore comparing 6 treated vs 6 untreated samples. Out of the 2,881,044 1kb-

windows genome-wide, 1,410,578 windows were tested for differential methylation and 41,460 windows were P<0.05. DMRs were assigned to genes using ChIPseeker R package (Yu, Wang and He, 2015) and TxDb.Hsapiens.UCSC.hg19.knownGene annotations. The number of windows assigned to each gene was compared between differentially expressed genes (DEGs) and non-DEGs. To avoid potential bias towards longer genes (longer genes are more likely to harbour more DMRs), we also calculated the ratio between total cumulative DMR length per gene and gene length.

### 4.2.10. *VDR* and *MREG* resequencing

Using Ion AmpliSeq Designer Version 6.17 we defined 242 amplicons covering six regions of the *VDR* locus, varying in length from 1.1 to 11kb. The six regions covered a total of ~40kb of the *VDR locus*. For *MREG locus* we defined 131 amplicons that covered nine regions and a total of ~20.6kb of the gene. The amplicons were sequenced by means of an Ion PGM machine and Ion 318 v2 chips. Individuals sequenced belong to a wider sample of unrelated healthy donors residing in the Basque Country, whose skin pigmentation was recorded by measuring the reflectance of the inner part of the arm at 685 nm (the same sample set of the Chapter 1 (from second sampling), see section 1.2.2). For sequencing, two sub-sets of 48 individuals were selected depending on their position on both ends of the sample distribution of reflectance values. These sub-sets represented thus two groups, one of 48 most lightly pigmented individuals and one of 48 most darkly pigmented individuals in the sample.

*Library preparation, emulsion PCR and enrichment*

Samples were amplified using the custom panel described above, using 10 ng of genomic DNA. DNA libraries were prepared using the Ion AmpliSeq DL8 chemistry and the Ion Chef instrument according to the manufacturer's recommendations. Libraries were quantified using the Ion Library Quantitation kit and pooled to an equimolar

concentration of 30 pM for template preparation. Template preparation, enrichment of beads containing the template and chip loading were performed using the Ion Chef instrument and the Ion PGM Hi Q Kit according to the manufacturer's recommendations.

Ion 318 v2 chips (8 samples per chip/12 chips) were sequenced on the Ion PGM instrument together with the Ion PGM Hi Q View Chef Supplies Kit. Primary sequencing data were aligned and reported relative to the Hg19 as the reference genome using the Torrent Suite Software v5.2.1 under default settings. Secondary sequence analyses were performed using the Coverage Analysis (v5.2.1.2) and the Variant Caller (v5.2.1.38) plugins.

*Population genetic analysis*

Average amplicon depth was 2041X. Three amplicons for which the coverage was <20X were discarded in all samples. This led to the removal of four possible SNPs. Amplicons were assembled into 6 regions for *VDR* and 9 regions for *MREG*. Each region was defined by the set of overlapping amplicons or amplicons in which the distance between them was not > 150bp, and which the total length for the region was > 2kb. Only biallelic SNPs were retained for further analysis. For comparative purposes, data for equivalent regions of chromosomes 2 and 12 from the 1000 genomes project populations (phase 3) were obtained from ftp://ftp.1000genomes.ebi.ac.uk/vol1/ftp/release/20130502. Tajima's D was estimated by means of VCF-kit (https://github.com/AndersenLab/VCF-kit). Simulations to obtain Tajima's D p-values for *VDR* and *MREG* regions were obtained by means of ms (Hudson, 2002; Hellenthal and Stephens, 2007) using the following command line for VDR: /ms 96 100000 -t 0.725 -r 0.695 1000 -I 3 0 96 0 -n 1 1.68202 -n 2 3.73683 -n 3 7.29205 -eg 0 2 116.010723 -eg 0 3 160.246047 -ma x 0.881098 0.561966 0.881098 x 2.79746 0.561966 2.79746 x -ema 0.028985 3 x 7.29314 x 7.29314 x x x x x -ej 0.028985 3 2 -ej 0.197963 2 1 -en 0.028985 2 0.287184 -en 0.303501 1 1 451984012. And for *MREG*:./ms 96 100000 -t 0.961 -r 3.504 1000 -I 3 0

96 0 -n 1 1.68202 -n 2 3.73683 -n 3 7.29205 -eg 0 2 116.010723 -eg 0 3 160.246047 -ma x 0.881098 0.561966 0.881098 x 2.79746 0.561966 2.79746 x -ema 0.028985 3 x 7.29314 x 7.29314 x x x x -ej 0.028985 3 2 -ej 0.197963 2 1 -en 0.028985 2 0.287184 -en 0.303501 1 1 783890995; which reflect the demographical model by Gutenkunst et *al*. (2009).

## 4.3. Results and discussion

### 4.3.1. Initial experiments

Optimization experiments in primary melanocyte cell cultures (3 HEMn-LP and 3 HEMn-DP) were performed to explore the effect of different 1,25$(OH)_2D_3$ concentrations and exposure times on the expression of selected melanogenic and vitamin D responsive genes. Melanogenic genes (*MITF*, *DCT* and *TYRP1*) were selected in order to have a preliminary view of the possible effect of vitamin D on melanogenesis. Vitamin D receptor (*VDR*) was selected as a control of vitamin D effect.

These experiments showed that, *DCT*, *MITF* and *VDR* have different basal expression, the highest corresponding to *DCT* and the lowest for *VDR*. Assay for *TYRP1* did not yield reliable results, so we focused on the other *loci*. There was a general trend to gene expression increase after incubation with 1,25$(OH)_2D_3$ for *DCT*, *MITF* and *VDR*. In fact, statistically significant differences (one-tailed paired t-test) are observed for *MITF* and *DCT* at 12h and 24h, at 1,25$(OH)_2D_3$ concentration of $10^{-7}$ M and $10^{-8}$ M with respect to their controls, whereas *VDR* is significant at a 1,25$(OH)_2D_3$ concentration of $10^{-8}$ M at 24h, and borders significance at $10^{-7}$ M at both times. There is more variance in *VDR* expression possibly due to the low expression observed (Figure 4.1). Nevertheless, immunocytochemistry with anti-VDR shows (in red) that the expression of this receptor is increased 12h after 1,25$(OH)_2D_3$ incubation ($10^{-7}$ M) (Figure 4.2). This increase of VDR

can be observed mainly in the nucleus although it can also be seen in the cytoplasm. It can also be observed that RXRα, the retoinoid X receptor alpha, with which VDR dimerizes, also increases and co-localizes in the nucleus (in green) (Figure 4.2). Western Blot results are in accordance with immunocytochemistry, showing an increase of VDR protein level after incubation with $1,25(OH)_2D_3$ at 12h, and even a higher increase after 18h (Figure 4.3).

We also measured melanin concentration in three cell lines (two HEMn-LP and one HEMn-DP) after incubation with $10^{-7}$M $1,25(OH)_2D_3$ for 18h, 24h and 36h. Although in darkly-pigmented cell line melanin content was similar in cells incubated with vitamin D and controls, in lightly-pigmented melanocytes there were small fold changes at 18h and 36h. For both light cell lines, melanin content increased about two-fold after 36h in relation to controls.

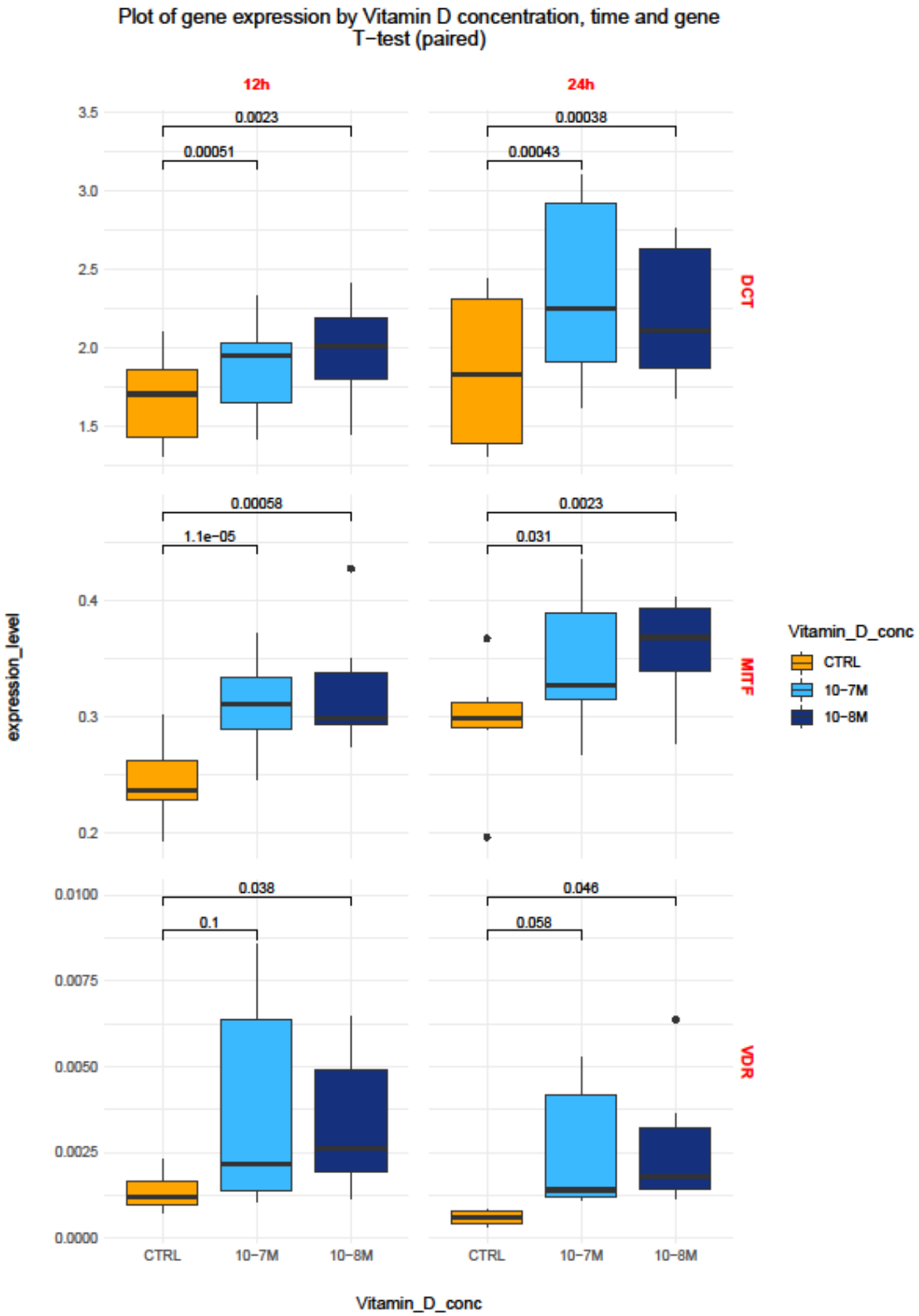


**Figure 4.1. Digital PCR analyses of gene expression of *DCT*, *MITF* and *VDR* after 12h and 24 incubation with $10^{-7}$ M and $10^{-8}$ M $1,25(OH)_2D_3$ and control in six melanocyte primary cell lines**. Significance for one-tailed paired T-test.

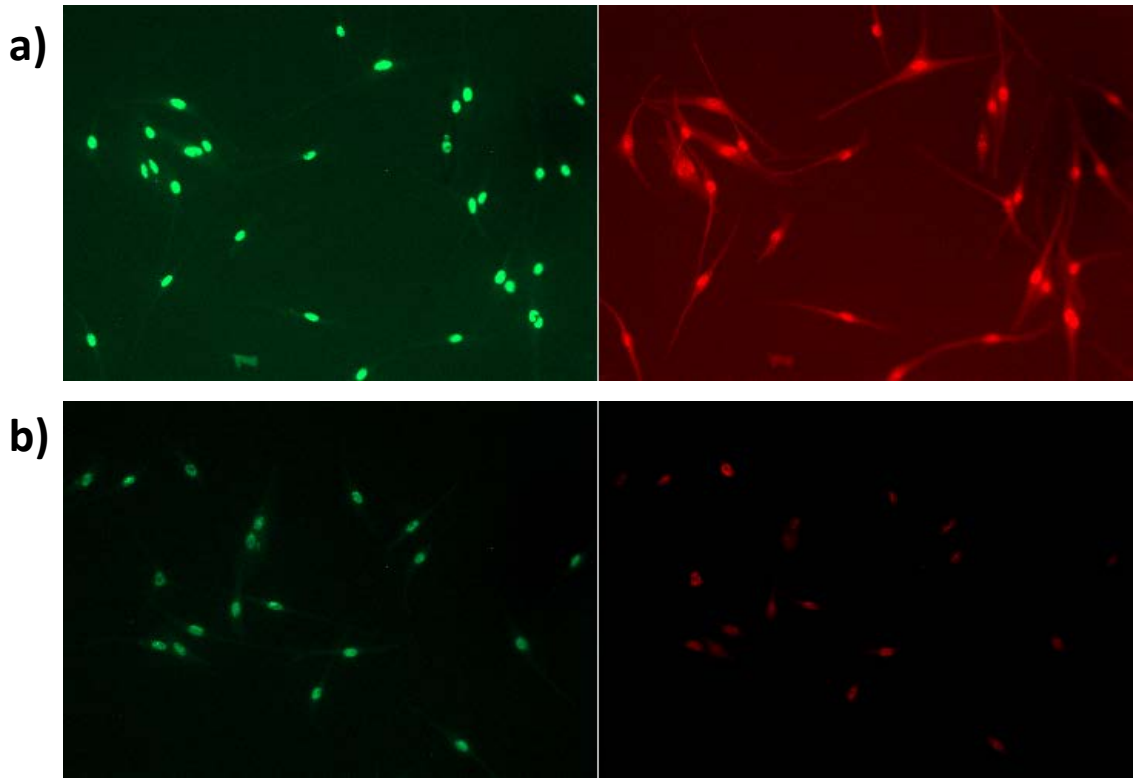


**Figure 4.2. Immunofluorescence assay in melanocytes incubated with 1,25(OH)$_2$D$_3$ (a), or control (b) after 12h**. In green *RXRα*, in red *VDR*.

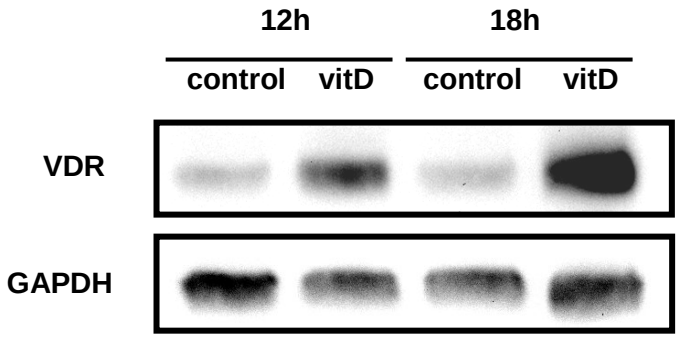


**Figure 4.3. Western Blot for vitamin D receptor (VDR) from melanocytes incubated with 1,25(OH)$_2$D$_3$ (vitD) or control after 12h and 18h**.

### 4.3.2. RNA-sequencing

Based on these results we decided to incubate our cell cultures with $10^{-7}$ M $1,25(OH)_2D_3$ (which is also in line with other reports, like that of Ramagopalan et *al*., 2010) and for an intermediate time of 18h.

Thus, nine different primary melanocyte cell lines were then subjected to $10^{-7}$ M $1,25(OH)_2D_3$ for 18h, alongside their corresponding controls. RNA-Seq data from these cell lines showed an average of 73.4+/-9.1 million reads per sample, of which an average of ~73% were high quality reads.

Differential expression analyses identified varying numbers of significant genes depending on the method used (i.e. at FDR<0.05 for dark, light and all together respectively, 22, 8 and 14 genes by edgeR; and 19, 61 and 19 genes by DESeq2. However, both methods showed very high correlation in fold-changes, suggesting that the estimated effect sizes are robust regardless of the method (Spearman's rho > 0.93, P < 2.2e-16). The genes whose expression is significantly different (FDR<0.05) in the global set of $10^{-7}$ M $1,25(OH)_2D_3$ treated samples vs. controls for DESeq2 and edgeR are shown in Tables S4.1-S4.6.

Overall, two genes stand out as overexpressed in treated samples independently of the method (DESeq2 and edgeR), when all samples are considered together and independently (dark melanocytes analysed independently and light melanocytes analysed independently) (Figure 4.4a,b): *SULT1C2* (sulfotransferase family 1C, member 2), and *CEBPD* (CCAAT enhancer binding protein, delta).

Regarding ***SULT1C2***, in vitro assays with recombinant human SULTs showed that 25OHD3 is selectively conjugated to 25OHD3-3-O-sulfate by human sulfotransferase 2A1 (*SULT2A1*) (Wong et *al*., 2018). 25OHD3 is the major circulating form of vitamin D3, and blood levels of 25OHD3 has been used as a marker of the vitamin D3 status. It is

unclear whether the formation of 25OHD3-3-O-sulfate from 25OHD3 could be considered a catabolic process or an alternative 25OHD3 storage form in the body (Higashi et *al*., 2014). It has been reported that SULT1C2 has no activity towards 7-Dehydrocholesterol, Vitamin D3, 25-OH-Vitamin D3 or Calcitriol (Kurogi et *al*., 2017). Nevertheless, in LS180 human colorectal adenocarcinoma cells, *SULT1C2* expression is also significantly increased by $1,25(OH)_2D_3$ treatment (Rondini et *al*., 2014; Barrett et *al*., 2016). Besides, activation of vitamin D receptor also increased *SULT1C2* expression in hepatocytes (Dubaisi et *al*., 2018). Thus, a similar storage/catabolic process could also exist in melanocytes for $1,25(OH)_2D_3$ and *SULT1C2*.

***CEBPD*** is an important transcription factor that enhances the transcription of other genes alone or as heterodimer with other members of the gene family. Interestingly, *CEBPA* and *CEBPB* are known to bind an enhancer region in *MITF* and regulating the pigmentation pathway in melanoma cells (Swoboda et *al*., 2018). Although there is no evidence for *CEBPD*, it could be possible to also regulate *MITF*.

Another interesting gene that is overexpressed in either all samples together, dark melanocytes analysed independently or light melanocytes analysed independently (although in light melanocytes only with the edgeR method) is ***CYP24A1*** (cytochrome P450 family 24 subfamily A member 1) (Figure 4.4c), which synthesizes a mitochondrial protein that initiates the degradation of 1,25-dihydroxyvitamin D3 (and 25-hydroxyvitamin D3) into 24-hydroxylated products which constitute the degradation products of the vitamin D molecule (Jones, Prosser and Kaufmann 2012). *CYP24A1* is a known target of vitamin D and VDR (Väisänen et *al*., 2005). The inactivation of $1,25(OH)_2D_3$ by CYP24A1 acts as a negative feedback and maintains vitamin D homeostasis. Genome-wide association studies (GWAS) have also identified variants at *CYP24A1* that contribute to serum levels of vitamin D (Jiang et *al*., 2018).

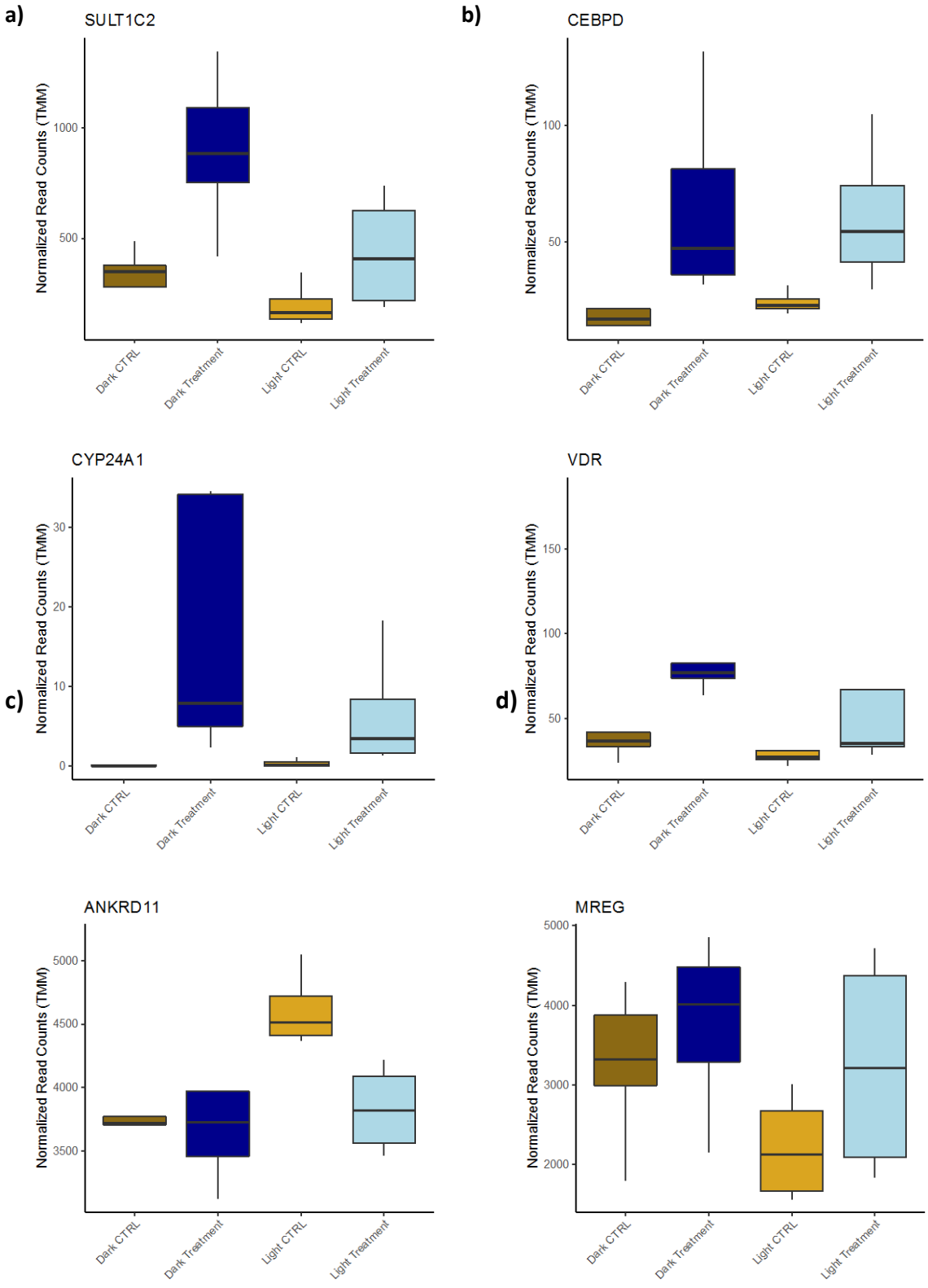


**Figure 4.4. Expression levels of selected differentially expressed genes before and after incubation with 1,25(OH)$_2$D$_3$.** All patterns FDR<0.05.

Both methods (edgeR and DESeq2) identify ***VDR*** as significantly increased in expression in dark samples analysed independently and when light and dark samples are analysed jointly (Figure 4.4d). The increase on *VDR* expression is not significant after multiple testing in the case of the light melanocytes alone (nominal p~0.012 for DESeq2 and p~0.006 for edgeR). This suggests that dark melanocytes are more responsive to active vitamin D than light melanocytes, at least through *VDR* signalling.

None of the classical genes associated to melanogenesis such as the melanocortin receptor 1 (*MC1R)*, tyrosinase (*TYR*), *MITF* or *DCT* were highlighted at a FDR value < 0.05 by edgeR or DESeq2. However, in light melanocytes, in contrast with dark melanocytes, there was a tendency of increased expression of melanogenic genes, including as *MITF, DCT, TYRP1, KIT* and *KITLG*, although not significant.

*Inferences on pigmentation genes*

Although the classical pigmentation genes were not significantly differentially expressed, by studying the GWAS catalog (Buniello et *al*., 2019), a collection of all published genome-wide association studies, we identified some genes associated with pigmentation-related traits among the differentially expressed genes in light melanocytes (as detected by DESeq2 FDR<0.05), such as *ANKRD11 and LRP5*. For example, ankyrin repeat domain 11 (***ANKRD11***) which associates with tan response, sunburns and hair colour in Europeans (Visconti et *al*., 2018; Kichaev et *al*., 2019) and also with squamous cell carcinoma (Liyanage et *al*., 2019), is under-expressed after $1,25(OH)_2D_3$ exposure (Figure 4.4e). *ANKRD11* is a chromatin regulator, suggesting that its decrease in expression induced by active vitamin D could impact the transcriptional levels of additional genes downstream. Furthermore, ANKRD11 protein is able to interact with p53 and enhance its transcriptional activity, while *ANKRD11* itself is also a target of p53 (Neilsen et *al*., 2008). Interestingly, there is experimental evidence supporting that the expression of both *MC1R* and *ANKRD11* are correlated (i.e. both being targets of several

super-enhancers within the *ANKRD11* gene body, GeneHancer ID: GH16J089480, Fishilevich et *al*., 2017).

***LRP5*** (LDL receptor related protein 5) is another gene associated with hair colour (Kichaev et *al*., 2019) and it is also associated with osteoporosis (Morris et *al*., 2019), which is a disease linked with vitamin D insufficiency (Holick, 2007).

Another gene to highlight is melanoregulin (***MREG***), which in this work is upregulated by vitamin D in light samples (and in all samples analysed together, with both methods) (Figure 4.4f), but without direct link with pigmentation traits by GWAS catalogue.

However, it has been reported that in mouse melanocytes, melanoregulin negatively regulates a shedding mechanism that drives melanosome transfer to keratinocytes (Wu et *al*., 2012), and Ohbayashi et *al*. (2012) demonstrated that melanoregulin is involved in the centripetal movement of melanosomes towards the nucleus, at least in mouse melan-a cells. Furthermore, based on experiments made on mouse retinal pigment epithelium, it has been proposed that melanoregulin is important for the formation and maturation of lysosomes and lysosome-related organelles (LROs) (Damek-Poprawa et *al*., 2009). In humans, in retinal pigment epithelium, *MREG* levels regulate pigment incorporation into melanosomes. Rachel et *al*. (2012) observed that loss of melanoregulin function increased while overexpression of *MREG* decreased pigment incorporation into melanosomes of the retinal pigment epithelium. However, the effect on the pigmentary phenotype of an overexpression of *MREG* in human melanocytes is not clear. Interestingly, *MREG* expression in melanocytes has been correlated with *MITF* expression ($r = 0.776$, $p = 3.33E-38$) (Hoek et *al*., 2008). Further studies regarding *MREG* function in melanocytes would help clarify its role in human pigmentation. However, it seems that it could be relevant for normal pigmentation.

*Genes associated with melanoma*

On the other hand, among the differentially expressed genes, there are several genes that have been related with melanoma (with DESeq2 or edgeR), both in dark and light melanocytes, although there are more abundant in light samples. In general, we found that tumour suppressor genes such as *PTEN* (phosphatase and tensin homolog) or *IGFBP5* (insulin like growth factor binding protein 5) are overexpressed after vitamin D treatment, while among underexpressed genes, there are several related with melanoma risk or progression or that have been reported to be overexpressed in melanoma.

***PTEN***, which is upregulated in light melanocytes, is one of the most important tumour suppressors, which takes part in important processes, such as regulation of cell growth and survival, promotion of apoptosis, inhibition of migration, proliferation and metabolism (Lee, Chen and Pandolfi, 2018). PTEN is a phosphatidylinositol-(3,4,5)-trisphosphates (PIP3) phosphatase that inhibits the phosphoinositide-3-kinase (PI3K)/AKT signalling pathway. Cao et *al*. (2013) demonstrated that UV irradiation triggers PTEN interaction with MC1R. After UV irradiation, α-MSH-MC1R complex recruits PTEN, protecting it from ubiquitination and degradation. Therefore, the stabilization of PTEN promotes the inhibition of PI3K/AKT signalling. Mutations on *PTEN* can lead to PI3K/AKT signalling hyperactivation and drive oncogenic transformation. Indeed, *PTEN* is mutated in a large number of cancers, including melanoma (Shain et *al*., 2015; Reddy, Miller and Tsao, 2017), and loss of heterozygosity of *PTEN* is observed in about 30% of melanomas (Conde-Pérez and Larue, 2012). PI3K/AKT signaling activation, via loss of *PTEN* function, can inhibit apoptosis in melanoma cells and induce growth and cell-survival (Conde-Pérez and Larue, 2012). Furthermore, *PTEN* loss has also been associated to resistance to *BRAF* inhibitors (Tímár et *al*., 2016, Zuo et *al*., 2018). Thus, the overexpression of *PTEN* shown in the light-pigmented melanocytes treated with $1,25(OH)_2D_3$ are in line with the anti-melanoma effects of vitamin D (Slominski et *al*., 2017).

Regarding dark melanocytes, we highlight the upregulation of *IGFBP5* and *GDF15* (growth differentiation factor 15). *IGFBP* has been reported to act as a tumour suppressor in melanoma. It has been proven that it is able to supress the proliferation and invasion of melanoma cells (Wang et *al*., 2015). *GDF15* has been reported to be upregulated in melanoma (Boyle et *al*., 2009) and in stage III and IV melanomas, high GDF15 serum levels were associated with poor prognosis (Weide et *al*., 2016). However, it has been reported to also exhibit antitumorigenic and pro-apoptotic activities (Ünal et *al*., 2015). Interestingly, *GDF15* is upregulated by *TP53* and UV irradiation increases its expression in human melanocytes (Yang et *al*., 2006).

On the other hand, there are many melanoma-related genes underexpressed in both dark and light melanocytes. When dark and light melanocytes are considered together, we observed the downregulation of *ST8SIA1* and *MYOF* (although there are not significant for dark and light melanocytes alone). For dark melanocytes alone, there are some other downregulated genes, such as *ALCAM, CD36, MAP2* or *LOX*. Finally, in light melanocytes there are several genes downregulated by vitamin D: *DHCR24, ECM1, MX2, CSPG4, NFATC2, LGALS3BP, IGFBP4, MCAM, NES, ENG, FASN, FOXM1, FAM129B* and *MMP2*.

***ST8SIA1*** gene encodes the Ganglioside GD3 synthase, which produces gangliosides GD3 and GT3. Ganglioside GD3 is known to be important in melanoma cells. Expression of GD3 has been associated with increased cell proliferation and invasion activity (Furukawa et *al*., 2012). Besides, GD3 also enhances cell adhesion to extracellular matrix in melanoma cells (Ohkawa et *al*., 2010). *ST8SIA1* is upregulated in melanoma in comparison with benign nevi (Sumantran, Mishra and Sudhakar, 2015). Furthermore, Miyata et *al*. (2014) showed that keratinocytes irradiated with UV are able to induce the expression of *ST8SIA1* in human melanocytes and suggested that this could promote the malignant transformation of melanocytes.

***MYOF*** (myoferlin), which is overexpressed in advanced melanoma (Zhang et *al*. 2018a), is involved in the proliferation, invasion and migration of tumour cells (Zhu et al., 2019).

***ALCAM*** (activated leukocyte cell adhesion molecule) is a member of a subfamily of immunoglobulin receptors. It is implicated in the processes of cell adhesion, migration and progression of malignant melanoma (Ofori-Acquah and King, 2008; Li et *al*., 2016). ***CD36*** (CD36 molecule) and ***LOX*** (lysyl oxidase) are also related with proliferation, angiogenesis, migration and metastasis in melanoma (Thorne et *al*., 2000; Osawa et *al*., 2013; Pascual et *al*., 2017).

Among melanoma-related genes underexpressed in light melanocytes, most of them are overexpressed in melanomas and have different functions: some of them are mainly related with extracellular matrix and cell adhesion (such as *ECM1, CSPG4* and *MCAM*), cell proliferation (*CSPG4, ENG, FOXM1*), inhibition of apoptosis (*DHCR24, NFATC2*) or invasion (*ENG, FAM129B, MMP2, MCAM*), although most of them participate in more than one process.

For instance, ***MCAM*** (melanoma cell adhesion molecule) plays a role in cell adhesion and it is essential for tumour initiation and progression (Wang et *al*., 2013b). However, its expression is higher in advanced melanomas and metastasis and correlates with aggressiveness and invasiveness. *MCAM* participates in multiple melanoma functions, such as inflammation, differentiation, adhesion, invasion, angiogenesis and metastasis (Lei et *al*., 2015). Interestingly, *MITF* has been reported to be able to repress *MCAM* in melanoblasts (Rao et *al*., 2016).

***CSPG4*** (chondroitin sulfate proteoglycan 4) encodes a melanoma-associated chondroitin sulfate proteoglycan that binds to the basement membrane heparan sulphate proteoglycan, perlecan, and is involved in cell adhesion (Tang et *al*., 2018a). Thus, it is important for the stabilization of cell-substratum interactions during early events of melanoma cell spreading on endothelial basement membranes. It is associated with

melanoma tumour formation, proliferation and malignant progression (Price et *al*., 2011; Dye et *al*., 2013). Furthermore, its expression has also been correlated to the resistance of melanoma to chemotherapeutics (Price et *al*., 2011). Interestingly, CSPG4 facilitates melanoma metastasis by the interaction with **MMP2** (matrix metallopeptidase 2) (Dye et *al*., 2013), which is also underexpressed in our light melanocytes treated with vitamin D. *MMP2* is principally involved in invasiveness (Hofmann et *al*., 2000; Dahal, Lee and Gupta, 2019).

***MX2*** (MX dynamin like GTPase 2) has been associated with melanoma and nevi predisposition by several independent GWAS performed in individuals of European descent (Barrett et *al*., 2011; Ransohoff et *al*., 2017; Duffy et *al*., 2018). Gibbs et *al*. (2015) also confirmed the association of rs45430 in *MX2* with melanoma. On the other hand, *MX2* has also been reported to be underexpressed in vitiligo (Dey-Rao and Sinha, 2017), whereas the melanoma variants in *MX2* associate with increased expression (Zhang et *al*., 2018b). Intriguingly, Sironi et *al*. (2014) reported evidence for recent positive selection at this gene in non-Africans.

***NFATC2*** (nuclear factor of activated T cells 2) and ***DHCR24*** (24-dehydrocholesterol reductase) have anti-apoptotic activity in melanoma cells (Di Stasi et *al*., 2005; Perotti et *al*., 2012). Although the principal function of *DHCR24* is to participate in the synthesis of cholesterol (Prabhu et *al*., 2016b), it was also reported to take part in the modulation of oxidative stress response (Zerenturk et *al*., 2013) and because of that, it can be important in melanoma. Indeed, Di Stasi et *al*. (2005) found an association between upregulation of *DHCR24* in melanoma metastases and resistance to oxidative stress-induced apoptosis. ***ENG*** (endoglin) and ***FAM129B*** (family with sequence similarity 129, member B) are also involved in melanoma proliferation and invasion (Old et *al*., 2009; Pardali et *al*., 2011; Tesic et *al*., 2015).

Overall, these results suggest a transcriptional response related with protection against malignancy, specifically in light-pigmented melanocytes. Hence, these observations are in line with the reported anti-melanoma effects of active vitamin D in both animal models and clinical data (Slominski et *al*., 2017).

Pathway analyses showed that in vitamin D treated melanocytes, as expected, the overrepresented pathways that were significant (FDR<0.05) were those related with "*vitamin D metabolism and pathway*" or "*Vitamin D receptor pathway*", confirming that the melanocytes did response to vitamin D treatment. These pathways were significant when all samples were analysed together and for dark melanocytes alone, with the genes significant for both DESeq2 and edgeR methods, in Panther (Mi, Muruganujan and Thomas, 2013) and Wikipathways databases (Kutmon et *al*., 2016).

### 4.3.3. Methylated DNA analysis

To understand the impact of $1,25(OH)_2D_3$ treatment on the regulatory landscape associated with these transcriptional changes, we performed methylated DNA immunoprecipitation sequencing (MeDIP-Seq) under the same experimental conditions as described above. We scanned the genome in 1kb windows for differential methylation after $1,25(OH)_2D_3$ exposure. Even if no window passed multiple testing criteria (probably due to the small sample size and the large amount of windows tested, around 1.4M), we found that genes with differential expression were enriched for differentially methylated regions (DMRs), with significant nominal P-values (P<0.05) (Figure 4.5). This trend was observed for both edgeR and DESeq2 differentially expressed genes, and was significant even correcting for gene length (Figure 4.6).

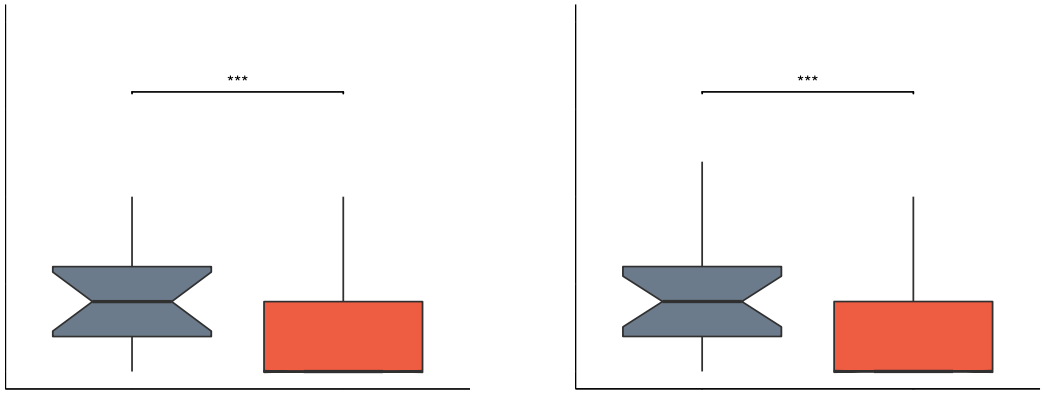


**Figure 4.5**. **Patterns of differentially methylated regions (DMRs) at differentially expressed genes (DEGs).** DEGs show significantly more DMRs than other genes (Wilcoxon tests P<0.002). EdgeR (left) and DESeq2 (right).

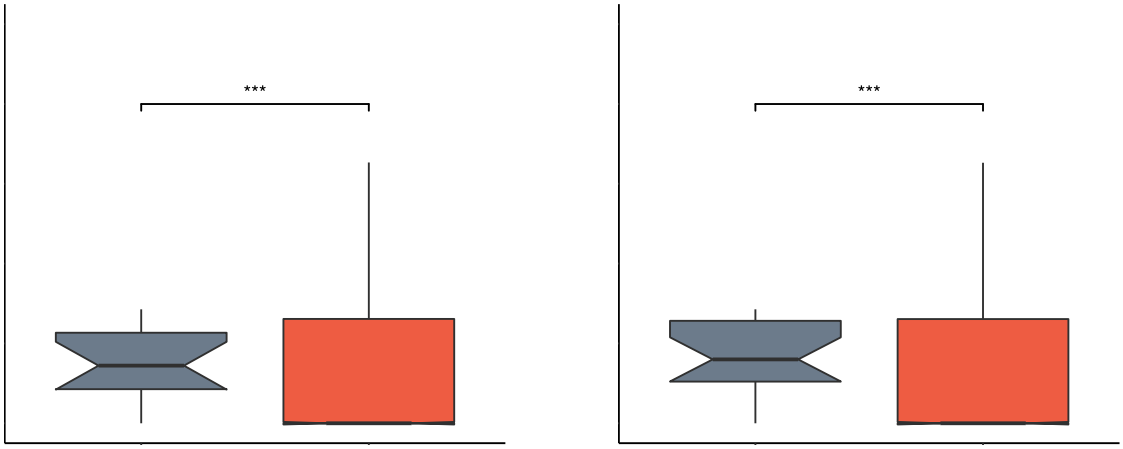


**Figure 4.6. Differentially expressed genes (DEGs) show significantly more differentially methylated length per kb than other genes** (Wilcoxon tests, P<0.02).

Among the differentially expressed genes with most DMRs (Table 4.1), we find *GAS7* gene (growth arrest specific 7), which harboured 7 DMRs (6 of them hypermethylated), encompassing the intronic regions of several isoforms. The function of *GAS7* in melanocytes is unclear, it has been associated to projections growth in neurons (Chao Chang and Lu, 2005). *ST8SIA1,* a possible target of *MITF* (Hoek et *al*., 2008), showed 6 intronic DMRs, *CEBPD* and *MREG* showed 5 and 4 respectively whereas *VDR* and *CYP24A1* showed two and one exonic DMR (Figure 4.7).

**Table 4.1. Differentially expressed genes (DEGs) in all samples together (light and dark) with the number of differentially methylated regions (DMR) they harbour.**

| DEG | DEG method | # DMRs P<0.05 |
|---|---|---|
| ***COL22A1*** | edgeR | 7 |
| ***GAS7*** | DESeq2 | 7 |
| ***ST8SIA1*** | DESeq2 | 6 |
| ***CEBPD*** | edgeR, DESeq2 | 5 |
| ***MREG*** | edgeR, DESeq2 | 4 |
| ***ABLIM3*** | DESeq2 | 3 |
| ***IGFBP5*** | edgeR | 3 |
| ***MX2*** | DESeq2 | 3 |
| ***MYOF*** | DESeq2 | 3 |
| ***PADI2*** | edgeR, DESeq2 | 3 |
| ***TPST1*** | edgeR, DESeq2 | 3 |
| ***NT5DC3*** | edgeR, DESeq2 | 2 |
| ***VDR*** | edgeR, DESeq2 | 2 |
| ***ZBTB16*** | edgeR | 2 |
| ***ADHFE1*** | DESeq2 | 1 |
| ***CYP24A1*** | edgeR, DESeq2 | 1 |
| ***FOXD3*** | DESeq2 | 1 |
| ***IL1R1*** | edgeR, DESeq2 | 1 |
| ***OLFML2A*** | edgeR, DESeq2 | 1 |
| ***YWHAQ*** | DESeq2 | 1 |
| ***FCMR*** | DESeq2 | 0 |
| ***PPP1R16B*** | edgeR | 0 |
| ***SULT1C2*** | edgeR, DESeq2 | 0 |

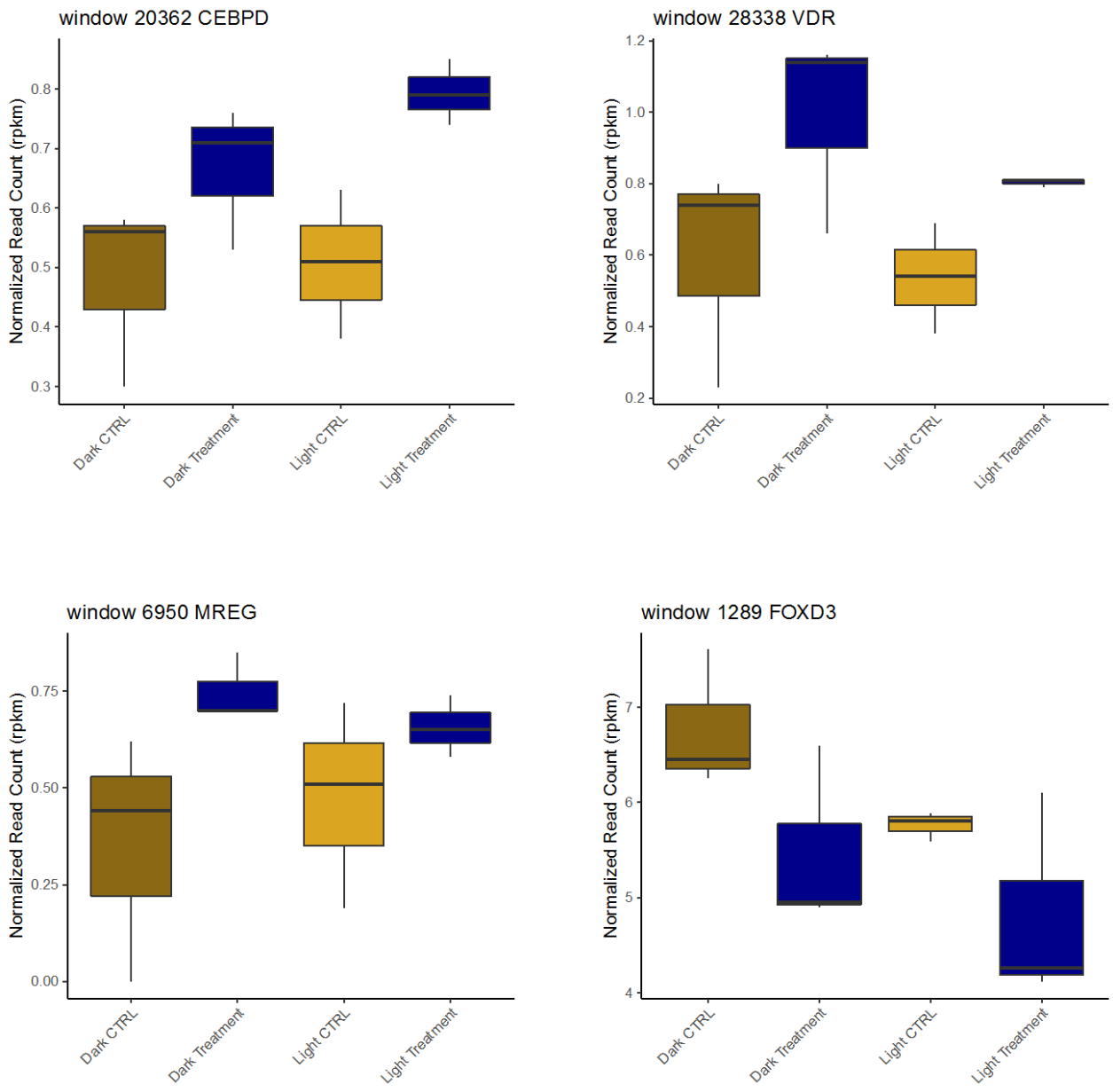


**Figure 4.7. DNA methylation levels before and after $1,25(OH)_2D_3$ treatment in some differentially expressed genes.** All patterns P<0.05.

The majority of DMRs in DEGs located within gene bodies (>75% in intronic regions), where the role of DNA methylation on transcription is poorly understood and can be both permissive or repressive (Lou et *al*., 2014). In contrast, DNA methylation in promoter regions typically associates with transcriptional silencing. *FOXD3* (forkhead box D3), which is underexpressed after the treatment (when analysing all samples together), showed a hypomethylated DMR 1.7kb upstream the gene, co-localizing with the promoter region of *FOXD3* and its antisense RNA gene *FOXD3-AS1* (Figure 4.7). The significant reduction of expression levels observed in *FOXD3* after $1,25(OH)_2D_3$ treatment suggests that the hypomethylation of the DMR might increase the expression of the antisense gene, leading to silencing of *FOXD3*. Interestingly, *FOXD3* can repress *MITF* expression (Curran et *al*., 2010; Wan, Hu and He, 2011) and it has suggested that it may be associated to tanning ability in a UK population, although it failed replication in other European cohorts (Visconti et *al*., 2018).

Another differentially expressed gene with DMRs in the promoter regions was the melanoma-related gene *MX2*. The gene, which was significantly undexpressed after vitamin D treatment, showed three hypermethylated DMRs spanning the promoter and introns of several isoforms (Figure 4.8). In line with these results, SNPs associated with melanoma risk in *MX2* have shown to alter DNA methylation levels in-between our reported DMR regions (Roos et *al*., 2017), supporting the role of DNA methylation mediating the transcriptional changes of *MX2* in melanocytes.

The enrichment of methylation changes at differentially expressed regions suggests a potential regulatory role of DNA methylation mediating the transcriptional response to $1,25(OH)_2D_3$ in melanocytes. Given the majority of the differentially methylated regions located outside promoters, future studies elucidating the role of gene body methylation on transcriptional activity will provide further insights into the mechanisms by which the detected DMRs mediate these transcriptional changes.

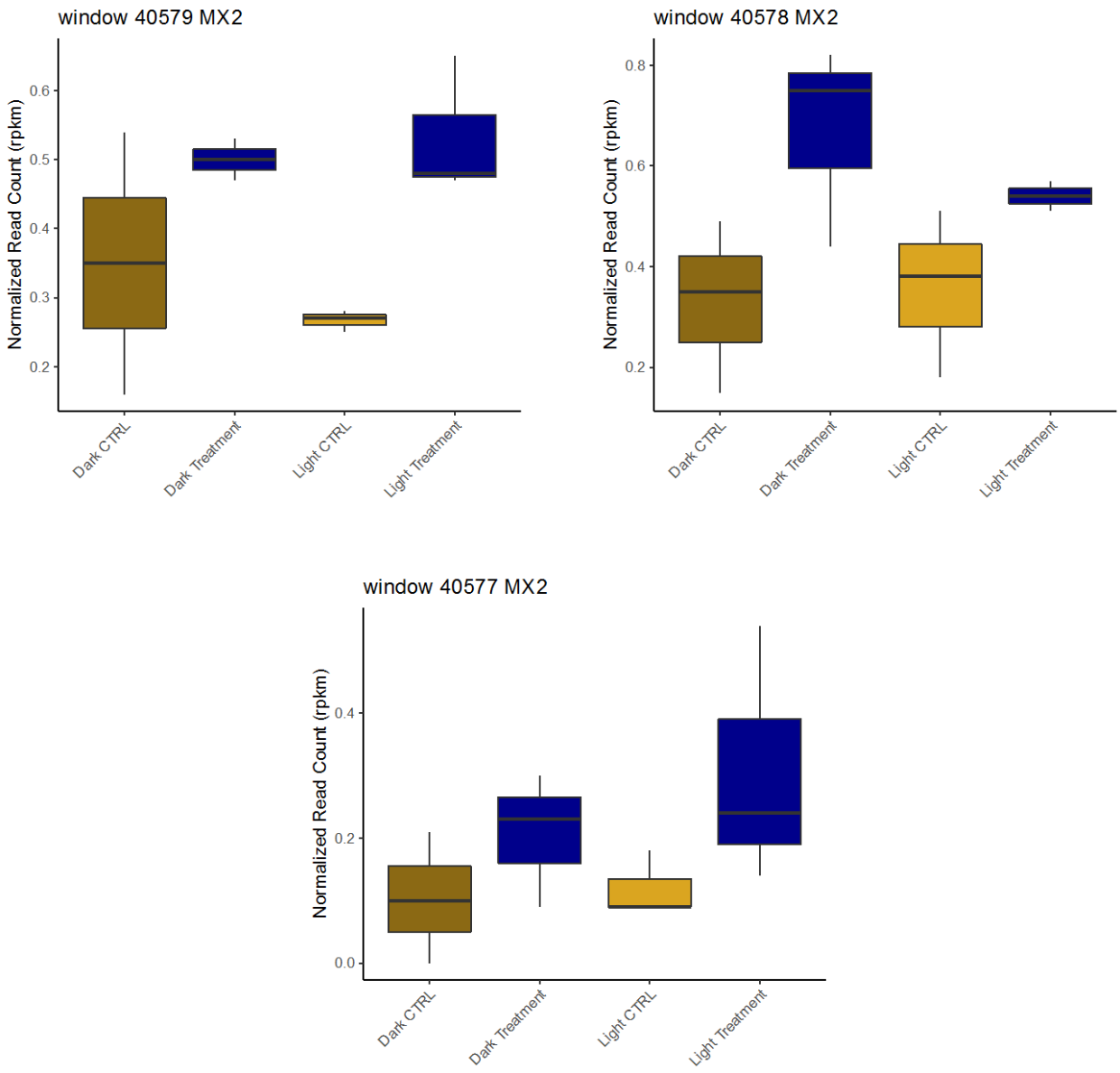


**Figure 4.8**. **DNA methylation levels of 3 differentially methylated regions (DMRs) associated to *MX2*, before and after 1,25(OH)$_2$D$_3$.** All patterns P<0.05

### 4.3.4. Assessing homogeneity of cell lines

We wanted to asses if cell lines with the same pigmentary phenotype (darkly or lightly pigmented) shared the same characteristics, and that the results obtained were not biased because of any particular cell line departuring from its suppossed pigmentation group.

For that, we performed a variant calling analysis using RNA-seq data and performed a PCA analysis adding data from the 1000G project worldwide populations. Figure 4.9 shows, that, in general, dark cell lines and light cell lines formed two separated groups. Dark cell lines were clustered near African population from 1000G project and light cell lines were located near the cluster of European population. However, two cell lines lied in an intermediate position. The darkly pigmented "DP1" cell line and the lightly pigmented "LP1" cell line did not group together with the rest of the cell lines of their corresponding pigmentary phenotype, and were closer from each other. Thus, we considered that these two cell lines may include bias in the results, so we decided to re-analyse the RNA-seq data excluding the DP1 and LP1 cell lines.

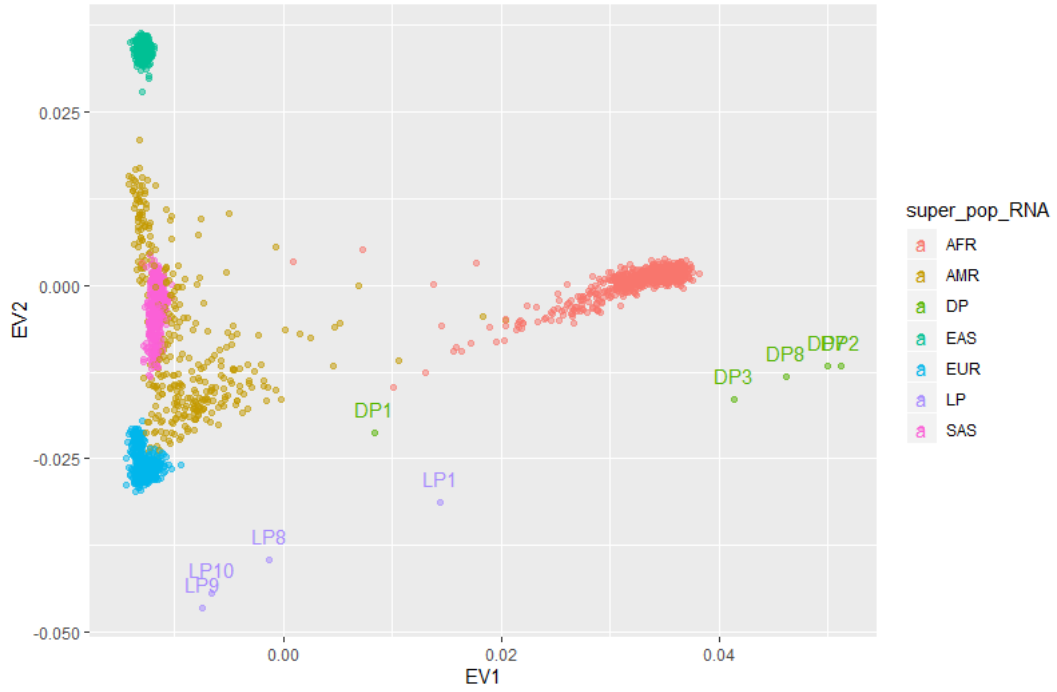


**Figure 4.9. Principal Component Analysis showing the first two components for SNP data from the cell lines and 1000G populations.** DP indicates dark cell lines and LP light cell lines. AFR: African, AMR: Admixed American, EAS: East Asian, EUR: European and SAS: South Asian.

### 4.3.5. RNA-sequencing excluding DP1 and LP1 cell lines

We performed a new RNA-seq analysis, this time using ony the DESeq2 method for differential expression analysis, from 3 HEMn-LP and 4 HEMn-DP (excluding the discordant cell lines DP1 and LP1). Differentially expressed genes (DEGs) obtained with the second analysis are listed in Tables S4.7-S4.12.

When all samples (dark and light) are considered together, we do not observe substantial differences with the initial analysis. We now observe some additional genes and a few of the previous ones (*FOXD3, GAS7, MX2* and *ST8SIA1*) do not reach statistical significance now, possibly due to the smaller sample size used. However, when analyzed separatedly, dark melanocytes, show a higher amount of DEGs in this second analysis. Interestingly, among the upregulated genes, ***SLC7A5*** (Solute carrier family 7 member 5) has recently been associated with pigmentation. Thus, Gaudel et *al*. (2020) have reported that *SLC7A5* is a target for *MITF* and that the inhibition of *SLC7A5* decreases melanogenesis.

As regards light melanocytes, nearly all the genes detected in the first analysis are also significant after excluding the LP1 cell line. However, we now observe a greater amount of DEGs, indicating a higher response to vitamin D (Tables S4.11 and S4.12).

In contrast with dark melanocytes, in light melanocytes incubated with vitamin D, ***MITF*** is upregulated (FDR = 0.027). Besides, although they are not statistically significant we also observe a tendency for increased expression in pigmentation-related genes such as *TYRP1, DCT, PAX3, SLC24A5* or *KIT*.

Apart from *MITF*, which is a central regulator of melanogenesis, several other genes indicate now a possible role of vitamin D in the regulation of pigmentation. The endothelin receptor type B (***EDNRB***), which is implicated in the regulation of melanogenesis by the endothelin pathway (Park, Lee and Cho, 2015), is also statistically significantly upregulated (FDR = 0.002), In this sense, we also observe an upregulation of ***GNAQ*** (G

protein subunit alpha q), which encodes a subunit of a G-protein, reported to interact with *EDNRB* in melanocytes (Urtatiz and Raamsdonk 2016).

*EDNRB* expression has also been reported to be upregulated by UV radiation in melanocytes, together with *MITF* (Tagashira et *al*., 2015). The upregulation of *EDNRB* by vitamin D has already been reported in mouse immature melanocytes by Watabe et *al*. (2002), together with an increase of tyrosinase activity. However, they did not observe similar results in mature melanocytes. In their experiments, the incubation of melanoblasts with endothelin 3 and vitamin D induced the increase of *MITF* expression, but not the incubation with vitamin D alone. Later on, Kawakami et *al*. (2014) performed a similar research, in this case using human melanoblasts and melanocytes from lighly pigmented individuals. Again, they observed an increase in tyrosinase activity after incubation with active vitamin D in melanoblasts and melanocytes, and also an increase in protein levels of the endothelin B receptor in melanoblasts. However, they did not report data for melanocytes regarding *EDNRB.* In contrast, in our experiments, we do observe an upregulation of both *MITF* and *EDNRB* after incubation with vitamin D alone. Our results suggest that *EDNRB* may regulate melanogenesis in human lightly pigmented melanocytes.

In addition, several genes implicated in melanosome biogenesis, protein trafficking and delivery to melanosomes and melanosome transport are also positively modulated by vitamin D and significative at FDR<0.05. The genes with the more evident roles in those functions are *VAMP7, STX12, BLOC1S6, RAB27A, RAB1A* and *KIF5B.*

The transport of cargo from endosomes to melanosomes (including the melanogenic proteins *TYR, TYRP1* and *DCT*), is mainly regulated by the BLOC complexes (biogenesis of lysosome-associated organelles complex) and AP-3 (Adaptor protein-3). In our data, we observe the upregulation of ***BLOC1S6***, which codifies a subunit of the BLOC-1 complex. Mutations in *BLOC1S6* are related with a subtype of Hermansky–

Pudlak síndrome (a genodermatosis with pigmentary disorders) (Serre, Busuttil and Botto, 2018). Besides, ***AP3S1*** (also upregulated) encodes a subunit of the AP3 adaptor complex, which is important for the transport of tyrosinase (Sitaram and Marks, 2013).

Proteins are delivered to melanosomes by membrane trafficking. This process requires the fusion of the membranes of tubular carriers of endosomes and melanosomes which is mediated by membrane-associated proteins called SNAREs (Soluble N-ethylmaleimide-sensitive factor attachment protein receptors). In our data we observe the upregulation of two important SNARES (among others): ***VAMP7*** (Vesicle associated membrane protein 7) and ***STX12*** (Syntaxin 12) (also know as *SXT13* or *STX14*). Both proteins are essential for cargo delivery into melanosomes (Jani et *al*., 2015). In particular, they are important for the correct trasnport of *TYRP1* (Dennis et *al*., 2016).

On the other hand, the small GTPases *RAB27A* and *RAB1A* that localize in the membrane of the melanosomes and *KIF5B* (Kinesin family member 5B) are important for melasonome transport. ***RAB1A*** participates in the microtubule-dependent anterograde transport (towards the pheriphey of the cell) of mature melanosomes (Ishida et *al*., 2012). ***RAB27A***, in turn, is involved in the actin dependent transport of mature melanosomes towards the tips of the dendrites, by recruiting myosin Va motor protein and assembly proteins (Jordens et *al*., 2006; Alzahofi et *al*., 2020). *RAB27A* is transcriptionally regulated by *MITF* (Chiaverini et *al*., 2008). Due to its function in controlling melanosome transport, it is also important for determination of constitutive pigmentation (Yoshida-Amano et *al*., 2012).

We also observe the upregulation of some kinesin-related genes (*KIF5B, KIF2A, KIF20B*), which are motor proteins that move along microtubules and participate in transport. In particular, ***KIF5B*** codifies the kinesin-1 heavy chain. Kinesin-1 is recruited by *RAB1A* for the regulation of melanosome tranrport (Ishida, Ohbayashi and Fukuda, 2015).

In addition to the above mentioned *loci,* there are also other genes related with endosome network and Golgi protein traficking that may be also relevant for melanosome biogenesis, including the sorting nexins *SNX3, SNX4, SNX6 and SNX18*, *TMED10, BORCS7* and *ARL8B* among others.

Other genes possibly related with pigmentation are ***OSTM1***, which was associated to fur color in mice (Chalhoub et *al*., 2003) and has been reported to be a target for MITF (Hoek et al., 2008), and ***RB1***, which has been reported to be a MITF cofactor, and may be involved in the activation *TYR* expression (Seberg, Van Otterloo and Cornell, 2017).

Pathway enrichment analysis

We perfomed a pathway overrepresentation analysis, based on the KEGG database, implemented in Webgestalt, and in light melanocytes treated with vitamin D, overrepresented pathways included "*Ubiquitin mediated proteolysis*", "*p53 signaling pathway*" and "*Endocytosis*". Ubiquitin mediated proteolysis is involved in nearly all cellular processes, including regulation of cell cycle, DNA repair, apoptosis or immune and inflammatory responses (Ciechanover, Orian and Schwartz, 2000). On the other hand, p53 is one of the most important tumour suppressor genes that is activated under stress conditions, regulating important functions such as cell cycle arrest, DNA repair, apoptosis and metabolic pathways (Fischer, 2017).

In this sense, $1,25(OH)_2D_3$ has been reported to increase the protein levels of p53 by non-genomic mechanism (Sequeira et *al*., 2012). In accordance with this, although we did not detect an upregulation in the expression of *TP53* gene (tumor protein p53), we did find some genes overexpressed in light melanocytes after vitamin D treatment that can be transcriptionally upregulated by the tumour suppressor p53. Among them, we find genes related with DNA repair and oxidative damage response, such as ***RRM2B, SESN1*** and ***SESN3***. Besides, some of the above mentioned downregulated genes, with a possible function in melanoma (such as *MCAM, MX2 or NFATC2)* have also been

reported to be transcriptionally repressed by p53 (Fischer, 2017). In addition, Junctional Mediating and Regulating Y protein (**JMY**), a known cofactor of p53 (Adighibe and Pezzella, 2018), is also upregulated.

P53 is also able to regulate its activity through a negative feedback mechanism, by inducing the expression of target genes. In our data, we observe the upregulation of its targets genes ***MDM2*** and ***CCNG1***. *MDM2* codifies a E3 ubiquitin ligase and is the principal inhibitor of p53 activity: through ubiquitination, which leads to degradation, or by binding the transcriptional activation domain of p53 (Wu et *al*., 1993; Haupt et *al*., 1997). Besides, *CCNG1* (Cyclin G1) activates *MDM2* (Okamoto et *al*., 2002). Thus, although we do not observe an increase in *TP53* expression, it may be due to the subsequent negative regulation by *MDM2*, after the activation of p53-dependent targets.

p53 is also related with pigmentation, especially for its role in UV-induced tanning response. Cui et *al*. (2007) demonstrated that *POMC* contains a p53 binding site and in response to UV exposure, *TP53* expression is upregulated in keratinocytes, leading to the induction of POMC and thus α-MSH, which then is secreted and binds to the MC1R receptor in melanocytes. Besides, genes encoding other melanogenic factors produced by keratinocytes also contain p53 binding sites (Box and Terzian, 2008).

However, the effect of p53 on melanocytes in relation with pigmentation is less clear, although it has been proposed to also influence melanogenesis through a direct effect on melanocytes themselves. For instance, *TYRP1* contains a p53-responsive element on its regulatory sequence and both *TYRP1* and *TYR* are upregulated by p53 (Nylander et *al*., 2000; Khlgatian et *al*., 2002). On the other hand, several studies have demonstrated the involvement of p53 in the response to UVB. Yang et *al*. (2006) analysed the expression profile of UV irradiated melanocytes and identified a set of p53-target genes, suggesting a role of p53 in the response to UV. López et *al*. (2015b) also

observed the upregulation of several p53-target genes and *TP53* itself in UV irradiated lightly and darkly pigmented melanocytes.

Regarding downregulated genes, in this second analysis we detect nearly all the genes detected on the first analysis and several more. Overall, we observe a decreased expression of several genes related with melanoma, suggesting that vitamin D may exert a protective function.

### 4.3.6. *VDR* and *MREG* resequencing

We resequenced *VDR* and *MREG* genes in order to analyse if the selection has affected these *loci*. *VDR* is the main effector of vitamin D pathway and *MREG* is one of the genes that could be implicated in the regulation of pigmentation. Resequencing was performed in a subset of 96 individuals from the Basque Country with different pigmentary phenotype: 48 of the least pigmented individuals and 48 of the most pigmented individuals from based on a reflectance distribution. We also compared our data with data from different populations of 1000 Genomes Project (1000G): Central Europeans (CEU), Tuscans from Italy (TSI) and Yoruba from African (YRI).

Both genes showed positive Tajima's D values in some of the regions sequenced in the samples from The Basque Country and in the European populations analysed from 1000G. Interestingly, in the African population (Yoruba) from 1000G, there were no significant positive Tajima's D values for any of the genes (Figures 4.9 and 4.10).

For the *VDR locus*, there were not substantial differences between the most lightly and most darkly pigmented individuals from the Basque Country. European populations from 1000G also show similar positive values. In contrast, in the African population there were negative Tajima's D values, which could indicate the effect of positive selection. European populations from 1000G also showed some regions with negative values in the extremes of the sequence, but showed positive values in other regions along the gene body (Figure 4.9).

Among the regions showing Tajima's D positive values, there is exon 5, which together with exons 3 and 4 codify for the DNA binding domain. There are also positive values in the region near exon 8, which codifies for one of the vitamin D binding domains. Therefore, it could be important for the *VDR* function of gene expression regulation.

For *MREG locus*, all European populations showed several regions with positive Tajima's D values and African population showed no signs of selection.

Positive Tajima's D values could indicate the effect of balancing selection on these *loci*. Balancing selection could arise from different situations. For instance, it is possible that heterozygotes could have an advantage above homozygotes in certain conditions. Another possibility is that different haplotypes could be advantageous depending on the ambient conditions, and in a changing environment, different haplotypes are maintained. In the case of VDR, due to its many functions, it is possible that some haplotypes could be beneficious for some of the functions and other haplotypes could be advantageous for another of its roles, and as a consequence, intermediate frequencies of different haplotypes are maintained. Different haplotypes could be also important in different stages of life, providing different advantages in early development, adulthood or pregnancy. In relation with pigmentation, one possibility is that different haplotypes are maintained due to different pressures depending on the solar irradiation: the need to be protected against solar irradiation in summer and more despigmented in winter to allow enough vitamin D synthesis.

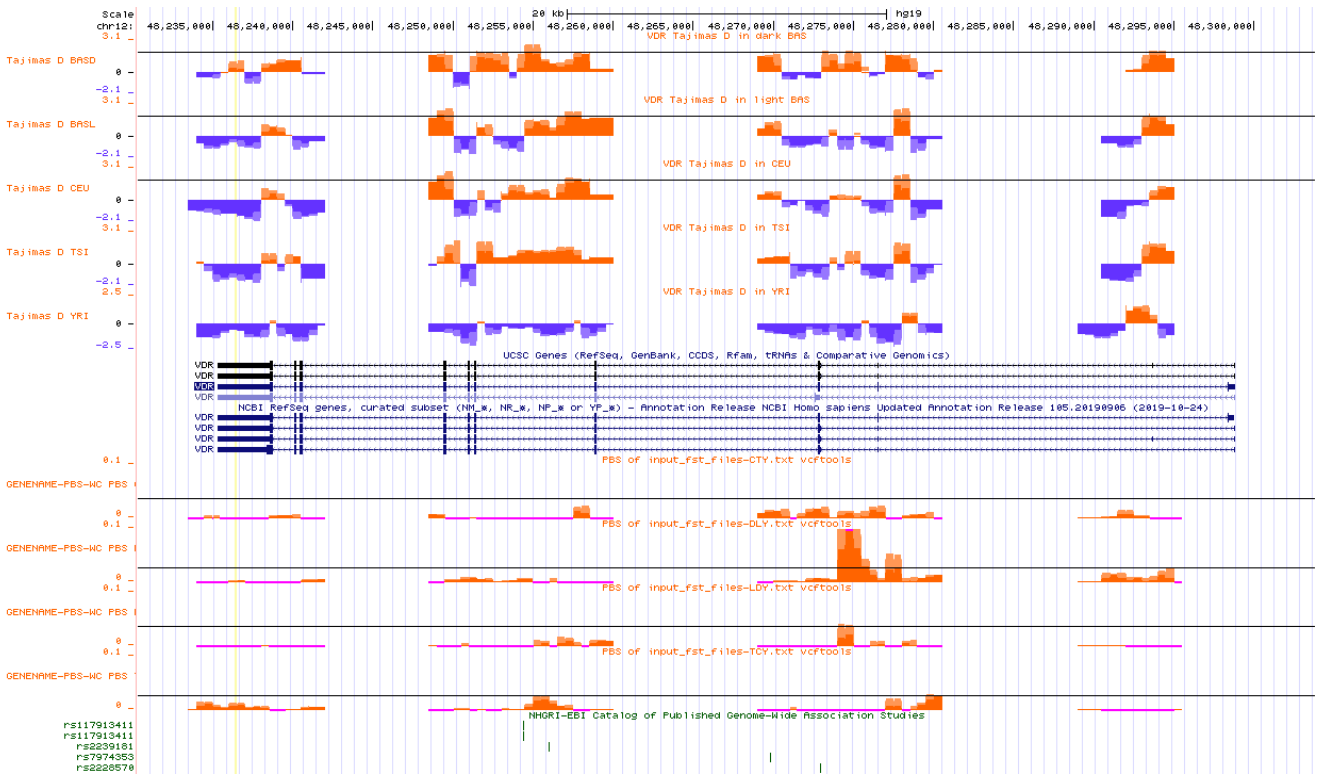


**Figure 4.9. Representation of Tajima's D values for *VDR locus* in the populations analysed visualized on UCSC Genome Browser.** Black lines indicate values of 2. BASL: most lightly pigmented Basque individuals; BASD: most darkly pigmented Basque individuals; CEU: Central Europeans, TSI: Tuscans from Italy; YRI: Yoruba from Africa.

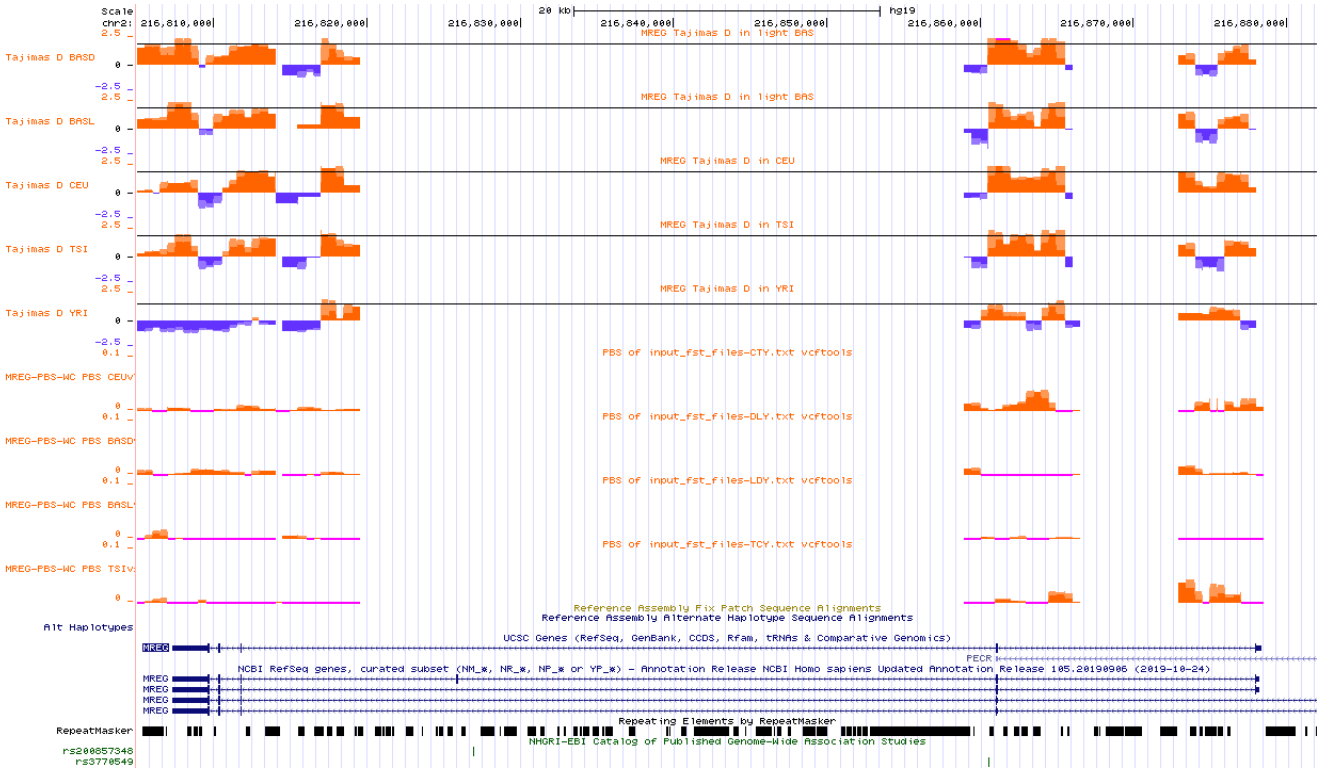


**Figure 4.10. Representation of Tajima's D values for *MREG locus* in the populations analysed visualized on UCSC Genome Browser.** Black lines indicate values of 2. BASL: most lightly pigmented Basque individuals; BASD: most darkly pigmented Basque individuals; CEU: Central Europeans; TSI: Tuscans from Italy; YRI: Yoruba from Africa

.

## 4.4. Conclusions

In conclusion, taking all these data in combination, expression analysis of melanocytes under treatment with $10^{-7}$ M $1,25(OH)_2D_3$ seems to be eliciting a response through its receptor *VDR*, which seems to initiate a mechanism of store or catabolism of $1,25(OH)_2D_3$.

Lightly and darkly pigmented melanocytes show different responses to vitamin D, which seems stronger in light melanocytes. Our results suggest an implication of vitamin D on pigmentation in light melanocytes. On one hand, by increasing expression of melanogenic genes and which could be mediated by the *EDNRB*, and on the other, by modulating melanosome biogenesis and transport.

In addition, the transcriptional profile modulated by vitamin D also showed many genes implicated in melanoma risk and progression, suggesting an anti-melanoma effect of active vitamin D that has been previously proposed (Slominski et *al*., 2017). Interestingly, this protective effect is more notable in light melanocytes, suggesting the influence of the pigmentary phenotype on the response to vitamin D.

## 4.5. Supplementary Material

**Table S4.1. Upregulated genes (FDR < 0.05) in 1,25(OH)$_2$D$_3$ treated samples vs. controls in ALL samples together (dark + light), with DESeq2 and/or edgeR methods (FDR values in brackets).**

| Gene symbol | Gene name | Method (FDR values) |
|---|---|---|
| ***ADHFE1*** | Alcohol dehydrogenase iron containing 1 | DESeq2 (0.0304) |
| ***CEBPD*** | CCAAT enhancer binding protein delta | EdgeR (1.29E-08)<br>DESeq2 (7.55E-07) |
| ***COL22A1*** | Collagen type XXII alpha 1 chain | EdgeR (0.0033) |
| ***CYP24A1*** | Cytochrome P450 family 24 subfamily A member 1 | EdgeR (6.07E-17)<br>DESeq2 (1.92E-06) |
| ***IGFBP5*** | Insulin like growth factor binding protein 5 | EdgeR (0.0038) |
| ***IL1R1*** | Interleukin 1 receptor type 1 | EdgeR (0.0011)<br>DESeq2 (3.89E-07) |
| ***MREG*** | Melanoregulin | EdgeR (0.0406)<br>DESeq2 (1.13E-05) |
| ***NT5DC3*** | 5'-nucleotidase domain containing 3 | EdgeR (2.12E-05)<br>DESeq2 (3.92E-10) |
| ***PADI2*** | Peptidyl arginine deiminase 2 | EdgeR (0.0101)<br>DESeq2 (7.04E-06) |
| ***PPP1R16B*** | Protein phosphatase 1 regulatory subunit 16B | EdgeR (0.0483) |
| ***SULT1C2*** | Sulfotransferase family 1C member 2 | EdgeR (7.66E-13)<br>DESeq2 (9.20E-17) |
| ***TPST1*** | Tyrosylprotein sulfotransferase 1 | EdgeR (0.0001)<br>DESeq2 (8.45E-08) |
| ***VDR*** | Vitamin D receptor | EdgeR (0.0004)<br>DESeq2 (5.45E-07) |
| ***YWHAQ*** | Tyrosine 3-monooxygenase/tryptophan 5-monooxygenase activation protein theta | DESeq2 (4.96E-05) |

**Table S4.2. Upregulated genes (FDR < 0.05) in 1,25(OH)$_2$D$_3$ treated samples vs. controls in DARK samples, with DESeq2 and/or edgeR methods (FDR values in brackets).**

| Gene symbol | Gene name | Method (FDR values) |
|---|---|---|
| ***CEBPD*** | CCAAT enhancer binding protein delta | EdgeR (6.83E-05) DESeq2 (0.0033) |
| ***COL16A1*** | Collagen type XVI alpha 1 chain | EdgeR (0.0392) DESeq2 (0.0002) |
| ***COL22A1*** | Collagen type XXII alpha 1 chain | EdgeR (1.87E-12) DESeq2 (8.10E-10) |
| ***CYP24A1*** | Cytochrome P450 family 24 subfamily A member 1 | EdgeR (1.97E-14) DESeq2 (0.0004) |
| ***EFR3B*** | EFR3 homolog B | EdgeR (0.0392) DESeq2 (0.0069) |
| ***GDF15*** | Growth differentiation factor 15 | DESeq2 (0.0489) |
| ***IGFBP5*** | Insulin like growth factor binding protein 5 | EdgeR (2.80E-06) DESeq2 (1.07E-06) |
| ***MAGED4*** | MAGE family member D4 | EdgeR (0.0007) DESeq2 (0.0048) |
| ***MCHR1*** | Melanin concentrating hormone receptor 1 | EdgeR (0.0455) |
| ***NT5DC3*** | 5'-nucleotidase domain containing 3 | EdgeR (0.0002) DESeq2 (8.60E-05) |
| ***PPP1R16B*** | Protein phosphatase 1 regulatory subunit 16B | EdgeR (0.005) |
| ***PRSS33*** | Serine protease 33 | EdgeR (6.83E-05) |
| ***SERPINB9*** | Serpin family B member 9 | EdgeR (0.0383) |
| ***SULT1C2*** | Sulfotransferase family 1C member 2 | EdgeR (1.88E-15) DESeq2 (5.77E-16) |
| ***TPST1*** | Tyrosylprotein sulfotransferase 1 | EdgeR (0.0005) DESeq2 (0.0026) |
| ***VDR*** | Vitamin D receptor | EdgeR (0.0007) DESeq2 (0.0048) |
| ***ZFYVE28*** | Zinc finger FYVE-type containing 28 | DESeq2 (0.0217) |

**Table S4.3. Upregulated genes (FDR < 0.05) in 1,25(OH)$_2$D$_3$ treated samples vs. controls in LIGHT samples, with DESeq2 and/or edgeR methods (FDR values in brackets).**

| Gene symbol | Gene name | Method (FDR values) |
|---|---|---|
| ***ATXN3*** | Ataxin 3 | DESeq2 (0.0211) |
| ***C7orf60*** | Chromosome 7 open reading frame 60 | DESeq2 (0.0250) |
| ***CCNG1*** | Cyclin G1 | DESeq2 (0.008) |
| ***CEBPD*** | CCAAT enhancer binding protein delta | EdgeR (0.0165)<br>DESeq2 (0.0363) |
| ***CNIH1*** | Cornichon family AMPA receptor auxiliary protein 1 | DESeq2 (0.0250) |
| ***CNOT7*** | CCR4-NOT transcription complex subunit 7 | DESeq2 (0.0190) |
| ***CYP24A1*** | Cytochrome P450 family 24 subfamily A member 1 | EdgeR (0.0201) |
| ***DSTN*** | Destrin, actin depolymerizing factor | DESeq2 (0.0211) |
| ***EID1*** | EP300 interacting inhibitor of differentiation 1 | DESeq2 (0.0211) |
| ***ESRP1*** | Epithelial splicing regulatory protein 1 | DESeq2 (0.0250) |
| ***LINC01531*** | Long intergenic non-protein coding RNA 1531 | DESeq2 (0.0325) |
| ***MAD2L1*** | Mitotic arrest deficient 2 like 1 | EdgeR (0.0130)<br>DESeq2 (0.0158) |
| ***METAP2*** | Methionyl aminopeptidase 2 | DESeq2 (0.0333) |
| ***MREG*** | Melanoregulin | DESeq2 (0.0051) |
| ***NDUFB5*** | NADH:ubiquinone oxidoreductase subunit B5 | DESeq2 (0.0268) |
| ***NUCKS1*** | Nuclear casein kinase and cyclin dependent kinase substrate 1 | DESeq2 (0.0178) |
| ***PIK3CB*** | Phosphatidylinositol-4,5-bisphosphate 3-kinase catalytic subunit beta | DESeq2 (0.0435) |
| ***PTEN*** | Phosphatase and tensin homolog | DESeq2 (0.0180) |
| ***RBM7*** | RNA binding motif protein 7 | DESeq2 (0.0211) |
| ***SCOC*** | Short coiled-coil protein | DESeq2 (0.0422) |
| ***SEC62*** | SEC62 homolog, preprotein translocation factor | DESeq2 (0.0087) |
| ***SERF1B*** | Small EDRK-rich factor 1B | EdgeR(6.28E-05)<br>DESeq2 (0.0051) |
| ***SOX4*** | SRY-box transcription factor 4 | DESeq2 (0.0305) |
| ***SUB1*** | SUB1 regulator of transcription | DESeq2 (0.0459) |
| ***SULT1C2*** | Sulfotransferase family 1C member 2 | EdgeR (0.0123)<br>DESeq2 (0.0055) |
| ***UACA*** | Uveal autoantigen with coiled-coil domains and ankyrin repeats | DESeq2 (0.0158) |
| ***WDR43*** | WD repeat domain 43 | DESeq2 (0.0459) |
| ***ZMAT3*** | Zinc finger matrin-type 3 | DESeq2 (0.0074) |

**Table S4.4. Downgulated genes (FDR < 0.05) in 1,25(OH)$_2$D$_3$ treated samples vs. controls in ALL samples together (dark + light), with DESeq2 and/or edgeR methods (FDR values in brackets).**

| Gene symbol | Gene name | Method (FDR values) |
|---|---|---|
| ***ABLIM3*** | Actin binding LIM protein family member 3 | DESeq2 (0.0460) |
| ***FCMR*** | Fc fragment of IgM receptor | DESeq2 (0.0219) |
| ***FOXD3*** | Forkhead box D3 | DESeq2 (0.0454) |
| ***GAS7*** | Growth arrest specific 7 | DESeq2 (0.0460) |
| ***MX2*** | MX dynamin like GTPase 2 | DESeq2 (0.0277) |
| ***MYOF*** | Myoferlin | DESeq2 (0.0460) |
| ***OLFML2A*** | Olfactomedin like 2A | EdgeR (0.0004)<br>DESeq2 (4.63E-05) |
| ***ST8SIA1*** | ST8 alpha-N-acetyl-neuraminide alpha-2,8-sialyltransferase 1 | DESeq2 (0.0275) |
| ***ZBTB16*** | Zinc finger and BTB domain containing 16 | EdgeR (0.0018) |

**Table S4.5. Downgulated genes (FDR < 0.05) in 1,25(OH)$_2$D$_3$ treated samples vs. controls in DARK samples, with DESeq2 and/or edgeR methods.**

| Gene symbol | Gene name | Method (FDR values) |
|---|---|---|
| ***ALCAM*** | Activated leukocyte cell adhesion molecule | EdgeR (0.0270)<br>DESeq2 (0.0048) |
| ***CD36*** | CD36 molecule | EdgeR (0.0296)<br>DESeq2 (0.0073) |
| ***LOX*** | Lysyl oxidase | DESeq2 (0.0376) |
| ***MAP2*** | Microtubule associated protein 2 | DESeq2 (0.0376) |
| ***MIR548AR*** | MicroRNA 548ar | EdgeR (0.0210) |
| ***PALMD*** | Palmdelphin | DESeq2 (0.0345) |
| ***RP11-562A8.4*** | | EdgeR (0.0373) |
| ***SORBS2*** | Sorbin and SH3 domain containing 2 | EdgeR (0.0461)<br>DESeq2 (0.0048) |
| ***SYNPR*** | Synaptoporin | EdgeR (0.0210) |
| ***ZBTB16*** | Zinc finger and BTB domain containing 16 | EdgeR (1.33E-09) |

**Table S4.6. Downgulated genes (FDR < 0.05) in 1,25(OH)$_2$D$_3$ treated samples vs. controls in LIGHT samples, with DESeq2 and/or edgeR methods (FDR values in brackets).**

| Gene symbol | Gene name | Method (FDR values) |
|---|---|---|
| ***ABLIM3*** | Actin binding LIM protein family member 3 | DESeq2 (0.0180) |
| ***ANKRD11*** | Ankyrin repeat domain 11 | DESeq2 (0.0479) |
| ***C11orf24*** | Chromosome 11 open reading frame 24 | DESeq2 (0.0459) |
| ***CEP170B*** | Centrosomal protein 170B | DESeq2 (0.0422) |
| ***COL4A2*** | Collagen type IV alpha 2 chain | DESeq2 (0.0051) |
| ***CSPG4*** | Chondroitin sulfate proteoglycan 4 | DESeq2 (0.0051) |
| ***DCHS1*** | Dachsous cadherin-related 1 | DESeq2 (0.0176) |
| ***DHCR24*** | 24-dehydrocholesterol reductase | EdgeR (0.0127)<br>DESeq2 (0.0051) |
| ***ECM1*** | Extracellular matrix protein 1 | EdgeR (0.0127)<br>DESeq2 (0.0051) |
| ***ENG*** | Endoglin | DESeq2 (0.0214) |
| ***FAM129B*** | Family with sequence similarity 129, member B | DESeq2 (0.0324) |
| ***FASN*** | Fatty acid synthase | DESeq2 (0.0248) |
| ***FCMR*** | Fc fragment of IgM receptor | DESeq2 (0.0105) |
| ***FHDC1*** | FH2 domain containing 1 | DESeq2 (0.0324) |
| ***FOXM1*** | Forkhead box M1 | DESeq2 (0.0251) |
| ***HRH2*** | Histamine receptor H2 | DESeq2 (0.0211) |
| ***IGFBP4*** | Insulin like growth factor binding protein 4 | DESeq2 (0.0126) |
| ***LGALS3BP*** | Galectin 3 binding protein | DESeq2 (0.0105) |
| ***LIMD1*** | LIM domains containing 1 | DESeq2 (0.0479) |
| ***LRP5*** | LDL receptor related protein 5 | DESeq2 (0.0364) |
| ***LY6E*** | Lymphocyte antigen 6 family member E | DESeq2 (0.0305) |
| ***MCAM*** | Melanoma cell adhesion molecule | DESeq2 (0.0135) |
| ***MMP2*** | Matrix metallopeptidase 2 | DESeq2 (0.0364) |
| ***MX2*** | MX dynamin like GTPase 2 | DESeq2 (0.0248) |
| ***NES*** | Nestin | DESeq2 (0.0145) |
| ***NFATC2*** | Nuclear factor of activated T cells 2 | DESeq2 (0.0051) |
| ***OLFML2A*** | Olfactomedin like 2A | EdgeR (0.0001)<br>DESeq2 (9.76E-07) |
| ***PCDHGC3*** | Protocadherin gamma subfamily C, 3 | DESeq2 (0.0211) |
| ***PLXNB3*** | Plexin B3 | DESeq2 (0.0331) |
| ***SDC3*** | Syndecan 3 | DESeq2 (0.0126) |
| ***SGK223*** | Homolog of rat pragma of Rnd2 | DESeq2 (0.0423) |
| ***SPON2*** | Spondin 2 | DESeq2 (0.0346) |
| ***SVIL*** | Supervillin | DESeq2 (0.0189) |

**Table S4.7. Upregulated genes (FDR < 0.05) in 1,25(OH)$_2$D$_3$ treated samples vs. controls in ALL samples together (dark + light), excluding DP1 and LP1 cell lines.**

| Gene symbol | Gene name | p-value | FDR |
|---|---|---|---|
| ***IGFBP5*** | Insulin like growth factor binding protein 5 | 1.21E-12 | 2.40E-08 |
| ***CYP24A1*** | Cytochrome P450 family 24 subfamily A member 1 | 1.84E-09 | 1.82E-05 |
| ***IL1R1*** | Interleukin 1 receptor type 1 | 4.25E-09 | 2.81E-05 |
| ***NT5DC3*** | 5'-nucleotidase domain containing 3 | 7.39E-09 | 3.66E-05 |
| ***CEBPD*** | CCAAT enhancer binding protein delta | 3.02E-08 | 0.0001 |
| ***SULT1C2*** | Sulfotransferase family 1C member 2 | 4.42E-08 | 0.0001 |
| ***VDR*** | Vitamin D receptor | 1.62E-06 | 0.0026 |
| ***TPST1*** | Tyrosylprotein sulfotransferase 1 | 2.03E-06 | 0.0031 |
| ***CTSL*** | Cathepsin L | 7.74E-06 | 0.0090 |
| ***YWHAQ*** | Tyrosine 3-monooxygenase/tryptophan 5-monooxygenase activation protein theta | 1.93E-05 | 0.0191 |
| ***PADI2*** | Peptidyl arginine deiminase 2 | 4.61E-05 | 0.0397 |
| ***ADHFE1*** | Alcohol dehydrogenase iron containing 1 | 5.58E-05 | 0.0410 |
| ***SPP1*** | Secreted phosphoprotein 1 | 5.87E-05 | 0.0416 |
| ***MREG*** | Melanoregulin | 6.34E-05 | 0.0434 |

**Table S4.8. Downregulated genes (FDR < 0.05) in 1,25(OH)$_2$D$_3$ treated samples vs. controls in ALL samples together (dark + light), excluding DP1 and LP1 cell lines.**

| Gene symbol | Gene name | p-value | FDR |
|---|---|---|---|
| ***OLFML2A*** | Olfactomedin like 2A | 3.45E-08 | 0.0001 |
| ***THBS1*** | Thrombospondin 1 | 7.81E-08 | 0.0001 |
| ***DACT1*** | Dishevelled binding antagonist of beta catenin 1 | 1.65E-07 | 0.0003 |
| ***NES*** | Nestin | 8.68E-07 | 0.0017 |
| ***PRIMA1*** | Proline rich membrane anchor 1 | 1.56E-06 | 0.0026 |
| ***FHDC1*** | FH2 domain containing 1 | 2.32E-06 | 0.0032 |
| ***HRH2*** | Histamine receptor H2 | 2.70E-06 | 0.0035 |
| ***SORBS2*** | Sorbin and SH3 domain containing 2 | 5.23E-06 | 0.0064 |
| ***COL1A2*** | Collagen type I alpha 2 chain | 9.85E-06 | 0.0108 |
| ***MYOF*** | Myoferlin | 1.26E-05 | 0.0132 |
| ***NFATC2*** | Nuclear factor of activated T cells 2 | 2.20E-05 | 0.0208 |
| ***MAML3*** | Mastermind like transcriptional coactivator 3 | 4.28E-05 | 0.0386 |
| ***AC010731.2*** | | 5.17E-05 | 0.0410 |
| ***SVIL*** | Supervillin | 4.97E-05 | 0.0410 |
| ***COL4A1*** | Collagen type IV alpha 1 chain | 5.44E-05 | 0.0410 |

**Table S4.9. Upregulated genes (FDR < 0.05) in $1,25(OH)_2D_3$ treated samples vs. controls in DARK samples (excluding DP1 cell line).**

| Gene symbol | Gene name | p-value | FDR |
|---|---|---|---|
| ***IGFBP5*** | Insulin like growth factor binding protein 5 | 4.36E-09 | 4.33E-05 |
| ***COL22A1*** | Collagen type XXII alpha 1 chain | 8.3E-09 | 5.52E-05 |
| ***NT5DC3*** | 5'-nucleotidase domain containing 3 | 3.24E-07 | 0.0010 |
| ***CYP24A1*** | Cytochrome P450 family 24 subfamily A member 1 | 6.67E-07 | 0.0016 |
| ***COL16A1*** | Collagen type XVI alpha 1 chain | 7.95E-07 | 0.0017 |
| ***SULT1C2*** | Sulfotransferase family 1C member 2 | 2.41E-06 | 0.0036 |
| ***KCNE4*** | potassium voltage-gated channel subfamily E regulatory subunit 4 | 2.23E-06 | 0.0036 |
| ***CEBPD*** | CCAAT enhancer binding protein delta | 2.76E-06 | 0.0039 |
| ***FAM222A*** | Family with sequence similarity 222 member A | 7.47E-06 | 0.0078 |
| ***DLL3*** | Delta like canonical Notch ligand 3 | 8.92E-06 | 0.0078 |
| ***TANGO2*** | Transport and golgi organization 2 homolog | 7.37E-06 | 0.0078 |
| ***ZFYVE28*** | Zinc finger FYVE-type containing 28 | 1.09E-05 | 0.0083 |
| ***NCCRP1*** | NCCRP1, F-box associated domain containing | 1.41E-05 | 0.0104 |
| ***CTSL*** | Cathepsin L | 1.64E-05 | 0.0105 |
| ***EPHX1*** | Epoxide hydrolase 1 | 1.64E-05 | 0.0105 |
| ***SLC7A5*** | Solute carrier family 7 member 5 | 1.59E-05 | 0.0105 |
| ***SLC5A10*** | Solute carrier family 5 member 10 | 2.48E-05 | 0.0141 |
| ***SLCO4A1*** | Solute carrier organic anion transporter family member 4A1 | 2.72E-05 | 0.0150 |
| ***KLHDC8B*** | Kelch domain containing 8B | 3.18E-05 | 0.0166 |
| ***VDR*** | Vitamin D receptor | 3.78E-05 | 0.0181 |
| ***CITED1*** | Cbp/p300 interacting transactivator with Glu/Asp rich carboxy-terminal domain 1 | 3.69E-05 | 0.0181 |
| ***PADI2*** | Peptidyl arginine deiminase 2 | 5.97E-05 | 0.0252 |
| ***SORBS3*** | Sorbin and SH3 domain containing 3 | 7.39E-05 | 0.0287 |
| ***TPRN*** | Taperin | 7.95E-05 | 0.0297 |
| ***IL1R1*** | Interleukin 1 receptor type 1 | 8.97E-05 | 0.0318 |
| ***TPST1*** | Tyrosylprotein sulfotransferase 1 | 0.0001 | 0.0407 |
| ***EFR3B*** | EFR3 homolog B | 0.0001 | 0.0412 |
| ***OSGIN1*** | Oxidative stress induced growth inhibitor 1 | 0.0001 | 0.0453 |
| ***TMEM51*** | Transmembrane protein 51 | 0.0001 | 0.0496 |

**Table S4.10. Downregulated genes (FDR < 0.05) in $1,25(OH)_2D_3$ treated samples vs. controls in DARK samples (excluding DP1 cell line).**

| Gene symbol | Gene name | p-value | FDR |
|---|---|---|---|
| ***F2R*** | Coagulation factor II thrombin receptor | 1.51E-09 | 3.00E-05 |
| ***SORBS2*** | Sorbin and SH3 domain containing 2 | 1.30E-08 | 6.44E-05 |
| ***MAP2*** | Microtubule associated protein 2 | 1.94E-08 | 7.71E-05 |
| ***THBS1*** | Thrombospondin 1 | 3.87E-07 | 0.0010 |
| ***SLC16A6*** | Solute carrier family 16 member 6 | 1.85E-06 | 0.0036 |
| ***LOX*** | Lysyl oxidase | 2.41E-06 | 0.0036 |
| ***TBL1XR1*** | TBL1X receptor 1 | 5.70E-06 | 0.0070 |
| ***NRCAM*** | Neuronal cell adhesion molecule | 5.55E-06 | 0.0070 |
| ***MARCKS*** | Myristoylated alanine rich protein kinase C substrate | 9.11E-06 | 0.0078 |
| ***GNG2*** | G protein subunit gamma 2 | 9.16E-06 | 0.0078 |
| ***KLF9*** | Kruppel like factor 9 | 9.53E-06 | 0.0078 |
| ***ALCAM*** | Activated leukocyte cell adhesion molecule | 8.71E-06 | 0.0078 |
| ***SPRED1*** | Sprouty related EVH1 domain containing 1 | 8.74E-06 | 0.0078 |
| ***DACT1*** | Dishevelled binding antagonist of beta catenin 1 | 1.03E-05 | 0.0081 |
| ***COL1A2*** | Collagen type I alpha 2 chain | 1.51E-05 | 0.0105 |
| ***GMFB*** | Glia maturation factor beta | 1.70E-05 | 0.0105 |
| ***MALAT1*** | Metastasis associated lung adenocarcinoma transcript 1 | 1.90E-05 | 0.0114 |
| ***SMIM15*** | Small integral membrane protein 15 | 2.24E-05 | 0.0130 |
| ***JPH1*** | Junctophilin 1 | 3.19E-05 | 0.0166 |
| ***EPHA3*** | EPH receptor A3 | 3.44E-05 | 0.0175 |
| ***ADAM23*** | ADAM metallopeptidase domain 23 | 3.85E-05 | 0.0181 |
| ***FHDC1*** | FH2 domain containing 1 | 4.35E-05 | 0.0200 |
| ***LRRC7*** | Leucine rich repeat containing 7 | 4.47E-05 | 0.0201 |
| ***TRIM2*** | Tripartite motif containing 2 | 5.35E-05 | 0.0235 |
| ***KAT2B*** | Lysine acetyltransferase 2B | 5.97E-05 | 0.0252 |
| ***GNG12*** | G protein subunit gamma 12 | 6.46E-05 | 0.0266 |
| ***MYEF2*** | Myelin expression factor 2 | 6.67E-05 | 0.0269 |
| ***SHC4*** | SHC adaptor protein 4p | 7.04E-05 | 0.0279 |
| ***TTLL7*** | Tubulin tyrosine ligase like 7 | 7.82E-05 | 0.0297 |
| ***ROCK2*** | Rho associated coiled-coil containing protein kinase 2 | 8.58E-05 | 0.0313 |
| ***AMMECR1*** | AMMECR nuclear protein 1 | 8.70E-05 | 0.0313 |
| ***PLSCR4*** | Phospholipid scramblase 4 | 0.0001 | 0.0351 |
| ***SRP9*** | Signal recognition particle 9 | 0.0001 | 0.0378 |
| ***FAM126A*** | Family with sequence similarity 126 member A | 0.0001 | 0.0378 |
| ***GAS2L3*** | Growth arrest specific 2 like 3 | 0.0001 | 0.0378 |
| ***PYGO1*** | Pygopus family PHD finger 1 | 0.0001 | 0.0405 |

| | | | |
|---|---|---|---|
| ***HDAC9*** | Histone deacetylase 9 | 0.0001 | 0.0405 |
| ***SCOC*** | Short coiled-coil protein | 0.0001 | 0.0412 |
| ***COL12A1*** | Collagen type XII alpha 1 chain | 0.0001 | 0.0412 |
| ***UBASH3B*** | Ubiquitin associated and SH3 domain containing B | 0.0001 | 0.0412 |
| ***STARD13*** | StAR related lipid transfer domain containing 13 | 0.0001 | 0.0446 |
| ***OLFML2A*** | Olfactomedin like 2A | 0.0001 | 0.0446 |
| ***TXNDC9*** | Thioredoxin domain containing 9 | 0.0001 | 0.0446 |
| ***RAB11FIP2*** | RAB11 family interacting protein 2 | 0.0001 | 0.0446 |
| ***CHL1*** | Cell adhesion molecule L1 like | 0.0001 | 0.0446 |
| ***DLC1*** | DLC1 Rho GTPase activating protein | 0.0001 | 0.0451 |
| ***TMEM65*** | Transmembrane protein 65 | 0.0001 | 0.0468 |
| ***EVI5*** | Ecotropic viral integration site 5 | 0.0001 | 0.0494 |
| ***DPY19L3*** | Dpy-19 like C-mannosyltransferase 3 | 0.0002 | 0.0496 |
| ***FEM1B*** | Fem-1 homolog B | 0.0001 | 0.0496 |
| ***FBXL17*** | F-box and leucine rich repeat protein 17 | 0.0002 | 0.0496 |
| ***MYOF*** | Myoferlin | 0.0002 | 0.0496 |

**Table S4.11. Upregulated genes (FDR < 0.05) in 1,25(OH)$_2$D$_3$ treated samples vs. controls in LIGHT samples (excluding LP1 cell line).**

| Gene symbol | Gene name | p-value | FDR |
|---|---|---|---|
| ***SH3BGRL*** | SH3 domain binding glutamate rich protein like | 1.99E-11 | 3.95E-07 |
| ***PPP1CB*** | Protein phosphatase 1 catalytic subunit beta | 6.53E-11 | 6.48E-07 |
| ***C21orf91*** | Chromosome 21 open reading frame 91 | 1.44E-10 | 9.56E-07 |
| ***LPAR6*** | Lysophosphatidic acid receptor 6 | 4.16E-10 | 1.78E-06 |
| ***SEMA3C*** | Semaphorin 3C | 4.50E-10 | 1.78E-06 |
| ***CLIC4*** | Chloride intracellular channel 4 | 6.97E-10 | 2.30E-06 |
| ***CASD1*** | CAS1 domain containing 1 | 1.70E-09 | 4.83E-06 |
| ***EID1*** | EP300 interacting inhibitor of differentiation 1 | 7.33E-09 | 1.38E-05 |
| ***NR1D2*** | Nuclear receptor subfamily 1 group D member 2 | 8.94E-09 | 1.38E-05 |
| ***SCAMP1*** | Secretory carrier membrane protein 1 | 9.09E-09 | 1.38E-05 |
| ***SESN3*** | Sestrin 3 | 7.70E-09 | 1.38E-05 |
| ***ZMAT3*** | Zinc finger matrin-type 3 | 6.40E-09 | 1.38E-05 |
| ***SLC2A13*** | Solute carrier family 2 member 13 | 1.48E-08 | 2.11E-05 |
| ***BMI1*** | BMI1 proto-oncogene, polycomb ring finger | 1.72E-08 | 2.28E-05 |
| ***TCEA1*** | Transcription elongation factor A1 | 3.05E-08 | 3.79E-05 |
| ***LRRC58*** | Leucine rich repeat containing 58 | 3.68E-08 | 4.06E-05 |

| | | | |
|---|---|---|---|
| ***TWF1*** | Twinfilin actin binding protein 1 | 3.64E-08 | 4.06E-05 |
| ***OSBPL8*** | Oxysterol binding protein like 8 | 4.18E-08 | 4.36E-05 |
| ***ARHGAP5*** | Rho GTPase activating protein 5 | 4.88E-08 | 4.84E-05 |
| ***MAT2B*** | Methionine adenosyltransferase 2B | 6.36E-08 | 5.49E-05 |
| ***MREG*** | Melanoregulin | 6.11E-08 | 5.49E-05 |
| ***OSTM1*** | Osteoclastogenesis associated transmembrane protein 1 | 6.12E-08 | 5.49E-05 |
| ***ARRDC3*** | Arrestin domain containing 3 | 7.06E-08 | 5.83E-05 |
| ***STX7*** | Syntaxin 7 | 7.58E-08 | 5.87E-05 |
| ***TMEM123*** | Transmembrane protein 123 | 7.69E-08 | 5.87E-05 |
| ***CCSAP*** | Centriole, cilia and spindle associated protein | 8.6E-08 | 6.37E-05 |
| ***SLC16A10*** | Solute carrier family 16 member 10 | 9.21E-08 | 6.52E-05 |
| ***WASL*** | WASP like actin nucleation promoting factor | 1.11E-07 | 7.60E-05 |
| ***FAM63B/ MINDY2*** | MINDY lysine 48 deubiquitinase 2 | 1.84E-07 | 0.0001 |
| ***TRIQK*** | Triple QxxK/R motif containing | 2.18E-07 | 0.0001 |
| ***RAB27A*** | RAB27A, member RAS oncogene family | 2.30E-07 | 0.0001 |
| ***C5orf24*** | Chromosome 5 open reading frame 24 | 2.55E-07 | 0.0001 |
| ***TROVE2/RO60*** | Ro60, Y RNA binding protein | 2.51E-07 | 0.0001 |
| ***ADAM10*** | ADAM metallopeptidase domain 10 | 2.74E-07 | 0.0001 |
| ***CMPK1*** | Cytidine/uridine monophosphate kinase 1 | 2.77E-07 | 0.0001 |
| ***ARPP19*** | cAMP regulated phosphoprotein 19 | 2.99E-07 | 0.0001 |
| ***PTEN*** | Phosphatase and tensin homolog | 3.28E-07 | 0.0001 |
| ***YTHDF3*** | YTH N6-methyladenosine RNA binding protein 3 | 5.11E-07 | 0.0002 |
| ***GOLT1B*** | Golgi transport 1B | 5.63E-07 | 0.0002 |
| ***PRKACB*** | Protein kinase cAMP-activated catalytic subunit beta | 5.94E-07 | 0.0002 |
| ***TMED5*** | Transmembrane p24 trafficking protein 5 | 5.83E-07 | 0.0002 |
| ***YWHAQ*** | Tyrosine 3-monooxygenase/tryptophan 5-monooxygenase activation protein theta | 5.78E-07 | 0.0002 |
| ***TCEAL8*** | Transcription elongation factor A like 8 | 6.32E-07 | 0.0002 |
| ***CDKN1B*** | Cyclin dependent kinase inhibitor 1B | 7.04E-07 | 0.0002 |
| ***RSL24D1*** | Ribosomal L24 domain containing 1 | 6.97E-07 | 0.0002 |
| ***NAA30*** | N-alpha-acetyltransferase 30, NatC catalytic subunit | 8.24E-07 | 0.0003 |
| ***BORCS7*** | BLOC-1 related complex subunit 7 | 8.43E-07 | 0.0003 |
| ***CPNE3*** | Copine 3 | 9.55E-07 | 0.0003 |
| ***HS2ST1*** | Heparan sulfate 2-O-sulfotransferase 1 | 9.62E-07 | 0.0003 |
| ***MTPN*** | Myotrophin | 1.03E-06 | 0.0003 |
| ***UBE2D1*** | Ubiquitin conjugating enzyme E2 D1 | 1.02E-06 | 0.0003 |
| ***EIF1AX*** | Eukaryotic translation initiation factor 1A X-linked | 1.14E-06 | 0.0004 |

| | | | |
|---|---|---|---|
| ***PCNP*** | PEST proteolytic signal containing nuclear protein | 1.11E-06 | 0.0004 |
| ***UBE2B*** | Ubiquitin conjugating enzyme E2 B | 1.15E-06 | 0.0004 |
| ***LINC01531*** | Long intergenic non-protein coding RNA 1531 | 1.29E-06 | 0.0004 |
| ***FAM199X*** | Family with sequence similarity 199, X-linked | 1.39E-06 | 0.0004 |
| ***CBFB*** | Core-binding factor subunit beta | 1.47E-06 | 0.0004 |
| ***RAB18*** | RAB18, member RAS oncogene family | 1.51E-06 | 0.0005 |
| ***PURB*** | Purine rich element binding protein B | 1.55E-06 | 0.0005 |
| ***UHMK1*** | U2AF homology motif kinase 1 | 1.61E-06 | 0.0005 |
| ***QKI*** | QKI, KH domain containing RNA binding | 1.77E-06 | 0.0005 |
| ***FOPNL / CEP20*** | FGFR1OP N-terminal like / centrosomal protein 20 | 1.86E-06 | 0.0005 |
| ***RASSF8*** | Ras association domain family member 8 | 1.90E-06 | 0.0005 |
| ***REEP3*** | Receptor accessory protein 3 | 2.03E-06 | 0.0006 |
| ***ETNK1*** | Ethanolamine kinase 1 | 2.17E-06 | 0.0006 |
| ***CCNG1*** | Cyclin G1 | 2.32E-06 | 0.0006 |
| ***COPS2*** | COP9 signalosome subunit 2 | 2.28E-06 | 0.0006 |
| ***RAP2A*** | RAP2A, member of RAS oncogene family | 2.30E-06 | 0.0006 |
| ***NDUFA5*** | NADH:ubiquinone oxidoreductase subunit A5 | 2.44E-06 | 0.0006 |
| ***PPP4R2*** | Protein phosphatase 4 regulatory subunit 2 | 2.54E-06 | 0.0007 |
| ***RBM7*** | RNA binding motif protein 7 | 2.84E-06 | 0.0007 |
| ***SEC62*** | SEC62 homolog, preprotein translocation factor | 3.18E-06 | 0.0008 |
| ***HPGD*** | 15-hydroxyprostaglandin dehydrogenase | 3.44E-06 | 0.0008 |
| ***DMXL1*** | Dmx like 1 | 3.55E-06 | 0.0008 |
| ***UBE2E1*** | Ubiquitin conjugating enzyme E2 E1 | 3.55E-06 | 0.0008 |
| ***C3orf58 / DIPK2A*** | divergent protein kinase domain 2A | 3.86E-06 | 0.0009 |
| ***MOB1B*** | MOB kinase activator 1B | 3.83E-06 | 0.0009 |
| ***RHOQ*** | Ras homolog family member Q | 3.77E-06 | 0.0009 |
| ***SLC6A15*** | Solute carrier family 6 member 15 | 3.83E-06 | 0.0009 |
| ***SIAH1*** | Siah E3 ubiquitin protein ligase 1 | 4.21E-06 | 0.0009 |
| ***GOPC*** | Golgi associated PDZ and coiled-coil motif containing | 4.35E-06 | 0.0010 |
| ***ARL5A*** | ADP ribosylation factor like GTPase 5A | 4.63E-06 | 0.0010 |
| ***POLR2M*** | RNA polymerase II subunit M | 4.75E-06 | 0.0010 |
| ***YOD1*** | YOD1 deubiquitinase | 4.79E-06 | 0.0010 |
| ***AP3S1*** | Adaptor related protein complex 3 subunit sigma 1 | 5.03E-06 | 0.0011 |
| ***TNPO1*** | Transportin 1 | 5.24E-06 | 0.0011 |
| ***UBL3*** | Ubiquitin like 3 | 5.27E-06 | 0.0011 |

| | | | |
|---|---|---|---|
| ***MMGT1*** | Membrane magnesium transporter 1 | 5.38E-06 | 0.0011 |
| ***PRELID3B*** | PRELI domain containing 3B | 5.46E-06 | 0.0011 |
| ***TMX3*** | Thioredoxin related transmembrane protein 3 | 5.45E-06 | 0.0011 |
| ***BMPR2*** | Bone morphogenetic protein receptor type 2 | 5.84E-06 | 0.0012 |
| ***NAA50*** | N-alpha-acetyltransferase 50, NatE catalytic subunit | 6.08E-06 | 0.0012 |
| ***SMNDC1*** | Survival motor neuron domain containing 1 | 6.04E-06 | 0.0012 |
| ***SPAST*** | Spastin | 6.13E-06 | 0.0012 |
| ***ZDHHC20*** | Zinc finger DHHC-type palmitoyltransferase 20 | 6.00E-06 | 0.0012 |
| ***ARL8B*** | ADP ribosylation factor like GTPase 8B | 6.75E-06 | 0.0013 |
| ***SOCS6*** | Suppressor of cytokine signaling 6 | 6.58E-06 | 0.0013 |
| ***SPOPL*** | Speckle type BTB/POZ protein like | 6.68E-06 | 0.0013 |
| ***VMA21*** | Vacuolar ATPase assembly factor VMA21 | 6.71E-06 | 0.0013 |
| ***GNA13*** | G protein subunit alpha 13 | 6.92E-06 | 0.0013 |
| ***SYPL1*** | Synaptophysin like 1 | 7.10E-06 | 0.0013 |
| ***NAMPT*** | Nicotinamide phosphoribosyltransferase | 7.17E-06 | 0.0013 |
| ***CNIH1*** | Cornichon family AMPA receptor auxiliary protein 1 | 7.58E-06 | 0.0014 |
| ***PELI2*** | Pellino E3 ubiquitin protein ligase family member 2 | 8.00E-06 | 0.0014 |
| ***BROX*** | BRO1 domain and CAAX motif containing | 8.76E-06 | 0.0015 |
| ***PPP1R2*** | Protein phosphatase 1 regulatory inhibitor subunit 2 | 8.92E-06 | 0.00160 |
| ***AMD1*** | Adenosylmethionine decarboxylase 1 | 9.49E-06 | 0.00160 |
| ***CFAP97*** | Cilia and flagella associated protein 97 | 9.62E-06 | 0.00160 |
| ***LYRM7*** | LYR motif containing 7 | 9.70E-06 | 0.00160 |
| ***LMBRD1*** | LMBR1 domain containing 1 | 9.85E-06 | 0.00160 |
| ***GPRIN3*** | GPRIN family member 3 | 1.00E-05 | 0.0017 |
| ***FAM8A1*** | Family with sequence similarity 8 member A1 | 1.01E-05 | 0.0017 |
| ***SSPN*** | Sarcospan | 1.05E-05 | 0.0017 |
| ***UBE2W*** | Ubiquitin conjugating enzyme E2 W | 1.09E-05 | 0.0018 |
| ***RICTOR*** | RPTOR independent companion of MTOR complex 2 | 1.11E-05 | 0.0018 |
| ***ATE1*** | Arginyltransferase 1 | 1.19E-05 | 0.0019 |
| ***FGFR1OP2*** | FGFR1 oncogene partner 2 | 1.21E-05 | 0.0019 |
| ***RPRD1A*** | Regulation of nuclear pre-mRNA domain containing 1A | 1.29E-05 | 0.0020 |
| ***RP11-63E9.1*** | | 1.31E-05 | 0.0020 |
| ***CPEB2*** | Cytoplasmic polyadenylation element binding protein 2 | 1.36E-05 | 0.0021 |
| ***NEK7*** | NIMA related kinase 7 | 1.36E-05 | 0.0021 |
| ***STAG2*** | Stromal antigen 2 | 1.37E-05 | 0.0021 |

| | | | |
|---|---|---|---|
| ***ARL1*** | ADP ribosylation factor like GTPase 1 | 1.44E-05 | 0.0021 |
| ***CD2AP*** | CD2 associated protein | 1.42E-05 | 0.0021 |
| ***FBXO28*** | F-box protein 28 | 1.45E-05 | 0.0021 |
| ***MDFIC*** | MyoD family inhibitor domain containing | 1.44E-05 | 0.0021 |
| ***MOB4*** | MOB family member 4, phocein | 1.45E-05 | 0.0021 |
| ***PRPS2*** | Phosphoribosyl pyrophosphate synthetase 2 | 1.44E-05 | 0.0021 |
| ***HSD17B12*** | Hydroxysteroid 17-beta dehydrogenase 12 | 1.48E-05 | 0.0021 |
| ***NADK2*** | NAD kinase 2, mitochondrial | 1.47E-05 | 0.0021 |
| ***CDC73*** | Cell division cycle 73 | 1.51E-05 | 0.0021 |
| ***EDNRB*** | Endothelin receptor type B | 1.54E-05 | 0.0022 |
| ***ESRP1*** | Epithelial splicing regulatory protein 1 | 1.59E-05 | 0.0022 |
| ***CNOT7*** | CCR4-NOT transcription complex subunit 7 | 1.70E-05 | 0.0024 |
| ***RB1*** | RB transcriptional corepressor 1 | 1.80E-05 | 0.0025 |
| ***PCMTD2*** | Protein-L-isoaspartate (D-aspartate) O-methyltransferase domain containing 2 | 1.86E-05 | 0.0026 |
| ***HIPK3*** | Homeodomain interacting protein kinase 3 | 1.89E-05 | 0.0026 |
| ***KCNJ13*** | Potassium inwardly rectifying channel subfamily J member 13 | 1.90E-05 | 0.0026 |
| ***RAB8B*** | RAB8B, member RAS oncogene family | 1.91E-05 | 0.0026 |
| ***VPS26A*** | VPS26, retromer complex component A | 2.04E-05 | 0.0027 |
| ***RAP1A*** | RAP1A, member of RAS oncogene family | 2.08E-05 | 0.0028 |
| ***JAZF1*** | JAZF zinc finger 1 | 2.16E-05 | 0.0028 |
| ***SERF1B*** | Small EDRK-rich factor 1B | 2.24E-05 | 0.0029 |
| ***VAMP7*** | Vesicle associated membrane protein 7 | 2.23E-05 | 0.0029 |
| ***ARL6IP1*** | ADP ribosylation factor like GTPase 6 interacting protein 1 | 2.26E-05 | 0.0029 |
| ***CHPT1*** | Choline phosphotransferase 1 | 2.31E-05 | 0.0030 |
| ***ITGB8*** | Integrin subunit beta 8 | 2.33E-05 | 0.0030 |
| ***HNMT*** | Histamine N-methyltransferase | 2.41E-05 | 0.0030 |
| ***KIF5B*** | Kinesin family member 5B | 2.44E-05 | 0.0030 |
| ***PI4K2B*** | Phosphatidylinositol 4-kinase type 2 beta | 2.47E-05 | 0.0030 |
| ***PPM1K*** | Protein phosphatase, Mg2+/Mn2+ dependent 1K | 2.42E-05 | 0.0030 |
| ***SDHD*** | Succinate dehydrogenase complex subunit D | 2.46E-05 | 0.0030 |
| ***TIA1*** | TIA1 cytotoxic granule associated RNA binding protein | 2.43E-05 | 0.0030 |
| ***BLOC1S6*** | Biogenesis of lysosomal organelles complex 1 subunit 6 | 2.53E-05 | 0.0031 |
| ***GTF2A1*** | General transcription factor IIA subunit 1 | 2.56E-05 | 0.0031 |
| ***USP12*** | Ubiquitin specific peptidase 12 | 2.63E-05 | 0.0032 |
| ***CEBPZOS*** | CEBPZ opposite strand | 2.68E-05 | 0.0032 |

| | | | |
|---|---|---|---|
| ***OXR1*** | Oxidation resistance 1 | 2.69E-05 | 0.0032 |
| ***RAB1A*** | RAB1A, member RAS oncogene family | 2.66E-05 | 0.0032 |
| ***HINT3*** | Histidine triad nucleotide binding protein 3 | 2.7E-05 | 0.0032 |
| ***BCAP29*** | B cell receptor associated protein 29 | 2.82E-05 | 0.0032 |
| ***LMAN1*** | Lectin, mannose binding 1 | 2.82E-05 | 0.0032 |
| ***NUDT4*** | Nudix hydrolase 4 | 2.79E-05 | 0.0032 |
| ***PCMTD1*** | Protein-L-isoaspartate (D-aspartate) O-methyltransferase domain containing 1 | 2.80E-05 | 0.0032 |
| ***ALG10B*** | ALG10 alpha-1,2-glucosyltransferase B | 3.02E-05 | 0.0034 |
| ***RBM27*** | RNA binding motif protein 27 | 3.00E-05 | 0.0034 |
| ***SOCS4*** | Suppressor of cytokine signaling 4 | 3.02E-05 | 0.0034 |
| ***ACTR2*** | Actin related protein 2 | 3.21E-05 | 0.0036 |
| ***CLIP4*** | CAP-Gly domain containing linker protein family member 4 | 3.26E-05 | 0.0036 |
| ***NUCKS1*** | Nuclear casein kinase and cyclin dependent kinase substrate 1 | 3.25E-05 | 0.0036 |
| ***ATAD1*** | ATPase family AAA domain containing 1 | 3.37E-05 | 0.0037 |
| ***BEX4*** | Brain expressed X-linked 4 | 3.38E-05 | 0.0037 |
| ***HOOK3*** | Hook microtubule tethering protein 3 | 3.55E-05 | 0.0038 |
| ***UBE2D3*** | Ubiquitin conjugating enzyme E2 D3 | 3.63E-05 | 0.0039 |
| ***RAP2C*** | RAP2C, member of RAS oncogene family | 3.94E-05 | 0.0041 |
| ***STXBP3*** | Syntaxin binding protein 3 | 4.07E-05 | 0.0042 |
| ***RAB30*** | RAB30, member RAS oncogene family | 4.13E-05 | 0.0042 |
| ***SYT14*** | Synaptotagmin 14 | 4.30E-05 | 0.0044 |
| ***SPCS3*** | Signal peptidase complex subunit 3 | 4.33E-05 | 0.0044 |
| ***DSTN*** | Destrin, actin depolymerizing factor | 4.43E-05 | 0.0045 |
| ***PSIP1*** | PC4 and SFRS1 interacting protein 1 | 4.44E-05 | 0.0045 |
| ***SMAD5*** | SMAD family member 5 | 4.40E-05 | 0.0045 |
| ***MAD2L1*** | Mitotic arrest deficient 2 like 1 | 4.55E-05 | 0.0045 |
| ***CRNDE*** | Colorectal neoplasia differentially expressed | 4.64E-05 | 0.0046 |
| ***WDFY1*** | WD repeat and FYVE domain containing 1 | 4.62E-05 | 0.0046 |
| ***ZNF644*** | Zinc finger protein 644 | 4.61E-05 | 0.0046 |
| ***SLC39A6*** | Solute carrier family 39 member 6 | 4.67E-05 | 0.0046 |
| ***APPL1*** | Adaptor protein, phosphotyrosine interacting with PH domain and leucine zipper 1 | 4.71E-05 | 0.0046 |
| ***LIMS1*** | LIM zinc finger domain containing 1 | 4.82E-05 | 0.0047 |
| ***ANP32E*** | Acidic nuclear phosphoprotein 32 family member E | 4.86E-05 | 0.0047 |
| ***DR1*** | Down-regulator of transcription 1 | 4.96E-05 | 0.0048 |
| ***MDM2*** | MDM2 proto-oncogene | 5.17E-05 | 0.0049 |
| ***HIST1H2AC*** | Histone cluster 1 H2A family member c | 5.36E-05 | 0.0050 |

| | | | |
|---|---|---|---|
| ***ZDHHC17*** | Zinc finger DHHC-type palmitoyltransferase 17 | 5.36E-05 | 0.0050 |
| ***CLDND1*** | Claudin domain containing 1 | 5.52E-05 | 0.0052 |
| ***C2orf69*** | Chromosome 2 open reading frame 69 | 5.69E-05 | 0.0053 |
| ***RRM2B*** | Ribonucleotide reductase regulatory TP53 inducible subunit M2B | 5.76E-05 | 0.0053 |
| ***C5orf15*** | Chromosome 5 open reading frame 15 | 5.87E-05 | 0.0054 |
| ***PJA2*** | Praja ring finger ubiquitin ligase 2 | 5.90E-05 | 0.0054 |
| ***ATG12*** | Autophagy related 12 | 6.05E-05 | 0.0055 |
| ***DCUN1D4*** | Defective in cullin neddylation 1 domain containing 4 | 6.02E-05 | 0.0055 |
| ***MBNL1*** | Muscleblind like splicing regulator 1 | 6.28E-05 | 0.0057 |
| ***MIER1*** | MIER1 transcriptional regulator | 6.29E-05 | 0.0057 |
| ***ZFYVE16*** | Zinc finger FYVE-type containing 16 | 6.27E-05 | 0.0057 |
| ***GALNT1*** | Polypeptide N-acetylgalactosaminyltransferase 1 | 6.40E-05 | 0.0057 |
| ***HECA*** | Hdc homolog, cell cycle regulator | 6.49E-05 | 0.0058 |
| ***PTBP3*** | Polypyrimidine tract binding protein 3 | 6.48E-05 | 0.0058 |
| ***TLK1*** | Tousled like kinase 1 | 6.54E-05 | 0.0058 |
| ***VPS4B*** | Vacuolar protein sorting 4 homolog B | 6.70E-05 | 0.0059 |
| ***DCBLD2*** | Discoidin, CUB and LCCL domain containing 2 | 6.77E-05 | 0.0059 |
| ***LYSMD3*** | LysM domain containing 3 | 7.27E-05 | 0.0063 |
| ***RAB10*** | RAB10, member RAS oncogene family | 7.27E-05 | 0.0063 |
| ***SEL1L*** | SEL1L adaptor subunit of ERAD E3 ubiquitin ligase | 7.36E-05 | 0.0063 |
| ***SVIP*** | Small VCP interacting protein | 7.33E-05 | 0.0063 |
| ***PGRMC2*** | Progesterone receptor membrane component 2 | 7.51E-05 | 0.0064 |
| ***DYNLT3*** | Dynein light chain Tctex-type 3 | 7.75E-05 | 0.0065 |
| ***NDUFB5*** | NADH:ubiquinone oxidoreductase subunit B5 | 7.69E-05 | 0.0065 |
| ***ST6GALNAC3*** | ST6 N-acetylgalactosaminide alpha-2,6-sialyltransferase 3 | 7.71E-05 | 0.0065 |
| ***SUB1*** | SUB1 regulator of transcription | 7.74E-05 | 0.0065 |
| ***FAM92A1 / CIBAR1*** | CBY1 interacting BAR domain containing 1 | 7.82E-05 | 0.0065 |
| ***SSR3*** | Signal sequence receptor subunit 3 | 7.89E-05 | 0.0066 |
| ***DCP2*** | Decapping mRNA 2 | 8.00E-05 | 0.0066 |
| ***RAB21*** | RAB21, member RAS oncogene family | 7.98E-05 | 0.0066 |
| ***SLC19A2*** | Solute carrier family 19 member 2 | 7.94E-05 | 0.0066 |
| ***PPP1CC*** | Protein phosphatase 1 catalytic subunit gamma | 8.07E-05 | 0.0066 |
| ***PTP4A1*** | Protein tyrosine phosphatase 4A1 | 8.25E-05 | 0.0067 |
| ***MIB1*** | Mindbomb E3 ubiquitin protein ligase 1 | 8.46E-05 | 0.0068 |
| ***NRAS*** | NRAS proto-oncogene, GTPase | 8.36E-05 | 0.0068 |

| | | | |
|---|---|---|---|
| ***SP3*** | Sp3 transcription factor | 8.40E-05 | 0.0068 |
| ***PSMD10*** | Proteasome 26S subunit, non-ATPase 10 | 8.69E-05 | 0.0068 |
| ***RBM43*** | RNA binding motif protein 43 | 8.6E-05 | 0.0068 |
| ***KPNA5*** | Karyopherin subunit alpha 5 | 9.04E-05 | 0.0071 |
| ***NT5C3A*** | 5'-nucleotidase, cytosolic IIIA | 9.09E-05 | 0.0071 |
| ***NDFIP2*** | Nedd4 family interacting protein 2 | 9.17E-05 | 0.0071 |
| ***HACD1*** | 3-hydroxyacyl-CoA dehydratase 1 | 9.35E-05 | 0.0072 |
| ***ZBTB33*** | Zinc finger and BTB domain containing 33 | 9.38E-05 | 0.0072 |
| ***PGM2L1*** | Phosphoglucomutase 2 like 1 | 9.46E-05 | 0.0072 |
| ***ARPC5*** | Actin related protein 2/3 complex subunit 5 | 9.69E-05 | 0.0074 |
| ***C7orf60*** | Chromosome 7 open reading frame 60 | 9.69E-05 | 0.0074 |
| ***GNAQ*** | G protein subunit alpha q | 9.74E-05 | 0.0074 |
| ***CAV2*** | Caveolin 2 | 9.93E-05 | 0.0075 |
| ***NT5DC3*** | 5'-nucleotidase domain containing 3 | 0.0001 | 0.0076 |
| ***MATR3*** | Matrin 3 | 0.0001 | 0.0079 |
| ***FEM1B*** | Fem-1 homolog B | 0.0001 | 0.0081 |
| ***SMIM14*** | Small integral membrane protein 14 | 0.0001 | 0.0082 |
| ***SOAT1*** | Sterol O-acyltransferase 1 | 0.0001 | 0.0083 |
| ***CCDC126*** | Coiled-coil domain containing 126 | 0.0001 | 0.0084 |
| ***ATP6AP2*** | ATPase H+ transporting accessory protein 2 | 0.0001 | 0.0086 |
| ***TFAM*** | Transcription factor A, mitochondrial | 0.0001 | 0.0086 |
| ***ZYG11B*** | Zyg-11 family member B, cell cycle regulator | 0.0001 | 0.0086 |
| ***ALG6*** | ALG6 alpha-1,3-glucosyltransferase | 0.0001 | 0.0086 |
| ***MOSPD1*** | Motile sperm domain containing 1 | 0.0001 | 0.0086 |
| ***DPP4*** | Dipeptidyl peptidase 4 | 0.0001 | 0.0087 |
| ***RSRP1*** | Arginine and serine rich protein 1 | 0.0001 | 0.0087 |
| ***ATP6V1A*** | ATPase H+ transporting V1 subunit A | 0.0001 | 0.0088 |
| ***ELK4*** | ETS transcription factor ELK4 | 0.0001 | 0.0088 |
| ***MBOAT2*** | Membrane bound O-acyltransferase domain containing 2 | 0.0001 | 0.0088 |
| ***PUM2*** | Pumilio RNA binding family member 2 | 0.0001 | 0.0088 |
| ***SNX3*** | Sorting nexin 3 | 0.0001 | 0.0088 |
| ***TMED10*** | Transmembrane p24 trafficking protein 10 | 0.0001 | 0.0088 |
| ***ZBTB10*** | Zinc finger and BTB domain containing 10 | 0.0001 | 0.0088 |
| ***FOXN2*** | Forkhead box N2 | 0.0001 | 0.0088 |
| ***SNX18*** | Sorting nexin 18 | 0.0001 | 0.0089 |
| ***FAM172A*** | Family with sequence similarity 172 member A | 0.0001 | 0.0089 |
| ***RHOBTB3*** | Rho related BTB domain containing 3 | 0.0001 | 0.0089 |
| ***SLC16A7*** | Solute carrier family 16 member 7 | 0.0001 | 0.0089 |

| | | | |
|---|---|---|---|
| ***TM9SF3*** | Transmembrane 9 superfamily member 3 | 0.0001 | 0.0089 |
| ***VCPIP1*** | Valosin containing protein interacting protein 1 | 0.0001 | 0.0090 |
| ***ZNF22*** | Zinc finger protein 22 | 0.0001 | 0.0091 |
| ***TMEM65*** | Transmembrane protein 65 | 0.0001 | 0.0093 |
| ***MZT1*** | Mitotic spindle organizing protein 1 | 0.0001 | 0.0093 |
| ***SLC5A3*** | Solute carrier family 5 member 3 | 0.0001 | 0.0094 |
| ***MOB1A*** | MOB kinase activator 1A | 0.0001 | 0.0096 |
| ***CTDSPL2*** | CTD small phosphatase like 2 | 0.0001 | 0.0097 |
| ***C3orf38*** | Chromosome 3 open reading frame 38 | 0.0001 | 0.0097 |
| ***PCGF5*** | Polycomb group ring finger 5 | 0.0001 | 0.0097 |
| ***RBPJ*** | Recombination signal binding protein for immunoglobulin kappa J region | 0.0001 | 0.0097 |
| ***TMEM126B*** | Transmembrane protein 126B | 0.0001 | 0.0098 |
| ***ABCD3*** | ATP binding cassette subfamily D member 3 | 0.0001 | 0.0100 |
| ***MMD*** | Monocyte to macrophage differentiation associated | 0.0001 | 0.0101 |
| ***DPY19L4*** | Dpy-19 like 4 | 0.0001 | 0.0101 |
| ***NMD3*** | NMD3 ribosome export adaptor | 0.0001 | 0.0101 |
| ***CISD2*** | CDGSH iron sulfur domain 2 | 0.0001 | 0.0102 |
| ***IPMK*** | Inositol polyphosphate multikinase | 0.0001 | 0.0102 |
| ***CPEB4*** | Cytoplasmic polyadenylation element binding protein 4 | 0.0001 | 0.0104 |
| ***KPNA4*** | Karyopherin subunit alpha 4 | 0.0001 | 0.0105 |
| ***SLC38A2*** | Solute carrier family 38 member 2 | 0.0001 | 0.0105 |
| ***SMCHD1*** | Structural maintenance of chromosomes flexible hinge domain containing 1 | 0.0001 | 0.0106 |
| ***BET1*** | Bet1 golgi vesicular membrane trafficking protein | 0.0001 | 0.0109 |
| ***TAPT1*** | Transmembrane anterior posterior transformation 1 | 0.0001 | 0.0109 |
| ***ZNF24*** | Zinc finger protein 24 | 0.0001 | 0.0109 |
| ***ATF2*** | Activating transcription factor 2 | 0.0001 | 0.0111 |
| ***FMR1*** | FMRP translational regulator 1 | 0.0001 | 0.0111 |
| ***KPNA3*** | Karyopherin subunit alpha 3 | 0.0001 | 0.0111 |
| ***PBRM1*** | Polybromo 1 | 0.0001 | 0.0111 |
| ***UBE2V2*** | Ubiquitin conjugating enzyme E2 V2 | 0.0001 | 0.0111 |
| ***PMS1*** | PMS1 homolog 1, mismatch repair system component | 0.0001 | 0.0111 |
| ***TWSG1*** | Twisted gastrulation BMP signaling modulator 1 | 0.0001 | 0. 0111 |
| ***UBE2J1*** | Ubiquitin conjugating enzyme E2 J1 | 0.0001 | 0.0113 |
| ***RFTN2*** | Raftlin family member 2 | 0.0001 | 0.0114 |
| ***HMGB1*** | High mobility group box 1 | 0.0001 | 0.0115 |

| | | | |
|---|---|---|---|
| ***ACAP2*** | ArfGAP with coiled-coil, ankyrin repeat and PH domains 2 | 0.0001 | 0.0119 |
| ***NCKAP1*** | NCK associated protein 1 | 0.0001 | 0.0119 |
| ***TVP23B*** | Trans-golgi network vesicle protein 23 homolog B | 0.0001 | 0.0119 |
| ***CYCS*** | Cytochrome c, somatic | 0.0002 | 0.0121 |
| ***ARMC1*** | Armadillo repeat containing 1 | 0.0002 | 0.0122 |
| ***SOCS5*** | Suppressor of cytokine signaling 5 | 0.0002 | 0.0123 |
| ***MBNL3*** | Muscleblind like splicing regulator 3 | 0.0002 | 0.0124 |
| ***TMEM41B*** | Transmembrane protein 41B | 0.0002 | 0.0126 |
| ***IGIP*** | IgA inducing protein | 0.0002 | 0.0126 |
| ***BTF3L4*** | Basic transcription factor 3 like 4 | 0.0002 | 0.0128 |
| ***ELMOD2*** | ELMO domain containing 2 | 0.0002 | 0.0128 |
| ***EPS15*** | Epidermal growth factor receptor pathway substrate 15 | 0.0002 | 0.0129 |
| ***RFK*** | Riboflavin kinase | 0.0002 | 0.0130 |
| ***UBE2K*** | Ubiquitin conjugating enzyme E2 K | 0.0002 | 0.0131 |
| ***MAN1A2*** | Mannosidase alpha class 1A member 2 | 0.0002 | 0.0132 |
| ***GLS*** | Glutaminase | 0.0002 | 0.0135 |
| ***TMEM33*** | Transmembrane protein 33 | 0.0002 | 0.0136 |
| ***PKD2*** | Polycystin 2, transient receptor potential cation channel | 0.0002 | 0.0136 |
| ***SLC35A3*** | Solute carrier family 35 member A3 | 0.0002 | 0.0136 |
| ***ATP6V1C1*** | ATPase H+ transporting V1 subunit C1 | 0.0002 | 0.0137 |
| ***LIN7C*** | Lin-7 homolog C, crumbs cell polarity complex component | 0.0002 | 0.0137 |
| ***FAM91A1*** | Family with sequence similarity 91 member A1 | 0.0002 | 0.0139 |
| ***PRKAR1A*** | Protein kinase cAMP-dependent type I regulatory subunit alpha | 0.0002 | 0.0140 |
| ***UACA*** | Uveal autoantigen with coiled-coil domains and ankyrin repeats | 0.0002 | 0.0140 |
| ***API5*** | Apoptosis inhibitor 5 | 0.0002 | 0.0140 |
| ***SERINC1*** | Serine incorporator 1 | 0.0002 | 0.0140 |
| ***YES1*** | YES proto-oncogene 1, Src family tyrosine kinase | 0.0002 | 0.0140 |
| ***TMED2*** | Transmembrane p24 trafficking protein 2 | 0.0002 | 0.0143 |
| ***LEPROTL1*** | Leptin receptor overlapping transcript like 1 | 0.0002 | 0.0145 |
| ***UBA2*** | Ubiquitin like modifier activating enzyme 2 | 0.0002 | 0.0145 |
| ***MSI2*** | Musashi RNA binding protein 2 | 0.0002 | 0.0145 |
| ***LINC00998 / SMIM30*** | Small integral membrane protein 30 | 0.0002 | 0.0146 |
| ***STRN*** | Striatin | 0.0002 | 0.0146 |
| ***ZHX1*** | Zinc fingers and homeoboxes 1 | 0.0002 | 0.0146 |
| ***CHURC1*** | Churchill domain containing 1 | 0.0002 | 0.0148 |

| | | | |
|---|---|---|---|
| ***TMX1*** | Thioredoxin related transmembrane protein 1 | 0.0002 | 0.0150 |
| ***DIMT1*** | DIMT1 rRNA methyltransferase and ribosome maturation factor | 0.0002 | 0.0150 |
| ***STYX*** | Serine/threonine/tyrosine interacting protein | 0.0002 | 0.0152 |
| ***DEK*** | DEK proto-oncogene | 0.0002 | 0.0153 |
| ***LCORL*** | Ligand dependent nuclear receptor corepressor like | 0.0002 | 0.0153 |
| ***FAM200B*** | Family with sequence similarity 200 member B | 0.0002 | 0.0154 |
| ***MTMR6*** | Myotubularin related protein 6 | 0.0002 | 0.0154 |
| ***UBXN4*** | UBX domain protein 4 | 0.0002 | 0.0154 |
| ***PPP4R3B*** | Protein phosphatase 4 regulatory subunit 3B | 0.0002 | 0.0155 |
| ***GABPA*** | GA binding protein transcription factor subunit alpha | 0.0003 | 0.0156 |
| ***RAB14*** | RAB14, member RAS oncogene family | 0.0003 | 0.0157 |
| ***ITM2B*** | Integral membrane protein 2B | 0.0003 | 0.0157 |
| ***ATP8A1*** | ATPase phospholipid transporting 8A1 | 0.0003 | 0.0158 |
| ***SGPP1*** | Sphingosine-1-phosphate phosphatase 1 | 0.0003 | 0.0158 |
| ***EFR3A*** | EFR3 homolog A | 0.0003 | 0.0160 |
| ***PHLDA1*** | Pleckstrin homology like domain family A member 1 | 0.0003 | 0.0160 |
| ***PLEKHF2*** | Pleckstrin homology and FYVE domain containing 2 | 0.0003 | 0.0162 |
| ***JMY*** | Junction mediating and regulatory protein, p53 cofactor | 0.0003 | 0.0164 |
| ***GNB4*** | G protein subunit beta 4 | 0.0003 | 0.0167 |
| ***HSD17B11*** | Hydroxysteroid 17-beta dehydrogenase 11 | 0.0003 | 0.0169 |
| ***AP1AR*** | Adaptor related protein complex 1 associated regulatory protein | 0.0003 | 0.0170 |
| ***CHIC1*** | Cysteine rich hydrophobic domain 1 | 0.0003 | 0.0172 |
| ***DLG1*** | Discs large MAGUK scaffold protein 1 | 0.0003 | 0.0173 |
| ***FAM126B*** | Family with sequence similarity 126 member B | 0.0003 | 0.0173 |
| ***FZD3*** | Frizzled class receptor 3 | 0.0003 | 0.0175 |
| ***TMTC3*** | Transmembrane O-mannosyltransferase targeting cadherins 3 | 0.0003 | 0.0175 |
| ***XIAP*** | X-linked inhibitor of apoptosis | 0.0003 | 0.0175 |
| ***LAMTOR3*** | Late endosomal/lysosomal adaptor, MAPK and MTOR activator 3 | 0.0003 | 0.0175 |
| ***PHF10*** | PHD finger protein 10 | 0.0003 | 0.0175 |
| ***RYBP*** | RING1 and YY1 binding protein | 0.0003 | 0.0175 |
| ***RALA*** | RAS like proto-oncogene A | 0.0003 | 0.0175 |
| ***ARF6*** | ADP ribosylation factor 6 | 0.0003 | 0.0176 |
| ***SLC35F5*** | Solute carrier family 35 member F5 | 0.0003 | 0.0177 |

| | | | |
|---|---|---|---|
| ***CUL4B*** | Cullin 4B | 0.0003 | 0.0177 |
| ***DUSP19*** | Dual specificity phosphatase 19 | 0.0003 | 0.0177 |
| ***SCYL2*** | SCY1 like pseudokinase 2 | 0.0003 | 0.0177 |
| ***GCC2*** | GRIP and coiled-coil domain containing 2 | 0.0003 | 0.0178 |
| ***LBR*** | Lamin B receptor | 0.0003 | 0.0178 |
| ***ZNF148*** | Zinc finger protein 148 | 0.0003 | 0.0180 |
| ***IMPAD1*** | Inositol monophosphatase domain containing 1 | 0.0003 | 0.0180 |
| ***CXorf57/ RADX*** | RPA1 related single stranded DNA binding protein, X-linked | 0.0003 | 0.0182 |
| ***B4GALT6*** | Beta-1,4-galactosyltransferase 6 | 0.0003 | 0.0183 |
| ***C1GALT1*** | Core 1 synthase, glycoprotein-N-acetylgalactosamine 3-beta-galactosyltransferase 1 | 0.0003 | 0.0183 |
| ***MAP4K5*** | Mitogen-activated protein kinase kinase kinase kinase 5 | 0.0003 | 0.0184 |
| ***SGTB*** | Small glutamine rich tetratricopeptide repeat containing beta | 0.0003 | 0.0184 |
| ***TSNAX*** | Translin associated factor X | 0.0003 | 0.0186 |
| ***FNIP2*** | Folliculin interacting protein 2 | 0.0003 | 0.0186 |
| ***PPP3R1*** | Protein phosphatase 3 regulatory subunit B, alpha | 0.0003 | 0.0186 |
| ***NXT2*** | Nuclear transport factor 2 like export factor 2 | 0.0004 | 0.0187 |
| ***CREBL2*** | cAMP responsive element binding protein like 2 | 0.0004 | 0.0189 |
| ***KIAA1033 / WASHC4*** | WASH complex subunit 4 | 0.0004 | 0.0189 |
| ***SLC39A10*** | Solute carrier family 39 member 10 | 0.0004 | 0.0189 |
| ***STT3B*** | STT3 oligosaccharyltransferase complex catalytic subunit B | 0.0004 | 0.0189 |
| ***RB1CC1*** | RB1 inducible coiled-coil 1 | 0.0004 | 0.0191 |
| ***C4orf3*** | Chromosome 4 open reading frame 3 | 0.0004 | 0.0192 |
| ***CACNA2D1*** | Calcium voltage-gated channel auxiliary subunit alpha2delta 1 | 0.0004 | 0.0192 |
| ***PGGT1B*** | Protein geranylgeranyltransferase type I subunit beta | 0.0004 | 0.0192 |
| ***NIPSNAP3A*** | Nipsnap homolog 3A | 0.0004 | 0.0194 |
| ***AFTPH*** | Aftiphilin | 0.0004 | 0.0195 |
| ***IPO7*** | Importin 7 | 0.0004 | 0.0196 |
| ***TOMM70A*** | Translocase of outer mitochondrial membrane 70A | 0.0004 | 0.0196 |
| ***SUGT1*** | SGT1 homolog, MIS12 kinetochore complex assembly cochaperone | 0.0004 | 0.0198 |
| ***TMEM64*** | Transmembrane protein 64 | 0.0004 | 0.0198 |
| ***BHLHE41*** | Basic helix-loop-helix family member e41 | 0.0004 | 0.0199 |
| ***FNBP1L*** | Formin binding protein 1 like | 0.0004 | 0.0199 |

| | | | |
|---|---|---|---|
| ***RNF13*** | Ring finger protein 13 | 0.0004 | 0.0199 |
| ***SHOC2*** | SHOC2 leucine rich repeat scaffold protein | 0.0004 | 0.0199 |
| ***UBE3A*** | Ubiquitin protein ligase E3A | 0.0004 | 0.0199 |
| ***ZDHHC2*** | Zinc finger DHHC-type palmitoyltransferase 2 | 0.0004 | 0.0200 |
| ***HIGD1A*** | HIG1 hypoxia inducible domain family member 1A | 0.0004 | 0.0202 |
| ***EXOC5*** | Exocyst complex component 5 | 0.0004 | 0.0204 |
| ***CREB1*** | cAMP responsive element binding protein 1 | 0.0004 | 0.0207 |
| ***DCUN1D1*** | Defective in cullin neddylation 1 domain containing 1 | 0.0004 | 0.0208 |
| ***STARD4*** | StAR related lipid transfer domain containing 4 | 0.0004 | 0.0210 |
| ***DNAJB9*** | DnaJ heat shock protein family (Hsp40) member B9 | 0.0004 | 0.0211 |
| ***ZBTB6*** | Zinc finger and BTB domain containing 6 | 0.0004 | 0.0211 |
| ***BTG1*** | BTG anti-proliferation factor 1 | 0.0004 | 0.0212 |
| ***ERGIC2*** | ERGIC and golgi 2 | 0.0004 | 0.0212 |
| ***C11orf58*** | Chromosome 11 open reading frame 58 | 0.0004 | 0.0214 |
| ***HAUS3*** | HAUS augmin like complex subunit 3 | 0.0005 | 0.0218 |
| ***TMEM50B*** | Transmembrane protein 50B | 0.0005 | 0.0224 |
| ***AZIN1*** | Antizyme inhibitor 1 | 0.0005 | 0.0225 |
| ***RCN2*** | Reticulocalbin 2 | 0.0005 | 0.0225 |
| ***CCDC6*** | Coiled-coil domain containing 6 | 0.0005 | 0.0225 |
| ***DCTN4*** | Dynactin subunit 4 | 0.0005 | 0.0227 |
| ***FSD1L*** | Fibronectin type III and SPRY domain containing 1 like | 0.0005 | 0.0229 |
| ***BTBD1*** | BTB domain containing 1 | 0.0005 | 0.0229 |
| ***LAMP2*** | Lysosomal associated membrane protein 2 | 0.0005 | 0.0229 |
| ***MAF*** | MAF bZIP transcription factor | 0.0005 | 0.0229 |
| ***TMEM167B*** | Transmembrane protein 167B | 0.0005 | 0.0231 |
| ***CAPZA1*** | Capping actin protein of muscle Z-line subunit alpha 1 | 0.0005 | 0.0231 |
| ***ELOVL5*** | ELOVL fatty acid elongase 5 | 0.0005 | 0.0231 |
| ***SOX4*** | SRY-box transcription factor 4 | 0.0005 | 0.0231 |
| ***ZNF277*** | Zinc finger protein 277 | 0.0005 | 0.0231 |
| ***TDRD3*** | Tudor domain containing 3 | 0.0005 | 0.0233 |
| ***NUDT21*** | Nudix hydrolase 21 | 0.0005 | 0.0239 |
| ***UBLCP1*** | Ubiquitin like domain containing CTD phosphatase 1 | 0.0005 | 0.0240 |
| ***ARMCX3*** | Armadillo repeat containing X-linked 3 | 0.0005 | 0.0240 |
| ***ARFIP1*** | ADP ribosylation factor interacting protein 1 | 0.0005 | 0.0242 |
| ***SMIM15*** | Small integral membrane protein 15 | 0.0005 | 0.0242 |
| ***STAM*** | Signal transducing adaptor molecule | 0.0005 | 0.0242 |

| | | | |
|---|---|---|---|
| ***SLC30A1*** | Solute carrier family 30 member 1 | 0.0005 | 0.0243 |
| ***KIF20B*** | Kinesin family member 20B | 0.0005 | 0.0243 |
| ***VAMP4*** | Vesicle associated membrane protein 4 | 0.0005 | 0.0243 |
| ***CAPZA2*** | Capping actin protein of muscle Z-line subunit alpha 2 | 0.0006 | 0.0244 |
| ***ACTR3*** | Actin related protein 3 | 0.0006 | 0.0245 |
| ***YIPF4*** | Yip1 domain family member 4 | 0.0006 | 0.0246 |
| ***CCDC110*** | Coiled-coil domain containing 110 | 0.0006 | 0.0248 |
| ***IL1R1*** | Interleukin 1 receptor type 1 | 0.0006 | 0.0249 |
| ***LNPEP*** | Leucyl and cystinyl aminopeptidase | 0.0006 | 0.0249 |
| ***MBLAC2*** | Metallo-beta-lactamase domain containing 2 | 0.0006 | 0.0249 |
| ***MED21*** | Mediator complex subunit 21 | 0.0006 | 0.0249 |
| ***EPHA5*** | EPH receptor A5 | 0.0006 | 0.0249 |
| ***GRPEL2*** | GrpE like 2, mitochondrial | 0.0006 | 0.0249 |
| ***ZBTB44*** | Zinc finger and BTB domain containing 44 | 0.0006 | 0.0249 |
| ***RASA2*** | RAS p21 protein activator 2 | 0.0006 | 0.0250 |
| ***ZFR*** | Zinc finger RNA binding protein | 0.0006 | 0.0250 |
| ***LYRM5 / ETFRF1*** | Electron transfer flavoprotein regulatory factor 1 | 0.0006 | 0.0250 |
| ***ATP11B*** | ATPase phospholipid transporting 11B | 0.0006 | 0.0252 |
| ***WDR43*** | WD repeat domain 43 | 0.0006 | 0.0253 |
| ***PIK3CB*** | Phosphatidylinositol-4,5-bisphosphate 3-kinase catalytic subunit beta | 0.0006 | 0.0254 |
| ***CELF2*** | CUGBP Elav-like family member 2 | 0.0006 | 0.0255 |
| ***LMBRD2*** | LMBR1 domain containing 2 | 0.0006 | 0.0256 |
| ***TMEM30A*** | Transmembrane protein 30A | 0.0006 | 0.0256 |
| ***MAGT1*** | Magnesium transporter 1 | 0.0006 | 0.0257 |
| ***SLC25A32*** | Solute carrier family 25 member 32 | 0.0006 | 0.0257 |
| ***RCHY1*** | Ring finger and CHY zinc finger domain containing 1 | 0.0006 | 0.0257 |
| ***CSNK1G3*** | Casein kinase 1 gamma 3 | 0.0006 | 0.0258 |
| ***TIAL1*** | TIA1 cytotoxic granule associated RNA binding protein like 1 | 0.0006 | 0.0258 |
| ***PRKAA1*** | Protein kinase AMP-activated catalytic subunit alpha 1 | 0.0006 | 0.0259 |
| ***TMEM167A*** | Transmembrane protein 167A | 0.0006 | 0.0260 |
| ***LARP4*** | La ribonucleoprotein 4 | 0.0006 | 0.0260 |
| ***SKAP2*** | Src kinase associated phosphoprotein 2 | 0.0006 | 0.0261 |
| ***VPS13C*** | Vacuolar protein sorting 13 homolog C | 0.0006 | 0.0263 |
| ***FAM160B1*** | Family with sequence similarity 160 member B1 | 0.0006 | 0.0264 |
| ***C5orf30 / MACIR*** | Macrophage immunometabolism regulator | 0.0007 | 0.0267 |
| ***APPBP2*** | Amyloid beta precursor protein binding protein 2 | 0.0007 | 0.0269 |
| ***TMEM215*** | Transmembrane protein 215 | 0.0007 | 0.0269 |

| | | | |
|---|---|---|---|
| ***RAB2A*** | RAB2A, member RAS oncogene family | 0.0007 | 0.0269 |
| ***SNX4*** | Sorting nexin 4 | 0.0007 | 0.0269 |
| ***DNAJC3*** | DnaJ heat shock protein family (Hsp40) member C3 | 0.0007 | 0.0269 |
| ***SEPSECS*** | Sep (O-phosphoserine) tRNA:Sec (selenocysteine) tRNA synthase | 0.0007 | 0.0270 |
| ***ABHD17B*** | Abhydrolase domain containing 17B, depalmitoylase | 0.0007 | 0.0271 |
| ***NT5DC1*** | 5'-nucleotidase domain containing 1 | 0.0007 | 0.0271 |
| ***TAX1BP1*** | Ax1 binding protein 1 | 0.0007 | 0.0271 |
| ***MITF*** | Microphthalmia-associated transcription fac | 0.0007 | 0.0271 |
| ***PTPN4*** | Protein tyrosine phosphatase non-receptor type 4 | 0.0007 | 0.0271 |
| ***SARAF*** | Store-operated calcium entry associated regulatory factor | 0.0007 | 0.0272 |
| ***MRPL42*** | Mitochondrial ribosomal protein L42 | 0.0007 | 0.0273 |
| ***CBX3*** | Chromobox 3 | 0.0007 | 0.0275 |
| ***DDX3Y*** | DEAD-box helicase 3 Y-linked | 0.0007 | 0.0275 |
| ***LLPH*** | LLP homolog, long-term synaptic facilitation factor | 0.0007 | 0.0275 |
| ***RBBP9*** | RB binding protein 9, serine hydrolase | 0.0007 | 0.0275 |
| ***ACER3*** | Alkaline ceramidase 3 | 0.0007 | 0.0278 |
| ***IREB2*** | Iron responsive element binding protein 2 | 0.0007 | 0.0279 |
| ***PTGES3*** | Prostaglandin E synthase 3 | 0.0007 | 0.0281 |
| ***ORMDL1*** | ORMDL sphingolipid biosynthesis regulator 1 | 0.0007 | 0.0284 |
| ***GLO1*** | Glyoxalase I | 0.0007 | 0.0285 |
| ***TRAPPC6B*** | Trafficking protein particle complex 6B | 0.0008 | 0.0287 |
| ***HP1BP3*** | Heterochromatin protein 1 binding protein 3 | 0.0008 | 0.0291 |
| ***PRRC1*** | Proline rich coiled-coil 1 | 0.0008 | 0.0291 |
| ***SSX2IP*** | SSX family member 2 interacting protein | 0.0008 | 0.0296 |
| ***AGPS*** | Alkylglycerone phosphate synthase | 0.0008 | 0.0298 |
| ***BNIP3L*** | BCL2 interacting protein 3 like | 0.0008 | 0.0298 |
| ***SMIM13*** | Small integral membrane protein 13 | 0.0008 | 0.0299 |
| ***EGLN1*** | Egl-9 family hypoxia inducible factor 1 | 0.0008 | 0.0299 |
| ***SLC25A24*** | Solute carrier family 25 member 24 | 0.0008 | 0.0299 |
| ***SET*** | SET nuclear proto-oncogene | 0.0008 | 0.0300 |
| ***RFX3*** | Regulatory factor X3 | 0.0008 | 0.0301 |
| ***SNX6*** | Sorting nexin 6 | 0.0008 | 0.0301 |
| ***NLK*** | Nemo like kinase | 0.0008 | 0.0302 |
| ***RAD21*** | RAD21 cohesin complex component | 0.0008 | 0.0302 |
| ***NPHP3*** | Nephrocystin 3 | 0.0008 | 0.0303 |
| ***PURA*** | Purine rich element binding protein A | 0.0008 | 0.0304 |
| ***PWAR6*** | Prader Willi/Angelman region RNA 6 | 0.0008 | 0.0304 |

| | | | |
|---|---|---|---|
| ***TMEM170B*** | Transmembrane protein 170B | 0.0008 | 0.0304 |
| ***PAWR*** | Pro-apoptotic WT1 regulator | 0.0008 | 0.0304 |
| ***GALNT3*** | Polypeptide N-acetylgalactosaminyltransferase 3 | 0.0008 | 0.0304 |
| ***NAP1L1*** | Nucleosome assembly protein 1 like 1 | 0.0008 | 0.0304 |
| ***ZMPSTE24*** | Zinc metallopeptidase STE24 | 0.0008 | 0.0305 |
| ***AF127936.9*** | | 0.0008 | 0.0305 |
| ***CDC42SE2*** | CDC42 small effector 2 | 0.0008 | 0.0306 |
| ***RALGPS2*** | Ral GEF with PH domain and SH3 binding motif 2 | 0.0009 | 0.0307 |
| ***SLC38A6*** | Solute carrier family 38 member 6 | 0.0009 | 0.0308 |
| ***CNOT6L*** | CCR4-NOT transcription complex subunit 6 like | 0.0009 | 0.0309 |
| ***KIAA1715 / LNPK*** | Lunapark, ER junction formation factor | 0.0009 | 0.0309 |
| ***RCBTB1*** | RCC1 and BTB domain containing protein 1 | 0.0009 | 0.0309 |
| ***STAM2*** | Signal transducing adaptor molecule 2 | 0.0009 | 0.0309 |
| ***PKN2*** | Protein kinase N2 | 0.0009 | 0.0310 |
| ***EIF5A2*** | Eukaryotic translation initiation factor 5A2p | 0.0009 | 0.0310 |
| ***CEP57*** | Centrosomal protein 57 | 0.0009 | 0.0312 |
| ***MICU3*** | Mitochondrial calcium uptake family member 3 | 0.0009 | 0.0312 |
| ***UFM1*** | Ubiquitin fold modifier 1 | 0.0009 | 0.0312 |
| ***CPSF6*** | Cleavage and polyadenylation specific factor 6 | 0.0009 | 0.0312 |
| ***CANX*** | Calnexin | 0.0009 | 0.0314 |
| ***ARMCX1*** | Armadillo repeat containing X-linked 1 | 0.0009 | 0.031 |
| ***ABCB5*** | ATP binding cassette subfamily B member 5 | 0.0009 | 0.0318 |
| ***ABCE1*** | ATP binding cassette subfamily E member 1 | 0.0009 | 0.0318 |
| ***COMMD2*** | COMM domain containing 2 | 0.0009 | 0.0321 |
| ***UEVLD*** | UEV and lactate/malate dehyrogenase domains | 0.0009 | 0.0321 |
| ***GTF2F2*** | General transcription factor IIF subunit 2 | 0.0009 | 0.0321 |
| ***KDM7A*** | Lysine demethylase 7A | 0.0009 | 0.0321 |
| ***UBXN2A*** | UBX domain protein 2A | 0.0009 | 0.0321 |
| ***ZNF654*** | zinc finger protein 654 | 0.0009 | 0.0321 |
| ***BNIP2*** | BCL2 interacting protein 2 | 0.0009 | 0.0325 |
| ***NFIB*** | Nuclear factor I B | 0.0010 | 0.0329 |
| ***METAP2*** | Methionyl aminopeptidase 2 | 0.0010 | 0.0330 |
| ***RIF1*** | Replication timing regulatory factor 1 | 0.0010 | 0.0337 |
| ***PRDX3*** | Peroxiredoxin 3 | 0.0010 | 0.0337 |
| ***FYTTD1*** | Forty-two-three domain containing 1 | 0.0010 | 0.0343 |

| | | | |
|---|---|---|---|
| ***HMGN3*** | High mobility group nucleosomal binding domain 3 | 0.0010 | 0.0343 |
| ***RP11-135F9.3*** | | 0.0010 | 0.0010 |
| ***FAM73A / MIGA1*** | Mitoguardin 1 | 0.0010 | 0.0349 |
| ***TWISTNB*** | Twist basic helix-loop-helix transcription factor 1 neighbor | 0.0010 | 0.0349 |
| ***VCPKMT*** | Valosin containing protein lysine methyltransferase | 0.0010 | 0.0349 |
| ***PAK2*** | p21 (RAC1) activated kinase 2 | 0.0011 | 0.0356 |
| ***AK3*** | Adenylate kinase 3 | 0.0011 | 0.0356 |
| ***CAB39*** | Calcium binding protein 39 | 0.0011 | 0.0356 |
| ***TAF1D*** | TATA-box binding protein associated factor, RNA polymerase I subunit D | 0.0011 | 0.0356 |
| ***BACH1*** | BTB domain and CNC homolog 1 | 0.0011 | 0.0356 |
| ***SLK*** | STE20 like kinase | 0.0011 | 0.0358 |
| ***CDC37L1*** | Cell division cycle 37 like 1 | 0.0011 | 0.0361 |
| ***SNRNP48*** | Small nuclear ribonucleoprotein U11/U12 subunit 48 | 0.0011 | 0.0364 |
| ***GBAS / NIPSNAP2*** | Nipsnap homolog 2 | 0.0011 | 0.0365 |
| ***SLC16A1*** | Solute carrier family 16 member 1 | 0.0011 | 0.0365 |
| ***FBXL3*** | F-box and leucine rich repeat protein 3 | 0.0011 | 0.0366 |
| ***TBC1D23*** | TBC1 domain family member 23 | 0.0011 | 0.0366 |
| ***PHC3*** | Polyhomeotic homolog 3 | 0.0011 | 0.0370 |
| ***CDC42EP3*** | CDC42 effector protein 3 | 0.0011 | 0.0372 |
| ***FBXL17*** | F-box and leucine rich repeat protein 17 | 0.0011 | 0.0372 |
| ***UBA3*** | Ubiquitin like modifier activating enzyme 3 | 0.0011 | 0.0373 |
| ***MORC3*** | MORC family CW-type zinc finger 3 | 0.0012 | 0.0376 |
| ***GMCL1*** | Germ cell-less 1, spermatogenesis associated | 0.0012 | 0.0376 |
| ***PPP3CB*** | Protein phosphatase 3 catalytic subunit beta | 0.0012 | 0.0377 |
| ***ACBD3*** | Acyl-CoA binding domain containing 3 | 0.0012 | 0.0380 |
| ***LPGAT1*** | Lysophosphatidylglycerol acyltransferase 1 | 0.0012 | 0.0382 |
| ***ATXN3*** | Ataxin 3 | 0.0012 | 0.0383 |
| ***RNF217*** | Ring finger protein 217 | 0.0012 | 0.0386 |
| ***TDRP*** | Testis development related protein | 0.0012 | 0.0390 |
| ***ATL3*** | Atlastin GTPase 3 | 0.0012 | 0.0392 |
| ***STX12*** | Syntaxin 12 | 0.0012 | 0.0392 |
| ***ODF2L*** | Outer dense fiber of sperm tails 2 like | 0.0012 | 0.0395 |
| ***DNAL1*** | Dynein axonemal light chain 1 | 0.0013 | 0.0395 |
| ***MAP9*** | Microtubule associated protein 9 | 0.0013 | 0.0395 |
| ***TMEM70*** | Transmembrane protein 70 | 0.0013 | 0.0397 |
| ***FAM69A*** | Family with sequence similarity 69 member A | 0.0013 | 0.0398 |
| ***IDS*** | Iduronate 2-sulfatase | 0.0013 | 0.0398 |

| | | | |
|---|---|---|---|
| ***RAB5A*** | RAB5A, member RAS oncogene family | 0.0013 | 0.0398 |
| ***SLC39A8*** | Solute carrier family 39 member 8 | 0.0013 | 0.0398 |
| ***ACTR6*** | Actin related protein 6 | 0.0013 | 0.0408 |
| ***ARL6IP5*** | ADP ribosylation factor like GTPase 6 interacting protein 5 | 0.0013 | 0.0408 |
| ***C1orf27 / ODR4*** | Odr-4 GPCR localization factor homolog | 0.0013 | 0.0408 |
| ***GSKIP*** | GSK3B interacting protein | 0.0013 | 0.0408 |
| ***LANCL1*** | LanC like 1 | 0.0013 | 0.0408 |
| ***SLC25A40*** | Solute carrier family 25 member 40 | 0.0013 | 0.0408 |
| ***APOOL*** | Apolipoprotein O like | 0.0013 | 0.0410 |
| ***ASPH*** | Aspartate beta-hydroxylase | 0.0013 | 0.0412 |
| ***TRAK2*** | Trafficking kinesin protein 2 | 0.0013 | 0.0414 |
| ***PRPF40A*** | Pre-mRNA processing factor 40 homolog A | 0.0014 | 0.0419 |
| ***SMAD4*** | SMAD family member 4 | 0.0014 | 0.0422 |
| ***SRSF10*** | Serine and arginine rich splicing factor 10 | 0.0014 | 0.0423 |
| ***EIF3E*** | Eukaryotic translation initiation factor 3 subunit E | 0.0014 | 0.0426 |
| ***ZFAND5*** | Zinc finger AN1-type containing 5 | 0.0014 | 0.0426 |
| ***ATP13A3*** | ATPase 13A3 | 0.0014 | 0.0427 |
| ***ERBB2IP*** | Erbb2 interacting protein | 0.0014 | 0.0430 |
| ***TOMM20*** | Translocase of outer mitochondrial membrane 20 | 0.0014 | 0.0430 |
| ***SNAPC3*** | Small nuclear RNA activating complex polypeptide 3 | 0.0014 | 0.0432 |
| ***RC3H1*** | Ring finger and CCCH-type domains 1 | 0.0015 | 0.0437 |
| ***FCHO2*** | FCH and mu domain containing endocytic adaptor 2 | 0.0015 | 0.0437 |
| ***HAS2*** | Hyaluronan synthase 2 | 0.0015 | 0.0437 |
| ***RNF138*** | Ring finger protein 138 | 0.0015 | 0.0438 |
| ***LINC00657 / NORAD*** | Non-coding RNA activated by DNA damage | 0.0015 | 0.0440 |
| ***C2orf49*** | Chromosome 2 open reading frame 49 | 0.0015 | 0.0447 |
| ***ALDH1L2*** | Aldehyde dehydrogenase 1 family member L2 | 0.0015 | 0.0447 |
| ***CPNE8*** | Copine 8 | 0.0015 | 0.0447 |
| ***DESI2*** | Desumoylating isopeptidase 2 | 0.0015 | 0.0448 |
| ***G3BP2*** | G3BP stress granule assembly factor 2 | 0.0015 | 0.0448 |
| ***UCHL5*** | Ubiquitin C-terminal hydrolase L5 | 0.0015 | 0.0451 |
| ***SLC35A5*** | Solute carrier family 35 member 5 | 0.0016 | 0.0457 |
| ***FBXL5*** | F-box and leucine rich repeat protein 5 | 0.0016 | 0.0460 |
| ***RNF2*** | Ring finger protein 2 | 0.0016 | 0.0460 |
| ***ABCA1*** | ATP binding cassette subfamily A member 1 | 0.0016 | 0.0465 |
| ***SESN1*** | Sestrin 1 | 0.0016 | 0.0465 |
| ***SLC9A6*** | Solute carrier family 9 member 6 | 0.0016 | 0.0465 |

| | | | |
|---|---|---|---|
| ***ARMT1*** | Acidic residue methyltransferase 1 | 0.0016 | 0.0466 |
| ***FMNL2*** | Formin like 2 | 0.0016 | 0.0466 |
| ***PEX1*** | Peroxisomal biogenesis factor 1 | 0.0016 | 0.0466 |
| ***DENND1B*** | DENN domain containing 1B | 0.0016 | 0.0467 |
| ***METTL9*** | Methyltransferase like 9 | 0.0016 | 0.0467 |
| ***TMPO*** | Thymopoietin | 0.0016 | 0.0467 |
| ***PTCHD4*** | Patched domain containing 4 | 0.0016 | 0.0467 |
| ***RNFT1*** | Ring finger protein, transmembrane 1 | 0.0016 | 0.0472 |
| ***DCK*** | Deoxycytidine kinase | 0.0016 | 0.0473 |
| ***LTN1*** | Listerin E3 ubiquitin protein ligase 1 | 0.0016 | 0.0473 |
| ***EIF4A2*** | Eukaryotic translation initiation factor 4A2 | 0.0017 | 0.0475 |
| ***SH3GLB1*** | SH3 domain containing GRB2 like, endophilin B1 | 0.0017 | 0.0475 |
| ***YAP1*** | Yes1 associated transcriptional regulator | 0.0017 | 0.0476 |
| ***VAPA*** | VAMP associated protein A | 0.0017 | 0.0476 |
| ***ANGEL2*** | Angel homolog 2 | 0.0017 | 0.0477 |
| ***PNPLA8*** | Patatin like phospholipase domain containing 8 | 0.0017 | 0.0481 |
| ***ACSL3*** | Acyl-CoA synthetase long chain family member 3 | 0.0017 | 0.0483 |
| ***SS18*** | SS18 subunit of BAF chromatin remodeling complex | 0.0017 | 0.0485 |
| ***PRPF39*** | Pre-mRNA processing factor 39 | 0.0017 | 0.0487 |
| ***KIAA1143*** | KIAA1143 | 0.0017 | 0.0492 |
| ***MED13*** | Mediator complex subunit 13 | 0.0018 | 0.0495 |
| ***KIF3A*** | Kinesin family member 3A | 0.0018 | 0.0497 |

**Table S4.12. Downregulated genes (FDR < 0.05) in 1,25(OH)$_2$D$_3$ treated samples vs. controls in LIGHT samples (excluding LP1 cell line).**

| Gene symbol | Gene name | p-value | FDR |
|---|---|---|---|
| ***OLFML2A*** | Olfactomedin like 2A | 4.92E-09 | 1.22E-05 |
| ***PRKCDBP* / CAVIN3** | Caveolae associated protein 3 | 5.21E-07 | 0.0002 |
| ***DHCR24*** | 24-dehydrocholesterol reductase | 3.34E-06 | 0.0008 |
| ***NFATC2*** | Nuclear factor of activated T cells 2 | 3.37E-06 | 0.0008 |
| ***ECM1*** | Extracellular matrix protein 1 | 9.25E-06 | 0.0016 |
| ***PCDHGC3*** | Protocadherin gamma subfamily C, 3 | 1.31E-05 | 0.0020 |
| ***FASN*** | Fatty acid synthase | 3.23E-05 | 0.0036 |
| ***ABLIM3*** | Actin binding LIM protein family member 3 | 3.34E-05 | 0.0037 |
| ***GIPC3*** | GIPC PDZ domain containing family member 3 | 3.36E-05 | 0.0037 |
| ***LGALS3BP*** | Galectin 3 binding protein | 3.45E-05 | 0.0037 |
| ***HRH2*** | Histamine receptor H2 | 3.72E-05 | 0.0039 |
| ***LIMD2*** | LIM domain containing 2 | 3.80E-05 | 0.0040 |
| ***MAL*** | Mal, T cell differentiation protein | 3.85E-05 | 0.0040 |
| ***DCHS1*** | Dachsous cadherin-related 1 | 4.10E-05 | 0.0042 |
| ***COL4A2*** | Collagen type IV alpha 2 chain | 5.04E-05 | 0.0048 |
| ***TOM1L2*** | Target of myb1 like 2 membrane trafficking protein | 7.23E-05 | 0.0063 |
| ***CSPG4*** | Chondroitin sulfate proteoglycan 4 | 8.44E-05 | 0.0068 |
| **CTC-251I16.1** | | 8.35E-05 | 0.0068 |
| ***PLEC*** | Plectin | 8.50E-05 | 0.0068 |
| ***FAM129B*** | Family with sequence similarity 129, member B | 8.59E-05 | 0.0068 |
| ***FCMR*** | Fc fragment of IgM receptor | 9.25E-05 | 0.0071 |
| ***TRIOBP*** | TRIO and F-actin binding protein | 0.0001 | 0.0081 |
| ***NES*** | Nestin | 0.0001 | 0.0088 |
| ***ENG*** | Endoglin | 0.0001 | 0.0099 |
| ***MCAM*** | Melanoma cell adhesion molecule | 0.0001 | 0.0111 |
| ***LY6E*** | Lymphocyte antigen 6 family member E | 0.0002 | 0.0119 |
| ***SYDE1*** | Synapse defective Rho GTPase homolog 1 | 0.0002 | 0.0127 |
| ***MAML3*** | MAML3 | 0.0002 | 0.0130 |
| ***MYL9*** | Myosin light chain 9 | 0.0002 | 0.0133 |
| ***SDC3*** | Syndecan 3 | 0.0002 | 0.0142 |
| ***HMGXB3*** | HMG-box containing 3 | 0.0002 | 0.0145 |
| ***AEBP1*** | AE binding protein 1 | 0.0002 | 0.0154 |
| ***MMP17*** | Matrix metallopeptidase 17 | 0.0002 | 0.0154 |
| ***SGK223*** | Homolog of rat pragma of Rnd2 | 0.0003 | 0.0157 |
| ***FHDC1*** | FH2 domain containing 1 | 0.0003 | 0.0171 |
| ***CD4*** | CD4 molecule | 0.0003 | 0.0173 |

| | | | |
|---|---|---|---|
| ***GPX1*** | Glutathione peroxidase 1 | 0.0004 | 0.0188 |
| ***GAS7*** | Growth arrest specific 7 | 0.0004 | 0.0191 |
| ***PCDH1*** | Protocadherin 1 | 0.0004 | 0.0203 |
| ***IGFBP4*** | Insulin like growth factor binding protein 4 | 0.0004 | 0.0204 |
| ***CEP170B*** | Centrosomal protein 170B | 0.0005 | 0.0221 |
| ***SVIL*** | Supervillin | 0.0005 | 0.0225 |
| ***HMG20B*** | High mobility group 20B | 0.0005 | 0.0225 |
| ***IFITM3*** | Interferon induced transmembrane protein 3 | 0.0005 | 0.0229 |
| ***FOXM1*** | Forkhead box M1 | 0.0006 | 0.0245 |
| ***PLOD1*** | Procollagen-lysine,2-oxoglutarate 5-dioxygenase 1 | 0.0006 | 0.0250 |
| ***PCDHGA12*** | Protocadherin gamma subfamily A, 12 | 0.0007 | 0.0270 |
| ***GBF1*** | Golgi brefeldin A resistant guanine nucleotide exchange factor 1 | 0.0007 | 0.0271 |
| ***GOLGA7B*** | Golgin A7 family member B | 0.0007 | 0.0271 |
| ***CYB5R3*** | Cytochrome b5 reductase 3 | 0.0007 | 0.0271 |
| ***SPON2*** | Spondin 2 | 0.0007 | 0.0272 |
| ***BCAR1*** | BCAR1 scaffold protein, Cas family member | 0.0007 | 0.0273 |
| ***MMP2*** | Matrix metallopeptidase 2 | 0.0007 | 0.0275 |
| ***B4GALNT4*** | Beta-1,4-N-acetyl-galactosaminyltransferase 4 | 0.0007 | 0.0286 |
| ***LRP5*** | LDL receptor related protein 5 | 0.0008 | 0.0292 |
| ***MX2*** | MX dynamin like GTPase 2 | 0.0008 | 0.0298 |
| ***MAGED2*** | MAGE family member D2 | 0.0008 | 0.0299 |
| ***HSPB7*** | Heat shock protein family B (small) member 7 | 0.0008 | 0.0305 |
| ***PLXNB3*** | Plexin B3 | 0.0008 | 0.0305 |
| ***ABHD17A*** | Abhydrolase domain containing 17A, depalmitoylase | 0.0009 | 0.0309 |
| ***CHPF*** | Chondroitin polymerizing factor | 0.0009 | 0.0309 |
| ***MFI2 /MELTF*** | Melanotransferrin | 0.0009 | 0.0318 |
| ***AURKAIP1*** | Aurora kinase A interacting protein 1 | 0.0009 | 0.0321 |
| ***PLOD3*** | Procollagen-lysine,2-oxoglutarate 5-dioxygenase 3 | 0.0009 | 0.0321 |
| ***HK1*** | Hexokinase 1 | 0.0010 | 0.0326 |
| ***MAP3K3*** | Mitogen-activated protein kinase kinase kinase 3 | 0.0010 | 0.0339 |
| ***KMT2D*** | Lysine methyltransferase 2D | 0.0012 | 0.0383 |
| ***CCDC85B*** | Coiled-coil domain containing 85B | 0.0012 | 0.0388 |
| ***LRP3*** | LDL receptor related protein 3 | 0.0013 | 0.0409 |
| ***PIP5K1C*** | Phosphatidylinositol-4-phosphate 5-kinase type 1 gamma | 0.0013 | 0.0412 |
| ***ACTB*** | Actin beta | 0.0014 | 0.0424 |
| ***S100A11*** | S100 calcium binding protein A11 | 0.0014 | 0.0427 |
| ***RHBDF2*** | Rhomboid 5 homolog 2 | 0.0014 | 0.0429 |
| ***ITGA5*** | Integrin subunit alpha 5 | 0.0015 | 0.0437 |

| | | | |
|---|---|---|---|
| ***CRIP2*** | Cysteine rich protein 2 | 0.0015 | 0.0437 |
| ***KIFC3*** | Kinesin family member C3 | 0.0015 | 0.0440 |
| ***TRAM2*** | Translocation associated membrane protein 2 | 0.0015 | 0.0447 |
| ***TMEM8A*** | Transmembrane protein 8A | 0.0016 | 0.0472 |
| ***C15orf52* / CCDC9B** | coiled-coil domain containing 9B | 0.0017 | 0.0479 |
| ***TSPO*** | Translocator protein | 0.0017 | 0.0481 |
| ***JUN*** | Jun proto-oncogene, AP-1 transcription factor subunit | 0.0018 | 0.0493 |
| ***OSBPL5*** | Oxysterol binding protein like 5 | 0.0018 | 0.0497 |

# Discussion

The purpose of the present work was to investigate the possible interaction between human skin pigmentation and skin immunity, by the analysis of two molecules with important roles in immune system: the antimicrobial peptide β-defensin 103, which plays pivotal roles in innate and adaptive immunity (Chessa et *al*., 2020; Shelley, Davidson and Dorin, 2020) and vitamin D, which possesses immunomodulatory activity (Baeke *et* al., 2010; Trochoutsou et *al*., 2015)

The discovery by Candille et *al*. (2007) that linked a mutation in the canine orthologue of human β-defensin 103 with black coat colour in dogs, led us to consider that human β-defensin 103 could also be implicated in skin pigmentation. Thus, we analysed the sequence diversity of *DEFB103* in individuals from the Basque Country with different level of pigmentation, as well as in samples from Africa, Asia, Australia and Europe. We detected 30 variants of which 15 had not been previously annotated: we detected two exonic variants, one missense variation leading to an aminoacidic change in the signal peptide, that was predicted to be benign, and a deletion in the second exon leading to a larger peptide, probably not functional. However, these mutations were rare. In addition, we did not find any mutation similar to that described by Candille et *al*. (2007) in dogs.

In humans, *DEFB103* is located in a copy number variant (CNV) region on chromosome 8p23.1, along with other β-defensin encoding gene. Thus, in addition to sequence variation, this is another source of variability that we explored. Our initial determination of copy number (CN) by Real-time quantitative PCR (RT-qPCR), showed unusual results, with a median of 2 copies per diploid genome, in contrast with data reported by other authors, which usually show a median of 4 copies (Hollox, 2008). Using the data of the re-sequencing of *DEFB103*, we estimated the minimum copy number on 13 samples (based on the number of different sequences detected) and observed discrepancies in three cases (the number of different sequences was higher than copy number estimated by RT-qPCR). Thus, we decided to analyse copy number with by a more reliable technique.

The β-defensin CNV has previously been extensively analysed by different methods, and several authors have compared the performance of different techniques for the analysis of this CNV. In general, RT-qPCR seem to be the technique with higher bias and discrepancy when comparing with other techniques (Fode et *al*., 2011; Perne et *al*., 2009; Zhang et *al*., 2014). Fernandez-Jimenez et *al*. (2011) observed that RT-qPCR is more sensitive to DNA concentration than the Paralog Ratio Test (PRT). However, they reported that comparable results are achieved by RT-qPCR and PRT if normalized amounts of input template DNA are used. Besides, they also observed that PRT is sensitive to DNA quality, due to the need of longer amplicons. In our experience however, RT-qPCR did not result a reliable technique given that it underestimated the copy number. However, Digital PCR (dPCR) did result a much better option because DNA concentration seems not to be limiting, since it is an end-point technique and the amplification efficiencies should not influence the results and results were much more accurate.

Furthermore, discordance in the estimates of samples with high copy numbers has also reported for MLPA and PRT (Armour et *al*., 2007). Zhang et *al*. (2014) reported that MLPA was the most accurate technique in comparison with RT-qPCR and PRT, although the concordance with PRT was high (90.52%). The main reason of the discrepancy was a mutation that was present in the binding site of the primer for one of the targeted paralogous pseudogenes. They observed that PRT underestimated the copy number by one in the samples carrying the mutation. This is an example of one of the main the disadvantages of PRT. Sequence variability in the paralogous *loci* used as a reference can hinder amplification and led to underestimation of the copy number. To minimize this problem, more paralog *loci* can be used at the same time. Triplex paralog test is now common and has been used for β-defensin CNV analysis (Aldhous et *al*., 2010; Fode et *al*., 2011; Jones et *al*., 2014). But it is dependant of the existence of paralogs for the target *loci*. Although we did not conduct a comparative analysis between dPCR, PRT

and MLPH, the simplicity of the technique and the amount of reaction-wells analysed made dPCR a robust and reliable technique. In this sense, next generation sequencing has also been used to analyse β-defensin CNV, with whole-genome sequencing (Handsaker et *al*., 2015) and exome sequencing data (Forni et *al*., 2015). Handsaker et *al*. (2015) also used Digital PCR to evaluate the results and they get high concordance (99.9%).

Thus, after evaluating the possibilities, we decided to use Digital PCR and obtained more accurate and reliable results, at least compared to standard RT-PCR.

The analysis of the copy number results in the most and the least pigmented (skin reflectance) Basque individuals showed no differences between the frequencies of the two groups. However, by analysing the copy number in samples from the different regions of Spain, we did observe a correlation between copy number and annual mean of incident UV-B radiation (J/m2). Thus, individuals from the provinces with less UV-B surface mean irradiation tend to have higher frequencies of lower copy numbers. This is suggesting to us that UV radiation could have been important in the evolution of the β-defensin CNV. Unfortunately, we did not have data of the pigmentation level of these individuals to test if the observed differences could be also related with pigmentation.

To further investigate the role of UV in relation with *DEFB103*, we analysed the effect of irradiating human keratinocytes regarding *DEFB103* expression, using keratinocytes derived from lightly and darkly pigmented individuals. Glaser et *al.* (2009) have already reported that UV irradiation was able to induce the expression of some antimicrobial peptides (AMPs), including HBD2 and HBD3. Felton et al. (2013) also analysed the upregulation of some AMPs on irradiated skin of healthy volunteers by immunohistochemistry and observed a high induction of some AMPs, but the upregulation of HBD3 was modest and it did not affect HBD2 .

In our results, there was substantial variability in the response to UV by keratinocytes, with, only 4 out of 6 cell lines showing and increase in the expression after UV irradiation. Inter-individual variation was also observed by Glasser et *al.* (2009) and in the experiments of Wolf-Horrell and D'Orazio (2014) with human skin explants. Anyway, although there was variance in the time and intensity of the response, we observed that all the light keratinocytes increased *DEFB103* expression, while only one of the dark cell lines responded, suggesting that the pigmentary phenotype could be relevant in the response to UV, at least for light keratinocytes.

In order to evaluate the magnitude of the response, we incubated the same cell lines with a pathogenic stimulus: Heat Killed *Staphylococcus aureus* (HKSA). Although HBD3 is known to have a potent activity against *Staphylococcus aureus* (Harder et *al*., 2001), and *DEFB103* is upregulated in infections *of S. aureous*, (Zanger et *al.*, 2010), in our experiments, not all the cell lines responded to HKSA, and also showed variability in the responses. In this case, the response was not seemingly related with pigmentary phenotype. Overall, as expected, the magnitude of the response was higher against HKSA. The fact that the response to HKSA was also variable, indicates that many factors could influence at the same time the expression of *DEFB103*, making it difficult to elucidate the effect of the stimulants.

Vitamin D has also been reported to positively modulate the expression of AMPs, specially cathelicidin, but also HBD2 and HBD3 (Wang et *al*., 2004; Dai et *al*., 2010). However, Peric et *al*., (2009) observed that in psoriatic keratinocytes, vitamin D downregulated HBD2 and HBD3 expression. In our results, vitamin D does not seem to induce a clear effect: only two cell lines increase *DEFB103* expression, while the other cell lines do not respond or show a decrease in the expression. As mentioned before, the effect on *DEFB103* and probably other AMPs depends on several factors, including the state of the cells and the presence of other inductors. For instance, UV irradiation

and vitamin D have been reported to differentially modulate the expression of some AMPs in healthy and injured skin (Peric et *al*., 2009; Felton et *al*., 2013).

On the other hand, our results suggest that UV increases the expression of *DEFB103*, especially in keratinocytes from lightly pigmented individuals. UV radiation has an immunosuppressive effect on the skin, as it supresses T-cell-mediated immune responses (Schwarz, 2010). However, UV also induces the expression of some AMPs, including HBD3, as we have observed in our results. Thus, it has been proposed that while UV supresses the adaptive immune system, it also induces the innate immune system, which prevents pathogen infections (Schwarz, 2010).

As an additional form of protection (namely, photoprotection), HBD3 could also mediate melanogenesis. To analyse this possibility, we incubated human melanocytes from dark and light pigmented individuals with HBD3 and analysed the transcriptional response, using gene expression microarrays. Melanocytes were incubated with wither wild-type peptide or a peptide carrying the mutation found in dogs.

At 24h after the incubation, we observed an upregulation of melanogenic genes in both dark and light melanocytes. We made a list of pigmentation-associated genes that are expressed in melanocytes, and confirmed that those genes were overrepresented among the HBD3-upregulated genes. In light melanocytes, the overrepresentation was more significant, suggesting again a possible relation with pigmentary phenotype. The effect on pigmentary genes was more significant with wild-type HBD3 in both dark and light cells, indicating that in humans the mutation may not be relevant.

However, based on our results we were not able to elucidate which of the melanogenic pathways is modulated by HBD3, because genes from different pathways were upregulated. Besides, in several melanogenic pathways, melanogenesis is promoted by activating proteins already present in the cell.

Even so, the most probably scenario is that HBD3 activates MC1R signalling pathway. In fact, the ability of HBD3 to bind MC1R has broadly been demonstrated (Candille et *al*., 2007, Beaumont et *al*., 2012; Swope et *al*., 2012, Nix et *al*., 2013, 2015), so it is the principal candidate. According to most authors, HBD3 does not seem to induce an increase of cAMP levels in melanocytes (Candille et *al*., 2007; Swope et *al*., 2012; Nix et *al*., 2013), but MC1R can also function through a cAMP-independent pathway. In this sense, Herraiz et *al.* (2011) reported that MC1R is able to transactivate the receptor KIT and activate ERK1/ERK2 MAPK pathways, leading to MITF activation.

However, we cannot rule out the possibility of HBD3 binding to other receptors, such as the endothelin B receptor (EDNRB) or the receptor tyrosine kinase KIT, which are both upregulated (although *EDNRB* only in light melanocytes). In fact, β-defensins are able to bind a variety of receptors, by electrostatic interactions, due to their cationic nature (Semple et *al*., 2012). In particular, HBD3 has been reported to bind some other G protein-coupled receptors, such as CCRC6, MCR3 and MC4R (Semple et *al*., 2010; Nix et *al*., 2015).

In addition, we also observed an increase in the expression of genes related with oxidative stress response and DNA repair. Interestingly, most of those genes have been reported to be modulated by α-MSH (Kokot et *al*., 2009; Song et *al*., 2009; Kadekaro et *al*., 2010, 2012; Abdel-Malek et *al*., 2014), suggesting that HBD3 may also induce other functions mediated by α-MSH.

Our results suggest that HBD3 is able to trigger melanogenesis and possibly other functions associated to MC1R signalling, in contrast with the inhibitory effect reported by other authors. Swope et *al.* (2012) defined HBD3 as a MC1R antagonist because it inhibited α-MSH-induced cAMP increase. Besides, Jarrett et *al*. (2015) also reported that HBD3 inhibits the protective effects of α-MSH, preventing the activation of the base and nucleotide excision repair (NER), involved in DNA repair. However, those effects are

only because of the inhibition of α-MSH binding to MC1R, but HBD3 do not decrease basal levels of MC1R signalling. HBD3 binding to MC1R is based on electrostatic interactions, which provides higher affinity (Nix et *al*., 2015), and thus, higher ability to compete with other ligands.

On the other hand, it has been reported that MC1R is also able activate other DNA repair mechanisms by cAMP-independent pathways, by the activation of ERK and AKT signalling (Castejón-Griñán et *al*., 2017). It remains possible that HBD3 could stimulate these responses. Interestingly, Castejón-Griñán et *al*. (2017) demonstrated that variant MC1R activates AKT to promote DNA repair. In receptors carrying variants associated with RHC phenotype, the cAMP signalling is impaired but they are able to activate MAPK (Herraiz et *al*., 2009, 2011). In this sense, Beaumont et *al.* (2012), observed that ERK activation induced by HBD3 was similar in HEK cells transfected with wild-type MC1R and with MC1R carrying some variants associated with RHC phenotype (V92M, R142H, R160W and D294H), although not in R151C and D84E. It would be interesting to analyse if HBD3 is able to bind variant MC1R and trigger melanogenesis or DNA repair pathways in melanocytes carrying some of MC1R variants.

The effect of HBD3 depends on the presence of other MC1R ligands such as α-MSH and ASIP, as it impedes their binding. In the absence of α-MSH, HBD3 can stimulate similar functions. In this sense, we speculated that melanocytes in culture, without complements, would loss pigmentation activity due to the absence of stimulatory factors and we propose that in these conditions, HBD3 promotes melanogenesis.

Another one of our goals was to explore the possible bidirectional influence between vitamin D and melanogenesis. One the one hand we wanted to analyse if vitamin D is able to directly influence melanocytes and trigger melanogenesis. And on the other hand, to analyse if the response to vitamin D is dependent of the pigmentary phenotype.

Transcriptional analysis of melanocytes from dark and light pigmented individuals treated with active vitamin D, showed a distinct response. Light melanocytes showed a greater amount of differentially expressed genes (DEGs). Among the upregulated genes we observed several associated with pigmentation, of which we highlight *MITF* and *EDNBR*.

Our results are in line with others that also showed vitamin D induced upregulation of *EDNRB* in melanoblasts, although not in melanocytes (Watabe et *al*., 2002; Kawakami et *al*., 2014). With our data, we demonstrate that melanocytes also increase the expression of *EDNRB* in response to vitamin D. Besides *EDNRB* expression has also been reported to be upregulated by UV radiation in melanocytes, together with *MITF* (Tagashira et *al*., 2015). Watabe et *al*. (2002) also observed an upregulation of *MITF* expression when incubating melanoblasts with vitamin D and endothelin-3 (EDN3) simultaneously, but not with vitamin D alone, which led them suggest that both were needed to induce melanogenesis. Now, we have observed in this work that vitamin D alone is able to increase the expression of both *MITF* and *EDNRB*. Endothelins are normally secreted by keratinocytes and UV increases the production of at least endothelin-1 (EDN1) (Imokawa et *al*., 1992). However, melanocytes are also able to secrete endothelins (Park et *al*., 2015). Thus, although we do not see an increase of any of the endothelins, melanocytes could have secreted END1 or 3 to the medium (autocrine regulation).

The effect on pigmentation is further supported by the upregulation of genes involved in melanosome biogenesis and transport. Thus, *VAMP7, STX12* and *BLOC1S6* among others play essential roles in delivering cargo to melanosomes, including the transport of the melanogenic enzymes *TYR* and *TYRP1* (Jani et *al*., 2015; Dennis et *al*., 2016). On the other hand, *RAB27A, RAB1A* and *KIF5B* control the transport of mature melanosomes towards the periphery of the cell (Jordens et *al.*, 2006; Alzahofi et *al*., 2020).

Another gene related with melanosome transport is *MREG* (melanoregulin), which is also significantly upregulated when all cell lines ae considered together. The function of melanoregulin in human skin melanocytes has not been studied yet. However, in mouse melanocytes it seems to regulate the centripetal movement of melanosomes towards the nucleus (Ohbayashi et *al*., 2012). Thus, *MREG* controls melanosome transport in the opposite direction of *RAB27A* and *RAB1A*. Thus, the overexpression of melanoregulin *a priori* does not fit with the general trend of melanosome biogenesis and transport proposed. However, the role of *MREG* in human melanocytes could differ from mice. Another possible explanation of this discrepancy can be related with the localization of *MREG*. *RAB27A* and *RAB1A* localize in the membrane of the mature melanosomes, whereas *RAB7* (not modulated in our data), which drives melanosome transport towards the nucleus, is associated to immature melanosomes (Jordens et *al*., 2006). It is possible that melanoregulin could also be associated to immature melanosomes, but further research is needed to elucidate the role of MREG in human pigmentation.

Based on our data, we propose that vitamin D can modulate melanogenesis in human lightly pigmented melanocytes, possibly by the endothelin pathway. In relation with this, Thompson, Jones and Aitken (2018) observed that in Caucasian adults, constitutive melanin density was associated with higher 25-hydroxyvitamin D serum concentration. They suggest an increased sun exposure as the reason, provided by a increased sun tolerance.

In addition, the above also suggests that vitamin D is mediating a protective effect, because on the one hand, we observe the modulation of several genes related with melanoma, with a tendency of the upregulation of tumour suppressor genes such as *PTEN*, and downregulation of several melanoma-associated genes, with functions related to extracellular matrix and cell adhesion, cell proliferation or invasion. Although the effect is more evident in light melanocytes, we also see this tendency in dark melanocytes. On the other, in vitamin D treated-light melanocytes we observe the

overrepresentation of the p53 pathway, indicating that vitamin D could modulate some of its functions through this pathway. In this sense, p53 target genes implicated in DNA repair and oxidative damage response were upregulated. On the other hand, p53 has also been reported to stimulate known VDR-target genes (Maruyama et *al*., 2006).

Although *TP53* itself is not upregulated in our data, it could be that *protein* levels of p53 can also be modulated by the non-genomic mechanism of vitamin D (Sequeira et *al*., 2012). Other possibility is that *TP53* upregulation has occurred earlier and at 18h and it is no longer transcribing. Controlling p53 levels is crucial for cell homeostasis. In this sense, we see upregulation of genes related with the negative feedback loop, which controls p53 activity. Among them, *MDM2* codifies an E3 ubiquitin ligase, which is the principal inhibitor of p53 activity. MDM2 induces p53 proteosomal degradation, by ubiquitination, or inhibits p53 function by binding to its transcriptional activation domain (Wu et *al*., 1993; Haupt et *al.*, 1997). Interestingly MDM2 has also been reported to inhibit the transcriptional activity of VDR (Heyne et *al*., 2015).

Some evidences also suggest that p53 could play a role in melanogenesis by acting directly on melanocytes. The effect of p53 on pigmentation is principally by the induction in keratinocytes of POMC derived peptides (Cui et *al*., 2007) and other melanogenic factors (Box and Terzian, 2008). However, it has been proposed that p53 could increase the expression of the melanogenic genes *TYR* and *TYRP1* (Nylander et *al*., 2000; Khlgatian et *al*., 2002).

In summary, we propose that skin pigmentation can be modulated by both human β-defensin 103 and active vitamin D. The response to both factors, especially in the case of vitamin D, seem to be related to pigmentary phenotype.

The most widely accepted hypothesis postulates that skin lightening was the consequence of an adaptive process to facilitate the synthesis of vitamin D (Loomis, 1967; Jablonski and Chaplin, 2000, 2010, 2017; Chaplin and Jablonski, 2009; Grant, 2016). However, while lighter skin is advantageous for the production of adequate levels of vitamin D, it is also more vulnerable to UVR-induced damage. Our results suggest that active vitamin D is able to induce melanogenesis in melanocytes derived from lightly pigmented skin. Therefore, it is possible that, after reaching adequate levels of vitamin D, vitamin D itself promotes pigmentation to induce tanning that would protect the skin. This mechanism would be of special relevance at intermediate latitudes, where solar irradiation level changes along the year. In this sense, skin depigmentation would be the result of different pressures: the need to allow enough vitamin D synthesis and the need to be protected against solar irradiation in summer.

# Conclusions

1. The resequencing analysis performed on *DEFB103* locus showed that, although we detected new variants, there were mostly in introns, and there are not common indel variants similar to the polymorphism found in dogs. If sequence variation do regulate pigmentation in humans, it may not be because of mutations similar to the dog's polymorphism.

2. Copy Number analysis of *DEFB103* showed that it might be a relation between pigmentation and copy number levels, or at least with UV-B radiation. In the Spanish samples analysed, frequencies of low copy numbers are higher in individuals from regions with lower solar incidence.

3. Experiments with human cell lines showed that UV irradiation is able to induce the expression of *DEFB103* in keratinocytes, although in comparison with bacterial derived inducers of β-defensin 103, the response to UV is lower. Besides, all light cell lines increased *DEFB103* expression, but only one dark cell line. Thus, we conclude that UV-mediated *DEFB103* upregulation could be related with pigmentary phenotype.

4. Both wild-type peptide and the peptide carrying the mutation found in dogs were able to upregulate melanogenic *loci* in light and dark melanocytes. However, the response was more significant in light melanocytes. HBD3 also modulated *loci* involved in DNA repair and oxidative stress response. Thus, we propose that HBD3 peptide could be a modulator of pigmentary genes in human melanocytes and that HBD3 might also be able to regulate functions known to be regulated by α-MSH, possibly by the direct activation of MC1R.

5. Vitamin D produces an increase in the expression of melanogenic genes, such as *MITF* and *loci* with important functions in melanosome biosynthesis and transport (*VAMP7, STX12, RAB27A, RAB1A* and *KIF5B*) in lightly-pigmented melanocytes. Thus, we propose that vitamin D can induce an upregulation of melanogenesis. Given the

upregulation of the endothelin B receptor (*EDNRB*) we propose that this could be mediated through the endothelin pathway.

6. Vitamin D also modulates the expression of genes that have been related with melanoma: overall it upregulates tumour suppressor genes, such as *PTEN*, and downregulates loci associated with malignant transformation. We propose that vitamin D can provide a protective effect that could prevent melanoma transformation.

7. Given the ability of vitamin D to modulate melanogenesis in lightly pigmented skin, we propose that vitamin D production in light skin could be an adaptive mechanism to allow tanning in months of higher UV irradiation, in order to protect skin from UV damages.

# References

Abdel-Malek ZA, Ross R, Trinkle L, et al. Hormonal effects of vitamin D3 on epidermal melanocytes. *J Cell Physiol*. 1988; Aug;136(2):273-80.

Abdel-Malek Z, Swope VB, Suzuki I, et al. Mitogenic and melanogenic stimulation of normal human melanocytes by melanotropic peptides. *PENAS USA.* 1995; Feb 28;92(5):1789-93.

Abdel-Malek ZA, Swope VB, Starner RJ, et al. Melanocortins and the melanocortin 1 receptor, moving translationally towards melanoma prevention. *Arch Biochem Biophys*. 2014; 563:4-12.

Abe S, Miura K, Kinoshita A, et al. Copy number variation of the antimicrobial-gene, defensin beta 4, is associated with susceptibility to cervical cancer*. J Hum Genet.* 2013; May;58(5):250-3.

Abiko Y, Nishimura M, Kusano K, et al. Upregulated expression of human beta defensin-1 and -3 mRNA during differentiation of keratinocyte immortalized cell lines, HaCaT and PHK16-0b. J *Dermatol Sci*. 2003; 31(3):225-228.

Abrisqueta M, Herraiz C, Pérez Oliva AB, et al. Differential and competitive regulation of human melanocortin 1 receptor signaling by b-arrestin isoforms. *J Cell Sci.* 2013; Aug 15;126(Pt 16):3724-37.

Abu Bakar S, Hollox EJ, Armour JA. Allelic recombination between distinct genomic locations generates copy number diversity in human β-defensins. *PNAS USA*. 2009; Jan 20;106(3):853-8.

Ada S, Sahin S, Boztepe G, et al. No additional effect of topical calcipotriol on narrow-band UVB phototherapy in patients with generalized vitiligo*. Photodermatol Photoimmunol Photomed*. 2005; 21:79–83.

Adetunji MO, Lamont SJ, Abasht B, et al. Variant analysis pipeline for accurate detection of genomic variants from transcriptome sequencing data. *PLoS One*. 2019; 14(9):e0216838.

Adighibe O, Pezzella F. The Role of JMY in p53 Regulation. *Cancers (Basel).* 2018; 10(6):173.

Ahn JH, Jin SH, Kang H. LPS induces melanogenesis through p38 MAPK activation in human melanocytes. *Arch Dermatol Res*. 2008; Jul;300(6):325-9.

Akira S, Uematsu S, Takeuchi O. Pathogen Recognition and Innate Immunity. *Cell*. 2006; Feb 24;124(4):783-801

Aldhous MC, Abu Bakar S, Prescott NJ, et al. Measurement methods and accuracy in copy number variation: failure to replicate associations of beta-defensin copy number with Crohn's disease. *Hum Mol Genet*. 2010; Dec 15;19(24):4930-8.

Ali RS, Falconer A, Ikram M, et al. Expression of the peptide antibiotics human beta defensin-1 and human beta defensin-2 in normal human skin. *J Invest Dermatol*. 2001; Jul;117(1):106-11.

Ali SM, Yosipovitch G. Skin pH: From basic science to basic skin care. *Acta Derm Venereol*. 2013; May;93(3):261-7.

Aloia JF. African Americans, 25-hydroxyvitamin D, and osteoporosis: a paradox. *Am J Clin Nutr.* 2008; 88(2):545S–50S

Alzahofi N, Welz T, Robinson CL, et al. Rab27a co-ordinates actin-dependent transport by controlling organelle-associated motors and track assembly proteins. *Nat Commun.* 2020; 11(1):3495.

Anderson TM, vonHoldt BM, Candille SI, et al. Molecular and Evolutionary History of Melanism in North American Gray Wolves. *Science*. 2009; Mar 6;323(5919):1339-43.

Antonacci F, Kidd JM, Marques-Bonet T, et al. Characterization of six human disease-associated inversion polymorphisms. *Hum Mol Genet*. 2009; Jul 15;18(14):2555-66.

Arab A, Hadi A, Moosavian SP, et al. The association between serum vitamin D, fertility and semen quality: A systematic review and meta-analysis. *Int J Surg*. 2019; Nov;71:101-109.

Arca E, Tastan HB, Erbil AH, et al. Narrow-band ultraviolet B as monotherapy and in combination with topical calcipotriol in the treatment of vitiligo. *J Dermatol*. 2006; 33:338–343.

Armas LAG, Dowell S, Akhter M, et al. Ultraviolet-B radiation increases serum 25-hydroxyvitamin D levels: the effect of UVB dose and skin color. *Am Acad Dermatol*. 2007; 57(4):588–593.

Armour JA, Sismani C, Patsalis PC, et al. Measurement of locus copy number by hybridisation with amplifiable probes. *Nucleic Acids Res*. 2000; Jan 15;28(2):605-9.

Armour JA, Palla R, Zeeuwen PL, et al. Accurate, high-throughput typing of copy number variation using paralogue ratios from dispersed repeats. *Nucleic Acids Res*. 2007;35(3):e19.

Baba H, Uchiwa H, Watanabe S. UVB irradiation increases the release of SCF from human epidermal cells. *J Invest Dermatol*. 2005; May;124(5):1075-7.

Bade B, Zdebik A, Wagenpfeil S, et al. Low serum 25-hydroxyvitamin d concentrations are associated with increased risk for melanoma and unfavourable prognosis. *PLoS One*. 2014; Dec 1;9(12):e112863.

Bae-Harboe YS, Park HY. Tyrosinase: a central regulatory protein for cutaneous pigmentation. *J Invest Dermatol.* 2012; Dec;132(12):2678-80.

Baeke F, Takiishi T, Korf H, et al. Vitamin D: modulator of the immune system. *Curr Opin Pharmacol*. 2010;10(4):482-496.

Barrett JH, Iles MM, Harland M, et al. Genome-wide association study identifies three new melanoma susceptibility loci. *Nat Genet*. 2011; Oct 9;43(11):1108-13.

Barrett KG, Fang H, Kocarek TA, et al. Transcriptional Regulation of Cytosolic Sulfotransferase 1C2 by Vitamin D Receptor in LS180 Human Colorectal Adenocarcinoma Cells. *Drug Metab Dispos*. 2016; Aug;44(8):1431-4.

Basu Mallick C, Iliescu FM, Möls M, et al. The light skin allele of SLC24A5 in South Asians and Europeans shares identity by descent. *PLoS Genet*. 2013; Nov;9(11):e1003912.

Bau DT, Gurr JR, Jan KY. Nitric oxide is involved in arsenite inhibition of pyrimidine dimer excision. *Carcinogenesis*. 2001; May;22(5):709-16.

Baxter LL, Watkins-Chow DE, Pavan WJ, et al. A curated gene list for expanding the horizons of pigmentation biology *Pigment Cell Melanoma Res*. 2018; 32(3):348–358.

Beaumont KA, Smit DJ, Liu YY, et al. Melanocortin-1 receptor-mediated signalling pathways activated by NDP-MSH and HBD3 ligands. P*igment Cell Melanoma Res*. 2012; May;25(3):370-4.

Behrens J, von Kries JP, Kühl M, et al. Functional interaction of beta-catenin with the transcription factor LEF-1. *Nature*. 1996; Aug 15;382(6592):638-42.

Bellei B, Flori E, Izzo E, et al. GSK3beta inhibition promotes melanogenesis in mouse B16 melanoma cells and normal human melanocytes. *Cell Signal.* 2008; Oct;20(10):1750-61.

Bellei B, Pitisci A, Catricalà C, et al. Wnt/b-catenin signaling is stimulated by α-melanocyte-stimulating hormone in melanoma and melanocyte cells: implication in cell differentiation. *Pigment Cell Melanoma Res*. 2011; Apr;24(2):309-25.

Bellono NW, Escobar IE, Oancea E. A melanosomal two-pore sodium channel regulates pigmentation. *Sci Rep*. 2016; 6, 26570

Bentley RW, Pearson J, Gearry RB, et al. Association of higher *DEFB4* genomic copy number with Crohn's disease. *Am J Gastroenterol*. 2010; Feb;105(2):354-9.

Bianchi ME. DAMPs, PAMPs and alarmins: all we need to know about danger. *J Leukoc Biol*. 2007; Jan;81(1):1-5.

Bikle DD, Nemanic MK, Whitney JO, et al. Neonatal Human Foreskin Keratinocytes Produce 1,25-Dihydroxyvitamin D3. Biochemistry. 1986a; Apr 8;25(7):1545-8.

Bikle DD, Nemanic MK, Gee E, et al. 1,25-Dihydroxyvitamin D3 production by human keratinocytes. Kinetics and regulation. *J Clin Invest*. 1986b; Aug;78(2):557-66.

Bikle DD. VITAMIN D: Newly Discovered Actions Require Reconsideration of Physiologic Requirements. *Trends Endocrinol Metab*. 2010; Jun;21(6):375-84.

Bikle DD. Vitamin D Metabolism and Function in the Skin. *Mol Cell Endocrinol*. 2011; Dec 5;347(1-2):80-9.

Bikle DD, Oda Y, Teichert A. The vitamin D receptor: a tumor suppressor in skin. *Discov Med*. 2011; Jan;11(56):7-17.

Bikle DD. Vitamin D receptor, a tumor suppressor in skin. *Can J Physiol Pharmacol*. 2015; May;93(5):349-54.

Bikle DD. Vitamin D: Newer concepts of its metabolism and function at the basic and clinical level. *J Endocr Soc.* 2020; Feb 8;4(2):bvz038.

Bin BH, Bhin J, Yang SH, et al. Membrane-Associated Transporter Protein (MATP) Regulates Melanosomal pH and Influences Tyrosinase Activity. *PLoS One*. 2015; Jun 9;10(6):e0129273.

Birke M, Schöpe J, Wagenpfeil S, et al. Association of Vitamin D Receptor Gene Polymorphisms With Melanoma Risk: A Meta-analysis and Systematic Review. *Anticancer Res*. 2020; Feb;40(2):583-595.

Björn LO. VitaminD synthesis may be independent of skin pigmentation only with UV of short wavelength. *J Invest Dermatol*. 2010; 130:2848–2850.

Bogh MK, Schmedes AV, Philipsen PA, et al. Vitamin D production after UVB exposure depends on baseline vitamin D and total cholesterol but not on skin pigmentation*. J Invest Dermatol*. 2010; 130:546–553.

Bolerazska B, Rabajdova M, Spakova I, et al. Current knowledge on the active form of Vitamin D synthesized in the skin and its effects on malignant melanoma. *Neoplasma*. 2017; 64(1):1-12.

Box NF, Terzian T. The role of p53 in pigmentation, tanning and melanoma. Pigment *Cell Melanoma Res*. 2008;21(5):525-533.

Boyle GM, Pedley J, Martyn AC, et al. Macrophage Inhibitory Cytokine-1 Is Overexpressed in Malignant Melanoma and Is Associated with Tumorigenicity. *J Invest Dermatol*. 2009; Feb;129(2):383-91.

Braff MH, Bardan A, Nizet V, et al. Cutaneous defense mechanisms by antimicrobial peptides. *J Invest Dermatol*. 2005; Jul;125(1):9-13.

Branda RF, Eaton JW. Skin color and nutrient photolysis: An evolutionary hypothesis. *Science*. 1978; Aug 18;201(4356):625-6.

Brożyna AA, Jozwicki W, Janjetovic Z, et al. Expression of vitamin D receptor (VDR) decreases during progression of pigmented skin lesions. *Hum Pathol.* 2011; May;42(5):618-31.

Brożyna AA, Jóźwicki W, Janjetovic Z, et al. Expression of Vitamin D-Activating Enzyme 1α-Hydroxylase (CYP27B1) Decreases during Melanoma Progression. *Hum Pathol*. 2013; March; 44(3): 374–387

Brożyna AA, Jóźwicki W, Slominski AT. Decreased VDR expression in cutaneous melanomas as marker of tumor progression: new data and analyses. *Anticancer Res.* 2014; Jun;34(6):2735-43.

Brożyna AA, Hoffman RM, Slominski AT. Relevance of Vitamin D in Melanoma Development, Progression and Therapy. *Anticancer Res*. 2020; Jan;40(1):473-489.

Buniello A, MacArthur JAL, Cerezo M, et al. The NHGRI-EBI GWAS Catalog of published genome-wide association studies, targeted arrays and summary statistics 2019. *Nucleic Acids Res*. 2019; Jan 8;47(D1):D1005-D1012.

Busca R, Ballotti R. Cyclic AMP a key messenger in the regulation of skin pigmentation. *Pigment Cell Res*. 2000; Apr;13(2):60-9.

Cabrera J (2011). DNAMR: Analysis of DNA microarray data. R package version 1.0.

Cadet J, Douki T. Formation of UV-induced DNA damage contributing to skin cancer development. *Photochem Photobiol Sci.* 2018; Dec 5;17(12):1816-1841.

Candille SI, Kaelin CB, Cattanach BM, et al. A β-defensin mutation causes black coat color in domestic dogs. *Science*. 2007 Nov 30;318(5855):1418-23.

Cao J, Wan L, Hacker E, et al. MC1R is a Potent Regulator of PTEN after UV Exposure in Melanocytes. *Mol Cell*. 2013; Aug 22;51(4):409-22.

Carlson JA, Linette GP, Aplin A, et al. Melanocyte Receptors: Clinical Implications and Therapeutic Relevance. *Dermatol Clin*. 2007; Oct;25(4):541-57, viii-ix.

Carsberg CJ, Ohanian J, Friedmann PS. Ultraviolet radiation stimulates a biphasic pattern of 1,2-diacylglycerol formation in cultured human melanocytes and keratinocytes by activation of phospholipases C and D. *Biochem J.* 1995 Jan 15;305 (Pt 2):471-7.

Carter NP. Methods and strategies for analyzing copy number variation using DNA microarrays. *Nat Genet*. 2007 Jul;39(7 Suppl):S16-21.

Cashman KD, Dowling KG, Škrabáková Z, et al. Vitamin D deficiency in Europe: pandemic? *Am J Clin Nutr.* 2016; Apr;103(4):1033-44.

Cattaruzza MS, Pisani D, Fidanza L, et al. 25-Hydroxyvitamin D serum levels and melanoma risk: a case-control study and evidence synthesis of clinical epidemiological studies. *Eur J Cancer Prev*. 2019; May;28(3):203-211.

Chadebech P, Goidin D, Jacquet C, et al. Use of human reconstructed epidermis to analyze the regulation of beta-defensin hBD-1, hBD-2, and hBD-3 expression in response to LPS. *Cell Biol Toxicol.* 2003 Oct;19(5):313-24.

Chalhoub N, Benachenhou N, Rajapurohitam V, et al. Grey-lethal mutation induces severe malignant autosomal recessive osteopetrosis in mouse and human. *Nat Med*. 2003; 9(4):399-406.

Chaiprasongsuk A, Janjetovic Z, Kim TK, et al. Protective effects of novel derivatives of vitamin D3 and lumisterol against UVB-induced damage in human keratinocytes involve activation of Nrf2 and p53 defense mechanisms. *Redox Biol*. 2019; Jun;24:101206.

Chao CC, Chang PY, Lu HH. Human Gas7 isoforms homologous to mouse transcripts differentially induce neurite outgrowth. *J Neurosci Res*. 2005; Jul 15;81(2):153-62.

Chaplin, G. Geographic distribution of environmental factors influencing human skin coloration. *Am J Phys Anthropol*. 2004; Nov;125(3):292-302.

Chaplin G, Jablonski NG. Vitamin D and the evolution of human depigmentation. *Am J Phys Anthropol*. 2009; 139, 451–461.

Cheli Y, Luciani F, Khaled M, et al. α-MSH and Cyclic AMP elevating agents control melanosome pH through a protein kinase A-independent mechanism. *J Biol Chem*. 2009 Jul 10;284(28):18699-706.

Chen TC, Chimeh F, Lu Z, et al. Factors that influence the cutaneous synthesis and dietary sources of vitamin D. *Arch Biochem Biophys*. 2007; Apr 15;460(2):213-7.

Chen J, Doroudi M, Cheung J, et al. Plasma membrane Pdia3 and VDR interact to elicit rapid responses to 1α,25(OH)(2)D(3). *Cell Signal*. 2013; Dec;25(12):2362-73.

Chessa C, Bodet C, Jousselin C, et al. Antiviral and Immunomodulatory Properties of Antimicrobial Peptides Produced by Human Keratinocytes. *Front Microbiol*. 2020;11:1155.

Chiaverini C, Beuret L, Flori E, et al. Microphthalmia-associated transcription factor regulates RAB27A gene expression and controls melanosome transport. *J Biol Chem*. 2008; 283(18):12635-12642.

Ciechanover A, Orian A, Schwartz AL. Ubiquitin-mediated proteolysis: biological regulation via destruction. *Bioessays*. 2000; 22(5):442-451.

Cingolani P, Platts A, Wang le L, et al. A program for annotating and predicting the effects of single nucleotide polymorphisms, SnpEff: SNPs in the genome of *Drosophila melanogaster* strain w1118; iso-2; iso-3. *Fly (Austin).* 2012;6(2):80-92

Conde-Pérez A, Larue L. PTEN and melanomagenesis. *Future Oncol*. 2012; Sep;8(9):1109-20.

Cui R, Widlund HR, Feige E, et al. Central role of p53 in the suntan response and pathologic hyperpigmentation. *Cell*. 2007;128(5):853-864.

Curran K, Lister JA, Kunkel GR, et al. Interplay between Foxd3 and Mitf regulates cell fate plasticity in the zebrafish neural crest. *Dev Biol*. 2010; Aug 1;344(1):107-18.

Dahal U, Le K, Gupta M. RNA m6A methyltransferase METTL3 regulates invasiveness of melanoma cells by matrix metallopeptidase 2. *Melanoma Res*. 2019; Aug;29(4):382-389.

Dai X, Sayama K, Tohyama M, et al. PPARγ mediates innate immunity by regulating the 1α,25-dihydroxyvitamin D3 induced hBD-3 and cathelicidin in human keratinocytes. *J Dermatol Sci*. 2010; Dec;60(3):179-86.

Damek-Poprawa M, Diemer T, Lopes VS, et al. Melanoregulin (MREG) Modulates Lysosome Function in Pigment Epithelial Cells. *J Biol Chem*. 2009; Apr 17;284(16):10877-89.

Daraghmeh AH, Bertoia ML, Al-Qadi MO, et al. Evidence for the vitamin D hypothesis: The NHANES III extended mortality follow-up. *Atherosclerosis*. 2016; Dec;255:96-101.

De Angelis C, Galdiero M, Pivonello C, et al. The role of vitamin D in male fertility: A focus on the testis. *Rev Endocr Metab Disord*. 2017; Sep;18(3):285-305.

De Filippis A, Fiorentino M, Guida L, et al. Vitamin D reduces the inflammatory response by *Porphyromonas gingivalis* infection by modulating human β-defensin-3 in human gingival epithelium and periodontal ligament cells. *Int Immunopharmacol*. 2017 Jun;47:106-117.

De Haes P, Garmyn M, Degreef H, et al. 1,25-Dihydroxyvitamin D3 inhibits ultraviolet B-induced apoptosis, Jun kinase activation, and interleukin-6 production in primary human keratinocytes. *J Cell Biochem*. 2003; 89:663-73.

De Haes P, Garmyn M, Verstuyf A, et al. 1,25-Dihydroxyvitamin D3 and analogues protect primary human keratinocytes against UVB-induced DNA damage. *J Photochem Photobiol B.* 2005; Feb 1;78(2):141-8.

Del Puerto C, Navarrete-Dechent C, Molgó M, et al. Immunohistochemical expression of vitamin D receptor in melanocytic naevi and cutaneous melanoma: a case–control study. *Br J Dermatol*. 2018; Jul;179(1):95-100.

DeLuca HF. Overview of general physiologic features and functions of vitamin D. *Am J Clin Nutr*. 2004; Dec;80(6 Suppl):1689S-96S.

Demeule M, Bertrand Y, Michaud-Levesque J, et al. Regulation of plasminogen activation: a role for melanotransferrin (p97) in cell migration. *Blood*. 2003; Sep 1;102(5):1723-31.

Denning MF. Specifying protein kinase C functions in melanoma. *Pigment Cell Melanoma Res*. 2012 Jul;25(4):466-76.

Dennis MK, Delevoye C, Acosta-Ruiz A, et al. BLOC-1 and BLOC-3 regulate VAMP7 cycling to and from melanosomes via distinct tubular transport carriers. *J Cell Biol*. 2016; 214(3):293-308.

Denzer N, Vogt T, Reichrath J. Vitamin D receptor (VDR) polymorphisms and skin cancer: A systematic review. *Dermatoendocrinol*. 2011; Jul;3(3):205-10.

De Smedt J, Van Kelst S, Boecxstaens V, et al. Vitamin D supplementation in cutaneous malignant melanoma outcome (ViDMe): a randomized controlled trial. *BMC Cancer*. 2017; Aug 23;17(1):562.

Dey-Rao R, Sinha AA. Vitiligo blood transcriptomics provides new insights into disease mechanisms and identifies potential novel therapeutic targets. *BMC Genomics*. 2017; Jan 28;18(1):109.

Dhople V, Krukemeyer A, Ramamoorthy A. The human beta-defensin-3, an antibacterial peptide with multiple biological functions. *Biochim Biophys Acta*. 2006 Sep;1758(9):1499-512.

Di Stasi D, Vallacchi V, Campi V, et al. DHCR24 gene expression is upregulated in melanoma metastases and associated to resistance to oxidative stress-induced apoptosis. *Int J Cancer*. 2005; Jun 10;115(2):224-30.

Dixon KM, Deo SS, Wong G, et al. Skin cancer prevention: A possible role of 1,25dihydroxyvitamin D3 and its analogs. *J Steroid Biochem Mol Biol*. 2005; Oct;97(1-2):137-43.

Dixon KM, Deo SS, Norman AW, et al. *In vivo* relevance for photoprotection by the vitamin D rapid response pathway. *J Steroid Biochem Mol Biol*. 2007; Mar;103(3-5):451-6.

Dixon KM, Norman AW, Sequeira VB, et al. 1α,25(OH)2-vitamin D and a nongenomic vitamin D analogue inhibit ultraviolet radiation-induced skin carcinogenesis. *Cancer Prev Res (Phila)*. 2011; Sep;4(9):1485-94.

Dobin A, Davis CA, Schlesinger F, et al. STAR: ultrafast universal RNAseq aligner. *Bioinformatics.* 2013; 29: 15–21.

Dubaisi S, Barrett KG, Fang H, et al. Regulation of cytosolic sulfotrasnferases in models of human hepatocyte development. *Drug Metab Dispos*. 2018; Aug;46(8):1146-1156.

Duffy DL, Zhu G, Li X, et al. Novel pleiotropic risk loci for melanoma and nevus density implicate multiple biological pathways. *Nat Commun*. 2018; Nov 14;9(1):4774.

Durazo-Arvizu RA, Camacho P, Bovet P, et al. 25-Hydroxyvitamin D in African-origin populations at varying latitudes challenges the construct of a physiologic norm. *Am J Clin Nutr*. 2014; Sep;100(3):908-14.

Dye DE, Medic S, Ziman M, et al. Melanoma biomolecules: independently identified but functionally intertwined. *Front Oncol*. 2013; Sep 24;3:252.

Egan KM, Signorello LB, Munro HM, et al. Vitamin D insufficiency among African-Americans in the southeastern United States: implications for cancer disparities (United States). *Cancer Causes Control*. 2008; Jun;19(5):527-35.

Elias PM, Menon G, Wetzel BK, et al. Evidence that stress to the epidermal barrier influenced the development of pigmentation in humans. *Pigment Cell Melanoma Res*. 2009; Aug;22(4):420-34.

Elias PM, Menon G, Wetzel BK, et al. Barrier Requirements as the Evolutionary "Driver" of Epidermal Pigmentation in Humans. *Am J Hum Biol*. 2010; Jul-Aug;22(4):526-37.

Elias PM, Williams ML. Basis for the gain and subsequent dilution of epidermal pigmentation during human evolution: The barrier and metabolic conservation hypotheses revisited. *Am J Phys Anthropol*. 2016; Oct;161(2):189-207.

Ellison TI, Smith MK, Gilliam AC, et al. Inactivation of the vitamin D receptor enhances susceptibility of murine skin to UV-induced tumorigenesis. *J Invest Dermatol*. 2008; Oct;128(10):2508-17.

Ericson MD, Singh A, Tala SR, et al. Human β‑Defensin 1 and β‑Defensin 3 (Mouse Ortholog mBD14) Function as Full Endogenous Agonists at Select Melanocortin Receptors. *J Med Chem*. 2018; Apr 26;61(8):3738-3744.

Fan Y, Zhang Y, Xu S, et al. Insights from ENCODE on Missing Proteins: Why β‑Defensin Expression Is Scarcely Detected. *J Proteome Res*. 2015 Sep 4;14(9):3635-44.

Fang S, Sui D, Wang Y, et al. Association of vitamin D levels with outcome in patients with melanoma after adjustment for C-reactive protein. *J Clin Oncol*. 2016; May 20;34(15):1741-7.

Farrar MD, Kift R, Felton SJ, et al. Recommended summer sunlight exposure levels fail to produce sufficient vitamin D status in UK adults of South Asian origin. *Am J Clin Nutr*. 2011; 94, 1219–1224.

Feldman D, Krishnan AV, Swami S, et al. The role of vitamin D in reducing cancer risk and progression. *Nat Rev Cancer*. 2014; May;14(5):342-57.

Fellermann K, Stange DE, Schaeffeler E, et al. A chromosome 8 gene-cluster polymorphism with low human beta-defensin 2 gene copy number predisposes to Crohn disease of the colon. *Am J Hum Genet*. 2006 Sep;79(3):439-48.

Fernandez-Jimenez N, Castellanos-Rubio A, Plaza-Izurieta L, et al. Analysis of β-defensin and Toll-like receptor gene copy number variation in celiac disease. *Hum Immunol*. 2010 Aug;71(8):833-6.

Fernandez-Jimenez N, Castellanos-Rubio A, Plaza-Izurieta L, et al. Accuracy in Copy Number Calling by qPCR and PRT: A Matter of DNA. *PLoS One*. 2011;6(12):e28910.

Fischer M. Census and evaluation of p53 target genes. Oncogene. 2017; 36(28):3943-3956.

Fishilevich S, Nudel R, Rappaport N, et al. GeneHancer: genome-wide integration of enhancers and target genes in GeneCards. *Database (Oxford)*. 2017 Jan 1;2017.

Fitzpatrick TB. The Validity and Practicality of Sun-Reactive Skin Types I Through VI. *Arch Dermatol*. 1988; Jun;124(6):869-71

Fluhr JW, Elias PM. Stratum corneum pH: Formation and function of the 'Acid Mantle'. *Exog Dermatol.* 2002; 1:163–175

Fode P, Jespersgaard C, Hardwick RJ, et al. Determination of Beta-Defensin Genomic Copy Number in Different Populations: A Comparison of Three Methods. *PLoS One*. 2011 Feb 22;6(2):e16768.

Ford L, Graham V, Wall A, et al. Vitamin D concentrations in an UK inner-city multicultural outpatient population. *Ann Clin Biochem.* 2006; 43:468e73

Forni D, Martin D, Abujaber R, et al. Determining multiallelic complex copy number and sequence variation from high coverage exome sequencing data. *BMC Genomics*. 2015 Nov 2;16:891.

Friedmann PS, Wren FE, Matthews JN. Ultraviolet stimulated melanogenesis by human melanocytes is augmented by di-acyl glycerol but not TPA. *J. Cell Physiol*. 1990 142, 334–341

Froy O. Regulation of mammalian defensin expression by Toll-like receptor-dependent and independent signalling pathways. *Cell Microbiol.* 2005 Oct;7(10):1387-97.

Fruitwala S, El-Naccache DW, Chang TL. Multifaceted immune functions of human defensins and underlying mechanisms. *Semin Cell Dev Biol*. 2019;88:163-172.

Fuller BB, Spaulding DT, Smith DR. Regulation of the catalycit activity of pre-existing tyrosinase in black and Caucasian human melanocyte cell cultures. *Exp Cell Res*. 2001 Jan 15;262(2):197-208.

Funasaka Y, Hayashi Y, Komoto M, et al. Modulation of melanocyte-stimulating hormone receptor expression on normal human melanocytes: evidence for a regulatory role of ultraviolet B, interleukin-1α, interleukin-1β, endothelin-1 and tumour necrosis factor-α. *Br J Dermatol*. 1998 Aug;139(2):216-24.

Furukawa K, Hamamura K, Ohkawa Y, et al. Disialyl gangliosides enhance tumor phenotypes with differential modalities. *Glycoconj J*. 2012; Dec;29(8-9):579-84.

Gambichler T, Bindsteiner M, Höxtermann S, et al. Serum 25-hydroxyvitamin D serum levels in a large German cohort of patients with melanoma. *Br J Dermatol.* 2013; Mar;168(3):625-8.

Ganz T. Defensins: antimicrobial peptides of innate immunity. *Nat Rev Immunol.* 2003 Sep;3(9):710-20.

Garcia RJ, Ittah A, Mirabal S, Figueroa J, et al. Endothelin 3 induces skin pigmentation in a keratin-driven inducible mouse model. *J Invest Dermatol.* 2008 Jan;128(1):131-42.

Gaudel C, Soysouvanh F, Leclerc J, et al. Regulation of Melanogenesis by the Amino Acid Transporter SLC7A5 [published online ahead of print, 2020 Mar 30]. *J Invest Dermatol*. 2020; S0022-202X(20)31209-4.

Giamarellos-Bourboulis EJ, Platzer M, Karagiannidis I, et al. High Copy Numbers of β-Defensin Cluster on 8p23.1, Confer Genetic Susceptibility, and Modulate the Physical Course of Hidradenitis Suppurativa/Acne Inversa. *J Invest Dermatol*. 2016 Aug;136(8):1592-1598.

Gibbs DC, Orlow I, Kanetsky PA, et al. Inherited genetic variants associated with occurrence of multiple primary melanoma. *Cancer Epidemiol Biomarkers Prev*. 2015; Jun;24(6):992-7.

Giglio S, Broman KW, Matsumoto N, et al. Olfactory receptor-gene clusters, genomic-inversion polymorphisms, and common chromosome rearrangements. *Am J Hum Genet*. 2001 Apr;68(4):874-83.

Gläser R, Röwert J, Mrowietz U. Hyperpigmentation due to topical calcipotriol and photochemotherapy in two psoriatic patients. *Br J Dermatol*. 1998; Jul;139(1):148-51.

Gläser R, Navid F, Schuller W, et al. UV-B radiation induces the expression of antimicrobial peptides in human keratinocytes in vitro and in vivo. *J Allergy Clin Immunol*. 2009 May;123(5):1117-23.

Goktas EO, Aydin F, Senturk N, et al. Combination of narrow band UVB and topical calcipotriol for the treatment of vitiligo. *J Eur Acad Dermatol Venereol*. 2006; 20:553–557.

Gonzalez-Curiel I, Trujillo V, Montoya-Rosales A, et al. 1,25-dihydroxyvitamin D3 induces LL-37 and HBD-2 production in keratinocytes from diabetic foot ulcers promoting wound healing: an in vitro model. *PLoS One*. 2014; Oct 22;9(10):e111355.

Gordon PR, Gilchrest BA. Human melanogenesis is stimulated by diacylglycerol. *J Invest Dermatol.* 1989 Nov;93(5):700-2.

Gordon-Thomson C, Gupta R, Tongkao-on W, et al. 1α,25 Dihydroxyvitamin D3 enhances cellular defences against UV-induced oxidative and other forms of DNA damage in skin. *Photochem Photobiol Sci*. 2012; Dec;11(12):1837-47.

Graffelman J. Exploring Diallelic Genetic Markers: The HardyWeinberg Package. *J Stat Softw*. 2015; 64(3), 1-23. URL http://www.jstatsoft.org/v64/i03/.

Grant WB. The UVB–vitamin D3–pigment hypothesis is alive and well. *Am J Phys Anthropol.* 2016; Dec;161(4):752-755.

Greaves M. Was skin cancer a selective force for black pigmentation in early hominin evolution? *Proc Biol Sci*. 2014; Feb 26;281(1781):20132955.

Groth M, Szafranski K, Taudien S, et al. High-resolution mapping of the 8p23.1 beta-defensin cluster reveals strictly concordant copy number variation of all genes. *Hum Mutat*. 2008 Oct;29(10):1247-54.

Groth M, Wiegand C, Szafranski K, et al. Both copy number and sequence variations affect expression of human DEFB4. *Genes Immun*. 2010 Sep;11(6):458-66.

Grichnik JM, Burch JA, Burchette J, et al. The SCF/KIT pathway plays a critical role in the control of normal human melanocyte homeostasis. *J Invest Dermatol*. 1998 Aug;111(2):233-8.

Gunathilake R, Schurer NY, Shoo BA, et al. pH-Regulated Mechanisms Account for Pigment-Type Differences in Epidermal Barrier Function. *J Invest Dermatol*. 2009; Jul;129(7):1719-29.

Guo H, Yang K, Deng F, et al. Wnt3a inhibits proliferation but promotes melanogenesis of melan-a cells. *Int J Mol Med*. 2012 Sep;30(3):636-42.

Gupta R, Dixon KM, Deo SS, et al. Photoprotection by 1,25 Dihydroxyvitamin D3 is associated with an increase in p53 and a decrease in nitric oxide products. *J Invest Dermatol*. 2007; Mar;127(3):707-15.

Gutenkunst RN, Hernandez RD, Williamson SH, et al. Inferring the Joint Demographic History of Multiple Populations from Multidimensional SNP Frequency Data. *PLoS Genet*. 2009; Oct;5(10):e1000695.

Hachiya A, Kobayashi A, Ohuchi A, et al. The paracrine role of stem cell factor/c-kit signalling in the activation of human melanocytes in ultraviolet-B-induced pigmentation. *J Invest Dermatol*. 2001 Apr;116(4):578-86.

Hagiwara M, Brindle P, Harootunian A, et al. Coupling of hormonal stimulation and transcription via the cyclic AMP-responsive factor CREB is rate limited by nuclear entry of protein kinase A. *Mol Cell Biol*. 1993 Aug;13(8):4852-9.

Handsaker RE, Van Doren V, Berman JR, et al. Large multi-allelic copy number variations in humans. *Nat Genet*. 2015 Mar;47(3):296-303.

Hara M, Yaar M, Gilchrest BA. Endothelin-1 of keratinocyte origin is a mediator of melanocyte dendricity. *J Invest Dermatol.* 1995 Dec;105(6):744-8.

Harder J, Bartels J, Christophers E, et al. A peptide antibiotic from human skin. *Nature*. 1997; 387(6636):861.

Harder J, Bartels J, Christophers E, et al. Isolation and characterization of human beta-defensin-3, a novel human inducible peptide antibiotic. *J Biol Chem*. 2001 Feb 23;276(8):5707-13.

Harder J, Meyer-Hoffert U, Wehkamp K, et al. Differential gene induction of human beta-defensins (hBD-1, -2, -3, and -4) in keratinocytes is inhibited by retinoic acid. *J Invest Dermatol*. 2004; 123(3):522-529.

Harder J, Dressel S, Wittersheim M, et al. Enhanced expression and secretion of antimicrobial peptides in atopic dermatitis and after superficial skin injury. *J Invest Dermatol*. 2010 May;130(5):1355-64.

Hardwick RJ, Machado LR, Zuccherato LW, et al. A worldwide analysis of beta-defensin copy number variation suggests recent selection of a high-expressing *DEFB103* gene copy in East Asia. *Hum Mutat*. 2011 Jul;32(7):743-50.

Hardwick RJ, Amogne W, Mugusi S, et al. β-defensin genomic copy number is associated with HIV load and immune reconstitution in sub-saharan Africans. *J Infect Dis*. 2012 Oct 1;206(7):1012-9.

Harris SS. Vitamin D and African Americans. *J Nutr*. 2006; Apr;136(4):1126-9.

Hartmann A, Lurz C, Hamm H, et al. Narrow-band UVB311nm vs. broadband UVB therapy in combination with topical calcipotriol vs. placebo in vitiligo. *Int J Dermatol*. 2005; 44:736–742.

Hattori H, Kawashima M, Ichikawa Y, et al. The epidermal stem cell factor is over-expressed in lentigo senilis: implication for the mechanism of hyperpigmentation. *J Invest Dermatol*. 2004 May;122(5):1256-65.

Haussler MR, Jurutka PW, Mizwicki M, et al. Vitamin D receptor (VDR)-mediated actions of 1α,25$(OH)_2$vitamin $D_3$: genomic and non-genomic mechanisms. *Best Pract Res Clin Endocrinol Metab*. 2011; Aug;25(4):543-59.

Haupt Y, Maya R, Kazaz A, et al. Mdm2 promotes the rapid degradation of p53. *Nature*. 1997;387(6630):296-299.

Heath AK, Kim IY, Hodge AM, et al. Vitamin D Status and Mortality: A Systematic Review of Observational Studies. *Int J Environ Res Public Health*. 2019; Jan 29;16(3). pii: E383.

Hellborg F, Qian W, Mendez-Vidal C, et al. Human wig-1, a p53 target gene that encodes a growth inhibitory zinc finger protein. *Oncogene*. 2001; Sep 6;20(39):5466-74.

Hellenthal G, Stephens M. msHOT: modifying Hudson's ms simulator to incorporate crossover and gene conversion hotspots. *Bioinformatics*. 2007; Feb 15;23(4):520-521

Henry J, Toulza E, Hsu CY, et al. Update on the epidermal differentiation complex. *Front Biosci (Landmark Ed*). 2012; Jan 1;17:1517-32.

Herraiz C, Jiménez-Cervantes C, Zanna P, et al. Melanocortin 1 receptor mutations impact differentially on signalling to the cAMP and the ERK mitogen-activated protein kinase pathways. *FEBS Lett*. 2009;583(19):3269-3274.

Herraiz C, Journé F, Abdel-Malek Z, et al. Signaling from the human melanocortin 1 receptor to ERK1 and ERK2 mitogen-activated protein kinases involves transactivation of cKIT. *Mol Endocrinol*. 2011 Jan;25(1):138-56.

Heyne K, Heil TC, Bette B, Reichrath J, Roemer K. MDM2 binds and inhibits vitamin D receptor. *Cell Cycle*. 2015;14(13):2003-2010.

Hida T, Wakamatsu K, Sviderskaya EV, et al. Agouti protein, mahogunin, and attractin in pheomelanogenesis and melanoblast-like alteration of melanocytes: a cAMP-independent pathway. Pigment *Cell Melanoma Res*. 2009; 22(5):623-634.

Higashi T, Goto A, Morohashi M, et al. Development and validation of a method for determination of plasma 25-hydroxyvitamin D3 3-sulfate using liquid chromatography/tandem mass spectrometry. *J Chromatogr B Analyt Technol Biomed Life Sci*. 2014; Oct 15;969:230-4.

Hii CS, Ferrante A. The Non-Genomic Actions of Vitamin D. *Nutrients.* 2016; Mar 2;8(3):135.

Hino S, Tanji C, Nakayama KI, et al. Phosphorylation of beta-catenin by cyclic AMP-dependent protein kinase stabilizes beta-catenin through inhibition of its ubiquitination. *Mol Cell Biol*. 2005 Oct;25(20):9063-72.

Hirsch T, Spielmann M, Zuhaili B, et al. Human beta-defensin-3 promotes wound healing in infected diabetic wounds. *J Gene Med*. 2009 Mar;11(3):220-8.

Hoek KS, Schlegel NC, Eichhoff OM, et al. Novel MITF targets identified using a two-step DNA microarray strategy. *Pigment Cell Melanoma Res*. 2008; Dec;21(6):665-76.

Hofmann UB, Westphal JR, Van Muijen GN, et al. Matrix metalloproteinases in human melanoma. *J Invest Dermatol*. 2000; Sep;115(3):337-44.

Holick MF, Smith E, Pincus S. Skin as the site of vitamin D synthesis and target tissue for 1,25-dihydroxyvitamin D3. Use of calcitriol (1,25-dihydroxyvitamin D3) for treatment of psoriasis. *Arch Dermatol*. 1987; Dec;123(12):1677-1683a.

Holick MF. Vitamin D: a millennium perspective. *J Cell Biochem*. 2003; 88(2):296–307.

Holick MF. Vitamin D deficiency. *N Engl J Med*. 2007; Jul 19;357(3):266-81.

Holick MF, Chen TC. Vitamin D deficiency: a worldwide problem with health consequences. *Am J Clin Nutr*. 2008; Apr;87(4):1080S-6S.

Holick MF. The vitamin D deficiency pandemic: Approaches for diagnosis, treatment and prevention. *Rev Endocr Metab Disord*. 2017; Jun;18(2):153-165.

Hollox EJ, Akrami SM, Armour JA. DNA copy number analysis by MAPH: molecular diagnostic applications. *Expert Rev Mol Diagn*. 2002 Jul;2(4):370-8.

Hollox EJ, Armour JA, Barber JC. Extensive normal copy number variation of a beta-defensin antimicrobial-gene cluster. *Am J Hum Genet.* 2003 Sep;73(3):591-600.

Hollox EJ. Copy number variation of beta-defensins and relevance to disease. *Cytogenet Genome Res*. 2008;123(1-4):148-55.

Hollox EJ, Barber JC, Brookes AJ, et al. Defensins and the dynamic genome: What we can learn from structural variation at human chromosome band 8p23.1. *Genome Res*. 2008a Nov;18(11):1686-97.

Hollox EJ, Huffmeier U, Zeeuwen PL, et al. Psoriasis is associated with increased beta-defensin genomic copy number. *Nat Genet*. 2008b Jan;40(1):23-5.

Hollox EJ, Armour JA. Directional and balancing selection in human beta-defensins. *BMC Evol Biol*. 2008 Apr 16;8:113.

Hong SP, Kim MJ, Jung MY, et al. Biopositive effects of low-dose UVB on epidermis: coordinate upregulation of antimicrobial peptides and permeability barrier reinforcement. *J Invest Dermatol*. 2008; Dec;128(12):2880-7.

Hosoi J, Abe E, Suda T, et al. Regulation of melanin synthesis of B16 mouse melanoma cells by 1 alpha, 25-dihydroxyvitamin D3 and retinoic acid. *Cancer Res*. 1985; Apr;45(4):1474-8.

Huber O, Korn R, McLaughlin J, et al. Nuclear localization of fl-catenin by interaction with transcription factor LEF-1. *Mech Dev*. 1996 Sep;59(1):3-10.

Hudson RR. Generating samples under a Wright-Fisher neutral model. *Bioinformatics*. 2002; Feb;18(2):337-8.

Huhtakangas JA, Olivera CJ, Bishop JE, et al. The vitamin D receptor is present in caveolae-enriched plasma membranes and binds 1 alpha,25(OH)2-vitamin D3 in vivo and in vitro. *Mol Endocrinol*. 2004; 18: 2660–2671.

Hutchinson PE, Osborne JE, Lear JT, et al. Vitamin D receptor polymorphisms are associated with altered prognosis in patients with malignant melanoma. *Clin Cancer Res*. 2000; Feb;6(2):498-504.

Hyter S, Coleman DJ, Ganguli-Indra G, et al. Endothelin-1 is a transcriptional target of p53 in epidermal keratinocytes and regulates ultraviolet induced melanocyte homeostasis. *Pigment Cell Melanoma Res*. 2013 Mar;26(2):247-58.

Imokawa G, Yada Y, Miyagishi M. Endothelins secreted from human keratinocytes are intrinsic mitogens for human melanocytes. *J Biol Chem*. 1992 Dec 5;267(34):24675-80.

Imokawa G, Miyagishi M, Yada Y. Endothelin-1 as a new melanogen: coordinated expression of its gene and the tyrosinase gene in UVB-exposed human epidermis. *J Invest Dermatol*. 1995 Jul;105(1):32-7.

Imokawa G, Yada Y, Kimura M. Signalling mechanisms of endothelin-induced mitogenesis and melanogenesis in human melanocytes. *Biochem J*. 1996 Feb 15;314 (Pt 1):305-12.

Imokawa G, Kobayasi T, Miyagishu M. Intracellular signalling mechanism leading to synergistic effects of endothelin-1 and stem cell factor on proliferation of cultured human melanocytes. Cross-talk via trans-activation of the tyrosine kinase c-kit receptor. *J Biol Chem*. 2000 Oct 27;275(43):33321-8.

Imokawa G, Ishida K. Inhibitors of intracellular signalling pathways that lead to stimulated epidermal pigmentation: perspective of anti-pigmenting agents. *Int J Mol Sc*i. 2014 May 12;15(5):8293-315

Ishida M, Ohbayashi N, Maruta Y, et al. Functional involvement of Rab1A in microtubule-dependent anterograde melanosome transport in melanocytes. *J Cell Sci*. 2012; 125(Pt 21):5177-5187.

Ishida M, Ohbayashi N, Fukuda M. Rab1A regulates anterograde melanosome transport by recruiting kinesin-1 to melanosomes through interaction with SKIP. *Sci Rep*. 2015; 5:8238.

Ishikawa T, Kanda N, Hau CS, et al. Histamine induces human beta-defensin-3 production in human keratinocytes. *J Dermatol Sci*. 2009; 56(2):121-127.

Ito S, IFPCS. The IFPCS presidential lecture: a chemist's view of melanogenesis. *Pigment Cell Res*. 2003 Jun;16(3):230-6.

Jablonski NG, Chaplin G. The evolution of human skin coloration. *J Hum Evol*. 2000; Jul;39(1):57-106.

Jablonski NG, Chaplin G. Human skin pigmentation as an adaptation to UV radiation. *Proc Natl Acad Sci USA*. 2010; 107,8962–8968

Jablonski NG, Chaplin G. The colours of humanity: the evolution of pigmentation in the human lineage. *Philos Trans R Soc Lond B Biol Sci*. 2017; Jul 5;372(1724). pii: 20160349.

Jagoda SV, Dixon KM. Protective effects of 1,25 dihydroxyvitamin D3 and its analogs on ultraviolet radiation-induced oxidative stress: a review. *Redox Rep*. 2020; Dec;25(1):11-16.

James CP, Bajaj-Elliott M, Abujaber R, et al. Human beta defensin (HBD) gene copy number affects HBD2 protein levels: impact on cervical bactericidal immunity in pregnancy. *Eur J Hum Genet*. 2018 Mar;26(3):434-439.

Jani RA, Purushothaman LK, Rani S, et al. STX13 regulates cargo delivery from recycling endosomes during melanosome biogenesis. *J Cell Sci*. 2015; 128(17):3263-3276.

Jarrett SG, Wolf Horrell EM, Boulanger MC, et al. Defining the Contribution of MC1R Physiological Ligands to ATR Phosphorylation at Ser435, a Predictor of DNA Repair in Melanocytes. *J Invest Dermatol*. 2015;135(12):3086-3095.

Jeayeng S, Wongkajornsilp A, Slominski AT, et al. Nrf2 in keratinocytes modulates UVB-induced DNA damage and apoptosis in melanocytes through MAPK signaling. *Free Radic Biol Med*. 2017; Jul;108:918-928.

Jiang X, O'Reilly PF, Aschard H, et al. Genome-wide association study in 79,366 European-ancestry individuals informs the genetic architecture of 25-hydroxyvitamin D levels. *Nat Commu*n. 2018; Jan 17;9(1):260.

Jones G, Prosser DE, Kaufmann M. 25-Hydroxyvitamin D-24-hydroxylase (CYP24A1): its important role in the degradation of vitamin D. *Arch Biochem Biophys*. 2012; Jul 1;523(1):9-18.

Jones EA, Kananurak A, Bevins CL, et al. Copy Number Variation of the Beta Defensin Gene Cluster on Chromosome 8p Influences the Bacterial Microbiota within the Nasopharynx of Otitis-Prone Children. *PLoS One*. 2014 May 27;9(5):e98269.

Jordens I, Westbroek W, Marsman M, et al. Rab7 and Rab27a control two motor protein activities involved in melanosomal transport. *Pigment Cell Res*. 2006; 19(5):412-423.

Kadalayil L, Rafiq S, Rose-Zerilli MJ, et al. Exome sequence read depth methods for identifying copy number changes. *Brief Bioinform*. 2015 May;16(3):380-92.

Kadekaro AL, Kavanagh R, Kanto H, et al. alpha-Melanocortin and endothelin-1 activate antiapoptotic pathways and reduce DNA damage in human melanocytes. *Cancer Res.* 2005 May 15;65(10):4292-9.

Kadekaro AL, Leachman S, Kavanagh RJ, et al. Melanocortin 1 receptor genotype: an important determinant of the damage response of melanocytes to ultraviolet radiation. *FASEB J*. 2010; Oct; 24(10): 3850–3860.

Kadekaro AL, Chen J, Yang J, et al. Alpha-melanocyte-stimulating hormone suppresses oxidative stress through a p53-mediated signaling pathway in human melanocytes. *Mol Cancer Res*. 2012; 10(6):778-786.

Kalus AA, Fredericks LP, Hacker BM, et al. Association of a genetic polymorphism (-44 C/G SNP) in the human *DEFB1* gene with expression and inducibility of multiple β-defensins in gingival keratinocytes. *BMC Oral Health*. 2009 Aug 27;9:21.

Kanda N, Ishikawa T, Watanabe S. Prostaglandin D2 induces the production of human beta-defensin-3 in human keratinocytes. *Biochem Pharmacol*. 2010; 79(7):982-989.

Katayama I, Ashida M, Maeda A, et al. Open trial of topical tacalcitol [1 alpha 24(OH)2D3] and solar irradiation for vitiligo vulgaris: Upregulation of c-Kit mRNA by cultured melanocytes. *Eur J Dermatol*. 2003; 13:372–376.

Kawakami T, Ohgushi A, Hirobe T, et al. Effects of 1,25-dihydroxyvitamin D3 on human epidermal melanocytes and melanoblasts. *J Dermatol Sci*. 2014; Oct;76(1):72-4.

Kerns JA, Cargill EJ, Clark LA, et al. Linkage and segregation analysis of black and brindle coat color in domestic dogs. *Genetics*. 2007; Jul;176(3):1679-89.

Khammissa RAG, Fourie J, Motswaledi MH, et al. The biological activities of vitamin D and its receptor in relation to calcium and bone homeostasis, cancer, immune and cardiovascular systems, skin biology, and oral health. *Biomed Res Int*. 2018; May 22;2018:9276380.

Khlgatian MK, Hadshiew IM, Asawanonda P, et al. Tyrosinase gene expression is regulated by p53. *J Invest Dermatol*. 2002;118(1):126-132.

Kiatsurayanon C, Niyonsaba F, Smithrithee R, et al. Host defense (Antimicrobial) peptide, human β-defensin-3, improves the function of the epithelial tight-junction barrier in human keratinocytes. *J Invest Dermatol*. 2014 Aug;134(8):2163-2173.

Kichaev G, Bhatia G, Loh PR, et al. Leveraging Polygenic Functional Enrichment to Improve GWAS Power. *Am J Hum Genet*. 2019; Jan 3;104(1):65-75.

Kim YJ, Hong CK, Seo SJ. Regulation of human beta-defensin 3 (hBD-3) in human keratinocyte (HaCaT) cell lines. *Annals of Dermatology*. 2003 15(1):1

Kim BJ, Rho YK, Lee HI, et al. The Effect of Calcipotriol on the Expression of Human β Defensin-2 and LL-37 in Cultured Human Keratinocytes. *Clin Dev Immunol*. 2009; 2009:645898.

Kim D, Langmead B, Salzberg SL. HISAT: a fast spliced aligner with low memory requirements. *Nat Methods*. 2015; Apr;12(4):357-60.

Kisich KO, Howell MD, Boguniewicz M, et al. The constitutive capacity of human keratinocytes to kill *Staphylococcus aureus* is dependent on beta-defensin 3. *J Invest Dermatol*. 2007 Oct;127(10):2368-80.

Koike S, Yamasaki K, Yamauchi T, et al. Toll-like receptors 2 and 3 enhance melanogenesis and melanosome transport in human melanocytes. *Pigment Cell Melanoma Res*. 2018; Sep;31(5):570-584.

Kokot A, Metze D, Mouchet N, et al. Alpha-melanocyte-stimulating hormone counteracts the suppressive effect of UVB on Nrf2 and Nrf-dependent gene expression in human skin. *Endocrinology*. 2009;150(7):3197-3206.

Krumm N, Sudmant PH, Ko A, et al. Copy number variation detection and genotyping from exome sequence data. *Genome Res*. 2012 Aug;22(8):1525-32.

Kullavanijaya P, Lim HW. Topical calcipotriene and narrow-band ultraviolet B in the treatment of vitiligo. *Photodermatol Photoimmunol Photomed.* 2004; 20:248–251.

Kurogi K, Sakakibara Y, Suiko M, et al. Sulfation of vitamin D3-related compounds—identification and characterization of the responsible human cytosolic sulfotransferases. *FEBS Lett*. 2017; Aug;591(16):2417-2425.

Kutmon M, Riutta A, Nunes N, et al. WikiPathways: capturing the full diversity of pathway knowledge. *Nucleic Acids Res*. 2016; Jan 4;44(D1):D488-94.

Laig M, Fekete C, Majumdar N. Digital PCR and the QuantStudio™ 3D Digital PCR System. *Methods Mol Biol*. 2020;2065:209-231.

Lee J, Youn JI. The photoprotective effect of 1,25-dihydroxyvitamin D3 on ultraviolet light B-induced damage in keratinocyte and its mechanism of action. *J Dermatol Sci*. 1998; Sep;18(1):11-8.

Lee YR, Chen M, Pandolfi PP. The functions and regulation of the PTEN tumour suppressor: new modes and prospects. *Nat Rev Mol Cell Biol*. 2018; Sep;19(9):547-562.

Lehmann B, Knuschke P, Meurer M. UVB-induced conversion of 7-dehydrocholesterol to 1 alpha,25-dihydroxyvitamin D3 (calcitriol) in the human keratinocyte line HaCaT. *Photochem Photobiol*. 2000; Dec;72(6):803-9.

Lehmann B, Rudolph T, Pietzsch J, et al. Conversion of vitamin D3 to 1alpha,25-dihydroxyvitamin D3 in human skin equivalents. *Exp Dermatol*. 2000; Apr;9(2):97-103.

Lehmann B, Genehr T, Knuschke P, et al. UVB-induced conversion of 7-dehydrocholesterol to 1alpha,25-dihydroxyvitamin D3 in an in vitro human skin equivalent model. *J Invest Dermatol*. 2001; Nov;117(5):1179-85.

Lehmann B, Sauter W, Knuschke P, et al. Demonstration of UVB induced synthesis of 1 alpha,25-dihydroxyvitamin D3 (calcitriol) in human skin by microdialysis. *Arch Dermatol Res*. 2003; Apr;295(1):24-8.

Lei X, Guan CW, Song Y, et al. The multifaceted role of CD146/MCAM in the promotion of melanoma progression. *Cancer Cell Int*. 2015; Feb 4;15(1):3.

Leone G, Pacifico A, Iacovelli P, et al. Tacalcitol and narrow-band phototherapy in patients with vitiligo. *Clin Exp Dermatol.* 2006; 31:200–205.

Lerchbaum E, Obermayer-Pietsch B. Vitamin D and fertility: a systematic review. *Eur J Endocrinol*. 2012; May;166(5):765-78.

Lev S, Yarden Y, Givol D. Dimerization and activation of the kit receptor by monovalent and bivalent binding of stem cell factor. *J Biol Chem*. 1992 Aug 5;267(22):15970-7.

Levy C, Khaled M, Fisher DE. MITF: master regulator of melanocyte development and melanoma oncogene. *Trends Mol Med*. 2006 Sep;12(9):406-14.

Li C, Liu Z, Zhang Z, et al. Genetic variants of the vitamin D receptor gene alter risk of cutaneous melanoma. *J Invest Dermatol.* 2007; Feb;127(2):276-80.

Li H, Durbin R. Fast and accurate short read alignment with Burrows-Wheeler Transform. *Bioinformatics*. 2010; Mar 1;26(5):589-95

Li L, Zhang Z, Ma T, et al. PRMT1 regulates tumor growth and metastasis of human melanoma via targeting ALCAM. *Mol Med Rep*. 2016; Jul;14(1):521-8.

Li H, Fan L, Zhu S, et al. Epilation induces hair and skin pigmentation through an EDN3/EDNRB-dependent regenerative response of melanocyte stem cells. *Sci Rep*. 2017 Aug 4;7(1):7272.

Liao Y, Smyth GK, Shi W. featureCounts: an efficient general purpose program for assigning sequence reads to genomic features. *Bioinformatics*. 2014; Apr 1;30(7):923-30.

Lienhard M, Grimm C, Morkel M, et al. MEDIPS: genome-wide differential coverage analysis of sequencing data derived from DNA enrichment experiments. *Bioinformatics*. 2014; Jan 15;30(2):284-6.

Linzmeier RM, Ganz T. Human defensin gene copy number polymorphisms: comprehensive analysis of independent variation in alpha- and beta-defensin regions at 8p22-p23. *Genomics*. 2005 Oct;86(4):423-30.

Liu L, Zhao C, Heng HH, et al. The human beta-defensin-1 and alpha-defensins are encoded by adjacent genes: two peptide families with differing disulfide topology share a common ancestry. *Genomics*. 1997 Aug 1;43(3):316-20.

Liu C, Li Y, Semenov M, et al. Control of beta-catenin phosphorylation/degradation by a dual-kinase mechanism. *Cell*. 2002 Mar 22;108(6):837-47.

Liu PT, Schenk M, Walker VP, et al. Convergence of IL-1beta and VDR activation pathways in human TLR2/1-induced antimicrobial responses. *PLoS One*. 2009; Jun 5;4(6):e5810.

Liu LH, Fan X, Xia ZK, et al. Angiotensin II stimulates melanogenesis via the protein kinase C pathway. *Exp Ther Med*. 2015 Oct;10(4):1528-1532.

Liyanage UE, Law MH, Han X, et al. Combined analysis of keratinocyte cancers identifies novel genome-wide loci. *Hum Mol Genet*. 2019;28(18):3148-3160.

Loomis WF. Skin-pigment regulation of vitamin-D biosynthesis in man. *Science*. 1967; Aug 4;157(3788):501-6.

López S, García O, Yurrebaso I, Flores C, et al. The Interplay between Natural Selection and Susceptibility to Melanoma on Allele 374F of SLC45A2 Gene in a South European Population. *PLoS One*. 2014 Aug 5;9(8):e104367.

López S, Alonso S, García de Galdeano A, et al. Melanocytes from dark and light skin respond differently after ultraviolet B irradiation: effect of keratinocyte conditioned medium. *Photodermatol Photoimmunol Photomed*. 2015a; 31: 149–158.

López S, Smith-Zubiaga I, García de Galdeano A, et al. Comparison of the Transcriptional Profiles of Melanocytes from Dark and Light Skinned Individuals under Basal Conditions and Following Ultraviolet-B Irradiation. *PLoS One*. 2015b;10(8):e0134911.

Lou S, Lee HM, Qin H, et al. Whole-genome bisulfite sequencing of multiple individuals reveals complementary roles of promoter and gene body methylation in transcriptional regulation. *Genome Biol*. 2014; Jul 30;15(7):408.

Love MI, Huber W, Anders S. Moderated estimation of fold change and dispersion for RNAseq data with DESeq2. *Genome Biol*. 2014; 15(12):550.

Luttrell LM, Lefkowitz RJ. The role of beta-arrestins in the termination and transduction of G-protein-coupled receptor signals. *J Cell Sci*. 2002 Feb 1;115(Pt 3):455-65.

Mackintosh JA. The antimicrobial properties of melanocytes, melanosomes and melanin and the evolution of black skin. *J Theor Biol*. 2001; Jul 21;211(2):101-13.

Majumdar N, Wessel T, Marks J. Digital PCR Modeling for Maximal Sensitivity, Dynamic Range and Measurement Precision. *PLoS One*. 2015 Mar 25;10(3):e0118833.

Makino T, Yamakoshi T, Mizawa M, et al. Ultraviolet B irradiation induces the expression of hornerin in xenotransplanted human skin. *Acta Histochem*. 2014; Jan;116(1):20-4.

Mandelcorn-Monson R, Marrett L, Kricker A, et al. Sun exposure, vitamin D receptor polymorphisms FokI and BsmI and risk of multiple primary melanoma. *Cancer Epidemiol*. 2011; Dec;35(6):e105-10.

Manggau M, Kim DS, Ruwisch L, et al. 1Alpha,25-dihydroxyvitamin D3 protects human keratinocytes from apoptosis by the formation of sphingosine-1-phosphate. *J Invest Dermatol*. 2001; Nov;117(5):1241-9.

Mansur CP, Gordon PR, Ray S, et al. Vitamin D, its precursors, and metabolites do not affect melanization of cultured human melanocytes*. J Invest Dermatol.* 1988; Jul;91(1):16-21.

Martínez-Cadenas C, López S, Ribas G, et al. Simultaneous purifying selection on the ancestral MC1R allele and positive selection on the melanoma-risk allele V60L in south Europeans. *Mol Biol Evol*. 2013; Dec;30(12):2654-65.

Maruyama R, Aoki F, Toyota M, et al. Comparative genome analysis identifies the vitamin D receptor gene as a direct target of p53-mediated transcriptional activation. *Cancer Res*. 2006;66(9):4574-4583.

Mason RS, Sequeira VB, Dixon KM, et al. Photoprotection by 1α,25-dihydroxyvitamin D and analogs: Further studies on mechanisms and implications for UV-damage. *J Steroid Biochem Mol Biol.* 2010; Jul;121(1-2):164-8.

Mazaika E, Homsy J. Digital Droplet PCR: CNV Analysis and Other Applications. *Curr Protoc Hum Genet*. 2014 Jul 14;82:7.24.1-13.

Medvedev P, Stanciu M, Brudno M. Computational methods for discovering structural variation with next-generation sequencing. *Nat Methods*. 2009 Nov;6(11 Suppl):S13-20.

Mehlotra RK, Dazard JE, John B, et al. Copy number variation within human β-defensin gene cluster influences progression to AIDS in the Multicenter AIDS Cohort Study. *J AIDS Clin Res*. 2012;3(10).

Mehlotra RK, Zimmerman PA, Weinberg A, et al. Variation in human β-defensin genes: new insights from a multipopulation study. *Int J Immunogenet*. 2013 Aug;40(4):261-9.

Meyer MB, Benkusky NA, Lee CH, et al. Genomic determinants of gene regulation by 1,25-dihydroxyvitamin D3 during osteoblast-lineage cell differentiation. *J Biol Chem*. 2014; Jul 11;289(28):19539-54.

Mi H, Muruganujan A, Thomas PD. PANTHER in 2013: modeling the evolution of gene function, and other gene attributes, in the context of phylogenetic trees. *Nucleic Acids Res*. 2013; Jan;41(Database issue):D377-86.

Milanese M, Segat L, Arraes LC, et al. Copy number variation of defensin genes and HIV infection in Brazilian children. *J Acquir Immune Defic Syndr*. 2009 Mar 1;50(3):331-3.

Miller JR, Hocking AM, Brown JD, et al. Mechanism and function of signal transduction by the Wnt/beta-catenin and Wnt/Ca2+ pathways. *Oncogene.* 1999 Dec 20;18(55):7860-72.

Mitchell BL, Zhu G, Medland SE, et al. Half the Genetic Variance in Vitamin D Concentration is Shared with Skin Colour and Sun Exposure Genes. *Behav Genet*. 2019; Jul;49(4):386-398.

Miyata M, Ichihara M, Tajima O, et al. UVB-irradiated keratinocytes induce melanoma-associated ganglioside GD3 synthase gene in melanocytes via secretion of tumor necrosis factor α and interleukin 6. *Biochem Biophys Res Commun*. 2014; Mar 7;445(2):504-10.

Mochly-Rosen D. Localization of protein kinases by anchoring proteins: a theme in signal transduction. *Science*. 1995 Apr 14;268(5208):247-51.

Moll PR, Sander V, Frischauf AM, et al. Expression Profiling of Vitamin D Treated Primary Human Keratinocytes. *J Cell Biochem*. 2007; Feb 15;100(3):574-92.

Morris JA, Kemp JP, Youlten SE, et al. An atlas of genetic influences on osteoporosis in humans and mice [published correction appears in Nat Genet. 2019 May;51(5):920]. *Nat Genet*. 2019;51(2):258-266.

Motakis ES, Nason GP, Fryzlewicz P, et al. Variance stabilization and normalization for one-color microarray data using a data-driven multiscale approach. *Bioinformatics*. 2006 Oct 15;22(20):2547-53.

Neilsen PM, Cheney KM, Li CW, et al. Identification of ANKRD11 as a p53 coactivator. *J Cell Sci.* 2008;121(Pt 21):3541-3552.

Nemere I, Safford SE, Rohe B, et al. Identification and characterization of 1,25D3-membrane-associated rapid response, steroid (1,25D3-MARRS) binding protein. *J Steroid Biochem Mol Biol*. 2004; May;89-90(1-5):281-5.

Newton-Bishop JA, Beswick S, Randerson-Moor J, et al. Serum 25-hydroxyvitamin D3 levels are associated with breslow thickness at presentation and survival from melanoma. *J Clin Oncol*. 2009; Nov 10;27(32):5439-44.

Nguyen AV, Soulika AM. The Dynamics of the skin's immune system. *Int J Mol Sci*. 2019; Apr 12;20(8). pii: E1811.

Nishizuka Y. Studies and perspectives of protein kinase C. *Science*. 1986 Jul 18;233(4761):305-12.

Niyonsaba F, Ogawa H, Nagaoka I. Human beta-defensin-2 functions as a chemotactic agent for tumour necrosis factor-alpha-treated human neutrophils. *Immunology*. 2004 Mar;111(3):273-81.

Niyonsaba F, Ushio H, Nakano N, et al. Antimicrobial peptides human beta-defensins stimulate epidermal keratinocyte migration, proliferation and production of proinflammatory cytokines and chemokines. *J Invest Dermatol*. 2007 Mar;127(3):594-604.

Niyonsaba F, Kiatsurayanon C, Chieosilapatham P, et al. Friends or Foes? Host defense (antimicrobial) peptides and proteins in human skin diseases. *Exp Dermatol*. 2017; Nov;26(11):989-998.

Nix MA, Kaelin CB, Ta T, et al. Molecular and Functional Analysis of Human β-Defensin 3 Action at Melanocortin Receptors. *Chem Biol.* 2013 Jun 20;20(6):784-95.

Nix MA, Kaelin CB, Palomino R, et al. Electrostatic Similarity Analysis of Human b-Defensin Binding in the Melanocortin System. *Biophys J.* 2015 Nov 3;109(9):1946-58

Nomura I, Goleva E, Howell MD, et al. Cytokine milieu of atopic dermatitis, as compared to psoriasis, skin prevents induction of innate immune response genes. *J Immunol*. 2003; 171:3262–9.

Norton HL, Kittles RA, Parra E, et al. Genetic Evidence for the Convergent Evolution of Light Skin in Europeans and East Asians. *Mol Biol Evol*. 2007; Mar;24(3):710-22.

Nurnberg B, Graber S, Gartner B, et al. Reduced serum 25-hydroxyvitamin D levels in stage IV melanoma patients. *Anticancer research*. 2009; 29:3669–3674.

Nylander K, Bourdon JC, Bray SE, et al. Transcriptional activation of tyrosinase and TRP-1 by p53 links UV irradiation to the protective tanning response. *J Pathol*. 2000;190(1):39-46.

Ofori-Acquah SF, King JA. Activated leukocyte cell adhesion molecule: a new paradox in cancer. *Transl Res*. 2008; Mar;151(3):122-8.

Ohbayashi N, Maruta Y, Ishida M, et al. Melanoregulin regulates retrograde melanosome transport through interaction with the RILP–p150Glued complex in melanocytes. *J Cell Sci*. 2012; Mar 15;125(Pt 6):1508-18.

Ohkawa Y, Miyazaki S, Hamamura K, et al. Ganglioside GD3 enhances ashesion signals and augments malignant properties of melanoma cells by recruiting integrins to glycolipid-enriched microdomains. *J Biol Chem*. 2010; Aug 27;285(35):27213-23.

Oikawa A, Nakayasu M. Stimulation of melanogenesis in cultured melanoma cells by calciferols. *FEBS Lett*. 1974 ;May 15;42(1):32-5.

Okamoto K, Li H, Jensen MR, et al. Cyclin G recruits PP2A to dephosphorylate Mdm2. *Mol Cell*. 2002; 9(4):761-771.

Old WM, Shabb JB, Houel S, et al. Functional proteomics identifies targets of phosphorylation by B-Raf signaling in melanoma. *Mol Cell*. 2009; Apr 10;34(1):115-31.

Orlow I, Roy P, Reiner AS, et al. Vitamin D receptor polymorphisms in patients with cutaneous melanoma. *Int J Cancer*. 2012; Jan 15;130(2):405-18.

Ortonne JP, Bissett DL. Latest insights into skin hyperpigmentation. *J Investig Dermatol Symp Proc*. 2008; Apr;13(1):10-4.

Osawa T, Ohga N, Akiyama K, et al. Lysyl oxidase secreted by tumour endothelial cells promotes angiogenesis and metastasis. *Br J Cancer*. 2013; Oct 15;109(8):2237-47.

Palumbo A, Solano F, Misuraca G, et al. Comparative action of dopachrome tautomerase and metal ions on the rearrangement of dopachrome. *Biochim Biophys Acta*. 1991 Nov 14;1115(1):1-5.

Paluncic J, Kovacevic Z, Jansson PJ, et al. Roads to melanoma: Key pathways and emerging players in melanoma progression and oncogenic signaling. *Biochim Biophys Acta*. 2016; Apr;1863(4):770-84.

Pardali E, van der Schaft DW, Wiercinska E, et al. Critical role of endoglin in tumor cell plasticity of Ewing sarcoma and melanoma. *Oncogene*. 2011; Jan 20;30(3):334-45.

Park HY, Russakovsky V, Ohno S, et al. The beta isoform of protein kinase C stimulates human melanogenesis by activating tyrosinase in pigment cells. *J. Biol. Chem*. 1993, 268, 11742-11749.

Park HY, Russakovsky V, Ao Y, et al. Alpha-melanocyte stimulating hormone-induced pigmentation is blocked by depletion of protein kinase C. *Exp Cell Res*. 1996 Aug 25;227(1):70-9.

Park HY, Perez JM, Laursen R, et al. Protein kinase C-beta activates tyrosinase by phosphorylating serine residues in its cytoplasmic domain. *J Biol Chem*. 1999 Jun 4;274(23):16470-8.

Park HY, Wu H, Killoran CE, et al. The receptor for activated C-kinase-I (RACK-I) anchors activated PKC-β on melanosomes. *J Cell Sci*. 2004 Jul 15;117(Pt 16):3659-68.

Park HY, Wu C, Yonemoto L, et al. MITF mediates cAMP-induced protein kinase C-β expression in human Melanocytes. *Biochem J*. 2006 May 1;395(3):571-8.

Park HY, Kosmadaki M, Yaar M, et al. Cellular mechanisms regulating human melanogenesis. *Cell Mol Life Sci*. 2009 May;66(9):1493-506.

Park PJ, Lee TR, Cho EG. Substance P stimulates endothelin 1 secretion via endothelin-converting enzyme 1 and promotes melanogenesis in human melanocytes. *J Invest Dermatol.* 2015; 135(2):551-559.

Pascual G, Avgustinova A, Mejetta S, et al. Targeting metastasis-initiating cells through the fatty acid receptor CD36. *Nature*. 2017; Jan 5;541(7635):41-45.

Pawlowska E, Wysokinski D, Blasiak J. Nucleotide Excision Repair and Vitamin D—Relevance for Skin Cancer Therapy. *Int J Mol Sci*. 2016; Apr 6;17(4):372.

Pazgier M, Hoover DM, Yang D, et al. Human beta-defensins. *Cell Mol Life Sci*. 2006 Jun;63(11):1294-313.

Peric M, Koglin S, Dombrowski Y, et al. Vitamin D Analogs Differentially Control Antimicrobial Peptide/''Alarmin''Expression in Psoriasis. *PLoS One*. 2009 Jul 22;4(7):e6340.

Pernet I, Reymermier C, Guezennec A, et al. Calcium triggers beta-defensin (hBD-2 and hBD-3) and chemokine macrophage inflammatory protein-3 alpha (MIP-3alpha/CCL20) expression in monolayers of activated human keratinocytes. *Exp Dermatol*. 2003;12(6):755-760.

Perne A, Zhang X, Lehmann L, et al. Comparison of multiplex ligation-dependent probe amplification and real-time PCR accuracy for gene copy number quantification using the beta-defensin locus. *Biotechniques.* 2009 Dec;47(6):1023-8.

Perotti V, Baldassari P, Bersani I, et al. NFATc2 is a potential therapeutic target in human melanoma. *J Invest Dermatol*. 2012; Nov;132(11):2652-60.

Petris MJ, Strausak D, Mercer JF. The Menkes copper transporter is required for the activation of tyrosinase. *Hum Mol Genet.* 2000 Nov 22;9(19):2845-51.

Picotto G, Liaudat AC, Bohl L, et al. Molecular aspects of vitamin D anticancer activity. *Cancer Inves*t. 2012; Oct;30(8):604-14.

Picardo M, Dell'Anna ML, Ezzedine K, et al. Vitiligo. Nat Rev Dis Primers. 2015 Jun 4;1:15011.

Pillai S, Bikle DD, Elias PM. 1,25-Dihydroxyvitamin D production and receptor binding in human keratinocytes varies with differentiation. *J Biol Chem*. 1988; Apr 15;263(11):5390-5.

Pilz S, Zittermann A, Obeid R, et al. The Role of Vitamin D in Fertility and during Pregnancy and Lactation: A Review of Clinical Data. *Int J Environ Res Public Health*. 2018; Oct 12;15(10).

Pinkel D, Segraves R, Sudar D, et al. High resolution analysis of DNA copy number variation using comparative genomic hybridization to microarrays. *Nat Genet*. 1998 Oct;20(2):207-11.

Powe CE, Evans MK, Wenger J, et al. Vitamin D-binding protein and vitamin D status of black Americans and white Americans. *N Engl J Med*. 2013; Nov 21;369(21):1991-2000.

Prabhu AV, Luu W, Li D, et al. DHCR7: A vital enzyme switch between cholesterol and vitamin D production. *Prog Lipid Res.* 2016a; Oct;64:138-151

Prabhu AV, Luu W, Sharpe LJ, et al. Cholesterol-mediated degradation of 7-dehydrocholesterol reductase switches the balance from cholesterol to vitamin D synthesis. *J Biol Chem*. 2016b; Apr 15;291(16):8363-73.

Price MA, Colvin Wanshura LE, Yang J, et al. CSPG4, a potential therapeutic target, facilitates malignant progression of melanoma. *Pigment Cell Melanoma Res*. 2011; Dec;24(6):1148-57.

Proksch E. pH in nature, humans and skin. *J Dermatol*. 2018; Sep;45(9):1044-1052.

Punnonen K, Yuspa SH. Ultraviolet light irradiation increases cellular diacylglycerol and induces translocation of diacylglycerol kinase in murine keratinocytes. *J Invest Dermatol*. 1992 Aug;99(2):221-6.

Rachel RA, Nagashima K, O'Sullivan TN, et al. Melanoregulin, Product of the dsu Locus, Links the BLOC-Pathway and Oa1 in Organelle Biogenesis. *PLoS One*. 2012; 7(9):e42446.

Ramagopalan SV, Heger A, Berlanga AJ, et al. A ChIP-seq defined genome-wide map of vitamin D receptor binding, Associations with disease and evolution. *Genome Res.* 2010; Oct;20(10):1352-60.

Ransohoff KJ, Wu W, Cho HG, et al. Two-stage genome-wide association study identifies a novel susceptibility locus associated with melanoma. *Oncotarget*. 2017; Mar 14;8(11):17586-17592.

Ranson M, Posen S, Mason RS. Human melanocytes as a target tissue for hormones: in vitro studies with 1 alpha-25, dihydroxyvitamin D3, alpha-melanocyte stimulating hormone, and beta-estradiol. *J Invest Dermatol.* 1988; Dec;91(6):593-8.

Rao C, Su Z, Li H, et al. Microphthalmia-associated transcription factor regulates skin melanoblast migration by repressing the melanoma cell adhesion molecule. *Exp Dermatol.* 2016; Jan;25(1):74-6.

R Core Team (2018). R: A language and environment for statistical computing. R Foundation for Statistical Computing, Vienna, Austria. URL https://www.R-project.org/.

Reddy BY, Miller DM, Tsao H. Somatic driver mutations in melanoma. *Cancer*. 2017, Jun 1;123(S11):2104-2117.

Reichrath J, Collins ED, Epple S, et al. Immunohistochemical detection of 1,25-dihydroxyvitamin D3 receptors (VDR) in human skin. A comparison of five antibodies. *Pathol Res Pract*. 1996; Mar;192(3):281-9.

Robinson MD, McCarthy DJ, Smyth GK. edgeR: a Bioconductor package for differential expression analysis of digital gene expression data. *Bioinformatics*. 2010; Jan 1;26(1):139-40.

Rodríguez-Jiménez FJ, Krause A, Schulz S, et al. Distribution of new human beta-defensin genes clustered on chromosome 20 in functionally different segments of epididymis. *Genomics*. 2003 Feb;81(2):175-83.

Rondini EA, Fang H, Runge-Morris M, et al. Regulation of human cytosolic sulfotransferases 1C2 and 1C3 by nuclear signalung pathways in LS180 colorectal adenocarcinoma cells. *Drug Metab Dispos*. 2014; Mar;42(3):361-8.

Ross AC, Manson JE, Abrams SA, et al. The 2011 report on dietary reference intakes for calcium and vitamin D from the Institute of Medicine: what clinicians need to know. *J Clin Endocrinol Metab*. 2011; Jan;96(1):53-8.

Roos L, Sandling JK, Bell CG, et al. Higher nevus count exhibits a distinct DNA methylation signature in healthy human skin: Implications for melanoma. *J Invest Dermatol*. 2017; Apr;137(4):910-920.

Rütter A, Schwarz T. Market hyperpigmentation in psoriatic plaque as a sequelae of combination therapy with UVB-311 and calcipotriol. *Hautarzt*. 2000; Jun;51(6):431-3.

Rybchyn MS, De Silva WGM, Sequeira VB, et al. Enhanced repair of UV-induced DNA damage by 1,25-Dihydroxyvitamin D3 in skin is linked to pathways that control cellular energy. *J Invest Dermatol.* 2018; May;138(5):1146-1156.

Saito H, Yasumoto K, Takeda K, et al. Melanocyte-specific microphthalmia-assoaciated transcription factor isoform activates its own gene promoter through physical interaction with lymphoid-enhancing factor 1. *J Biol Chem*. 2002 Aug 9;277(32):28787-94.

Samuel S, Sitrin MD. Vitamin D's role in cell proliferation and differentiation. *Nutr Rev*. 2008; Oct;66(10 Suppl 2):S116-24.

Sánchez-Más J, Guillo LA, Zanna P, et al. Role of G protein-coupled receptor kinases in the homologous desensitization of the human and mouse melanocortin 1 receptors. *Mol Endocrinol*. 2005 Apr;19(4):1035-48.

Saternus R, Pilz S, Gräber S, et al. A Closer Look at Evolution: Variants (SNPs) of Genes Involved in Skin Pigmentation, Including EXOC2, TYR, TYRP1, and DCT, Are Associated With 25(OH)D Serum Concentration. *Endocrinology*. 2015; Jan;156(1):39-47.

Schepsky A, Bruser K, Gunnarsson GJ, et al. The microphthalmia-associated transcription factor Mitf interacts with beta-catenin to determine target gene expression. *Mol Cell Biol*. 2006 Dec;26(23):8914-27.

Schibli DJ, Hunter HN, Aseyev V, et al. The solution structures of the human beta-defensins lead to a better understanding of the potent bactericidal activity of HBD3 against *Staphylococcus aureus*. *J Biol Chem*. 2002 Mar 8;277(10):8279-89.

Schleicher RL, Sternberg MR, Looker AC, et al. National Estimates of Serum Total 25-Hydroxyvitamin D and Metabolite Concentrations Measured by Liquid Chromatography-Tandem Mass Spectrometry in the US Population during 2007-2010. *J Nutr*. 2016; May;146(5):1051-61.

Schouten JP, McElgunn CJ, Waaijer R, et al. Relative quantification of 40 nucleic acid sequences by multiplex ligation-dependent probe amplification. *Nucleic Acids Res*. 2002 Jun 15;30(12):e57.

Schuch AP, Moreno NC, Schuch NJ, et al. Sunlight damage to cellular DNA: Focus on oxidatively generated lesions. *Free Radic Biol Med*. 2017; Jun;107:110-124.

Schwarz T. The dark and the sunny sides of UVR-induced immunosuppression: photoimmunology revisited. *J Invest Dermatol*. 2010;130(1):49-54.

Scott MC, Suzuki I, Abdel-Malek ZA. Regulation of the human melanocortin 1 receptor expression in epidermal melanocytes by paracrine and endocrine factors and by ultraviolet radiation. *Pigment Cell Res.* 2002 Dec;15(6):433-9.

Seberg HE, Van Otterloo E, Cornell RA. Beyond MITF: Multiple transcription factors directly regulate the cellular phenotype in melanocytes and melanoma. *Pigment Cell Melanoma Res.* 2017; 30(5):454-466.

Seidensticker MJ, Behrens J. Biochemical interactions in the wnt pathway. *Biochim Biophys Acta*. 2000 Feb 2;1495(2):168-82.

Semple F, Webb S, Li HN, et al. Human beta-defensin 3 has immunosuppressive activity in vitro and in vivo. *Eur J Immunol*. 2010 Apr;40(4):1073-8.

Semple F, Dorin JR. β-Defensins: multifunctional modulators of infection, inflammation and more? *J Innate Immun*. 2012; 4(4):337-48.

Serre C, Busuttil V, Botto JM. Intrinsic and extrinsic regulation of human skin melanogenesis and pigmentation. *Int J Cosmet Sci*. 2018; 40(4):328-347

Sequeira VB, Rybchyn MS, Tongkao-On W, et al. The role of the vitamin D receptor and ERp57 in photoprotection by 1α,25-dihydroxyvitamin D3. *Mol Endocrinol*. 2012; Apr;26(4):574-82.

Setty SR, Tenza D, Sviderskaya EV, et al. Cell-specific ATP7A transport sustains copper-dependent tyrosinase activity in melanosomes. *Nature*. 2008 Aug 28;454(7208):1142-6.

Shain AH, Yeh I, Kovalyshyn I, et al. The Genetic Evolution of Melanoma from Precursor Lesions. *N Engl J Med.* 2015; Nov 12;373(20):1926-36.

Shelley JR, Davidson DJ, Dorin JR. The Dichotomous Responses Driven by β-Defensins. *Front Immunol*. 2020;11:1176.

Shen Y, Ha W, Zeng W, et al. Exome sequencing identifies novel mutation signatures of UV radiation and trichostatin A in primary human keratinocytes. *Sci Rep*. 2020; Mar 18;10(1):4943.

Shin MH, Lee Y, Kim MK, Lee DH, Chung JH. UV increases skin-derived 1α,25-dihydroxyvitamin D3 production, leading to MMP-1 expression by altering the balance of vitamin D and cholesterol synthesis from 7-dehydrocholesterol. *J Steroid Biochem Mol Biol*. 2019; Dec;195:105449.

Sironi M, Biasin M, Cagliani R, et al. Evolutionary Analysis Identifies an MX2 Haplotype Associated with Natural Resistance to HIV-1 Infection. *Mol Biol Evol*. 2014; Sep;31(9):2402-14.

Sitaram A, Marks MS. Mechanisms of protein delivery to melanosomes in pigment cells. Physiology (Bethesda). 2012; 27(2):85-99.

Slominski A, Tobin DJ, Shibahara S, et al. Melanin Pigmentation in Mammalian Skin and Its Hormonal Regulation. *Physiol Rev*. 2004 Oct;84(4):1155-228.

Slominski AT, Brożyna AA, Zmijewski MA, et al. Vitamin D signaling and melanoma: role of vitamin D and its receptors in melanoma progression and management. *Lab Invest*. 2017; Jun;97(6):706-724.

Song X, Mosby N, Yang J, Xu A, Abdel-Malek Z, Kadekaro A et al. alpha-MSH activates immediate defense responses to UV-induced oxidative stress in human melanocytes. *Pigment Cell Melanoma Res*. 2009; 22(6):809-818.

Song EJ, Gordon-Thomson C, Cole L, et al. 1α,25-Dihydroxyvitamin D3 reduces several types of UV-induced DNA damage and contributes to photoprotection. *J Steroid Biochem Mol Biol*. 2013; Jul;136:131-8.

Song HJ, Lee SH, Choi GS, et al. Repeated ultraviolet irradiation induces the expression of Toll-like receptor 4, IL-6, and IL-10 in neonatal human melanocytes. *Photodermatol Photoimmunol Photomed*. 2018; Mar;34(2):145-151.

Sørensen OE, Cowland JB, Theilgaard-Mönch K, et al. Wound healing and expression of antimicrobial peptides/polypeptides in human keratinocytes, a consequence of common growth factors. *J Immunol*. 2003 Jun 1;170(11):5583-9.

Sørensen OE, Thapa DR, Rosenthal A, et al. Differential regulation of beta-defensin expression in human skin by microbial stimuli. *J Immunol*. 2005 Apr 15;174(8):4870-9.

Spath L, Ulivieri A, Lavra L, et al. Antiproliferative Effects of 1α-OHvitD3 in Malignant Melanoma: Potential Therapeutic implications. *Sci Rep*. 2017; Jan 11;7:40370.

Stranger BE, Forrest MS, Dunning M, et al. Relative impact of nucleotide and copy number variation on gene expression phenotypes. *Science*. 2007 Feb 9;315(5813):848-53.

Stuart PE, Hüffmeier U, Nair RP, et al. Association of β-defensin copy number and psoriasis in three cohorts of European origin. *J Invest Dermatol.* 2012 Oct;132(10):2407-2413.

Sugawara H, Harada N, Ida T, et al. Complex low-copy repeats associated with a common polymorphic inversion at human chromosome 8p23. *Genomics*. 2003 Aug;82(2):238-44.

Sumantran VN, Mishra P, Sudhakar N. Microarray analysis of differentially expressed genes regulating lipid metabolism during melanoma progression. *Indian J Biochem Biophys*. 2015; Apr;52(2):125-31.

Supp DM, Karpinski AC, Boyce ST. Expression of human β-defensins HBD-1, HBD-2, and HBD-3 in cultured keratinocytes and skin substitutes. *Burns*. 2004; Nov;30(7):643-8.

Suryo Rahmanto Y, Bal S, Loh KH, et al. Melanotransferrin: Search for a function. *Biochim Biophys Acta*. 2012; Mar;1820(3):237-43.

Suzuki I, Tada A, Ollmann MM, et al. Agouti signaling protein inhibits melanogenesis and the response of human melanocytes to alpha-melanotropin. *J Invest Dermatol*. 1997 Jun;108(6):838-42.

Suzuki A, Ozono K, Kubota T, et al. PTH/cAMP/PKA signaling facilitates canonical Wnt signaling via inactivation of glycogen synthase kinase-3β in osteoblastic Saos-2 cells. *J Cell Biochem.* 2008 May 1;104(1):304-17.

Swoboda A, Soukup R, Kinslechner K, et al. STAT3 promotes melanoma metastasis by CEBP-induced repression of the MITF pigmentation pathway. Prepint at https://www.biorxiv.org/content/10.1101/422832v1 (2018).

Swope VB, Jameson JA, McFarland KL, et al. Defining MC1R Regulation in Human Melanocytes by Its Agonist α-Melanocortin and Antagonists Agouti Signaling Protein and β-Defensin 3. J *Invest Dermatol.* 2012 Sep;132(9):2255-62.

Swope VB, Abdel-Malek ZA. Significance of the Melanocortin 1 and Endothelin B Receptors in Melanocyte Homeostasis and Prevention of Sun-Induced Genotoxicity. *Front Genet*. 2016 Aug 17;7:146.

Tada A, Suzuki I, Im S, et al. Endothelin-1 is a paracrine growth factor that modulates melanogenesis of human melanocytes and participates in their responses to ultraviolet radiation. *Cell Growth Differ*. 1998 Jul;9(7):575-84.

Tagashira H, Miyamoto A, Kitamura S, et al. UVB Stimulates the Expression of Endothelin B Receptor in Human Melanocytes via a Sequential Activation of the p38/MSK1/CREB/MITF Pathway Which Can Be Interrupted by a French Maritime Pine Bark Extract through a Direct Inactivation of MSK1. *PLoS One*. 2015; 10(6):e0128678.

Takahashi M, Matsuda F, Margetic N, et al. Automated Identification of Single Nucleotide Polymorphisms from Sequencing Data. *Proc IEEE Comput Soc Bioinform Conf*. 2002;1:87-93.

Takeda K, Yasumoto K, Takada R, et al. Induction of melanocyte-specific microphthalmia-associated transcription factor by Wnt-3a*. J Biol Chem.* 2000 May 12;275(19):14013-6.

Tam I, Dzierżęga-Lęcznar A, Stępień K. Differential expression of inflammatory cytokines and chemokines in lipopolysaccharide-stimulated melanocytes from lightly and darkly pigmented skin. *Exp Dermatol*. 2019; May;28(5):551-560.

Tang CH, Wei W, Liu L. Regulation of DNA Repair by S-Nitrosylation. *Biochim Biophys Acta*. 2012; Jun;1820(6):730-5.

Tang F, Lord MS, Stallcup WB, et al. Cell surface chondroitin sulphate proteoglycan 4 (CSPG4) binds to the basement membrane heparan sulphate proteoglycan, perlecan, and is involved in cell adhesion. *J Biochem*. 2018a; May 1;163(5):399-412

Tang L, Fang W, Lin J, et al. Vitamin D protects human melanocytes against oxidative damage by activation of Wnt/β-catenin signaling. *Lab Invest*. 2018b; Dec;98(12):1527-1537.

Tapia CV, Falconer M, Tempio F, et al. Melanocytes and melanin represent a first line of innate immunity against *Candida albicans*. *Med Mycol*. 2014; Jul;52(5):445-54.

Taudien S, Gäbel G, Kuss O, et al. Association studies of the copy-number variable ß-defensin cluster on 8p23.1 in adenocarcinoma and chronic pancreatitis. *BMC Res Notes*. 2012 Nov 13;5:629.

Tesic N, Kamensek U, Sersa G, et al. Endoglin (CD105) silencing mediated by shRNA under the control of endothelin-1 promoter for targeted gene therapy of melanoma. *Mol Ther Nucleic Acids*. 2015; May 5;4:e239.

Thompson MJW, Jones G, Aitken DA. Constitutive melanin density is associated with higher 25-hydroxyvitamin D and potentially total body BMD in older Caucasian adults via increased sun tolerance and exposure. *Osteoporos Int*. 2018;29(8):1887-1895.

Thorne RF, Marshall JF, Shafren DR, et al. The integrins alpha3beta1 and alpha6beta1 physically and functionally associate with CD36 in human melanoma cells. Requirement for extracellular domain of CD36. *J Biol Chem*. 2000; Nov 10;275(45):35264-75.

Tian J, Xu C (2013). MaXact: Exact max-type Cochran-Armitage trend test (CATT). R package version 0.2.1. https://CRAN.R-project.org/package=MaXact

Tímár J, Vizkeleti L, Doma V, et al. Genetic progression of malignant melanoma. *Cancer Metastasis Rev*. 2016; Mar;35(1):93-107.

Timerman D, McEnery-Stonelake M, Joyce CJ, et al. Vitamin D deficiency is associated with a worse prognosis in metastatic melanoma. *Oncotarget*. 2017; Jan 24;8(4):6873-6882.

Tomita Y, Torinuki W, Tagami H. Stimulation of human melanocytes by vitamin D3 possibly mediates skin pigmentation after sun exposure. *J Invest Dermatol*. 1988; Jun;90(6):882-4.

Trochoutsou AI, Kloukina V, Samitas K, et al. Vitamin-D in the Immune System: Genomic and Non-Genomic Actions. *Mini Rev Med Chem*. 2015;15(11):953-963.

Ünal B, Alan S, Başsorgun Cİ, et al. The divergent roles of growth differentiation factor-15 (GDF-15) in benign and malignant skin pathologies. *Arch Dermatol Res*. 2015; Sep;307(7):551-7.

Urtatiz O, Van Raamsdonk CD. Gnaq and Gna11 in the Endothelin Signaling Pathway and Melanoma. *Front Genet.* 2016; 7:59.

Wu X, Bayle JH, Olson D, et al. The p53-mdm-2 autoregulatory feedback loop. *Genes Dev.* 1993; 7(7A):1126-1132.

Väisänen S, Dunlop TW, Sinkkonen L, et al. Spatio-temporal activation of chromatin on the human CYP24 gene promoter in the presence of 1alpha,25-Dihydroxyvitamin D3. *J Mol Biol*. 2005; Jul 1;350(1):65-77.

van Kilsdonk JWJ, Jansen PAM, van den Bogaard EH, et al. The Effects of human beta-defensins on skin cells *in vitro*. *Dermatology*. 2017;233(2-3):155-163.

Vantieghem K, De Haes P, Bouillon R, et al. Dermal fibroblasts pretreated with a sterol Delta7-reductase inhibitor produce 25-hydroxyvitamin D3 upon UVB irradiation. *J Photochem Photobiol B*. 2006; Oct 2;85(1):72-8.

Visconti A, Duffy DL, Liu F, et al. Genome-wide association study in 176,678 Europeans reveals genetic loci for tanning response to sun exposure. *Nat Commun*. 2018; May 8;9(1):1684.

Voulgaris N, Papanastasiou L, Piaditis G, et al. Vitamin D and aspects of female fertility. *Hormones (Athens)*. 2017; Jan;16(1):5-21.

Wain LV, Odenthal-Hesse L, Abujaber R, et al. Copy number variation of the beta-defensin genes in europeans: no supporting evidence for association with lung function, chronic obstructive pulmonary disease or asthma. *PLoS One*. 2014 Jan 3;9(1):e84192.

Wan P, Hu Y, He L. Regulation of melanocyte pivotal transcription factor MITF by some other transcription factors. *Mol Cell Biochem*. 2011; Aug;354(1-2):241-6.

Wang TT, Nestel FP, Bourdeau V, et al. Cutting edge: 1,25-dihydroxyvitamin D3 is a direct inducer of antimicrobial peptide gene expression. *J Immunol*. 2004; Sep 1;173(5):2909-12.

Wang TT, Tavera-Mendoza LE, Laperriere D, et al. Large-scale in silico and microarray-based identification of direct 1,25-dihydroxyvitamin D3 target genes. *Mol Endocrinol.* 2005; Nov;19(11):2685-95.

Wang TT, Dabbas B, Laperriere D, et al. Direct and indirect induction by 1,25-dihydroxyvitamin D3 of the NOD2/CARD15-defensin beta2 innate immune pathway defective in Crohn disease. *J Biol Chem*. 2010; 285:2227–2231

Wang CQF, Akalu YT, Suarez-Farinas M, et al. IL-17 and TNF synergistically modulate cytokine expression while suppressing melanogenesis: potential relevance to psoriasis. *J Invest Dermatol*. 2013a; Dec;133(12):2741-2752.

Wang HF, Chen H, Ma MW, et al. miR-573 regulates melanoma progression by targeting the melanoma cell adhesion molecule. *Oncol Rep*. 2013b; Jul;30(1):520-6.

Wang J, Ding N, Li Y, et al. Insulin-like growth factor binding protein 5 (IGFBP5) functions as a tumor suppressor in human melanoma cells. *Oncotarget*. 2015; Aug 21;6(24):20636-49.

Wang Y, Viennet C, Robin S, et al. Precise role of dermal fibroblasts on melanocyte pigmentation. *J Dermatol Sci*. 2017a; Nov;88(2):159-166.

Wang J, Vasaikar S, Shi Z, et al. WebGestalt 2017: a more comprehensive, powerful, flexible and interactive gene set enrichment analysis toolkit. *Nucleic Acids Res*. 2017b; Jul 3;45(W1):W130-W137.

Watabe H, Soma Y, Kawa Y, et al. Differentiation of murine melanocyte precursors induced by 1,25-dihydroxyvitamin D3 is associated with the stimulation of endothelin B receptor expression. *J Invest Dermatol.* 2002; Sep;119(3):583-9.

Weaver S, Dube S, Mir A, et al. Taking qPCR to a higher level: Analysis of CNV reveals the power of high throughput qPCR to enhance quantitative resolution. *Methods*. 2010 Apr;50(4):271-6.

Webb AR, Kazantzidis A, Kift RC, et al. Colour Counts: Sunlight and Skin Type as Drivers of Vitamin D Deficiency at UK Latitudes. *Nutrients*. 2018; Apr 7;10(4).

Weide B, Schäfer T, Martens A, et al. High GDF-15 serum levels independently correlate with poorer overall survival of patients with tumor-free stage III and unresectable stage IV melanoma. *J Invest Dermatol.* 2016; Dec;136(12):2444-2452.

White SH, Wimley WC, Selsted ME. Structure, function, and membrane integration of defensins. *Curr Opin Struct Biol*. 1995 Aug;5(4):521-7.

Whyte MP, Thakker RV. Rickets and osteomalacia. *Medicine*. 2005; 33(12), 70–74.

Wickham, H. ggplot2: Elegant Graphics for Data Analysis. Springer-Verlag New York, 2016.

Wilde S, Timpson A, Kirsanow K, et al. Direct evidence for positive selection of skin, hair, and eye pigmentation in Europeans during the last 5,000 y. *Proc Natl Acad Sci USA*. 2014; Apr 1;111(13):4832-7.

Willie B, Gare J, King CL, et al. A preliminary assessment of Toll-like receptor and β-defensin gene polymorphisms in Papua New Guinea - what does it mean for HIV/AIDS? *PNG Med J*. 2017 Mar-Jun;60(1-2):51-59.

Wittersheim M, Cordes J, Meyer-Hoffert U, et al. Differential expression and in vivo secretion of the antimicrobial peptides psoriasin (S100A7), RNase 7, human beta-defensin-2 and -3 in healthy human skin. *Exp Dermatol.* 2013 May;22(5):364-6.

Wolf Horrell E, D'Orazio J. UV-independent induction of beta defensin 3 in neonatal human skin explants. *F1000Res.* 2014, 3:288

Wolfe BL, Trejo J. Clathrin-dependent mechanisms of G protein-coupled receptor endocytosis. *Traffic*. 2007 May;8(5):462-70.

Wong G, Gupta R, Dixon KM, et al. 1,25-Dihydroxyvitamin D and three low-calcemic analogs decrease UV-induced DNA damage via the rapid response pathway. *J Steroid Biochem Mol Bio*l. 2004; May;89-90(1-5):567-70.

Wong T, Wang Z, Chapron BD, et al. Polymorphic human Sulfotransferase 2A1 mediates the formation of 25-Hydroxyvitamin D 3 -3-O-sulfate: a major circulating Vitamin D metabolite in humans. *Drug Metab Dispos*. 2018; Apr;46(4):367-379.

Wu M, Hemesath TJ, Takemoto CM, et al. c-Kit triggers dual phosphorylations, which couple activation and degradation of the essential melanocyte factor Mi. *Genes Dev*. 2000 Feb 1;14(3):301-12.

Wu H, Park HY. Protein kinase C-beta-mediated complex formation between tyrosinase and TRP-1. *Biochem Biophy Res Commun*. 2003 Nov 28;311(4):948-53.

Wu J, Saint-Jeannet JP, Klein PS. Wnt–frizzled signaling in neural crest formation. *Trends Neurosci.* 2003 Jan;26(1):40-5.

Wu Z, Hoover DM, Yang D, et al. Engineering disulfide bridges to dissect antimicrobial and chemotactic activities of human β-defensin 3. *PNAS USA*. 2003 Jul 22;100(15):8880-5.

Wu XS, Masedunskas A, Weigert R, et al. Melanoregulin regulates a shedding mechanism that drives melanosome transfer from melanocytes to keratinocytes. *Proc Natl Acad Sci USA*. 2012; Jul 31;109(31):E2101-9.

Wyatt C, Lucas RM, Hurst C, et al. Vitamin D deficiency at melanoma diagnosis is associated with higher Breslow thickness. *PLoS One*. 2015; May 13;10(5):e0126394.

Yada Y, Higuchi K, Imokawa G. Effects of endothelins on signal transduction and proliferation in human melanocytes. *J Biol Chem*. 1991 Sep 25;266(27):18352-7.

Yamaguchi Y, Itami S, Watabe H, et al. Mesenchymal–epithelial interactions in the skin: increased expression of dickkopf1 by palmoplantar fibroblasts inhibits melanocyte growth and differentiation. *J Cell Biol*. 2004 Apr 26;165(2):275-85.

Yamaguchi Y, Passeron T, Hoashi T, et al. Dickkopf 1 (DKK1) regulates skin pigmentation and thickness by affecting Wnt/β-catenin signaling in keratinocytes. *FASEB J*. 2008 Apr;22(4):1009-20.

Yamaguchi Y, Hearing VJ. Physiological factors that regulate skin pigmentation. *Biofactors*. 2009 Mar-Apr;35(2):193-9.

Yanagisawa M, Kurihara H, Kimura S, et al. A novel potent vasoconstrictor peptide produced by vascular endothelial cells. *Nature*. 1988 Mar 31;332(6163):411-5.

Yang D, Chertov O, Bykovskaia SN, et al. Beta-defensins: linking innate and adaptive immunity through dendritic and T cell CCR6. *Science*. 1999 Oct 15;286(5439):525-8.

Yang D, Biragyn A, Kwak LW, et al. Mammalian defensins in immunity: more than just microbicidal. *Trends Immunol*. 2002 Jun;23(6):291-6.

Yang G, Zhang G, Pittelkow MR, et al. Expression profiling of UVB response in melanocytes identifies a set of p53-target genes. *J Invest Dermatol*. 2006; Nov;126(11):2490-506.

Yao R, Zhang C, Yu T, et al. Evaluation of three read-depth based CNV detection tools using whole-exome sequencing data. *Mol Cytogenet*. 2017 Aug 23;10:30.

Yasumoto K, Takeda K, Saito H, et al. Microphthalmia-associated transcription factor interacts with LEF-1, a mediator of Wnt signaling. *EMBO J*. 2002 Jun 3;21(11):2703-14.

Yohn JJ, Morelli JG, Walchak SJ, et al. Cultured human keratinocytes synthesize and secrete endothelin-1. *J Invest Dermatol*. 1993 Jan;100(1):23-6.

Yoshida H, Kunisada T, Grimm T, et al. Review: melanocyte migration and survival controlled by SCF/c-kit expression. *J Investig Dermatol Symp Proc*. 2001 Nov;6(1):1-5.

Yoshida-Amano Y, Hachiya A, Ohuchi A, et al. Essential role of RAB27A in determining constitutive human skin color. PLoS One. 2012; 7(7):e41160.

Yu G, Wang LG, He QY. ChIPseeker: an R/Bioconductor package for ChIP peak annotation, comparison and visualization. *Bioinformatics*. 2015; 31(14):2382-2383

Yuan XH, Jin ZH. Paracrine regulation of melanogenesis. *Br J Dermatol.* 2018; Mar;178(3):632-639.

Yuen AW, Jablonski NG. Vitamin D: in the evolution of human skin colour. *Med Hypotheses.* 2010; Jan;74(1):39-44.

Zanger P, Holzer J, Schleucher R, et al. Severity of *Staphylococcus aureus* infection of the skin is associated with inducibility of human beta-defensin 3 but not human beta-defensin 2. *Infect Immun.* 2010 Jul;78(7):3112-7.

Zeljic K, Kandolf-Sekulovic L, Supic G, et al. Melanoma risk is associated with vitamin D receptor gene polymorphisms. *Melanoma Res*. 2014; Jun;24(3):273-9.

Zerenturk EJ, Sharpe LJ, Ikonen E, et al. Desmosterol and DHCR24: Unexpected new directions for a terminal step in cholesterol synthesis. *Prog Lipid Res*. 2013; Oct;52(4):666-80.

Zhang X, Müller S, Möller M, et al. 8p23 beta-defensin copy number determination by single-locus pseudogene-based paralog ratio tests risk bias due to low-frequency sequence variations. *BMC Genomics*. 2014 Jan 24;15:64.

Zhang Z, Zhang Y, Evans P, et al. RNA-Seq 2G: Online Analysis Of Differential Gene Expression With Comprehensive Options Of Statistical Methods. Prepint at https://www.biorxiv.org/content/10.1101/122747v2 (2017).

Zhang W, Zhou P, Meng A, et al. Down-regulating Myoferlin inhibits the vasculogenic mimicry of melanoma via decreasing MMP-2 and inducing mesenchymal-to-epithelial transition. *J Cell Mol Med*. 2018a; Mar;22(3):1743-1754.

Zhang T, Choi J, Kovacs MA, et al. Cell-type–specific eQTL of primary melanocytes facilitates identification of melanoma susceptibility genes. *Genome Res*. 2018b; Nov;28(11):1621-1635.

Zhou XJ, Cheng FJ, Lv JC, et al. Higher DEFB4 genomic copy number in SLE and ANCA-associated small vasculitis. *Rheumatology* (Oxford). 2012 Jun;51(6):992-5.

Zhu W, Zhou B, Zhao C, et al. Myoferlin, a multifunctional protein in normal cells, has novel and key roles in various cancers. *J Cell Mol Med*. 2019; Nov;23(11):7180-7189.

Zittermann A, Iodice S, Pilz S, et al. Vitamin D deficiency and mortality risk in the general population: a meta-analysis of prospective cohort studies. *Am J Clin Nutr*. 2012; Jan;95(1):91-100.

Zsebo KM, Williams DA, Geissler EN, et al. Stem cell factor is encoded at the Sl locus of the mouse and is the ligand for the c-kit tyrosine kinase receptor. *Cell*. 1990 Oct 5;63(1):213-24.

Zuo Q, Liu J, Huang L, et al. AXL/AKT axis mediated-resistance to BRAF inhibitor depends on PTEN status in melanoma. *Oncogene*. 2018; Jun;37(24):3275-3289.